eman ta zabal zazu

Universidad del País Vasco

Euskal Herriko Unibertsitatea

Design, elaboration, characterization and evaluation of niosome formulations for gene delivery to retina and brain

Mohamed Ahmed Ahmed Mashal

Vitoria-Gasteiz 2020

NanoBioCel

Grupo de Micro y Nano Tecnologías, Biomateriales y Células

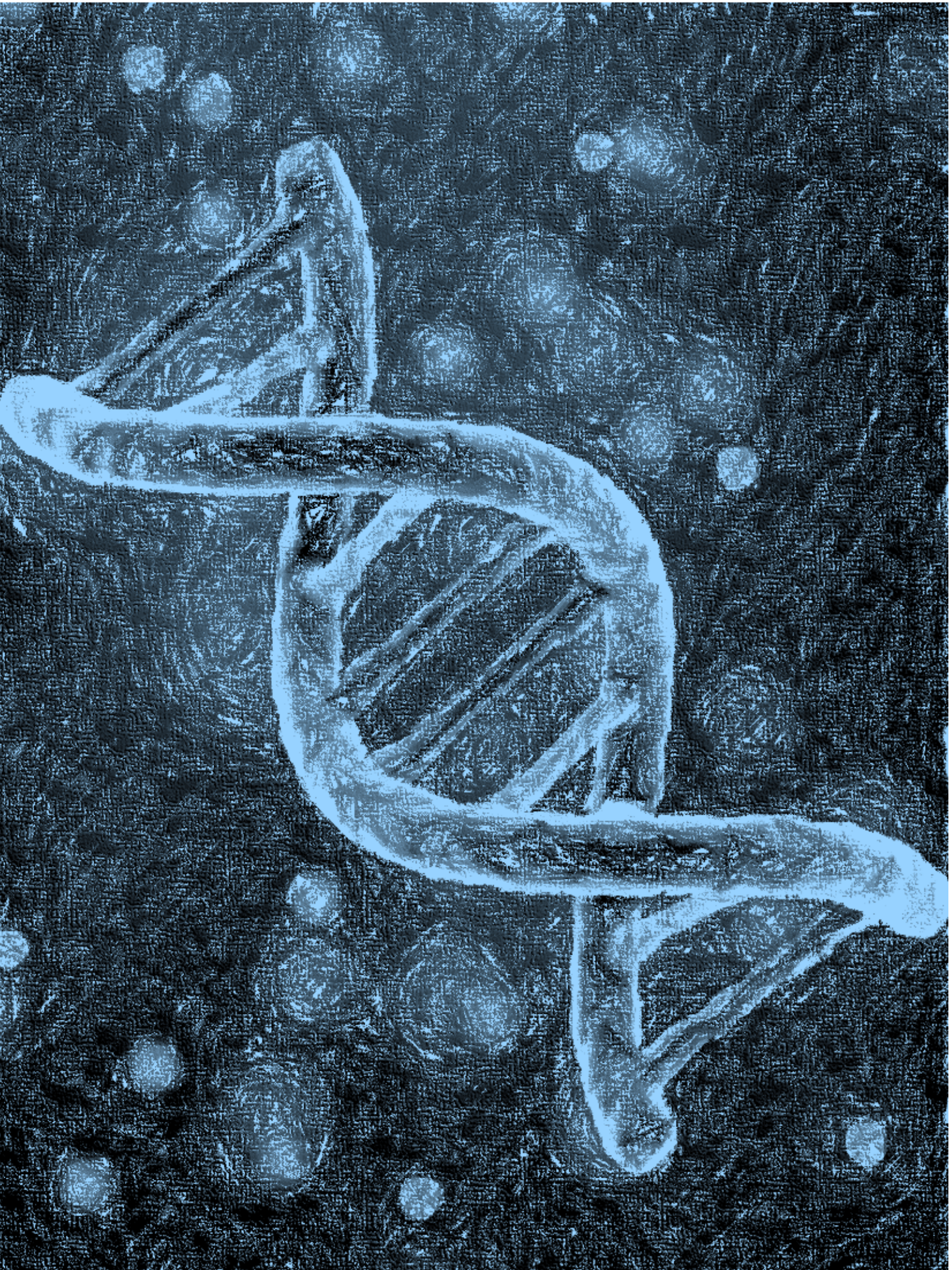

eman ta zabal zazu

Universidad del País Vasco

Euskal Herriko Unibertsitatea

Design, elaboration, characterization and evaluation of niosome formulations for gene delivery to retina and brain

Mohamed Ahmed Ahmed Mashal

NanoBiocel Group, Laboratory of Pharmaceutics

University of the Basque Country (UPV/EHU)

Faculty of Pharmacy

Vitoria-Gasteiz, 2020

eman ta zabal zazu

Universidad del País Vasco

Euskal Herriko Unibertsitatea

Design, elaboration, characterization and evaluation of niosome formulations for gene delivery to retina and brain

Mohamed Ahmed Ahmed Mashal

NanoBiocel Group, Laboratory of Pharmaceutics

University of the Basque Country (UPV/EHU)

Faculty of Pharmacy

Vitoria-Gasteiz, 2020

ACKNOWLEDGMENTS

First and to the greatest extent, praises and thanks to the Allah, the Almighty, for His showers of blessings during the way of my research work.
It is said that “If you're not thankful to people, you're not thankful to God”. Therefore, I have to say that the completion of this thesis would have been impossible without the love, support, guidance and encouragement of many individuals.

I would like to begin by expressing my deepest gratitude to my dearest supervisor Prof. Dr. Jose Luis Pedraz for giving me the opportunity to work on this thesis in his laboratory. He taught me the preciseness in science and the good practice in the lab. I feel myself privileged for being able to work under his experienced supervision towards accomplishing this research successfully. Honestly, I’ve always considered prof. Dr. Pedraz and Angela as my family in Spain. Dr. Pedraz, I can't thank you enough for all that you have done for me!

It is with great pleasure that I am expressing my thanks and appreciations to my dearest supervisor, Prof. Dr. Gustavo Puras, to whom I am immensely indebted. I truly thank him for being so enthusiastic about the work, for his great scientific guidance, reviewing the thesis manuscript and for his decent constructive comments.

I can’t express enough thanks to my soul mate, wife and co-worker, Dr. Noha Attia, for what no words can describe. Noha, without your dedications, support, and patience, obtaining my Ph.D. would have been totally impossible.

Research is an exciting journey of discovery. Thus, I extend my gratitude to all co-authors for their sincere invaluable support. The human, alongside with the scientific support from all members of the team was a continuous feeling throughout the whole journey in the lab.

Lastly, I own my warmest thanks to my dear ones, my Mom (Layla) and all my family members.

ACKNOWLEDGMENT FOR THE FINANCIAL SUPPORT

This project was supported by the Basque Country Government (CGIC10/172), Spanish Ministry of Education (Grant CTQ2017-84415-R, MAT2015-69967-C3-1R), the Generalitat de Catalunya (2014/SGR/624), and the Instituto de Salud Carlos III (CB06_01_0019, CB06_01_1028). The authors also wish to thank the intellectual and technical assistance from the ICTS “NANBIOSIS”, more specifically by the Drug Formulation Unit (U10) of the CIBER in Bioengineering, Biomaterials, and Nanomedicine (CIBER-BBN) at the University of Basque Country (UPV/EHU). Technical and human support provided by SGIker (UPV/EHU) is gratefully acknowledged.

ACKNOWLEDGMENT TO THE EDITORIALS

Authors would like to thank the editorials for granting permission to reuse their previously published articles in this thesis.

Mashal Mohamed, et al. "Retinal gene delivery enhancement by lycopene incorporation into cationic niosomes based on DOTMA and polysorbate 60."Journal of Controlled Release 254 (2017): 55-64.

Mashal Mohamed, et al. "Non-viral vectors based on cationic niosomes as efficient gene delivery vehicles to central nervous system cells into the brain."International journal of pharmaceutics 552.1-2 (2018): 48-55.

Mashal, Mohamed, et al. "Gene delivery to the rat retina by non-viral vectors based on chloroquine-containing cationic niosomes."Journal of Controlled Release 304 (2019): 181-190.

Man cannot remake himself without suffering,
for he is both the marble and the sculptor.

"Man, The Unknown" Alexis Carrel

Table of Contents

Chapter 1

Introduction

Chapter1

1.1.Gene therapy background

1.1.1. History

Gene therapy could be characterized as genetic material transfer in order to modify cells *in vitro*, *in vivo* and *ex vivo* mediated by transcription and/or translation. These modifications -obtained by recombinant nucleic acids, viruses, or genetically engineered microorganisms- are intended to repair, regulate, replace or even edit cells' genome (1). Despite the simplicity of this concept, the application of gene therapy strongly depends on designing a suitable long-term delivery system without adverse effects. Nearly seven decades ago, Frederick Griffith elucidated the transformation of the non-virulent type of pneumococcal bacteria into the virulent type. Several years later, in 1944, Avery, Macleod and McCarty described a genetic information carried in the form of deoxyribonucleic acid (DNA) that was responsible for the transformation of the pneumococcus bacteria. Years later, Watson and Crick identified DNA double-helix structure in 1953. This discovery was built on the previous work of Maurice Wilkins, in 1952, that had obtained extremely excellent X-ray diffraction photographs of DNA. The Wilkins' results were synchronized with those of Rosalind Franklin, in 1952, that had photographed a few different DNA fibers, and ultimately produced diffraction patterns using X-ray crystallography (1). After that, Howard Temin the stated r in 1961 that virus could transfer genetic material. One year later, in 1962, Maclaw Szybalski was the first researcher to transfer genes into mammalian cells. Theodore Friedmann and Richard Roblin subsequently in 1972 cited the Rogers' idea that "good DNA" could be used to replace faulty DNA in people with genetic defects, which was published in 1970 as the first recommendation to treat genetic diseases by gene therapy (2). At the same year, 1970, Hamilton Smith (Nobel prize laureate in 1978) discovered the restriction enzymes, which break DNA molecules at sites where a particular sequence of nucleotides occurs (3). Rogers and Pfuderer performed the first viral gene therapy trial in 1973, Based on the theory that viruses could be useful tools to introduce genetic materials into cells. Their study has opened the door for further discussion on the ethical aspects and rationale of gene therapy. Interestingly, in 1977, Fredrick Sanger (who won the Nobel prize twice) and his colleagues introduced the chain-termination method for sequencing DNA molecules

(4). This was a major achievement and allowed long stretches of DNA to be rapidly and accurately sequenced. In 1983, the polymerase chain reaction (PCR) technique was discovered by Kary Mullis, a breakthrough that enabled scientists to rapidly amplify DNA (5).

1.1.2. Clinical trials and commercial products of gene therapy

After decades of research, cell and gene therapies are moving from bench lab to bedside. Since the year 1989 (first gene therapy clinical trial), more than 2600 clinical trials for gene therapy have been approved globally till the year 2017 (Figure 1) (6).

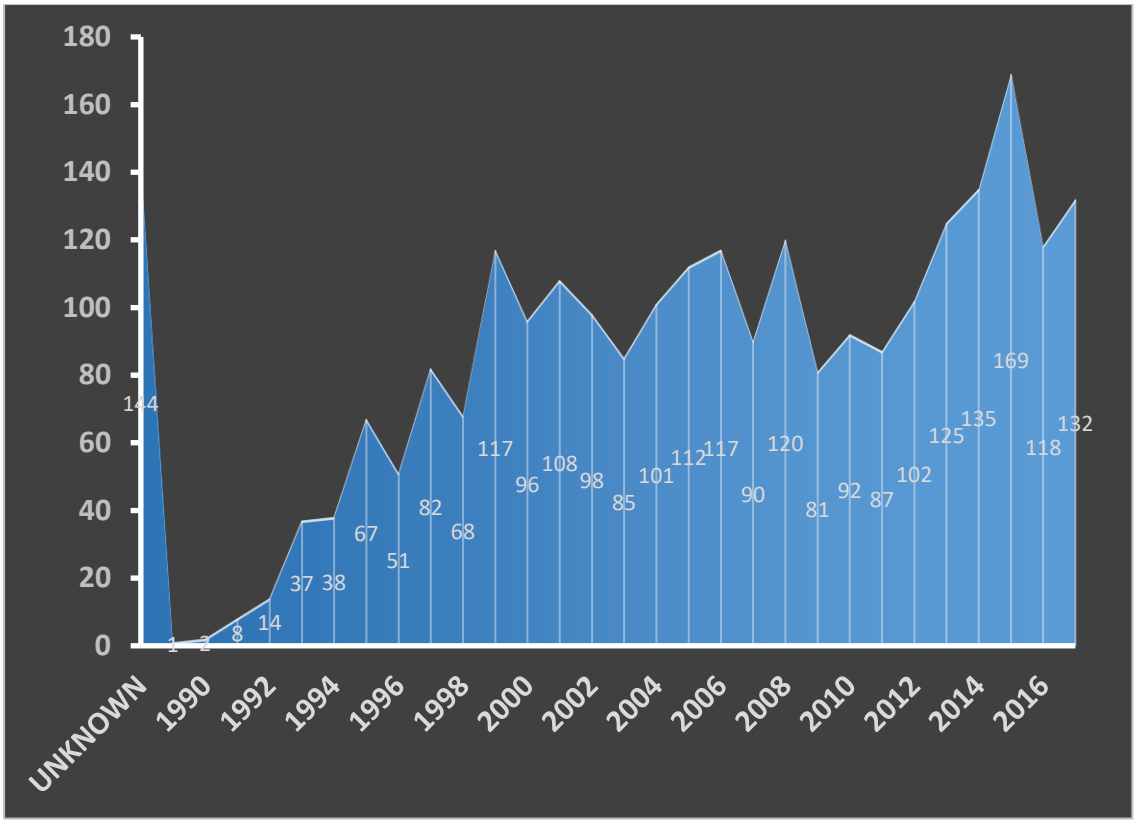

Figure 1. The number of gene therapy clinical trials approved worldwide 1989-2017 (6).

In 1990 the 4-year-old DeSilva with severe combined immune deficiency (SCID) became the first patient to undergo gene therapy in the United States. This trial was authorized by the NIH Recombinant DNA Advisory Committee (RAC) and the Food and Drug Administration (FDA). Functional adenosine deaminase (ADA) genes

were transferred by retroviral vectors into the cultured T cells. The T lymphocytes with the corrected gene were reinfused back into the patient about 12 days after blood was drawn. Also, at the NIH Clinical Center in1991, Cynthia a 9-years-old girl underwent another trial. Unfortunately, in 1999 the 18-year-old Jesse Gelsinger with inherited enzyme deficiency was the first victim of gene therapy after 4 days of injection with a genetically altered adenovirus into his liver. This was a direct reason for severe handicap in the research field of this technology (7). The field of gene therapy was shaken again in 2002, when a three-year-old boy with SCID treated in a French trial developed leukemia. Therefore, gene therapy clinical trials were halted again (8). Nevertheless, Gendicine (recombinant human p53 adenovirus) was approved in 2003 by the China Food and Drug Administration (CFDA) as a first gene therapy product to treat head and neck cancer (9). In 2007, British doctors performed the world's first gene therapy operation to treat Leber Congenital Amaurosis due to RPE65 mutations via ocular subretinal injection of adeno-associated virus (AAV) gene vector (10). In 2012, the first gene therapy drug approved by the European Medicines Agency (EMA) was Glybera (alipogene tiparvovec). Glybera is an AAV vector engineered to express lipoprotein lipase for the treatment of lipoprotein lipase

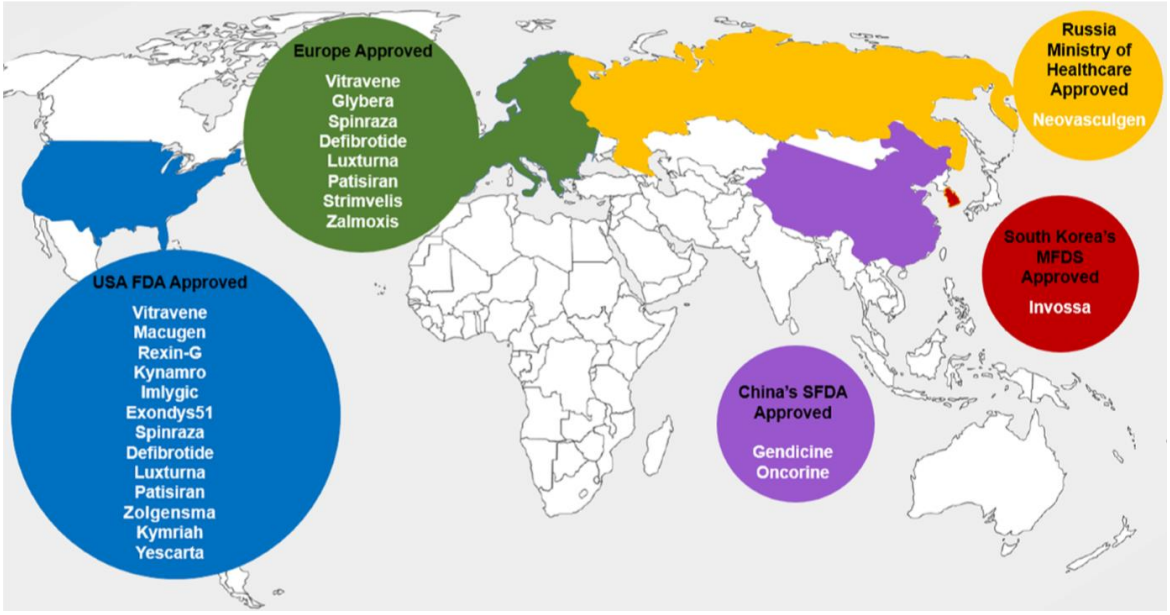

deficiency (11).

Figure 2. Distribution countries of approval gene therapy drugs (12)

The year of 2017 is considered the distinguished starting point for gene therapy in the United States. In August 2017, kymriah® was approved by the FDA as the first gene therapy product to be marketed for treatment of acute lymphoblastic leukemia. In the same year, Yescarta®, was approved by FDA for treating large B-cell lymphoma. Furthermore, by December 2017, the FDA-approved Luxturna® became the first *in vivo* gene therapy drug to treat Leber congenital amaurosis LCA (a rare inherited eye disease). Recently, Zolgensma® became the first gene therapy approved by FDA in 2019 to treat children less than two years of age with spinal muscular atrophy (SMA), a leading hereditary cause of infant mortality.

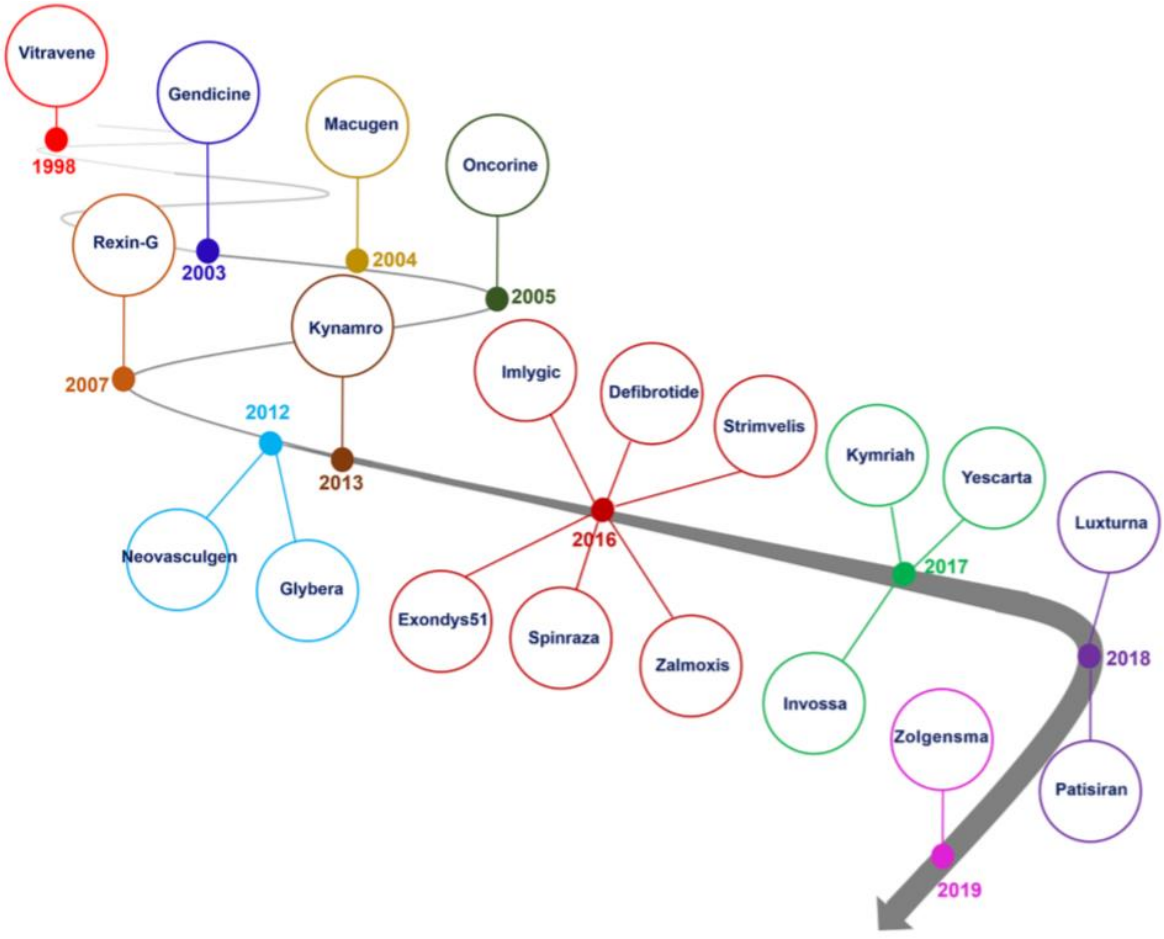

Figure 3. Timeline of gene therapy development (12)

Such recently approved drugs for human use based on gene, along with advances on revolutionary genome editing technologies, suggest that gene therapy can become a regular medical option into the clinical practice.

One of the organs that is considered an enticing gene therapy target is the eye, because of its accessibility and its immune privilege. The vision process is highly complex, and requires coordination of numerous components in both eye and brain. Moreover, the retina of the eye represents a part of the central nervous system (CNS) and is actually a brain tissue. Although the RPE65 gene therapy (via viral carriers) has paved the way for the treatment of retinal diseases. Some other genes are too large to be carried into the retina via viral carriers, such as the gene causing Stargardt's hereditary maculopathy.

The Retinostat® is a gene therapy that is currently in phase I clinical trial for the wet subtype of age-related macular degeneration (AMD). It inhibits blood vessel growth by expressing angiostatin and endostatin proteins. On the other side, the sFLT gene (carried on AAV vector) was injected subretinal to block the vascular endothelial growth factor (VEGF) (13). Table 1 depicts some gene therapy clinical trials for eye disorders at different stages. In a CNS clinical trial (NCT01454596), the gene for epidermal growth factor receptor (EGFRvIII) was incorporated in retrovirus to treat patients with glioblastoma. A retroviral vector transporting a chimeric antigen receptor (CAR) for the EGFRvIII tumor antigen, can be used to mediate genetic transfer of CAR with high efficiency (14). Table 2 elaborates more on the gene therapy clinical trials for CNS disorders.

Table 1. Gene therapy clinical trials on eye diseases (15).

Company	Product	indications	Phase	Expected reporting date
GenSight Biologics	GS010	Leber Hereditary Optic Neuropathy	Ph III (REVERSE & RESCUE)	Topline data for RESCUE expected Q1 2019; filing for market authorization expected in Europe in Q4 2019 and in the U.S. in H2 2020
Nightstar Therapeutics	NSR-REP1	Choroideremia	Ph III	Complete enrollment 1H 2019; data anticipated 2020
REGENXBIO	RGX-314	Wet Age-Related Macular Degeneration (wet AMD)	Ph IIb	Trial expected to initiate in 2H 2019
AGTC	rAAV2tYF-CB- hRS1	X-linked Retinitis Pigmentosa	Ph I/II	Interim data updates from dose-escalation and expansion groups expected in Q3 and Q4 of 2019
GenSight Biologics	GS030	Retinitis Pigmentosa	Ph I/II	Early findings expected 1H 2019; topline results expected 4Q 2020
4D Molecular Tx	4D-110	Choroideremia	Ph I	Clinical trial to initiate in 2019
Adverum Biotechnologies	ADVM-022	Wet AMD	Ph I	Enrollment update in 1H 2019; interim data in Q1 2020
AGTC / Bionic Sight	Undisclosed	Advanced retinal disease	IND preparation	IND to be submitted in 1H 2019

Table 2. Gene therapy clinical trials on CNS diseases (15).

Company	Product	Indications	Phase	Expected reporting date
AveXis / Novartis	AVXS-101	SMA Type 1	MAA filing, BLA submission, J-NDA filing (Japan)	Responses from EMA, FDA, MHLW (Japan) expected mid-2019
bluebird bio	Lenti-D	Cerebral Adrenoleukodystrophy	Ph III	To be initiated in 2019
Ziopharm Oncology	Controlled IL-13 + Libtayo	recurrent glioblastoma	Ph II	Trial to initiate in 1H 2019
ReNeuron	CTX product candidate	Stroke disability	Ph IIb	Ongoing; top-line data expected in early 2020
uniQure	AMT-130	Huntington's disease	Ph I/II	Trial to initiate in 2H 2019
Kolon Life Science	KLS-2031	Neuropathic pain	Ph I/IIA	Trial to initiate by EOY 2019
Axovant	AXO-AAV- GM1	GM1 gangliosidosis	Ph I	Expected to initiate trial in 1H 2019, with initial data expected in 2H 2019
Voyager	VY-AADC	Parkinson's disease	Ph I	Provide 12-month data in Q2 2019
AveXis / Novartis	AVXS-201	genetic ALS (SOD1)	Pre-IND	IND submission expected in late 2018/early 2019
PTC Therapeutics	TBD	Friedreich ataxia	pre-IND	Expected to submit IND in 2019
REGENXBIO	RGX-181	late-infantile neuronal ceroid lipofuscinosis type 2 (CLN2) disease	Pre-IND	IND submission anticipated in 2H 2019
Voyager	VY-HTT01	Huntington's disease	IND submission	Submit IND in 2019
Voyager	VY-SOD102	ALS-SOD1	Pre-IND	Submit IND in 2019

1.1.3. Gene therapy strategies

Currently, various gene therapy strategies do exist. Such strategies could be categorized into: (1) gene replacement for the monogenic diseases, (2) gene addition to treat acquired diseases, (3) gene editing to introduce targeted changes in host genome, and (4) alteration of gene expression by targeting RNA. The treatment may take place outside of the body (*ex vivo*) or inside the body (*in vivo*). Modified viruses or other vectors are used as gene delivery systems To deliver the gene into the genome into the cells.

The significant potential of using plasmids for gene therapy has been recognized since 1990. Selecting the right composition of a plasmid is fundamental to ensure the success of gene therapy. There are many factors and elements to be considered when choosing the plasmid backbone such as: cloning or expression safety, plasmid size, antibiotic resistance, restriction sites in multiple cloning site (MCS), promoter, terminator, ribosome binding site (RBS) sequence, or protein modifications (adding a tag or a fusion protein to the plasmid to further understand the function of a specific gene) (16). Both figure 4 and table 3 describe different elements of the plasmid.

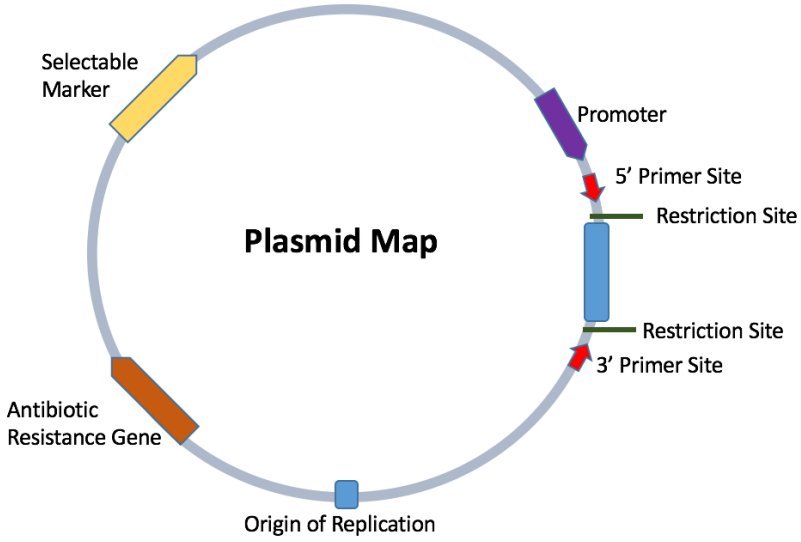

Figure 4. A representative map of the main features of a plasmid vector. (17)

Table 3. Plasmid elements and their description. (17)

Plasmid Element	Description
Origin of Replication (ORI)	DNA sequence which allows initiation of replication within a plasmid by recruiting transcriptional machinery proteins
Antibiotic Resistance Gene	Allows for selection of plasmid-containing bacteria.
Multiple Cloning Site (MCS)	Short segment of DNA which contains several restriction sites allowing for the easy insertion of DNA. In expression plasmids, the MCS is often downstream from a promoter.
Insert	Gene, promoter or other DNA fragment cloned into the MCS for further study.
Promoter Region	Drives transcription of the target gene. Vital component for expression vectors: determines which cell types the gene is expressed in and amount of recombinant protein obtained.
Selectable Marker	The antibiotic resistance gene allows for selection in bacteria. However, many plasmids also have selectable markers for use in other cell types.
Primer Binding Site	A short single-stranded DNA sequence used as an initiation point for PCR amplification or sequencing. Primers can be exploited for sequence verification of plasmids

Plasmids are simpler and cheaper to make, ship and store compared with viral and RNA-based vectors and have a much longer shelf life. The modular nature of plasmids also allows enables simple molecular cloning, making them easy to manipulate and design for therapeutic use. In addition, the plasmids can be distributed repeatedly, unlike viruses. Most plasmid DNA preparations include many topological plasmid variations, including supercoiled (the preferred topology), but also the undesirable linear and open circular forms of the plasmid. In order to deliver their

payload, Plasmids require vectors, physical forces, or advanced modifications for uptake and nuclear localization. Since plasmids are non-replicating episomes, the expression of transgenes is transient and diluted by cell division. The dinucleotides of unmethylated cytosine-phosphate-guanine (CpG) are more widespread in bacterial DNA than in mammalian DNA. They have the ability to be recognized by the mammalian immune system via toll-like receptor (TLR)-9, and are potentially precipitating not only in transgene silencing, but also in immune response (18).

RNA precursors are essential targets in genetic therapies. Antisense oligonucleotides (ASOs) are single-stranded (ss) DNA or RNA sequences that can be used for silencing overexpressed proteins in toxic "gain of function" diseases. They can target RNA for degradation, preventing the translation of a specific RNA into protein and altering the splicing of pre-mRNA. ssDNA complementary to mRNA could be used to block the translation of specific mRNA (19).

Aptamers are short, single-stranded DNA or RNA (ssDNA or ssRNA) molecules that can bind to a specific target, including proteins, peptides, carbohydrates, small molecules, toxins, and even living cells. Aptamers are selected from a large oligonucleotide library through a process called SELEX (Sequential Evolution of Ligands by Exponential Enrichment) (20).

Recently, the gene editing tool CRISPR/Cas9 (Clustered Regularly Interspaced Short Palindromic Repeats/ CRISPR-associated protein 9) was used (figure 5). Cas9 is an RNA-guided DNA endonuclease enzyme that uses CRISPR sequences as a guide to identify and cleave specific strands of DNA complementing the CRISPR sequence in order to mediate genome alteration with high precision. Unlike the previous gene editing techniques such as Transcription Activators-Like Effective Nucleases (TALENS) this technology is simple, easy to use and inexpensive. However, they have limitations, such as narrow targeting range and potential for off-target mutagenesis (21).

But with higher precision, one of the approaches based on the CRISPR technique is prime editing technology tool, which both specifies the target location and encodes the desired edit. The prime technique writes new genetic information directly

into a specified DNA site using a catalytically impaired Cas9 endonuclease fused to an engineered reverse transcriptase, programmed with a prime editing guide RNA (pegRNA). It rewrites DNA by cutting just one strand to add, delete, or substitute base pairs that can edit more genetic mutation forms than genome-editing approaches like CRISPR-Cas9 (22).

RNA interference (RNAi) is formulated and presented as a small double-stranded (ds) RNA intended to down-regulate its target transcript (i.e., mRNA) and protein. Nonetheless, for long-term knockdown, a more robust strategy is to use another RNAi route, by delivering synthetic microRNA (miRNA) (24). Additionally, short interfering RNAs (siRNAs) can downregulate a selected mRNA gene that appears to degrade through the RNA-interfering silencing complex (RISC). The platforms siRNA and ASO are both nucleic acids containing antisense strand designed to identify a target mRNA. Though, ASOs have one strand while siRNAs have two, which can reduce cost and simplify delivery (25).

In 2018, Alnylam launched the ONPATTRO® (patisiran) drug which has been approved by the FDA as the first siRNA-based therapy for the rare hereditary disease transthyretin-mediated amyloidosis in adult patients (26).

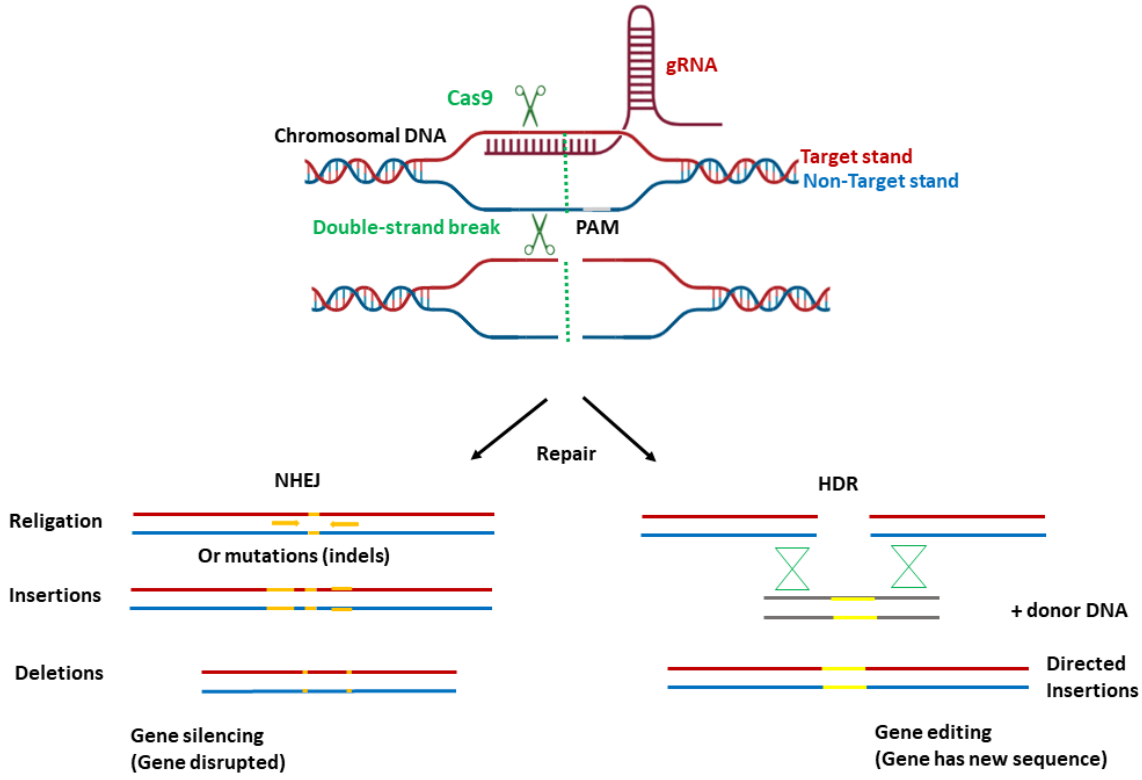

Figure 5. CRISPR/Cas9-mediated DNA cleavage and simplified repair mechanism (23).

1.2.Gene delivery vectors

Current gene delivery vehicles, namely vectors, are classified mainly into two classes: the viral and the non-viral vectors.

1.2.1.**Viral vectors**

Viruses are attractive gene-delivery vehicles due to their ability for efficient nucleic acid delivery to specific cell type while escaping host cell immune surveillance. Moreover, they may exploit the cellular machinery to encourage their replication (27). Viral delivery system is based on a virus with nucleic acid coated by capsid protein and in many cases further by an envelope structure. One or more viral structural genes are deleted to deactivate the virus from spread in the host organism (28). Viral vectors had been designed for temporary short-term and permanent long-term expression, and can be conveyed by both RNA and DNA viruses with either single-stranded or double-

stranded genomes (29). However, many disadvantages and safety issues are related to the use of viral vectors such as complex and expensive production, limited carrying capacity, broad tropism, oncogenicity, mutagenicity, immunogenicity and inflammatory responses (30). Recently, chimeric viral vectors have been developed in a trial to overcome the limitations of each viral species, by combining suitable features of two or more different viruses into one (31).

The retroviral capsid is an enveloped shell of protein with size of 80-100 nm. It has an average packaging capacity of 8 kb. Retroviral vector integrates in the host cell genome, by using reverse transcriptase in a stable and permanent manner. Replication-competent and replication-defective are the two types of retroviral vectors. Retrovirus are mainly applied in studies for tissue repair and engineering due to their capability of infecting dividing cells without developing any immunogenic viral proteins (32).

Lentiviruses, subtype of retrovirus, are able to integrate into non-dividing cells. The lentiviral genome is similar to other retroviruses; however, it contains six other genes -two regulatory genes and four accessory genes- that code for proteins essential for viral replication, binding, infection, and release. Lentivirus common example is the human immuno- deficiency virus type 1 (HIV-1). Lentiviral vectors seem to be less mutagenic than their retroviral counterparts (33).

Adenoviruses are icosahedral, non-enveloped, ds DNA viruses with a size of 70 nm, and a genome size of about 36 kb. They are the most widely used viral vectors able to overcome the limitations of other viral vectors as the retrovirus Among the 50 different serotypes of adenovirus, the types 2 and 5 are the most frequently used ones (34). The packaging capacity of dsDNA adenoviruses is about 7.5 kb of foreign DNA with short-term episomal expression with broad range of host cells. In addition, there is a possibility to hybridize adenovirus vectors with sleeping beauty transposase system for chromosomal integration or with CRISPR/Cas9 nuclease for gene editing (35).

The AAV is a small (22 nm in diameter) nonpathogenic parvovirus with a non-enveloped, icosahedral capsid. Its genome is composed of a linear, ss DNA. It is used

to target a variety of different types of tissues according to the types of capsid of different AAV serotypes. Their replications within a host cell nucleus requires either a helper virus or genotoxic stress conditions. It has a packaging capacity less than 4 kb. In gene therapy trials, there is a great interest in AAV-based trials in monogenetic diseases (32).

Herpes simplex virus, the virus responsible for famous cold sore, has a genome that composed of a dsDNA (152 kb in length) that coding up to 90 specific viral proteins. It consists of icosahedral protein shell that is coated by a viral envelope. It has a high insert capacity (> 30 kb). It has the potential to infect a host and then remain latent for a while before reappearing again. Moreover, its neurotropic nature enables it to infect neural cells, so may assist in gene therapy of various neural disease (32).

1.2.2. **Non-viral vectors**

Delivery systems using non-viral carriers is a promising tool for gene therapy because of their repeated administration capability and their appealing safety profile (36). Non-viral vectors are of lower cost, cheaper and easier-to-manufacture alternative to the viral vectors. Physical and chemical gene carriers are the two broad categories of non-viral vectors. However, tremendous achievements have been made in this field recently, clinical application of non-viral-vectors in gene therapy is still hampered by the lack of highly effective gene delivery techniques (37).

1.2.2.1. **Physical gene delivery methods**

These simple gene delivery methods (summarized in figure 6) facilitate gene transfer by physical forces to overcome the barrier function of cell membrane. The genetic material is delivered into cells without no particulate or viral system (38).

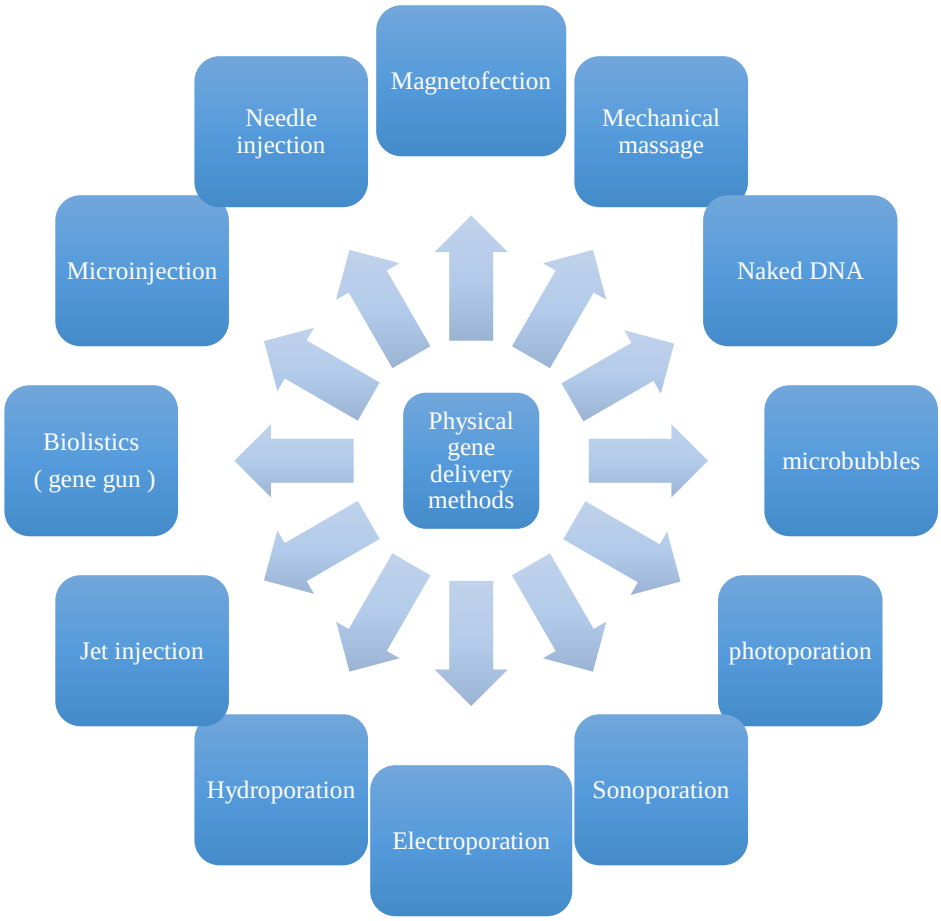

Figure 6. Different methods used of the physical gene delivery.

1.2.2.2. Chemical gene delivery methods

Chemical vectors are the second subcategory of non-viral vectors based on wide range of molecules and macromolecules (summarized in figure 7). In general, chemical vectors are in the form of nanoparticles that are able to mimic some viral function required for gene delivery (39). Theses carriers form electrostatic complexes with the genetic material.

Inorganic nanoparticles have been reported as non-viral gene delivery vehicles, such as gold nanoparticles, iron oxide nanoparticles, quantum dots, carbon nanotubes, graphene, silica and calcium phosphate. Generally, there are three approaches to use inorganic nanoparticles in gene delivery. The first approach involves conjugation of genetic material onto the inorganic nanoparticle with a responsive linker. The second approach involves direct use of positively charged inorganic nanoparticles to form a complex with the negatively charged genetic material. The third approach involves the use of cationic

amphiphilic polymers to aid in the complex formation between genetic material and the inorganic nanoparticle (40).

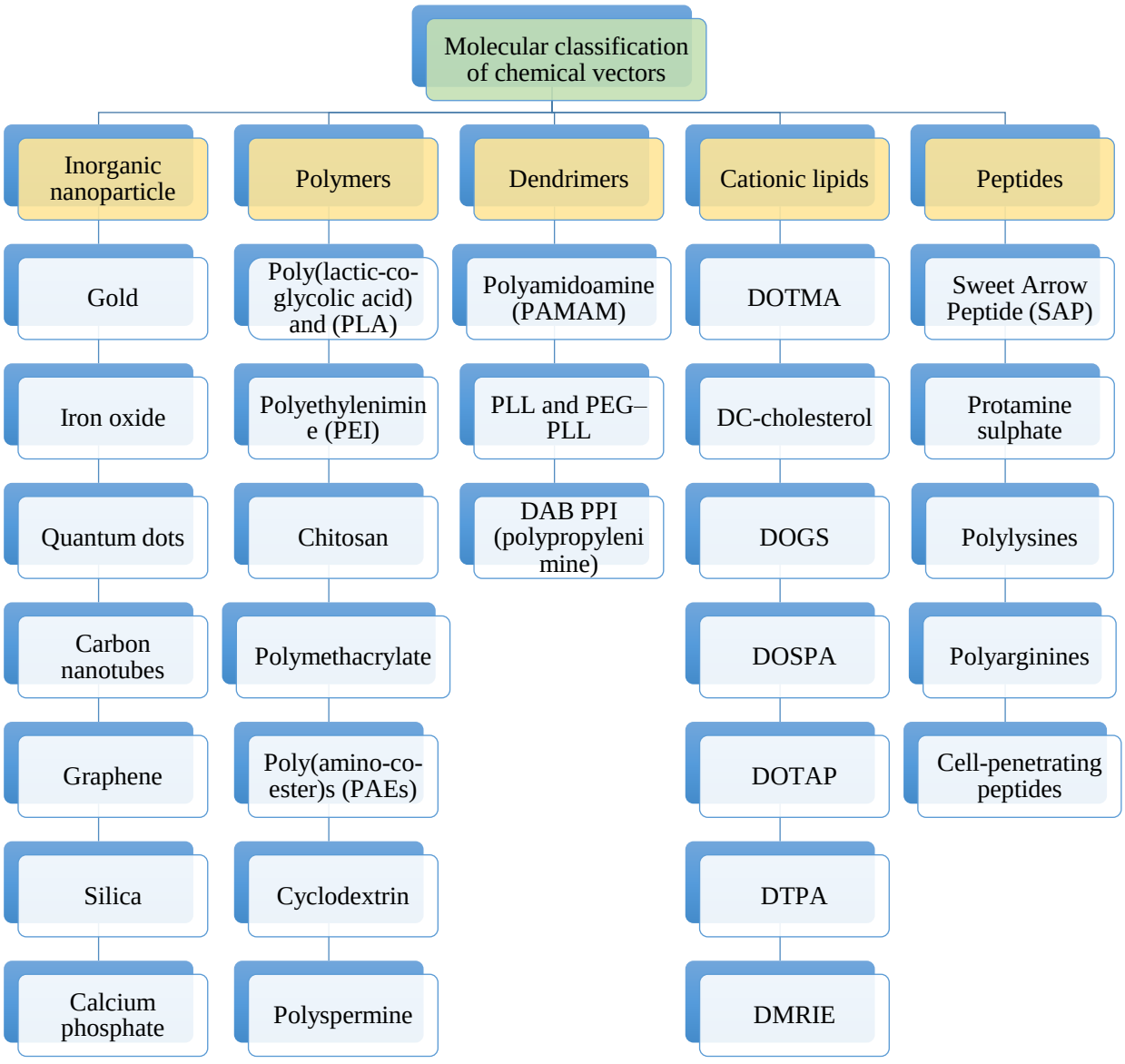

Figure 7. Molecular classification of chemical gene carriers.

Polymers of various architectures may shape nano- or micro-sized particles, according to the synthesis method. For gene delivery purposes, biocompatibility and biodegradability are important parameters to take into account when polymer vehicle is elaborated. The polymer's surface functionality plays a pivotal role in conjugating biomolecules for therapeutic targeting into different cells (41). Polymeric nanoparticles can overcome many hurdles of the gene delivery process, as poor cellular uptake, low

transfection efficiency, lysosomal degradation, and off-target effects. There are three main approaches that can be applied to polymeric nanoparticles when formulated with genetic materials as non-viral vehicles. The first approach is to condense DNA with polymers (polyplexes) as in case of poly ethylenimine, poly (L-lysine), polyamidoamine, and poly (β-amino acid)s chitosan. The second approach depends on encapsulating DNA in polymeric matrix or reservoir [ex: polylactide, poly(lactide-co-glycolide), and poly (β-amino ester)s chitosan]. The third approach compromises complexing DNA to the surface of polymeric nanoparticles (e.g. poly alkyl cyanoacrylate, polylactide, poly(lactide-co-glycolide) chitosan (grafted with cationic polysaccharides or surfactants) (42).

Dendrimers are highly branched three dimensional macromolecules emerged from a new class of polymers named "cascade molecules"(43). Dendrimers are gene delivery vehicles with interesting properties due to their functional group's high density, monodispersing features, well-defined shape and multivalences. However, toxicity due to high cationic charge is a major concern, especially with higher generation dendrimers. Poly amidoamine/ PAMAMs (the most widely researched dendrimers for gene delivery) are well characterized dendrimer species. They are advantageous thanks to their water solubility and lack of immunogenicity. Moreover, the modification to their terminal amine group facilitates the binding to various hosts or target molecules. The transfection reagent SuperFect® (by Qiagen), as a PAMAM dendrimer, depicts high yield gene transfer into primary human retinal pigment epithelial (RPE) cells (44).

Peptides (single and multifunctional) nanocarriers possess essential characteristics as non-viral gene delivery systems. Peptides are able to condense DNA through electrostatic and hydrophobic interactions. Besides, cell penetrating peptides mediate direct cellular entry via membrane translocation or facilitate endosomal escape after endocytosis. Moreover, peptides activate cytosolic transport and can function as nuclear localization signal as in case of protamine polypeptide. Many peptides act as targeting ligands to specific cell and/or tissue types (45).

Cationic lipids are interesting materials for gene delivery applications. In 1987, Felgner et al., synthesize DOTMA (1,2-di-O-octadecenyl-3-trimethylammonium propane (chloride salt) as the first cationic lipid for DNA delivery (46). Since that date, cationic lipids become one of the most important tools for the delivery of DNA, RNA and many other therapeutic molecules. They are easily designed, synthesized and characterized. Most of cationic lipids share the same common four domains structure, cationic head groups, hydrophobic portions, linker bonds between both domains, and backbone domain (as illustrated in figure 8). (47).

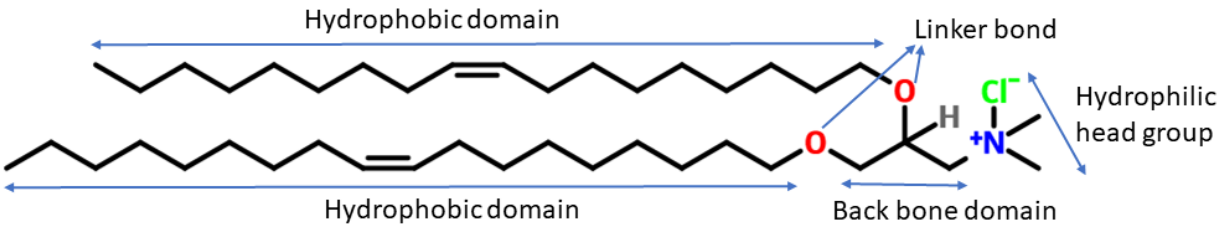

Figure 8. General structure of the cationic lipid DOTMA.

Interestingly, cationic lipids play various roles in the transfection process. The positive charge of the head group binds electrostatically to the negative charge of phosphate group in nucleic acids to form a complex. Also, it facilitates cellular uptake of nucleic acid by direct interaction with cell membrane negatively-charged glycoproteins and proteoglycans. Additionally, the positively-charged lipid protects genetic material against intracellular and extracellular nucleases. Moreover, it triggers endosomal escape by proton sponge effect (48). The hydrophobic domain structure determines the phase transition temperature and the fluidity of the bilayer and influences the stability of the nano formulation, the protection of DNA from nucleases, the endosomal escape, the release of DNA from complex, and the nuclear penetration (49). On the other hand, the positive surface charge is known to reduce the half-life of circulating complex in blood. Therefore, neutral polymers as polyethylene glycol (PEG) could be used for surface shielding to mitigate the excessive positive charge to prolong the half-life (50). The hydrophobic and hydrophilic moieties of cationic lipids are connected by a linker bond, commonly are ether, ester, amide, and carbamate groups.

In general, ether bonds, as in cationic lipid DOTMA, render better gene delivery efficiency (51). While, the backbone domain (most commonly glycerol-based) separates the headgroup from the hydrophobic domain, and acts as a scaffold on which the cationic lipid is built (49). For gene delivery, cationic lipids can be formulated in many structures, as liposomes, nano-emulsions, solid lipid nanoparticles, nanostructured lipid carriers, niosomes, and lipopolysomes (illustrated in figure 9).

1.3. Cationic lipid-based formulations

Liposomes are artificial self-assembled spherical vesicles enclosing a small volume of aqueous solution in a lipid bilayer. Liposomes consist mainly of phospholipids (the major component of biological membranes) (52). Generally, successful gene delivery via liposomes can be boosted by the aid of helper lipids. Helper lipids are neutral lipids that enhance the effectiveness and stability of cationic lipid-based delivery formulations. They can broadly bind to cell surfaces and form cone-shape geometry favoring the formation hexagonal II phase. That phase is known to promote endosomal release of the plasmid (are assumed to act as a membrane fusion promoter). Dioleoyl phosphatidyl ethanolamine (DOPE) is an efficient helper lipid for *in vitro* gene transfection via cationic liposomes (53). Cationic liposomes are extensively tested as gene delivery systems for nucleic acid therapeutics, siRNA and plasmid DNA. Polyethylene glycol (PEG), as a shielding agent, enhances the efficacy and tolerability of cationic liposomes in systemic delivery (54). Although, there are many advantages for using cationic liposomes, as their biodegradability and biocompatibility, many drawbacks limit their use as, phospholipid oxidation, short half-life, cell toxicity and low stability.

***Nano*-emulsions** a colloidal particulate system consist of oil core in water stabilized by surfactants. The addition of cationic substance to squalene is an example for cationic nano-emulsions as a good candidate in drug and gene delivery (55). A cationic emulsion containing castor oil and DC-Chol was used to deliver plasmids through portal vein injection in mice. Medium chain triglycerides, soybean oil, and squalene were used to prepare emulsions for gene delivery and represent the inner phase of the emulsion (56).

Solid lipid nanoparticles **(SLN)** were presented in 1990 as a substitute delivery system to liposomes, emulsions and polymeric nanoparticles. SLNs are composed of solid fat which is dispersed in an aqueous phase in the presence of surfactants to enhance its stability. The proper selection of lipids and surfactants can affect the particle size, stability, loaded molecules and behaviors of release. Their lipid components are solid at both body and ambient temperature (57).

Nanostructured lipid carriers **(NLCs)** are spherical structures with a mixed solid and liquid matrix, having an aqueous core surrounded by a lipid bilayer. There are three major types of NLC: cationic, neutral, and targeting-modified NLC. Cationic NLCs can be used as carriers for negatively charged substance, including proteins, polypeptides, oligonucleotides, RNAs and DNAs (58) NLC have many clinical applications because of superior biocompatibility, high biodegradability and low immunogenicity. They are used in the delivery of nucleic acids including distinct miRNA molecules for cancer gene therapy.

Niosomes are self-assembled non-ionic surfactant vesicles. They are composed of three main components: (1) a non-ionic surfactant such as polysorbates; (2) a neutral helper lipid such as cholesterol, squalene and lycopene; (3) a cationic lipid such as DOTMA. The incorporation of non-ionic molecules in niosomes reduces the undesirable toxicity of cationic lipids showing better cellular viability profiles compared to their corresponding anionic or cationic counterparts (59). Niosomes have first emerged as a vesicle delivery system in the 70s in the field of cosmetics industry. Thanks to their capability to encapsulate both hydrophobic and hydrophilic drugs, niosomes are reported as potential carriers for the delivery of drugs such as doxorubicin, vaccines, insulin, siRNA. They have many applicable therapeutic effects (e.g. anti-Alzheimer, anti-cancer, anti-oxidant, anti-diabetics and anti-microbial) and can be administrated via various methods, as intravenously, orally (e.g., Flurbiprofen); ocular (e.g., Chloramphenicol, Acetazolamide, Fluconazole), and topically (e.g., Erythromycin, Minoxidil, Rofecoxib) (60). Niosomes are highly stable, yet slightly leakier than liposomes. In comparison to liposomes, niosomes can be formulated at a lower cost, longer stability and less toxicity. Moreover, researchers highlighted on the

biocompatible, biodegradable pharmaceutics and low immunogenic features of their components (non-ionic surfactants, helper lipids as well as charged molecules). Niosomes have been widely used as oligonucleotide carriers. The formulation of niosomes, by the method of solvent emulsification-evaporation technique, managed to deliver pCMS-EGFP plasmid to the retina and brain. The results proved that niosomes could protect DNA from degradation and introduced good trafficking pattern with good chemical and physical stability and relatively smaller sizes. In addition, niosomes can also be used as vectors in DNA vaccines which provide a simple, stable and cost-effective solution compared with liposomes. Niosomes can also assist as a delivery system for targeting stem cells (60).

Lipopolysomes are multifunctional nanocarriers composed by combining polymersomes and liposomes. Lipopolysomes have the ability for simultaneous encapsulation of hydrophobic and hydrophilic molecules (61). The vector resulted by co-formulation of plasmid DNA and lipopolysomes is called lipopolyplexes. In non-viral gene delivery systems this term (lipopolyplexes) conclude a diverse component of lipids and polymers co-formulated with genetic materials. One advantage of lipopolyplexes vehicles is that they have the potential to be targeted to specific cell types by attaching peptide targeting ligands on the surface, thus increasing both the transfection efficiency and selectivity for disease targets such as cancer cells (62).

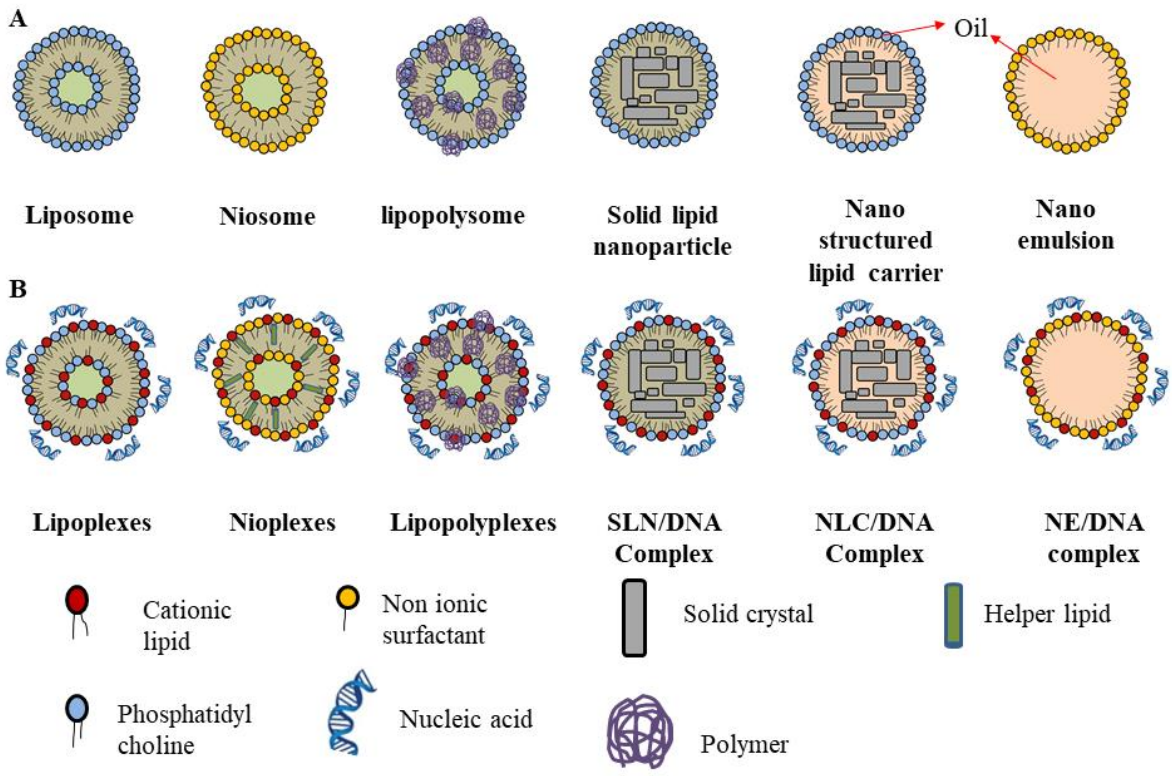

Figure 9. Different vectors (A) and vector/DNA complexes (B) containing cationic lipid.

1.4.Gene delivery barriers

On their way to the target cells *in vivo*, gene delivery systems must circumvent several extracellular and intracellular barriers (portrayed in figure 10). Therefore, the design of innovative optimal non-viral vectors is a great challenge to surpass these hurdles.

1.4.1. Extracellular barriers

Whatever the administration route is (e.g., inhalation, intramuscular injection, gavage, intravascular injection, oral, etc.), gene delivery vector will be inevitably in contact with the extracellular environment. Basically, these extracellular barriers

include lipid bilayer membrane, many blood components and endothelial barriers. Additional extracellular barriers need to be overcome by the vehicle when specific tissues need to be targeted, such as the brain, the eye or the lungs (37). The control of unwanted immune responses is the way to success of gene therapy strategies. Gene vectors are potentially able to trigger immune responses as lymphocytes. Moreover, enzymes such as lipases and nucleases can degrade the nano-formulation and the genetic payload and therefore interfere with transfection efficiency (63). The viral and non-viral vectors have been shown to induce an immune response. However, this activation has been most associated with viral vectors. The injection of cationic lipoplexes in the circulation cause the release of TNFα and IFNγ into the serum as inflammatory response chemokines. This may be as a result of unmethylated CpG motifs on the plasmid DNA and the subsequent recognition by TLRs (64).Extracellular barrier to be overcome strongly depend on the organ to be treated as well as the route of administration.

In the systemic circulation, blood flows to every organ and tissue in the body. Generally, intravenous administration is the most studied route of administration of non-viral gene delivery systems. Once gene vehicles are introduced into the circulation, they are subject to enzymatic degradation, serum proteins inactivation, complement-mediated clearance and reticuloendothelial system recognition (66). Formed blood elements (erythrocytes, leukocytes, and platelets) and serum proteins (albumin, immunoglobulins, and fibronectin) have a negative surface charge which interacts with the net positive charge of non-viral vector/DNA complex leading to aggregation or dissociation of the complex (67).

The delivery of non-viral gene vector to the lung is usually hampered by the pulmonary architecture, the presence of respiratory secretions (mucus and lung surfactant), the clearance mechanisms, and the activation of the immune system. According to the lung disease (e.g., cystic fibrosis, asthma, emphysema and lung cancer), the target cells can vary from epithelial cells, alveolar cells, macrophages, respiratory stem cells or endothelial cells (68). The respiratory secretions bind to the

complexes and sterically obstruct their way to the target cells limiting their diffusions and effectiveness.

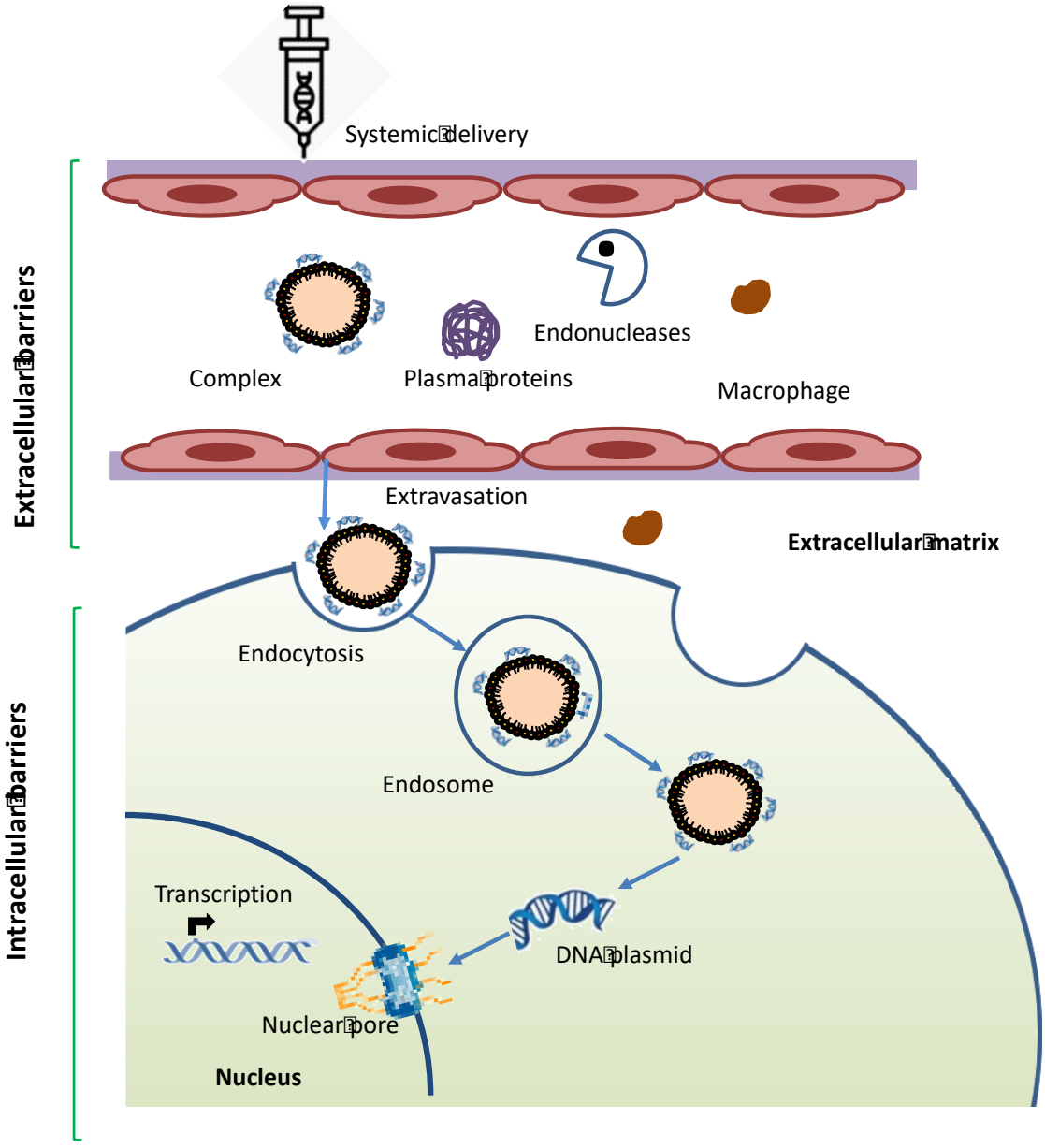

Figure 10. Extracellular and intracellular barriers, adapted from (65)

The blood-brain barrier (BBB) represents a huge obstacle upon systemic delivery of non-viral vector/DNA complexes into the brain. BBB is composed of brain microvascular endothelial cells, pericytes, astrocytes, tight junctions, and basal laminae (69). Many approaches exploit the receptor-mediated uptake of molecules such as transferrin, lactoferrin and insulin to cross the BBB, since receptors of those molecules

are expressed on many cell types, including neurons and the capillary endothelial cells of the BBB. Another approach uses peptidomimetic monoclonal antibodies (known as a molecular Trojan horse) to target specific receptors on the BBB and induce receptor-mediated transcytosis of the non-viral vector into the CNS. Other strategy includes transient mechanical disruption of the BBB and RNAi-mediated knockdown of tight junction proteins (70). Local administration to the brain, either by injection or by infusion is investigated in many pre-clinical studies. Intranasal delivery is another non-invasive means to deliver non-viral gene carriers to the brain, with the ability to pass the BBB and transfect and express the encoded proteins (71).

With regard to the eye, it is a highly compartmentalized and immune-privileged organ that offers interesting advantages as a gene therapy target (72). However, relevant biological barriers such as cornea, sclera, aqueous humor, blood-retinal barriers (BRB), choroidal and conjunctival blood flow, lymphatic clearance, and tear dilution need to be deeply considered. The BRB, which is composed of tight epithelial junctions, limits the delivery of non-viral vector/DNA complexes to the retina via systemic administration. Two strategies were suggested to overcome such BRB, (1) by using vectors smaller than 100 nm, and (2) by the use of ligand-targeted vectors that recognize specific receptors in the BRB (37).

1.4.2. **Intracellular barriers**

Gene delivery systems have to overcome many intracellular barriers extending from cell surface to nuclear entry for successful gene therapy. The non-viral vector/DNA complex enter the cells either by ligand-receptor binding interaction (receptor-mediated endocytosis) or by charge-mediated interactions with proteoglycans on cell membranes. Thus, the vesicles are susceptible to a cascade processes of complex uptake, endolysosomal escape, trafficking to the nucleus, vehicle unpacking and nuclear entry (73).

Being up taken into cells is not the only limiting barrier, however it is one of the most limiting steps affecting non-viral vehicle efficiency. Endocytosis is a vesicle-mediated process that can be mediated by five main endocytic pathways: clathrin-

mediated endocytosis (CME), caveolae-mediated endocytosis (CvME), clathrin-caveolae-independent endocytosis, macropinocytosis and phagocytosis (74).

Lysosomes are membrane-bound intracellular organelles with an acidic pH (4-5). They have an essential role for degradation and recycling of macromolecules delivered by endocytosis, phagocytosis, and autophagy (75). The ability of many non-viral vehicles to deliver nucleic acid efficiently may be attributed to their strong buffering capacity (pH ranges from 5 to 7). Such strong buffering capacity prevents the acidification of endosomes by acting as ‘proton sponges’ (48).

Productive gene transfer requires DNA to eventually cross the nuclear envelope through nuclear pore complexes (NPCs) before initiation of transcription. In the absence of cell division, the intact nuclear envelope impedes the entry of carrier-plasmid complexes (76). Various approaches were used to improve plasmids’ nuclear targeting, such as: complexation of plasmids with peptides, proteins, ligands, polymers, and inclusion of transcription factor-binding sites (77). As well, nuclear localization sequence (NLS) peptides can be directly bound to the DNA in order to promote its transport to the nucleus by the importins (78).

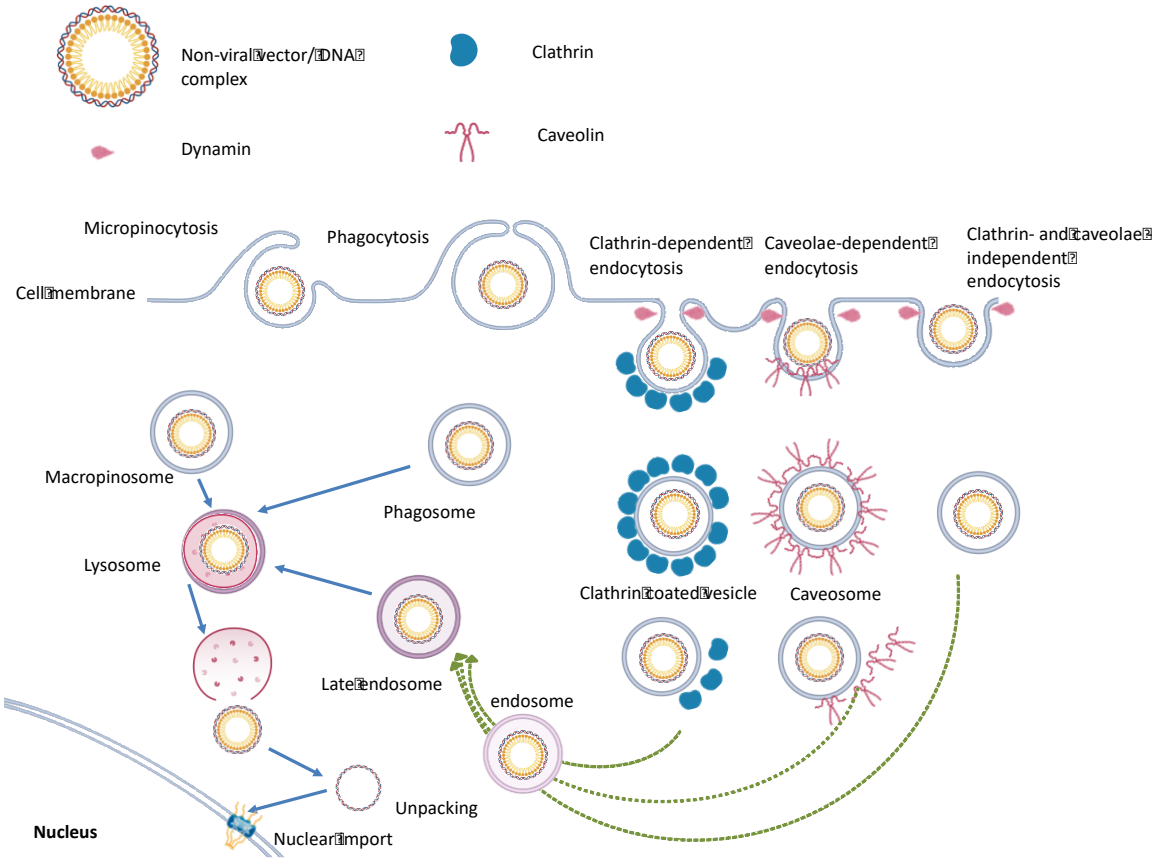

Figure 11. Mechanisms of cellular uptake of non-viral vector/DNA complex.

1.5.Stability of formulations

Chemical non-viral vectors are liquid formulations which upon storage are susceptible to stability problems. In general, nanoparticles are extremely unstable due to their high surface energy and they tend to change themselves or react with substances to reach a relatively stable state. Changes during storage and/or shipping requires preparation of freshly lipid/DNA complexes before every single use. Nevertheless, an acceptable stability is essential for pharmaceutical development and commercialization. Generally, physical stability affects the shelf-life of non-viral vector that is related to many parameters, such as: uniformity of size distribution, PDI, zeta potential, lamellar changes, aggregations and/or fusion (79). The change in such parameters may be considered as a function of pH, temperature, buffer concentration, ionic strength, storage time, etc. (80).

The physical stability study upon storage at different temperature (mainly at 25°C, 4°C, -20°C and -80°C) is one of the basic stability studies. Freezing could alter the membrane structure, and consequently the shape, of Lipofectamine 2000® vesicles and enhance their gene delivery action without compromising cell viability in many cell lines (81). Generally, the changes in physical characteristics by freezing of vesicles can lead to decrease or increase in transfection efficiency. The storage at subzero temperature may be a good substitute for storage at 4°C due to hydrolytic degradation caused by excess bulk water of aqueous formulation leading to less stable formulation on long-term storage. Nonetheless, cryopreservation at -80°C was used for the storage of liposomes, its use for DNA complexes may be unlogic as the addition of cryoprotectants as DMSO and sugars may affect the transfection efficacy and viability of the DNA complexes. In addition, cryopreservation had a damaging effect at the molecular levels specially on the DNA molecules (82).

The biological stability of chemical non-viral vectors refers to the interaction of DNA with different components in the biological system. Better understanding of their interactions is essential to establish specific design criteria. The aggregation of DNA by serum proteins and degradation by DNase enzymes are essential obstacles in the stability of DNA vectors. Interestingly, PEG coating tends to provide the protection of DNA against the serum degradation hazards (83).

1.6.References

1. Wirth T, Parker N, Ylä-Herttuala S. History of gene therapy. Gene. 2013;525(2):162-9.
2. Friedmann T, Roblin R. Gene therapy for human genetic disease? Science. 1972;175(4025):949-55.
3. Kelly Jr TJ, Smith HO. A restriction enzyme from Hemophilus influenzae: II. Base sequence of the recognition site. Journal of molecular biology. 1970;51(2):393-409.
4. Totomoch-Serra A, Marquez MF, Cervantes-Barragán DE. Sanger sequencing as a first-line approach for molecular diagnosis of Andersen-Tawil syndrome. F1000Research. 2017;6.
5. Bartlett JM, Stirling D. A short history of the polymerase chain reaction. PCR protocols: Springer; 2003. p. 3-6.
6. Ginn SL, Amaya AK, Alexander IE, Edelstein M, Abedi MR. Gene therapy clinical trials worldwide to 2017: An update. The journal of gene medicine. 2018;20(5):e3015.

7. Marshall E. Gene therapy death prompts review of adenovirus vector. Science. 1999;286(5448):2244-5.
8. Check E. Second cancer case halts gene-therapy trials. Nature Publishing Group; 2003.
9. Zhang W-W, Li L, Li D, Liu J, Li X, Li W, et al. The first approved gene therapy product for cancer Ad-p53 (Gendicine): 12 years in the clinic. Human gene therapy. 2018;29(2):160-79.
10. Bainbridge JW, Smith AJ, Barker SS, Robbie S, Henderson R, Balaggan K, et al. Effect of gene therapy on visual function in Leber's congenital amaurosis. New England Journal of Medicine. 2008;358(21):2231-9.
11. Ylä-Herttuala S. Endgame: glybera finally recommended for approval as the first gene therapy drug in the European union. Molecular Therapy. 2012;20(10):1831-2.
12. Shahryari A, Saghaeian Jazi M, Mohammadi S, Razavi Nikoo H, Nazari Z, Hosseini ES. Development and Clinical Translation of Gene Therapy for Genetic Disorders. Frontiers in genetics. 2019;10:868.
13. Bright Focus Foundation. Gene therapy for eye disease 2018, Octobar 24 [Available from: https://www.brightfocus.org/macular/article/gene-therapy-eye-disease.
14. Eskilsson E, Røsland GV, Solecki G, Wang Q, Harter PN, Graziani G, et al. EGFR heterogeneity and implications for therapeutic intervention in glioblastoma. Neuro-oncology. 2017;20(6):743-52.
15. Alliance for regenerative medicine. Select Near-Term Clinical Trial Milestones & Data Readouts: 2019+ 2019, March [Available from: https://alliancerm.org/.
16. genomecompiler.
how to choose the perfect vector for your molecular biology experiment 2016, March 21 [Available from: http://www.genomecompiler.com/how-to-choose-the-perfect-vector/.
17. addgene. Plasmids 101: What is a plasmid? 2014, jan 14 [Available from: https://blog.addgene.org/plasmids-101-what-is-a-plasmid.
18. Hardee CL, Arévalo-Soliz LM, Hornstein BD, Zechiedrich L. Advances in non-viral DNA vectors for gene therapy. Genes. 2017;8(2):65.
19. Weiler J, Hunziker J, Hall J. Anti-miRNA oligonucleotides (AMOs): ammunition to target miRNAs implicated in human disease? Gene therapy. 2006;13(6):496.
20. Pang X, Cui C, Wan S, Jiang Y, Zhang L, Xia L, et al. Bioapplications of cell-SELEX-generated aptamers in cancer diagnostics, therapeutics, theranostics and biomarker discovery: a comprehensive review. Cancers. 2018;10(2):47.
21. Ran FA, Hsu PD, Wright J, Agarwala V, Scott DA, Zhang F. Genome engineering using the CRISPR-Cas9 system. Nature protocols. 2013;8(11):2281.
22. Anzalone AV, Randolph PB, Davis JR, Sousa AA, Koblan LW, Levy JM, et al. Search-and-replace genome editing without double-strand breaks or donor DNA. Target. 2019;5(3).
23. Lipocalyx. VIROMER® CRISPR FOR RNP DELIVERY 2019, Octobar, [Available from: https://viromer-transfection.com/crispr.
24. Keeler AM, Elmallah MK, Flotte TR. Gene therapy 2017: progress and future directions. Clinical and translational science. 2017;10(4):242-8.

25. Watts JK, Corey DR. Gene silencing by siRNAs and antisense oligonucleotides in the laboratory and the clinic. The Journal of pathology. 2012;226(2):365.
26. Morrison C. Alnylam prepares to land first RNAi drug approval. Nature Publishing Group; 2018.
27. Robbins PD, Ghivizzani SC. Viral vectors for gene therapy. Pharmacology & therapeutics. 1998;80(1):35-47.
28. Lundstrom K, Boulikas T. Viral and non-viral vectors in gene therapy: technology development and clinical trials. Technology in cancer research & treatment. 2003;2(5):471-85.
29. Lundstrom K. Gene therapy applications of viral vectors. Technology in cancer research & treatment. 2004;3(5):467-77.
30. Puras G, Mashal M, Zárate J, Agirre M, Ojeda E, Grijalvo S, et al. A novel cationic niosome formulation for gene delivery to the retina. Journal of Controlled Release. 2014;174:27-36.
31. Tomanin R, Scarpa M. Why do we need new gene therapy viral vectors? Characteristics, limitations and future perspectives of viral vector transduction. Current gene therapy. 2004;4(4):357-72.
32. Warnock JN, Daigre C, Al-Rubeai M. Introduction to viral vectors. Viral Vectors for Gene Therapy: Springer; 2011. p. 1-25.
33. Escors D, Breckpot K. Lentiviral vectors in gene therapy: their current status and future potential. Archivum immunologiae et therapiae experimentalis. 2010;58(2):107-19.
34. Gardlík R, Pálffy R, Hodosy J, Lukács J, Turna J, Celec P. Vectors and delivery systems in gene therapy. Medical Science Monitor. 2005;11(4):RA110-RA21.
35. Lundstrom K. Viral vectors in gene therapy. diseases. 2018;6(2):42.
36. Lam AP, Dean D. Progress and prospects: nuclear import of nonviral vectors. Gene therapy. 2010;17(4):439.
37. Villate-Beitia I, Puras G, Zarate J, Agirre M, Ojeda E, Pedraz JL. First insights into non-invasive administration routes for non-viral gene therapy. Gene Therapy-Principles and Challenges: IntechOpen; 2015.
38. Du X, Wang J, Zhou Q, Zhang L, Wang S, Zhang Z, et al. Advanced physical techniques for gene delivery based on membrane perforation. Drug delivery. 2018;25(1):1516-25.
39. Pichon C, Billiet L, Midoux P. Chemical vectors for gene delivery: uptake and intracellular trafficking. Current opinion in biotechnology. 2010;21(5):640-5.
40. Loh XJ, Lee T-C, Dou Q, Deen GR. Utilising inorganic nanocarriers for gene delivery. Biomaterials science. 2016;4(1):70-86.
41. Amreddy N, Babu A, Muralidharan R, Munshi A, Ramesh R. Polymeric nanoparticle-mediated gene delivery for lung cancer treatment. Polymeric Gene Delivery Systems: Springer; 2017. p. 233-55.
42. Vasir JK, Labhasetwar V. Polymeric nanoparticles for gene delivery. Expert Opin Drug Deliv. 2006;3(3):325-44.
43. Dufes C, Uchegbu IF, Schätzlein AG. Dendrimers in gene delivery. Advanced drug delivery reviews. 2005;57(15):2177-202.
44. Chaplot SP, Rupenthal ID. Dendrimers for gene delivery–a potential approach for ocular therapy? Journal of Pharmacy and Pharmacology. 2014;66(4):542-56.

45. Raad M, Teunissen EA, Mastrobattista E. Peptide vectors for gene delivery: from single peptides to multifunctional peptide nanocarriers. Nanomedicine (Lond). 2014;9(14):2217-32.
46. Felgner PL, Gadek TR, Holm M, Roman R, Chan HW, Wenz M, et al. Lipofection: a highly efficient, lipid-mediated DNA-transfection procedure. Proceedings of the National Academy of Sciences. 1987;84(21):7413-7.
47. Zhi D, Bai Y, Yang J, Cui S, Zhao Y, Chen H, et al. A review on cationic lipids with different linkers for gene delivery. Advances in colloid and interface science. 2018;253:117-40.
48. Nguyen J, Szoka FC. Nucleic acid delivery: the missing pieces of the puzzle? Accounts of chemical research. 2012;45(7):1153-62.
49. Zhi D, Zhang S, Wang B, Zhao Y, Yang B, Yu S. Transfection efficiency of cationic lipids with different hydrophobic domains in gene delivery. Bioconjugate chemistry. 2010;21(4):563-77.
50. Ramamoorth M, Narvekar A. Non viral vectors in gene therapy-an overview. Journal of clinical and diagnostic research: JCDR. 2015;9(1):GE01.
51. Jones CH, Chen C-K, Ravikrishnan A, Rane S, Pfeifer BA. Overcoming nonviral gene delivery barriers: perspective and future. Molecular pharmaceutics. 2013;10(11):4082-98.
52. Gao X-z, Huang L-b. Cationic liposome-mediated gene transfer. Gene therapy. 1995;2(10):710-22.
53. Ropert C. Liposomes as a gene delivery system. Brazilian journal of medical and biological research. 1999;32(2).
54. MacLachlan I. Liposomal formulations for nucleic acid delivery. Antisense drug technology: principles, strategies, and applications. 2007;2:237-70.
55. Brito LA, Chan M, Shaw CA, Hekele A, Carsillo T, Schaefer M, et al. A cationic nanoemulsion for the delivery of next-generation RNA vaccines. Mol Ther. 2014;22(12):2118-29.
56. Liu CH, Yu SY. Cationic nanoemulsions as non-viral vectors for plasmid DNA delivery. Colloids Surf B Biointerfaces. 2010;79(2):509-15.
57. Naseri N, Valizadeh H, Zakeri-Milani P. Solid lipid nanoparticles and nanostructured lipid carriers: structure, preparation and application. Advanced pharmaceutical bulletin. 2015;5(3):305.
58. Wang H, Liu S, Jia L, Chu F, Zhou Y, He Z, et al. Nanostructured lipid carriers for MicroRNA delivery in tumor gene therapy. Cancer cell international. 2018;18(1):101.
59. Grijalvo S, Puras G, Zárate J, Sainz-Ramos M, Qtaish NA, López T, et al. Cationic Niosomes as Non-Viral Vehicles for Nucleic Acids: Challenges and Opportunities in Gene Delivery. Pharmaceutics. 2019;11(2):50.
60. Ge X, Wei M, He S, Yuan W-E. Advances of non-ionic surfactant vesicles (niosomes) and their application in drug delivery. Pharmaceutics. 2019;11(2):55.
61. Su C-W, Chiang C-S, Li W-M, Hu S-H, Chen S-Y. Multifunctional nanocarriers for simultaneous encapsulation of hydrophobic and hydrophilic drugs in cancer treatment. Nanomedicine. 2014;9(10):1499-515.
62. Bofinger R, Zaw-Thin M, Mitchell NJ, Patrick PS, Stowe C, Gomez-Ramirez A, et al. Development of lipopolyplexes for gene delivery: A comparison of the effects

of differing modes of targeting peptide display on the structure and transfection activities of lipopolyplexes. Journal of Peptide Science. 2018;24(12):e3131.
63. Saffari M, Moghimi HR, Dass CR. Barriers to liposomal gene delivery: from application site to the target. Iranian journal of pharmaceutical research: IJPR. 2016;15(Suppl):3.
64. Gottfried LF, Dean DA. Extracellular and intracellular barriers to non-viral gene transfer. Novel gene therapy approaches: IntechOpen; 2013.
65. Yin H, Kanasty RL, Eltoukhy AA, Vegas AJ, Dorkin JR, Anderson DG. Non-viral vectors for gene-based therapy. Nature Reviews Genetics. 2014;15(8):541.
66. Jones CH, Chen CK, Ravikrishnan A, Rane S, Pfeifer BA. Overcoming nonviral gene delivery barriers: perspective and future. Mol Pharm. 2013;10(11):4082-98.
67. Simoes S, Slepushkin V, Pires P, Gaspar R, Pedroso de Lima MC, Duzgunes N. Human serum albumin enhances DNA transfection by lipoplexes and confers resistance to inhibition by serum. Biochim Biophys Acta. 2000;1463(2):459-69.
68. Sanders N, Rudolph C, Braeckmans K, De Smedt SC, Demeester J. Extracellular barriers in respiratory gene therapy. Adv Drug Deliv Rev. 2009;61(2):115-27.
69. Dong X. Current Strategies for Brain Drug Delivery. Theranostics. 2018;8(6):1481-93.
70. O'Mahony AM, Godinho BM, Cryan JF, O'Driscoll CM. Non-viral nanosystems for gene and small interfering RNA delivery to the central nervous system: formulating the solution. J Pharm Sci. 2013;102(10):3469-84.
71. Harmon BT, Aly AE, Padegimas L, Sesenoglu-Laird O, Cooper MJ, Waszczak BL. Intranasal administration of plasmid DNA nanoparticles yields successful transfection and expression of a reporter protein in rat brain. Gene Ther. 2014;21(5):514-21.
72. Liu MM, Tuo J, Chan CC. Gene therapy for ocular diseases. Br J Ophthalmol. 2011;95(5):604-12.
73. Davis ME. Non-viral gene delivery systems. Curr Opin Biotechnol. 2002;13(2):128-31.
74. Hansen CG, Nichols BJ. Molecular mechanisms of clathrin-independent endocytosis. J Cell Sci. 2009;122(Pt 11):1713-21.
75. Appelqvist H, Petra Wäster, Katarina Kågedal, and Karin Öllinger. . The lysosome: From waste bag to potential therapeutic target. Journal of molecular cell biology. 2013;5(4):214-26.
76. Bai H, Lester GMS, Petishnok LC, Dean DA. Cytoplasmic transport and nuclear import of plasmid DNA. Biosci Rep. 2017;37(6).
77. Lam AP, Dean DA. Progress and prospects: nuclear import of nonviral vectors. Gene Ther. 2010;17(4):439-47.
78. Bremner KH, Seymour LW, Logan A, Read ML. Factors influencing the ability of nuclear localization sequence peptides to enhance nonviral gene delivery. Bioconjug Chem. 2004;15(1):152-61.
79. Armengol X, Estelrich J. Physical stability of different liposome compositions obtained by extrusion method. Journal of microencapsulation. 1995;12(5):525-35.
80. Grit M, Crommelin DJ. Chemical stability of liposomes: implications for their physical stability. Chemistry and physics of lipids. 1993;64(1-3):3-18.

81. Sork H, Nordin JZ, Turunen JJ, Wiklander OP, Bestas B, Zaghloul EM, et al. Lipid-based transfection reagents exhibit cryo-induced increase in transfection efficiency. Molecular Therapy-Nucleic Acids. 2016;5:e290.
82. Lin C, Tsai S. The effect of cryopreservation on DNA damage, gene expression and protein abundance in vertebrate. Italian Journal of Animal Science. 2012;11(1):e21.
83. Zagorovsky K, Chou LY, Chan WC. Controlling DNA-nanoparticle serum interactions. Proc Natl Acad Sci U S A. 2016;113(48):13600-5.

Chapter 2

Objectives

Gene therapy approach aims to treat both inherited and acquired diseases by delivering a therapeutic genetic material or its regulatory elements to target cells. The future of gene therapy depends mainly on the success to design optimal vector. Viral and non-viral vectors have been used as gene delivery carriers. In spite of the fact that viral vectors have the advantage of high gene transfection, the use of viral vectors is limited due to their side effects. Thus, non-viral vectors, have been developed and applied in gene therapy for their advantages, such as its safety, high gene capacity, stability, chemical design flexibility, and low immunogenic response. Therefore, the main objective of this thesis to design novel niosome formulations, containing novel helper lipid, able to deliver genes to eye and brain, safely and effectively.

1. To study the effect of lycopene, as natural helper lipid, in niosome formulation based on cationic lipid (DOTMA) and non-ionic surfactant (polysorbate 60), to boost transfection efficiency in retinal pigment epithelial (RPE-19) cells, without compromising cell viability and using it to transfect rat retina *in vivo*.

2. To investigate the-lycopene containing-niosomes to transfect NT2 cells, primary cortical culture as well as brain cortex of rats, as safe and efficient non-viral vectors to deliver DNA into the CNS to face many neurological disorders.

3. To ensure the role and importance of helper molecule to turn on transfection efficiency. Niosomes formulation was probed with different cationic lipid {2,3-di (tetradecyloxy) propan-1-amine (hydrochloride salt)} and different helper molecule (chloroquine diphosphate) to transfect rat retinal cells. the incorporation of chloroquine within nano formulations, rather than as a co-treatment of the cells, could open a new avenue for in vivo retinal gene delivery.

Chapter 3

Retinal gene delivery enhancement by lycopene incorporation into cationic niosomes based on DOTMA and polysorbate 60

Retinal gene delivery enhancement by lycopene incorporation into cationic niosomes based on DOTMA and polysorbate 60

Mohamed Mashal[a,1], Noha Attia[a,b,1], Gustavo Puras[a,c], Gema Martínez-Navarrete[c,d], Eduardo Fernández[c,d], Jose Luis Pedraz[a,c,]

[a] NanoBioCel Group, Laboratory of Pharmaceutics, School of Pharmacy, University of the Basque Country (UPV/EHU), Paseo de la Universidad 7, 01006 Vitoria-Gasteiz, Spain
[b] Histology and Cell Biology Department, Faculty of Medicine, University of Alexandria, Alexandria, Egypt
[c] Networking Research Centre of Bioengineering, Biomaterials and Nanomedicine (CIBER-BBN), Vitoria-Gasteiz, Spain
[d] Neuroprothesis and Neuroengineering Research Group, Miguel Hernández University, Elche, Spain

Journal of Controlled Release 254 (2017) 55–64

ABSTRACT

The present study aimed to evaluate the incorporation of the natural lipid lycopene into niosome formulations based on cationic lipid DOTMA and polysorbate 60 non-ionic surfactant to analyze the potential application of this novel formulation to deliver genetic material into the rat retina. Both niosomes with and without lycopene were prepared by the reverse phase evaporation method and physicochemically characterized in terms of size, zeta potential, polydispersity index and capacity to condense, release and protect the DNA against enzymatic digestion. In vitro experiments were performed in ARPE-19 cells after complexion of niosomes with pCMS-EGFP plasmid at appropriate cationic lipid/DNA ratios. At 18/1 mass ratio, nioplexes containing lycopene had nanometric size, positive zeta potential, low polydispersity and were able to condense, release and protect DNA. Percentage of transfected cell was around 35% without compromising cell viability. The internalization pathways studies revealed a preference to caveolae mediated endocytosis and macropinocytosis, which could circumvent lysosomal degradation. Both subretinal and intravitreal administrations to the rat retina showed that nioplexes were able to transfect efficiently the outer segments of the retina, which offer reasonable hope for the treatment of many inherited retinal diseases by a safe non-viral vector formulation after the less invasive intravitreal administration.

Keywords: Niosomes, Lycopene, Gene therapy, Retina, Non-viral vectors, Nanotechnology

3.1.Introduction

The abnormal expression or activity of numerous retinal proteins has been linked to the pathogenesis of several blinding retinal disorders with a genetic background, such as Leber congenital amaurosis [1], age-related macular degeneration [2] or retinitis pigmentosa [3]. Unfortunately, most of these devastating conditions do not have effective treatment at the moment. Although novel approaches, such as enzyme/protein replacement and stem cell-based therapies have shown recently promising results, gene therapy is by far the most well-developed field of research for the treatment of both inherited and acquired retinal disorders [4,5]. The unique anatomical and histological features of the eye provide both benefits and challenges for the progress in gene-based ocular therapeutics [6].

In the last decade, many viral and non-viral gene delivery approaches have been developed for the treatment of many retinal pathologies [7,8]. Compared with their counterparts, non-viral vectors have attracted great attention as safer alternative to deliver genetic material, since they can circumvent many safety issues that are still associated with viral gene delivery systems, such as immunogenicity, mutagenicity and oncogenic effects [9]. Consequently, the use of non-viral vectors in clinical trials has increased since 2004, while that of viral vector has decreased significantly [10]. Actually, cationic lipids and cationic polymers are the most commonly used non-viral vectors [10,11]. However, to date, one of the main problems that non-viral formulations have to face, in order to reach the clinical practice, is their limited transfection efficiency. Therefore, research activity on this area merits special attention for the scientific community [12].

As drug delivery system, niosomes have received growing attention by time for being osmotically active and chemically stable formulations [13]. Besides, when it comes to easy handling and low toxicity, they are considered quite advantageous over the well-known liposomes [14].

However, their use as gene delivery systems has been poorly studied, although some recent results have revealed their appealing properties to transfect efficiently brain and retinal cells in rats [15–17].

Niosomes, for gene delivery purposes, are self-assembled vesicular nano carrier systems composed typically by non-ionic surfactant, “helper” and cationic lipids [18]. The non-ionic “electrically neutral” surfactants enhance the stability of niosome formulations [19]. Additionally, cationic lipids form complexes by electrostatic interactions upon the addition of negatively charged genetic material [15,16], and “helper” lipids have a marked influence on both the physicochemical and biological properties of niosome gene carriers [15,17,20].

Recently, it has been reported on the literature the flattering properties of the “helper” lipid squalene (a natural lipid that belongs to the terpenoid family) in cationic niosome gene delivery formulations. Therefore, we decided to investigate the effect that lycopene, another natural lipid, could have on a niosome formulation based on cationic lipid N-[1-(2,3-dioleoyloxy)propyl]-N,N,N-trimethylammonium chlor-ide (DOTMA) and non-ionic surfactant polysorbate 60.

Lycopene is a carotenoid that contains 40 carbon and 56 hydrogen atoms (Fig. 1-C). Classically, it is known to be one of the most potent natural antioxidants that mediate cytoprotective, immunomodulatory and anticancer activities [21].

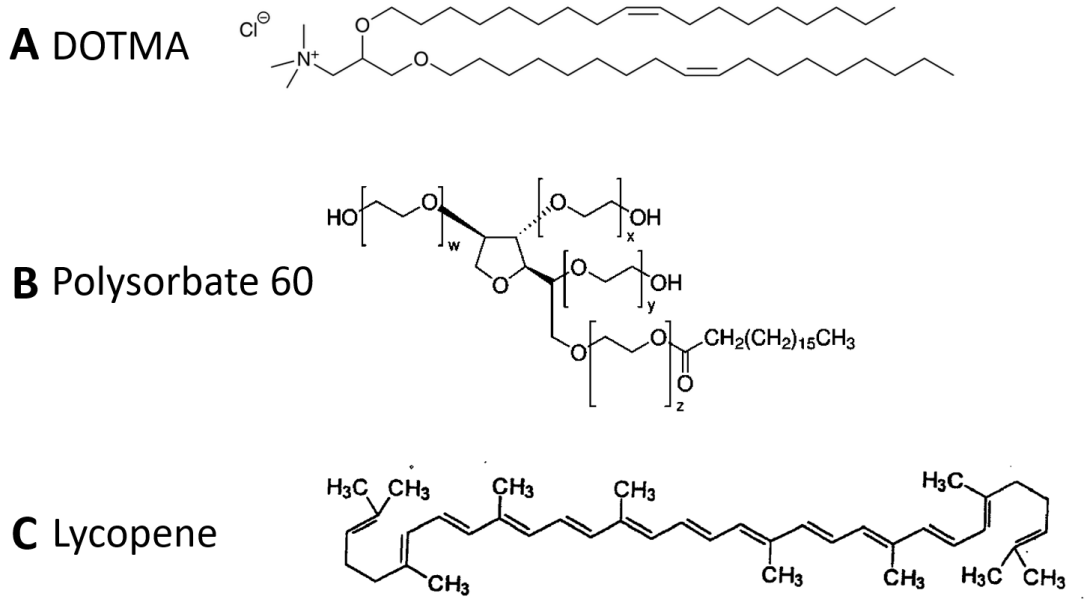

Fig. 1. Chemical structures of the cationic lipid, N-[1-(2,3-dioleoyloxy)propyl]-N,N,N-trimethylammonium chloride (DOTMA) (A), Polysorbate 60 (B), and Lycopene (C).

Additionally, lycopene can be found at high concentration levels in the eye, where it has shown both anti-inflammatory and anti-angiogenic effects [22].

We designed two novel niosome vector formulations for retinal gene delivery purposes based on the same cationic lipid N-[1-(2,3-dioleoy-loxy)propyl]-N,N,N-trimethylammonium chloride (DOTMA) and the same non-ionic surfactant polysorbate 60, in the absence/presence of lycopene (DP60 and DP60L, respectively). Both niosomes were elabo-rated by the solvent emulsification-evaporation technique and com-pared in terms of particle size, polydispersity index (PDI) and zeta potential. Upon the addition of the reported pCMS-EGFP plasmid at different cationic lipid/DNA ratios (w/w), nioplexes were obtained and characterized by size, PDI, morphology, and the ability to condense, release and protect the DNA from enzymatic digestion. In vitro experiments were performed to compare the behavior of both vectors in ARPE-19 cells regarding their cellular uptake, transfection efficiency, viability, and internalization mechanism. Following the in vitro characterization, the most promising formulation was administered to rat eyes via intravitreal and subretinal injection in order to evaluate transfection efficiency by confocal microscopy in both whole-mount and sagittal cross sections of the retina.

3.2.Materials and methods

3.2.1. Production of cationic niosomes

Niosomes were elaborated with slight modifications of the previously described reverse phase evaporation method [23]. Briefly, 5 mg of cationic lipid DOTMA D (Avanti Polar Lipids Inc., Alabama, USA) and 26 mg of polysorbate 60 P60 (0.5%, w/v, Sigma-Aldrich, Madrid, Spain) with/without 1 mg lycopene L (Sigma-Aldrich, Madrid, Spain) were dissolved in 1 ml of organic solvent, dichloromethane (Panreac, Barcelona, Spain). The emulsions were obtained by sonication of such organic phase with 5 ml milliQ water for 30 s at 45 W (Branson Sonifier 250®, Branson Ultrasonics Corporation, Danbury, USA). Dichloro-methane was removed from emulsions by evaporation under magnetic agitation for 2 h leaving the cationic nanoparticles in the aqueous medium. The corresponding molar ratios of both DP60 and DP60L formulations were 1:4 and 1:4:0.4, respectively.

3.2.2. Plasmid propagation and elaboration of nioplexes

pCMS-EGFP plasmid (5541 bp, Plasmid Factory, Bielefeld, Germany), was propagated in Escherichia coli DH5-α and purified using the Qiagen endotoxin-free plasmid purification Maxi-prep kit (Qiagen, California, USA) according to the manufacturer's instructions. The purified plasmid DNA was quantified by measuring absorbance at 260 nm in a NanoDrop® Spectrophotometer (Thermo Fisher Scientific Inc. Denver, USA). The purity of the plasmid was verified by agarose gel electrophoresis (Bio-Rad, Madrid, Spain) in Tris Borate-EDTA buffer, pH 8.0 (TBE buffer). DNA bands were detected using GelRed™ (Bio-Rad, Madrid, Spain) to stain DNA, and images were observed with a ChemiDoc™ MP Imaging System (Bio-Rad, Madrid, Spain). The stock solution of pCMS-EGFP plasmid (0.5 mg/ml) was estimated to be around 0.14 μM.

Both DP60 and DP60L nioplexes (niosome/DNA complexes) were elaborated by mixing an appropriate volume of a stock solution of pCMS-EGFP plasmid (0.5 mg/ml) with different volumes of the niosome suspensions (1 mg cationic lipid/ml) to obtain different cationic lipid/DNA mass ratios (w/w). The mixture was left for 30 min at room temperature to enhance electrostatic interaction between the cationic niosomes and the negatively charged plasmid.

3.2.3. Characterization of niosomes/nioplexes

Particle size and polydispersity index (PDI) were determined by dynamic light scattering (DLS) with Zetasizer Nano ZS (Malvern Instruments, UK). Determination of zeta potential by Laser Doppler
Velocimetry (LDV) was carried out with the same instrument, where samples were dispersed in a 0.1 mM NaCl solution. Particle size, reported as hydrodynamic diameter, was obtained by cumulative analysis. All measurements were carried out in triplicate.

The morphology of both niosomes and nioplexes was assessed by Transmission Electron Microscopy (TEM). Briefly, 5 μl of each sample was adhered onto glow discharged carbon coated grids for 60 s. The remaining liquid was removed by blotting on paper filter. Samples were visualized under TEM, Tecnai G2 20 Twin (FEI, Eindhoven, The Netherlands), operating at an accelerating voltage of 200 keV in a bright-field image mode. Digital images were acquired with an Olympus SIS Morada digital camera.

The capacity of niosomes to condense, release and protect DNA from enzymatic digestion was performed by agarose gel electrophoresis assay. Naked DNA or niosome-complexed DNA samples (200 ng of plasmid/20 μl) were run on a 0.8% w/v agarose gel, stained with GelRed™. The gel was immersed in a Tris–acetate–EDTA buffer and exposed for 30 min to 120 V. Bands were observed under a digital ChemiDoc™ MP Imaging System (Bio-Rad, Madrid, Spain). To analyze the release of DNA from both formulations at different mass ratios, 20 μl of a 2% SDS solution (Sigma-Aldrich, Madrid, Spain) was added to the samples. Protection capacity of nioplexes against enzymatic diges-tion was studied after adding DNase I (Sigma-Aldrich, Madrid, Spain) at a final concentration of 1 U DNase I/2.5 μg DNA. Afterwards, the mixtures were incubated at 37 °C for 30 min. Finally, 2% SDS solution was added to release DNA from nioplexes. The integrity of DNA was determined in comparison to untreated DNA.

3.2.4. Cell culture and in vitro transfection assays

ARPE-19 cells from the American Type Culture Collection (ATCC, CRL-2302™) were seeded in 24-well plates at a density of 9×10^4 cells/ well, with 300 μl of complete medium, formed of D-MEM/F-12 containing 10% fetal bovine serum (Gibco®, California, USA). 24 h later, the medium was removed and cells were washed with serum-free Opti-MEM® solution (Gibco®, California, USA). Then, cells were exposed to nioplexes (1.25 μg DNA), at different cationic lipid/DNA mass ration (w/w), diluted in serum-free Opti-MEM® solution for 4 h at 37 °C. After the incubation time, transfection medium was removed and cells were washed thoroughly with PBS. Next complete medium was added and cells were allowed to grow for further 72 h until

fluorescence microscopy imaging (Nikon TSM) and FACSCalibur flow cytometer analysis (BD Biosciences, USA) to determine transfection efficiency. To analyze cell viability, cells were stained with Propidium Iodide (Sigma-Aldrich, Madrid, Spain) prior to flow cytometry analysis. Experiments with uncomplexed DNA and with Lipofectamine™ 2000 (Invitrogen, California, USA) were considered as negative and positive controls, respectively. As a minimum, 10.000 events were collected and analyzed for each sample. Each formulation was analyzed by triplicate.

3.2.5. Cell uptake and intracellular distribution of nioplexes

To determine cellular uptake of nioplexes, ARPE-19 cells were transfected as mentioned in the previous 3.2.4 section, but in this case, nioplexes were prepared with FITC-labeled plasmid (pCMS-EGFP) (DareBio, Madrid, Spain). After 2, 3 and 4 h of incubation time with the vectors at 37 °C, transfection medium was removed and cells were washed thoroughly with PBS, detached, and analyzed by FACSCalibur flow cytometer (BD Biosciences, USA) using the FL1 channel (Ex/ Em = 490/525 nm). For each sample, 10.000 events were collected and analyzed. Cellular uptake data were expressed as the percentage of FITC-positive cells. Naked DNA was used as a negative control. Each formulation was analyzed by triplicate.

The intracellular distributions of the complexes were visualized by confocal laser scanning microscopy (CLSM; Olympus Fluoview500). Briefly, cells were seeded on coverslips-containing 24-well plates and treated with both nioplexes. After 2 and 4 h of incubation, coverslips were washed several times with PBS, fixed with 3.7% paraformaldehyde (PFA, Sigma-Aldrich, Madrid, Spain) and then mounted on Dapi Fluoromount-G from Southern Biotech (Birmingham, AL, USA).

3.2.6. Intracellular trafficking studies

The endocytosis mechanisms involved in the uptake of both nioplexes were evaluated by colocalization of nioplexes (prepared with FITC-pCMSEGFP) with different fluorescently labeled endocytosis markers, all obtained from Invitrogen (California, USA). To illustrate caveolae raft-mediated or clathrin-mediated endocytosis, we used AlexaFluor® 555-Cholera Toxin (10 μg/ml) and AlexaFluor®

546-Transferrin (50 μg/ml), respectively. Additionally, 0.15 μM AlexaFluor® 594-labeled dextran (anionic, 10,000 MW), were used to analyze macropinocytosis pathway. Briefly, cells at appropriate density were seeded on coverslips-containing 24-well plates and co-incubated with FITC-labeled nioplexes and one of the three aforementioned markers for 4 h. Next, transfection medium was removed and cells were washed twice with PBS, fixed with a 3.7% PFA. Preparations were mounted on Dapi Fluoromount-G and visualized with an Olympus Fluoview 500 confocal microscopy under sequential acquisition to avoid overlap of fluorescent emission spectra. Colocalization was first assessed qualitatively by the occurrence of yellow pixels resulting from the spatial overlap of green (pseudo color of nioplexes) and red pixels (pseudo color of endocytosis marker) from two separate channels. Colocalization between markers and nioplexes from images was then quantified by the Mander's colocalization coefficient (M). NIH Fiji© program was used to analyze images. The tone of each image was adjusted and overlapped to give a merged picture by digital processing. A minimum of three optical sections per sample were analyzed in three independent experiments [24].

3.2.7. Intravitreal and subretinal administrations

All experimental procedures were carried out in accordance with the Spanish and European Union regulations for the use of animals in research and the Association for Research in Vision and Ophthalmology (ARVO) statement for the use of animals in ophthalmic and vision research and supervised by the Miguel Hernandez University Standing Committee for Animal Use in Laboratory.

Nioplexes were injected intravitreally and subretinally in four adult female Sprague–Dawley rats (6–7 weeks old, 200–300 g weight) each. 4 μl of nioplexes suspension (containing 100 ng of plasmid) were injected under an operating microscope (Zeiss OPMI® pico; Carl Zeiss Meditec GmbH, Jena, Germany) with the aid of a Hamilton microsyringe (Hamilton Co., Reno, NV). A bent 33-gauge needle was used to inject into the vitreous of the left eyes, immediately adjacent to the ora serrata without touching the lens. To deliver nioplexes into the subretinal space, the needle was introduced through a sclerotomy (1–2 mm) posterior to ora serrata and in a tangential

direction toward the posterior retinal pole along the subretinal space. Successful administration was confirmed by the appearance of a partial retinal detachment by direct ophthalmoscopy of the eye fundus through the operating microscope. The untreated right eyes served as negative control. Commercially available Lipofectamine™ 2000 was used as positive control.

3.2.8. Analysis of EGFP expression

Three days post-injection, rats were sacrificed and perfused with 0.9% saline followed by 4% PFA in 0.1 M PBS at 4 °C. Native EGFP was analyzed in whole-mount retinal preparations using immunohistochemistry, EGFP protein expression was then evaluated in fresh-frozen retinal sections. Briefly, both eyes were enucleated, and the anterior segments, including the lens, were removed. Posterior eyecups were fixed in PBS containing 4% paraformaldehyde. Samples were then immersed in a graded series of sucrose solutions, 15%, 20% and 30% in PBS overnight at 4 °C for cryoprotection. Eyecups were embedded and oriented in optimal cutting temperature (O.C.T.)™ compound (Tissue-Tek®, Sakura Finetek Europe B.V., Alphen and den Rijn, Netherlands) and frozen in 2-methylbutane cooled in liquid nitrogen at −60 °C. Vertical sections of 16 μm thick were obtained using cut with a cryostat (HM 550; Microm International GmbH, Walldorf, Germany), mounted on SuperFrost® Plus microscope slides (VWR International BVBA, Leuven, Belgium). Prior to immunostaining, the frozen sections were blocked through non-specific staining with 10% normal donkey serum for 1 h with 0.5% Triton X-100 (Sigma-Aldrich, Madrid, Spain), then incubated overnight at 4 °C with combinations of primary antibodies: Chicken anti-GFP (Invitrogen, California, USA), rabbit anti-NeuN (Millipore, MA, USA) and rabbit anti-recoverin (Millipore, MA, USA). Primary antibodies were visualized using Alexa Fluor 488 and Alexa Fluor 555-conjugated secondary antibodies (Invitrogen, California, USA). Cell nuclei were counterstained with Hoechst 33,342 (Sigma-Aldrich, Madrid, Spain), mounted with anti-fading medium and examined by CLSM.

Immunofluorescence and EGFP expression were evaluated using a Leica TCS SPE spectral confocal microscope (Leica Microsystems GmbH, Wetzlar, Germany). Images were processed, montaged and composed digitally using ImageJ (NIH,

Bethesda, MD) and Adobe® Photoshop® CS5.1 software (Adobe Systems Inc., CA, USA).

3.2.9. Statistical analysis

Statistical analysis was completed with the InStat programme (GraphPad Software, San Diego, CA, USA). Differences between groups at significance levels of 95% were calculated by the ANOVA and the Student's t-test. In all cases, P values < 0.05 were regarded as significant. Normal distribution of samples was assessed by the Kolmogorov-Smirnov test and the homogeneity of the variance by the Levene test. Data were presented as mean ± SD, unless stated otherwise.

3.3.Results

3.3.1. Physicochemical characterization of niosomes and nioplexes

Table 1 summarizes the particle size, zeta potential (ZP) and polydispersity index (PDI) of both DP60 and DP60L niosomes. The size of niosomes increased from 66 to 102 nm when lycopene was incorporated into the niosome formulation. Regarding ZP values, the addition of lycopene decreased ZP to 34 mV in DP60L, compared to 45 mV in DP60, while no true difference in PDI vales was observed between both niosomes (0.46 and 0.44 for DP60 and DP60L formulations, respectively).

Table 1

Physical characterization of DP60 and DP60L niosomes regarding particle size (nm); Polydispersity index (PDI), and Zeta potential (mV). Data represent mean ± SD (n = 3).

Particle	Size (nm)	PDI	Zeta potential (mV)
DP60 niosome	66.49 ± 1.17	0.46±0.02	45.30±1.57
DP60L niosome	101.60 ± 2.48	0.44±0.02	33.80±1.13

The physicochemical characterization of both DP60 and DP60L nioplexes at different cationic lipid/DNA mass ratios (w/w) is summarized in Fig. 2. Fig. 2-A depicts size and ZP values of both nioplexes at different ratios (from 6/1 to 22/1). The size of DP60 nioplexes (light bars) varied between 146 nm at 14/1 cationic lipid/DNA mass

ratio to 89 nm at 22/1 mass ratio. Regarding size of nioplexes based on DP60 (dark bars), the highest value was observed at 6/1 mass ratio (154 nm), while the lowest one, was found as well at 22/1 ratio (90 nm). In general, slight modifications on sizes were observed between both DP60 and DP60L based nioplexes at different cationic lipid/DNA ratios. PDI values did not exceed 0.45 in all nioplexes (data not shown). Concerning ZP, readings were clearly higher in DP60 nioplexes, surpassing their DP60L counterpart at all cationic lipid/DNA mass ratios tested. As illustrated in Fig. 2-B, the morphology of both nioplexes, assessed by TEM, exhibited a pattern of discrete imperfectly spherical morphology with no aggregates. Fig. 2-C represents gel retardation assays of both DP60 and DP60L nioplexes prepared at different cationic lipid/DNA ratios (6/1, 12/1, 18/1 and 22/1). Both niosomes were able to complex partially the DNA, since faint SC bands were observed on 4, 7, 10 and 13 wells. However, the DNA bound to both niosomes was released upon the addition of SDS, as can be observed on lanes 5, 8, 11 and 14. Moreover, complexed DNA to both niosome formulations was protected from enzymatic digestion, since clear SC bands were detected on lanes 6, 9, 12 and 15. No SC bands were observed on lanes 3, which suggest that the enzyme worked properly.

3.3.2. In vitro transfection and viability studies in ARPE-19 cells

As can be observed in Fig. 3A, all cationic lipid/DNA mass ratios (w/w) studied above 6/1 clearly depicted higher percentage of transfection with DP60L nioplexes compared to their DP60 counterpart. The percentage of ARPE-19 cells transfected with DP60 nioplexes was in the range of 3–4%. Nonetheless, in the case of DPL60 niosomes, an increase in the percentage of transfected cells proportionally to the cationic lipid/DNA mass ratio was observed. The maximum percentage of transfection with DPL60 niosomes was obtained at cationic lipid/ DNA ratio 18/1 (34.4%), although it was significantly lower ($p < 0.05$) to that obtained with commercial reagent Lipofectamine™2000 (42.6%). Then, the percentage of transfected cells with DP60L niosomes decreased to 28.2% at 22/1 ratio. Meanwhile, naked DNA plasmid did not show any transfection (data not shown). Both vectors did not hamper cell viability that was over 90% at all ratios studied. However, viability in cells transfected with commercial

reagent Lipofectamine™2000 significantly decreased to 82% ($p < 0.05$). The micrographs obtained in (Fig. 3B) demonstrated that transfected ARPE-19 cells maintained a normal morphology with both nioplexes even with high cationic lipid/DNA mass ratios.

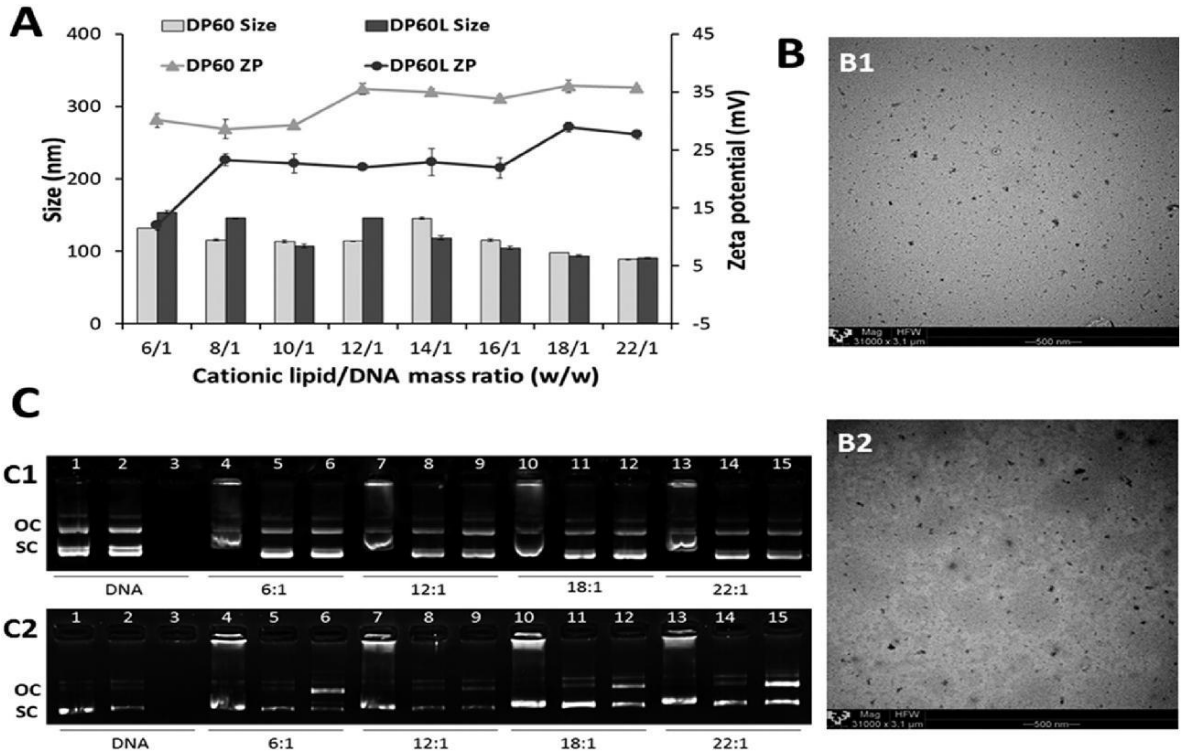

Fig. 2. Physicochemical characterization of nioplexes. A) Effect of cationic lipid/DNA mass ratio (w/w) on both particle size (bars) and zeta potential (lines). Each data point represents the mean ± SD (n = 3). TEM of DP60 (B1) and DP60L nioplexes (B2) at ratio of 18/1 cationic lipid/DNA mass ratio (w/w). Scale bar = 500 nm. Binding, SDS-induced release and protection of DNA at different cationic lipid/DNA mass ratios (w/w) of nioplexes based on both DP60 (C1) and DP60L (C2) visualized by agarose electrophoresis. Lanes 1–3 correspond to uncomplexed DNA; lanes 4–6, cationic lipid/DNA mass ratio 6/1; lanes 7–9, cationic lipid/DNA mass ratio 12/1; lanes 10–12, cationic lipid/DNA mass ratio 18/1; lanes 13–15, cationic lipid/DNA mass ratio 22/1. Nioplexes were treated with SDS (lanes 2, 5, 8, 11 and 14) and DNase I + SDS (lanes 3, 6, 9, 12 and 15). OC: open circular form, SC: supercoiled form.

3.3.3. Cell uptake studies

Nioplexes at cationic lipid/DNA mass ratio of best transfection, 18/ 1, were used to determine uptake percentage in ARPE-19 cells. Fig. 4-A features the percentage of FITC-positive cells quantified by flow cytometry. In general, the uptake percentage increased over time for both formulations. Additionally, DP60 uptake values (50.5%, 62.4%; and 75.5%) were significantly higher ($p < 0.05$) than values of DP60L uptake (5.8%, 11.1% and 23%) at the time points tested, respectively.

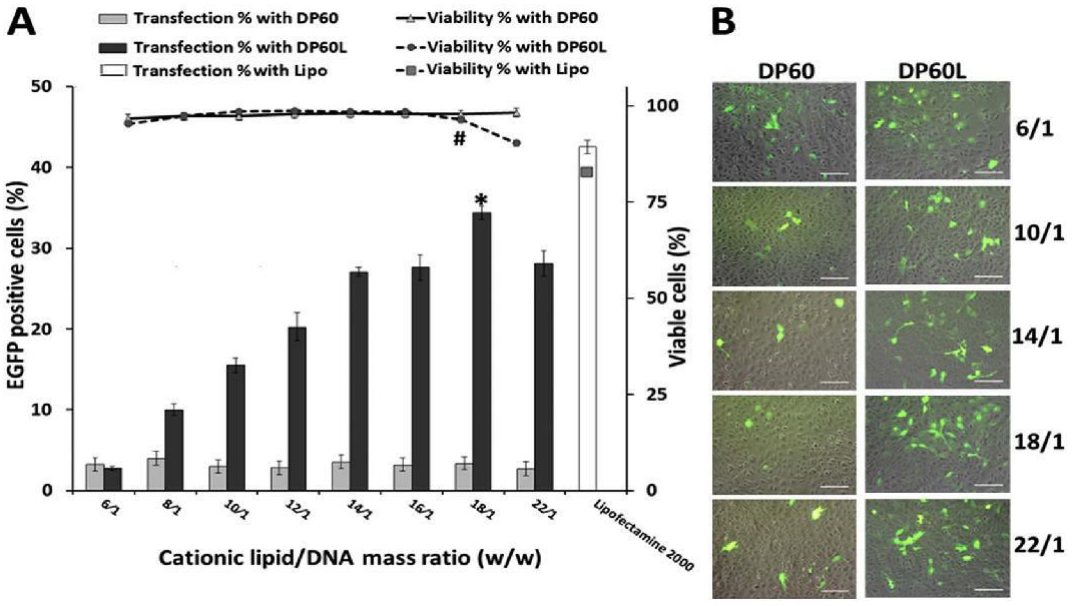

Fig. 3. In vitro transfection efficiency and cell viability in ARPE-19 cells at 72 h post-transfection. (A) Flow cytometry-based evaluation of the percentage of EGFP-positive cells (bars) and percentage of viable cells (lines) at different cationic lipid/DNA mass ratios (w/w). Values represent mean ± SD (n = 3). (*$P < 0.05$ vs. Lipofectamine™2000 transfection). ($^{\#}P < 0.05$ vs. Lipofectamine™2000 viability). (B) Overlay of fluorescence and phase-contrast micrographs of ARPE-19 cells 72 h post-transfection at different cationic lipid/DNA mass ratios (w/w). Scale bar = 100 μm.

Confocal micrographs were obtained after 2 and 4 h of incubation to visualize the progress of complex internalization over time. Fig. 4-B showed that both nioplexes were homogeneously distributed within the cytoplasm 2 h of incubation. However, after 4 h of incubation, cytoplasmic aggregates of DP60 complexes were discerned compared to their DP60L counterparts that maintained their relative homogeneous cytoplasmic distribution.

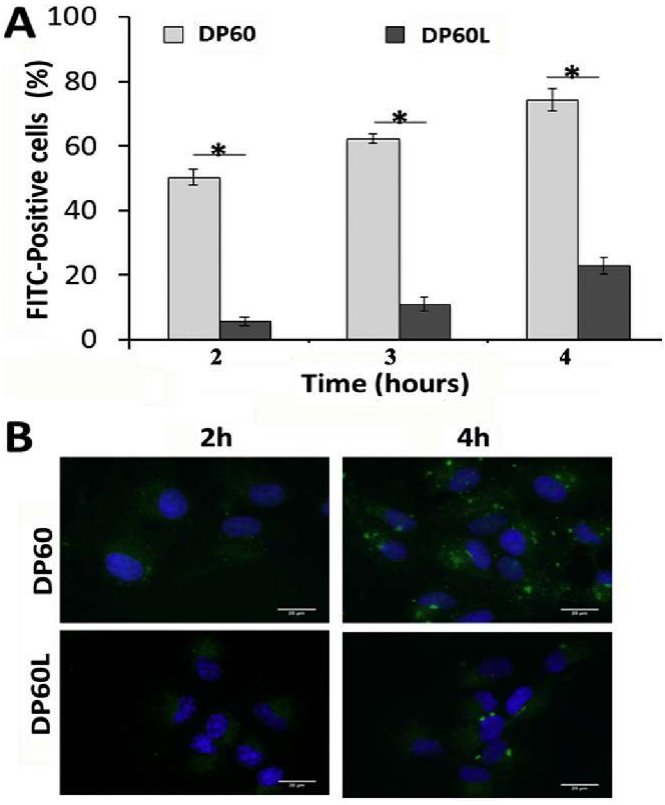

Fig. 4. Uptake of FITC-labeled nioplexes in ARPE-19 cells. Both DP60 and DP60L at a mass ratio of 18/1 (w/w). (A) Percentage of FITC-positive cells. Data represent mean ± SD (n = 3). *p < 0.05. (B) Fluorescence micrographs of ARPE-19 cells at 2 h and 4 h of incubation with FITC-labeled DP60 and DP60L nioplexes (green). Nuclei stained with Dapi (blue). Original magnification 63×. Scale bar = 20 μm. (For inter-pretation of the references to color in this figure legend, the reader is referred to the web version of this article.)

3.3.4. Cell internalization studies

Fig. 5 illustrates that DP60 nioplexes (green) highly co-localized with each one of the three different endocytosis markers used (red), resulting in yellowish signals that were quantified by Mander's overlap coefficient. Values of $M \geq 0.6$ indicated a positive co-localization. However, DP60L complexes, co-localized mainly with cholera toxin ($M = 0.76 \pm 0.04$) and dextran ($M = 0.76 \pm 0.07$) endocytosis markers, whereas no positive co-localization was observed with transferrin ($M = 0.53 \pm 0.03$).

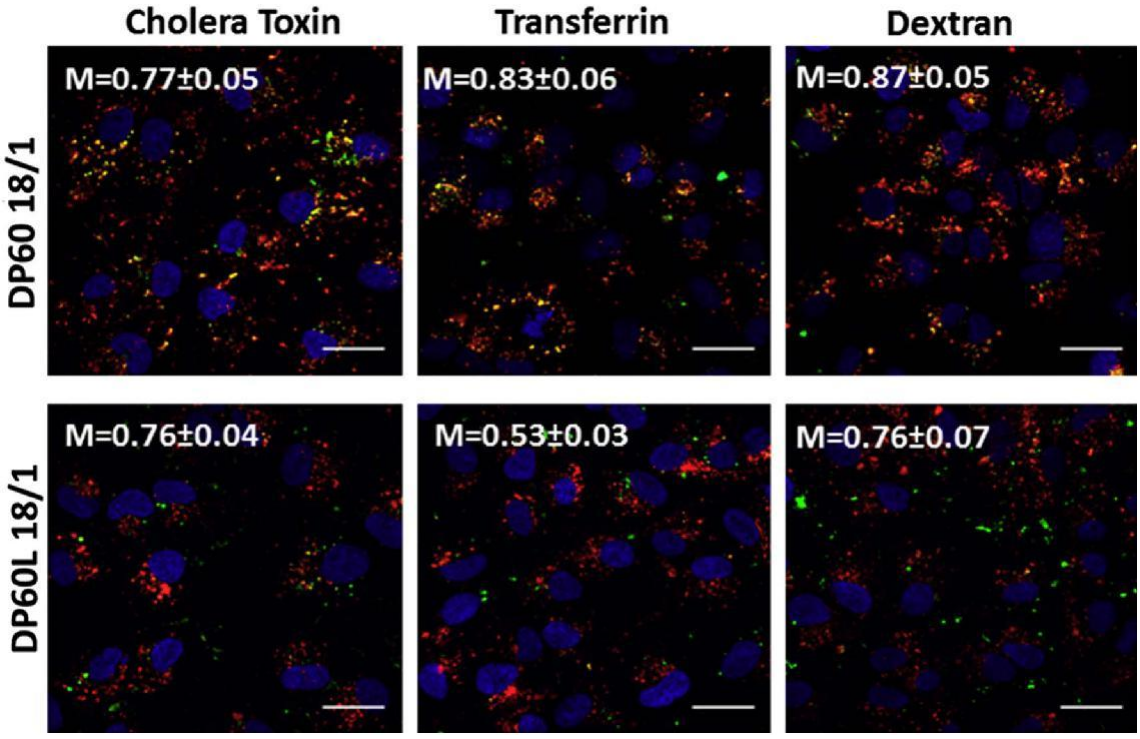

Fig. 5. Three-channel overlay RGB images of ARPE-19 cells showing nioplexes with FITC-labeled pCMS-EGFP (green) and one of the endocytosis markers in red (AlexaFluor® 555-Cholera Toxin, AlexaFluor® 546-Transferrin or AlexaFluor® 594-dextran). Presence of yellow/orange color represents the overlay of an endocytic marker and nioplexes. (M = Mander's overlap coefficient). Original magnification 63×, Scale bar = 25 μm. (For interpretation of the references to color in this figure legend, the reader is referred to the web version of this article.)

3.3.5. Histology and immunofluorescence analysis of EGFP expression in vivo

After 72 h of intravitreal administration of DP60L nioplexes, EGFP expression in the rat retina was analyzed by CLSM (Fig. 6). The analysis of whole-mount preparations (Fig. 6-A, B) revealed native EGFP-expression in some ganglion cells containing NeuN immunoreactivity (red color) as well as in some cells in contact with a typical microglial-like morphology, while no fluorescence was detected in control retina (data not shown). Fig. 7 shows vertical retinal sections where EGFP expression was detected in both ganglion cell layer (GCL) labeled with anti-NeuN (red color), and outer segments (OS) of photoreceptors with anti-Recoverin, a marker of photoreceptors

(red color) after intravitreal (Fig. 7-A, B) and subretinal injection (Fig. 7-C, D), regardless the route of administration. Both positive controls of rat retinae transfected with Lipofectamine™ 2000 and negative controls of non-transfected retinae can be observed in the Supplementary data section (Fig. S1).

3.4.Discussion

Due to its appealing chemical structure, the commercially available cationic lipid DOTMA has been widely used for gene delivery applications [25]. As shown in Fig. 1-A, its structure is composed of a polar head-group, two non-polar hydrophobic chains, a linker and a back-bone, which classically are known as the four domains that rule gene transfection process [26].

We combined DOTMA with the non-ionic surfactant polysorbate 60, in a niosome formulation at a molar ratio of 1:4 respectively, in order to enhance cell tolerance [27] and provide a steric barrier to avoid aggregation [28]. It has been reported on the literature that the presence of PEG chains in the chemical structure of polysorbates (Fig. 1-B) provides physicochemical stability to lipid formulations [29], conserves effectiveness over time and boosts transfection efficiency [30]. Compared with polysorbate 80, another polysorbate that has been widely used in the elaboration of niosome formulations for gene delivery applications, [15–17,31] polysorbate 60 could offer some important advances. For instance, the lack of double bonds in the hydrocarbon chains (Fig. 1-B) could provide low permeability of the vesicles, and therefore better stability of niosome membranes [29]. Additionally, compared with other hydrophilic surfactants such as polysorbates 80, 40 or 20, the low hydrophilic-lipophilic balance (HLB) value of polysorbate 60 (14.9) could help to solubilize lycopene more efficiently [31]. The addition of the natural and non-polar lipid lycopene (Fig. 1-C) into niosome bilaminar membrane could increase its fluidity, disturb membrane packing, and consequently vesicle susceptibility to environmental stresses [32].

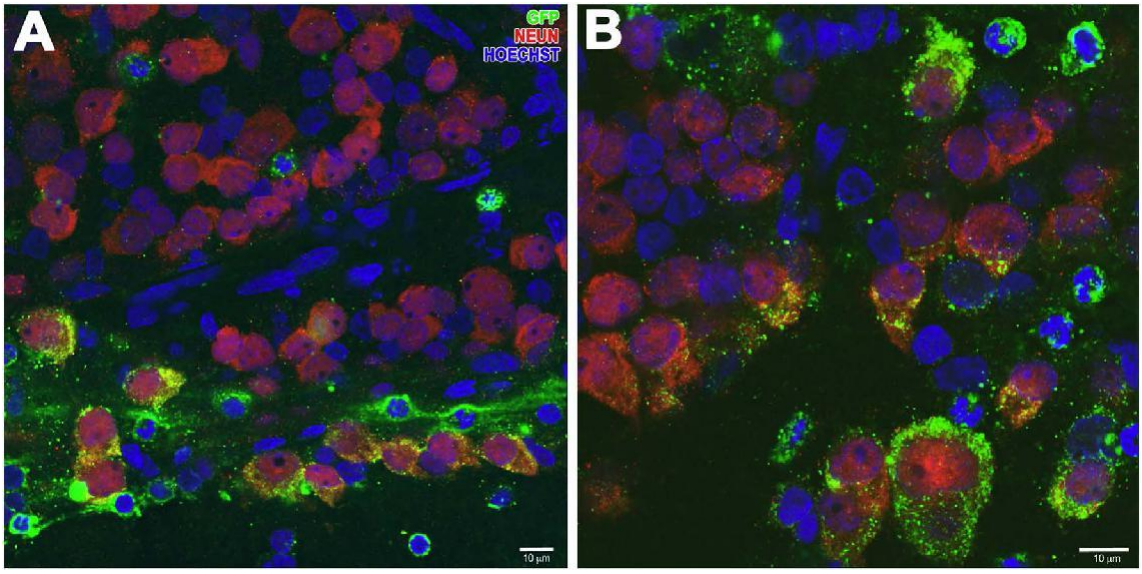

Fig. 6. Immunohistochemical study of EGFP expression in retinal whole-mount preparations 3 days after intravitreal administration of DP60L nioplexes. Partial colocalization of EGFP (green color) with NeuN-positive ganglion cells (red) was observed in the ganglion cell layer (GCL) (red). EGFP expression was observed as well in some cells with typical microglial morphology in GCL (NeuN-negative cells). Nuclei were stained with Hoechst 33342 (blue). Scale bars: 10 µm. (For interpretation of the references to color in this figure legend, the reader is referred to the web version of this article.)

Once elaborated by the reverse phase elaboration method, both DP60 and DP60L niosomes showed appropriate size (in the nanometric scale) and PDI values (below 0.5) for gene delivery purposes (Table 1). High positive ZP values (> +25 mV) ensure long-lasting stability [33], spontaneous electrostatic interaction with DNA, as well as binding of the resulting nioplexes to the negatively charged components of the cell membrane prior to cellular uptake [26].

To elaborate nioplexes, we added pCMS-EGFP reporter plasmid to both niosome formulations at different cationic lipid/DNA mass ratios, since otherwise, the complex assembly process could be slowed down [34]. The slight changes discerned in the size of nioplexes (100–150 nm, Fig. 2-A), at the mass ratios studied, might be due to the delicate balance of different events involved in the multistep self-assembled complex formation, such as: electrostatic interaction, further membrane merging, lipid mixing

and aggregate growth [34]. Regarding the ZP values, the gradual increase of superficial charge along with cationic lipid/DNA ratios (w/w) suggests the capacity of cationic niosomes to bind to and neutralize the negatively charged phosphate groups of DNA [17]. Lycopene addition reduced ZP value of DP60L nioplexes, compared to DP60, at all ratios studied. This fact could be explained by the perturbation of the lipid membrane bilayer, which could dissipate the electrical potential (Fig. 2-A) [35]. In any case, both formulations could function as gene delivery carriers, since the positively charged complexes could interact electrostatically with the anionic cell coat, inducing early steps of the endocytosis process [36]. The high positive ZP value of both DP60 and DP60L nioplexes, especially at 18/1 mass ratio (42 and 27 mV, respectively), could ensure the discrete morphology and absence of aggregates observed by TEM micrographs (Fig. 2-B) [[37].].

Among other factors that can influence on the transfection process, the electrostatic interactions between the negatively charged phosphate groups of the DNA and the positively charged amine groups of the cationic niosomes merits special attention [15–17,38]. We observed by agarose gel electrophoresis assay that at all cationic lipid/DNA ratios tested, both niosomes were able to condense, release and protect the DNA from enzymatic digestion (Fig. 2-C1and C2).

Once we evaluated that our formulations were biotechnologically suitable for gene delivery purposes, we proceeded to evaluate their biological performance in ARPE-19 cells.

ARPE-19 cell line has a normal karyotype and has functional and structural properties similar to retinal pigment epithelia (RPE) in vivo, expresses RPE-specific markers, hence it is considered a suitable transfection model to investigate our vectors' effectiveness and safety before its application in vivo [39]. It has been reported that the non-ionic nature of surfactants makes niosomes well tolerated by cells [40]. Our results in Fig. 3 show higher cell viability values in cells transfected with both nioplexes when compared with cells transfected with Lipofectamine™ 2000. Additionally, we observed under the fluorescence microscope that cells transfected with both nioplexes maintained their normal morphology, even at high cationic lipid/DNA ratios (Fig. 3-

B). Although the percentage of transfected cells with DP60L niosomes at 18/1 mass ratio was significantly lower than that obtained with commercially available Lipofectamine™ 2000, our niosomes formulation was better tolerated by ARPE-19 cells. Therefore, it could be an interesting alternative to Lipofectamine™ 2000, since some authors have reported damage on the retina associated to the in vivo administration of Lipofectamine™ 2000 in the eye [41]. Regarding the transfection efficiency, the lipid composition is considered a primary limiting factor that affects to this process [25]. We clearly observed in Fig. 3 the impact that lycopene had on transfection efficiency in ARPE-19 cells, since values were clearly higher when lycopene was present in the niosome formulation. Although the exact mechanism of lycopene action has not yet been fully elucidated, some authors suggest the existence of a lycopene receptor and/or transporter in the nuclear membrane of cells [42].

Additionally, other study has documented the capacity of lycopene to modulate transcription [43]. Such effect could be either by direct interactions with transcription factors such as nuclear factor-kappa, or by indirect modifications of transcriptional activity. In any case, further research is still needed to determine the exact mechanism [44]. The ascending transfection percentages obtained by DP60L at high mass ratios might be attributed, partially, to the triggering effect of free niosomes absorbed on to the cell membrane. At higher cationic lipid/DNA mass ratios, there is a large excess of cationic lipid to DNA, therefore a population of free niosomes is expected [45]. This free cationic lipid could prolong cellular retention or decreases degradation rate of DNA [25]. Nonetheless, additional experiments are needed to elucidate the detailed mechanisms involved.

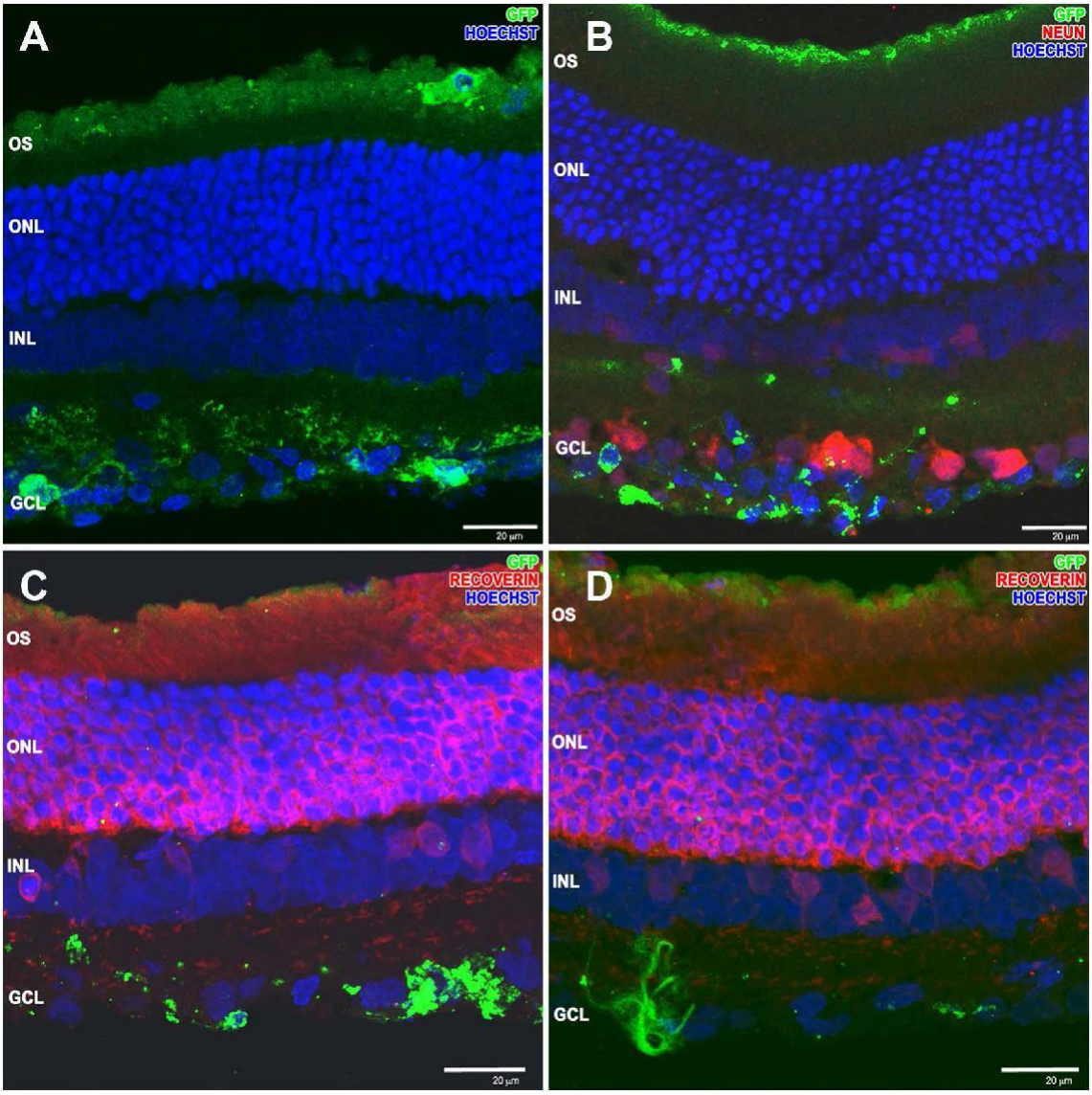

Fig. 7. Confocal fluorescence micrographs of retinal cross-sections after 3 days of intravitreal (A,B) and subretinal (C,D) administration of DP60L nioplexes. After intravitreal injections, EGFP fluorescence was observed in glial cells in the GCL, and in the outer segments of the photoreceptors. Localization of EGFP after subretinal injections was detected as well in OS of photoreceptors (stained with recoverin, in red) and some microglial cells. Cell nuclei were counterstained with Hoechst 33342 (blue). Scale bars: 20 µm. (For interpretation of the references to color in this figure legend, the reader is referred to the web version of this article.)

To determine whether enhanced internalization was among the effects that lycopene incorporation could have in niosome formulations, we studied the percentage of cellular uptake of both DP60 and DP60L formulations at the mass ratio of best transfection efficiency (18/1) in ARPE-19 cells at different times (Fig. 4). Surprisingly, flow cytometry studies showed that lycopene addition clearly reduced the percentage of cellular uptake at all times studies when compared to DP60 formulation (Fig. 4-A). Such reduction in the cellular uptake could probably be due to the lower zeta potential of DP60L formulation compared with DP60 (Fig. 2-A).

Additionally, CLSM studied (Fig. 4-B), excluded mere electrostatic adherence of cationic nioplexes to the negatively charged surface of ARPE-19 cell, since a clear intracellular distribution of both nioplexes was observed in the case of both formulations. In any case, the cytoplasmatic distribution of both nioplexes showed a different behavior. Whereas DP60L nioplexes maintained a homogeneous distribution in the cytoplasm over the time, DP60 nioplexes showed some aggregates at 4 h. The differences observed in the cytoplasmatic distribution of both formulations could suggest different internalization pathways. Therefore, and motivated by the differences observed between both formulation in terms of transfection efficiency and cellular uptake, we next studied the cellular trafficking of both nioplexes at the mass ratio of best transfection efficiency (18/1). Three of the pathways most employed in the uptake processes were assayed; clathrin-mediated endocytosis (CME), caveola-mediated endocytosis (CvME) and macropinocytosis (Fig. 5) [9]. The performance of non-viral vectors is known to be clearly affected by their distinct cellular internalization pathway, taking into account the variable effectiveness of every pathway in the release of DNA into the cytoplasm, which is one of the critical steps in the eventual transgene expression [34]. Although there is not a clear consensus in the scientific community, it is widely accepted that the endolysosomal fate is the hallmark feature of CME [37,46]. In the other hand, CvME and macropinocytosis are widely related to non-acidic and non-digestive routes of cellular uptake [47,48]. Therefore, our results observed in Fig. 5 suggest that internalization of DP60L via these last pathways could be advantageous

over CME internalization, in terms of both DNA delivery and integrity, since it could avoid lysosomal degradation [9].

Once the intracellular trafficking of both DP60 and DP60L nioplexes was studied, next, we performed a preliminary in vivo study to evaluate the transfection efficiency of DP60L vectors in rat retina after both intravitreal (IV) and subretinal (SR) administrations. These routes are considered the most clinically viable options to deliver genetic material to the back of the eye in an effective way. IV injection has been extensively studied thanks mainly to its relative easiness and to the capacity to deliver high doses of genetic material to retinal cells. Additionally, it is less invasive and traumatic than the counterpart SR administration [49]. Typically, after IV injection, the delivered genes are expressed, mainly, in the ganglion cell layer (GCL) of the retina [16]. Among many applications, transfection at this level could be of clinical importance for the treatment of glaucoma, a devastating eye disease that is considered the first cause of blindness worldwide [50]. However, our in vivo data showed not only a good and uniformly distributed EGFP expression at this level (Fig. 6 and Fig. 7-A, B), but also we observed EGFP expression in some of the outer segments (OS) of photoreceptors (Fig. 7-A, B), which suggests a partial diffusion of our DPL60 niosomes through the different layers of the retina. Diffusion of nioplexes could be probably explained by the PEG chains of the polysorbate 60 non-ionic tensioactive which could prevent aggregations with fibrillar structures in the retina. In any case, for further clinical applications, where the volume of the human vitreous is significantly bigger than the volume of the rat vitreous, we should also consider the possible electrostatic interactions between the positively charged niosome based complexes and the negatively charged components of the vitreous such as hyaluronans, proteoglycans, hyalocytes or proteins. These interactions could affect to the final performance of the formulation. To avoid this scenario, positively charged complexes could be coated with negatively charged compounds such us hyaluronic acid, which has been recently reported that can enhance retinal gene delivery after intravitreal injection [51].

Transfection at the outer layers of the retina is highly desirable from a therapeutic point of view, since to date, mutations in over 200 genes expressed in photoreceptors and RPE cells have been associated with many inherited retinal disorder, that until know, do not have curative treatment, such as Retinitis Pigmentosa, Stargardt Disease, Age-related Macular Degeneration, or Leber's Congenital Amaurosis, [16] to name just a few. Although being able to deliver the EGFP gene to the same layers as IV administration (Fig. 7-C,D), SR injection bears the risk of retinal detachment [49]. Therefore, our preliminary in vivo study offers reasonable hope to target the outer retina by the much safer IV instead of SR administration route, which relevant clinical implications.

3.5.Conclusion

This work describes the elaboration and characterization of a novel non-viral formulation based on DOTMA cationic lipid and polysorbate 60 non-ionic surfactant. Interestingly, the incorporation of natural lipid- lycopene- to the formulation clearly increased transfection efficiency in ARPE-19 cells, without affecting cell viability, probably due to the particular endocytosis pathway, where CvME and macro-pinocytosis pathways could avoid DNA degradation in the lysosome. In vivo administrations to the rat retina showed that DP60L niosomes were able to transfect the outer segments of the retina, which offer reason-able hope for the treatment of many inherited retinal diseases by a safe non-viral formulation after IV administration.

3.6.Acknowledgment

This project was partially supported by the University of the Basque Country UPV/EHU (UFI 11/32), by the Research Chair in Retinosis Pigmentosas “Bidons Egara”, the Spanish Ministry of Education (Grant Nos. CTQ2010-20541, CTQ2010-14897), the Basque Government (Department of Education, University and Research, predoctoral BFI-2011-2226 grant), and by Spanish Grant Nos. MAT2012-39290-C02-01, MAT2015-69967-C3-1-R, SAF2013-42347-R, and IPT-2012-0574-300000. Technical and human support provided by SGIker (UPV/ EHU) is gratefully acknowledged. The authors also wish to thank the intellectual and technical assistance

from the ICTS "NANBIOSIS", more specifically by the Drug Formulation Unit (U10) of the CIBER in Bioengineering, Biomaterials, and Nanomedicine (CIBER-BBN) at the University of Basque Country (UPV/EHU).

3.7. Supplementary data

Supplementary data to this article can be found online at http://dx.doi.org/10.1016/j.jconrel.2017.03.386.

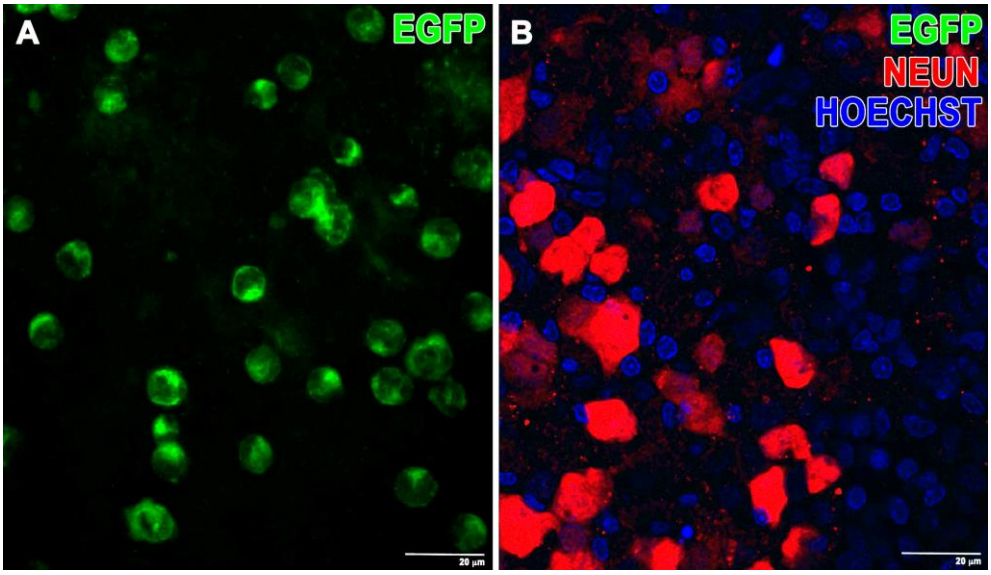

Fig. S1. Confocal imaging of whole mount retinas. A) EGFP expression 3 days after intravitreal injection of lipoplexes based on commercially available lipofectamine. B) Non-transfected retina from a right eye used as negative control. EGFP (green color), NeuN-positive ganglion cells (red color). Nuclei were stained with Hoechst 33342 (blue color). Scale bars: 20 μm.

3.8.References

[1] Q. Zheng, Y. Ren, R. Tzekov, Y. Zhang, B. Chen, J. Hou, C. Zhao, J. Zhu, Y. Zhang, X. Dai, Differential proteomics and functional research following gene therapy in a mouse model of Leber congenital amaurosis, PLoS One 7 (2012) e44855.

[2] S.S. Whitmore, R.F. Mullins, Transcriptome changes in age-related macular degeneration, BMC Med. 10 (2012) 1.

[3] V. Shinde, P. Kotla, C. Strang, M. Gorbatyuk, Unfolded protein response-induced dysregulation of calcium homeostasis promotes retinal degeneration in rat models of autosomal dominant retinitis pigmentosa, Cell Death Dis. 7 (2016) e2085.

[4] A. Koirala, S.M. Conley, M.I. Naash, A review of therapeutic prospects of non-viral gene therapy in the retinal pigment epithelium, Biomaterials 34 (2013) 7158–7167.

[5] S.E. Boye, S.L. Boye, A.S. Lewin, W.W. Hauswirth, A comprehensive review of retinal gene therapy, Mol. Ther. 21 (2013) 509–519.

[6] J. Stein-Streilein, Mechanisms of immune privilege in the posterior eye, Int. Rev. Immunol. 32 (2013) 42–56.

[7] S.L. Ginn, I.E. Alexander, M.L. Edelstein, M.R. Abedi, J. Wixon, Gene therapy clinical trials worldwide to 2012–an update, J. Gene Med. 15 (2013) 65–77.

[8] P.C. Issa, R.E. MacLaren, Non-viral retinal gene therapy: a review, Clin. Exp. Ophthalmol. 40 (2012) 39–47.

[9] S. Xiang, H. Tong, Q. Shi, J.C. Fernandes, T. Jin, K. Dai, X. Zhang, Uptake mechanisms of non-viral gene delivery, J. Control. Release 158 (2012) 371–378.

[10] M. Ramamoorth, A. Narvekar, Non-viral vectors in gene therapy-an overview, J. Clin. Diagn. Res. 9 (2015) GE01–GE06.

[11] M. Morille, C. Passirani, A. Vonarbourg, A. Clavreul, J.-P. Benoit, Progress in developing cationic vectors for non-viral systemic gene therapy against cancer, Biomaterials 29 (2008) 3477–3496.

[12] A.V. Oliveira, A. Marcelo, A.M.R. da Costa, G.A. Silva, Evaluation of cystamine-modified hyaluronic acid/chitosan polyplex as retinal gene vector, Mater. Sci. Eng.C58 (2016) 264–272.

[13] R. Rajera, K. Nagpal, S.K. Singh, D.N. Mishra, Niosomes: a controlled and novel drug delivery system, Biol. Pharm. Bull. 34 (2011) 945–953.

[14] K.M. Kazi, A.S. Mandal, N. Biswas, A. Guha, S. Chatterjee, M. Behera, K. Kuotsu, Niosome: a future of targeted drug delivery systems, J. Adv. Pharm. Technol. Res. 1 (2010) 374–380.

[15] E. Ojeda, G. Puras, M. Agirre, J. Zarate, S. Grijalvo, R. Eritja, L. DiGiacomo, G. Caracciolo, J.-L. Pedraz, The role of helper lipids in the intracellular disposition and transfection efficiency of niosome formulations for gene delivery to retinal pigment epithelial cells, Int. J. Pharm. 503 (2016) 115–126.

[16] G. Puras, G. Martinez-Navarrete, M. Mashal, J. Zarate, M. Agirre, E. Ojeda, S. Grijalvo, R. Eritja, A. Diaz-Tahoces, M. Aviles-Trigueros, E. Fernandez, J.L. Pedraz, Protamine/DNA/niosome ternary non-viral vectors for gene delivery to the retina: the role of protamine, Mol. Pharm. 12 (2015) 3658–3671.

[17] G. Puras, M. Mashal, J. Zarate, M. Agirre, E. Ojeda, S. Grijalvo, R. Eritja, A. Diaz-Tahoces, G. Martinez Navarrete, M. Aviles-Trigueros, E. Fernandez, J.L. Pedraz, A novel cationic niosome formulation for gene delivery to the retina, J. Control.Release 174 (2014) 27–36.

[18] C. Marianecci, L. Di Marzio, F. Rinaldi, C. Celia, D. Paolino, F. Alhaique, S. Esposito, M. Carafa, Niosomes from 80s to present: the state of the art, Adv. Colloid Interf. Sci. 205 (2014) 187–206.

[19] A.S. Dukhin, P.J. Goetz, How non-ionic "electrically neutral" surfactants enhance electrical conductivity and ion stability in non-polar liquids, J. Electroanal. Chem. 588 (2006) 44–50.

[20] M. Ramezani, M. Khoshhamdam, A. Dehshahri, B. Malaekeh-Nikouei, The influence of size, lipid composition and bilayer fluidity of cationic liposomes on the transfection efficiency of nanolipoplexes, Colloids Surf. B: Biointerfaces 72 (2009) 1–5.

[21] G. Krishnamoorthy, K. Selvakumar, P. Venkataraman, P. Elumalai, J. Arunakaran, Lycopene supplementation prevents reactive oxygen species mediated apoptosis in Sertoli cells of adult albino rats exposed to polychlorinated biphenyls, Interdiscip. Toxicol. 6 (2013) 83–92.

[22] P.S. Bernstein, F. Khachik, L.S. Carvalho, G.J. Muir, D.-Y. Zhao, N.B. Katz, Identification and quantitation of carotenoids and their metabolites in the tissues of the human eye, Exp. Eye Res. 72 (2001) 215–223.

[23] F. Szoka, D. Papahadjopoulos, Procedure for preparation of liposomes with large internal aqueous space and high capture by reverse-phase evaporation, Proc. Natl. Acad. Sci. 75 (1978) 4194–4198.

[24] V. Zinchuk, O. Grossenbacher-Zinchuk, Quantitative colocalization analysis of confocal fluorescence microscopy images, Curr. Protoc. Cell Biol. 4.19 (supplement 39) (2008) 4.19-1–4.19-16 (4.16. 11-14.16. 19).

[25] Y.K. Song, D. Liu, Free liposomes enhance the transfection activity of DNA/lipid complexes in vivo by intravenous administration, Biochim. Biophys. Acta 1372 (1998) 141–150.

[26] D.A. Balazs, W. Godbey, Liposomes for use in gene delivery, J. Drug Deliv. 2011 (2010).

[27] A. del Pozo-Rodriguez, D. Delgado, M.A. Solinis, A.R. Gascon, J.L. Pedraz, Solid lipid nanoparticles: formulation factors affecting cell transfection capacity, Int. J. Pharm. 339 (2007) 261–268.

[28] F. Liu, J. Yang, L. Huang, D. Liu, Effect of non-ionic surfactants on the formation of DNA/emulsion complexes and emulsion-mediated gene transfer, Pharm. Res. 13 (1996) 1642–1646.

[29] G. Abdelbary, N. El-Gendy, Niosome-encapsulated gentamicin for ophthalmic controlled delivery, AAPS Pharm. SciTech. 9 (2008) 740–747.

[30] O. Meyer, D. Kirpotin, K. Hong, B. Sternberg, J.W. Park, M.C. Woodle, D. Papahadjopoulos, Cationic liposomes coated with polyethylene glycol as carriers for oligonucleotides, J. Biol. Chem. 273 (1998) 15621–15627.

[31] L.D. Rhein, Surfactants in Personal Care Products and Decorative Cosmetics, third ed., CRC Press, Boca Raton, 2007.

[32] S. Xia, C. Tan, Y. Zhang, S. Abbas, B. Feng, X. Zhang, F. Qin, Modulating effect of lipid bilayer-carotenoid interactions on the property of liposome encapsulation, Colloids Surf. B: Biointerfaces 128 (2015) 172–180.

[33] S. Szunerits, R. Boukherroub, Introduction to Plasmonics: Advances and Applications, CRC Press, 2015.

[34] L. Wasungu, D. Hoekstra, Cationic lipids, lipoplexes and intracellular delivery of genes, J. Control. Release 116 (2006) 255–264.

[35] W.S. Sung, I.S. Lee, D.G. Lee, Damage to the cytoplasmic membrane and cell death caused by lycopene in Candida albicans, J. Microbiol. Biotechnol. 17 (2007)
1797–1804.

[36] F. Sakurai, R. Inoue, Y. Nishino, A. Okuda, O. Matsumoto, T. Taga, F. Yamashita, Y. Takakura, M. Hashida, Effect of DNA/liposome mixing ratio on the physico-chemical characteristics, cellular uptake and intracellular trafficking of plasmid DNA/cationic liposome complexes and subsequent gene expression, J. Control. Release 66 (2000) 255–269.

[37] L.M. Bareford, P.W. Swaan, Endocytic mechanisms for targeted drug delivery, Adv.

[38] E. Ojeda, G. Puras, M. Agirre, J. Zárate, S. Grijalvo, R. Pons, R. Eritja, G. Martinez-Navarrete, C. Soto-Sánchez, E. Fernandez, Niosomes based on synthetic cationic lipids for gene delivery: the influence of polar head-groups on the transfection efficiency in HEK-293, ARPE-19 and MSC-D1 cells, Org. Biomol. Chem. 13 (2015) 1068–1081.

[39] A.V. Kuznetsova, A.M. Kurinov, M.A. Aleksandrova, Cell models to study regulation of cell transformation in pathologies of retinal pigment epithelium, J. Ophthalmol. 2014 (2014) 801787.

[40] K. Aramaki, J. Yamada, Y. Tsukijima, T. Maehara, D. Aburano, Y. Sakanishi, K. Kitao, Formation of bilayer membrane and niosomes by double-tailed poly-glyceryl-type nonionic surfactant, Langmuir 31 (2015) 10664–10671.

[41] S. Kachi, Y. Oshima, N. Esumi, M. Kachi, B. Rogers, D.J. Zack, P.A. Campochiaro, Nonviral ocular gene transfer, Gene Ther. 12 (2005) 843–851.

[42] A. Liu, N. Pajkovic, Y. Pang, D. Zhu, B. Calamini, A.L. Mesecar, R.B. van Breemen, Absorption and subcellular localization of lycopene in human prostate cancer cells, Mol. Cancer Ther. 5 (2006) 2879–2885.

[43] P. Palozza, R.E. Simone, A. Catalano, M.C. Mele, Tomato lycopene and lung cancer prevention: from experimental to human studies, Cancers (Basel) 3 (2011) 2333–2357.

[44] Y. Sharoni, M. Danilenko, N. Dubi, A. Ben-Dor, J. Levy, Carotenoids and transcription, Arch. Biochem. Biophys. 430 (2004) 89–96.

[45] J.G. Smith, T. Wedeking, J.H. Vernachio, H. Way, R.W. Niven, Characterization and in vivo testing of a heterogeneous cationic lipid-DNA formulation, Pharm. Res. 15 (1998) 1356–1363.

[46] A. El-Sayed, H. Harashima, Endocytosis of gene delivery vectors: from clathrin-dependent to lipid raft-mediated endocytosis, Mol. Ther. 21 (2013) 1118–1130.

[47] A. Ferrari, V. Pellegrini, C. Arcangeli, A. Fittipaldi, M. Giacca, F. Beltram, Caveolae-mediated internalization of extracellular HIV-1 tat fusion proteins visualized in real time, Mol. Ther. 8 (2003) 284–294.

[48] S. Xiang, X. Zhang, Cellular Uptake Mechanism of Non-viral Gene Delivery and Means for Improving Transfection Efficiency, INTECH Open Access Publisher, 2013.

[49] K.I. Berns, The Parvoviruses, Springer Science & Business Media, 2013.

[50] M. Almasieh, A.M. Wilson, B. Morquette, J.L. Cueva Vargas, A. Di Polo, The molecular basis of retinal ganglion cell death in glaucoma, Prog. Retin. Eye Res. 31 (2012) 152–181.

[51]T.F. Martens, K. Remaut, H. Deschout, J.F. Engbersen, W.E. Hennink, M.J. van Steenbergen, J. Demeester, S.C. De Smedt, K. Braeckmans, Coating nanocarriers with hyaluronic acid facilitates intravitreal drug delivery for retinal gene therapy, J. Control. Release 202 (2015) 83–92.

Chapter 4

Non-viral vectors based on cationic niosomes as efficient gene delivery vehicles to central nervous system cells into the brain

Non-viral vectors based on cationic niosomes as efficient gene delivery vehicles to central nervous system cells into the brain

Mohamed Mashal[a,1], Noha Attia[a,b,1], Cristina Soto-Sánchez[c,d], Gema Martínez-Navarrete[c,d], Eduardo Fernández[c,d], Gustavo Puras[a,c,*], José Luis Pedraz[a,c,*]

[a] NanoBioCel Group, Laboratory of Pharmaceutics, School of Pharmacy, University of the Basque Country (UPV/EHU), Paseo de la Universidad 7, 01006 Vitoria-Gasteiz, Spain [b] Histology and Cell Biology Department, Faculty of Medicine, University of Alexandria, Alexandria, Egypt [c] Biomedical Research Networking Centre in Bioengineering, Biomaterials and Nanomedicine (CIBER-BBN), Spain [d] Neuroprothesis and Neuroengineering Research Group, Miguel Hernández University, Elche, Spain

Abstract

Development of safe and efficient non-viral vectors to deliver DNA into the CNS represents a huge challenge to face many neurological disorders. We elaborated niosomes based on DOTMA cationic lipid, lycopene "helper" lipid and polysorbate 60 as non-ionic surfactants for gene delivery to the CNS. Niosomes, and their corresponding nioplexes obtained after the addition of the pCMS-EGFP plasmid, were characterized in terms of size, charge, morphology and capacity to condense, release and protect DNA. In vitro experiments were performed in NT2 cells to evaluate transfection efficiency, viability, cellular uptake and intracellular distribution. Additionally, transfection in primary cortex cells were performed prior to brain administration into rat cerebral cortex. Data obtained showed that nioplexes exhibited not only adequate physicochemical properties for gene delivery applications, but also relevant transfection efficiencies (17%), without hampering viability (90%). Interestingly, In vivo experiments depicted promising protein expression in both cortical glial cells and blood vessels.

Keywords: Central nervous system, Gene therapy, Non-viral vectors, Niosomes, Cationic lipids

4.1.Introduction

Gene therapy concept relies on the introduction of genetic material into target cells to modify protein expression for therapeutic purposes (Pezzoli et al., 2012). Over the time has emerged as a promising strategy for the treatment of many diseases. From a practical point of view, the nervous system transfection represents a huge challenge to address many devastating neurological disorders such as Parkinson or Alzheimer diseases (Nobre and Almeida, 2011) that are difficult to treat with traditional pharmacology approaches, mainly due to the brain physical barriers that drugs need to overcome after systemic administration and the complexity of the system (Nagabhushan Kalburgi et al., 2013). However, nowadays, gene therapy clinical trials for neurological disorders are still few in number, mainly due to the lack of safe and suitable approaches to deliver genetic material to targets cells (Yin et al., 2014). Non-viral vectors have received increasing attention thanks to their flattering properties such as; easy elaboration, low cytotoxicity, immune tolerance and lack of oncogenic effects. Additionally, it is possible to use larger DNA inserts (Mansouri et al., 2004; Tang and Szoka, 1997). Therefore, a notable shift of preclinical studies has occurred from viral to non-viral vectors in various applications, including neurological disorders (Peluffo et al., 2015). However, the expression of genes delivered via such vectors is typically low, which justifies the need for further research in this topic. Among non-viral vectors, niosomes have recently emerged as promising gene delivery systems (Attia et al., 2017; Ochoa et al., 2014; Ojeda et al., 2016c; Puras et al. 2014, 2015). Basically, niosomes are non-phospholipid liposome like vesicles, with a bilayer structure (Ojeda et al., 2016a). Compared to liposomes, niosomes are recognized for their low cost and superior chemical and storage stabilities (Rajera et al., 2011). The typical components of a niosome formulation include the cationic lipid, which electrostatically interacts with negatively charged genetic material to form complexes, known as nioplexes (Agirre et al., 2015). The “helper” lipid, which enhances physicochemical properties of the formulation and the intracellular disposition of the complexes (Ojeda et al., 2016b), and the non-ionic surfactants, which increase the stability of the formulation and avoid aggregation between vesicles (Huang et al., 2011). Among cationic lipids, DOTMA has been widely used to elaborate lipid nanoparticles for gene delivery applications, mainly

due to its high aqueous solubility and its appealing chemical structure, which includes a polar head-group, a linker, a backbone and a hydrophobic domain (Rezaee et al., 2016). Lycopene is a natural carotenoid known for its potent antioxidant properties (Krishnamoorthy et al., 2013). Recently, has been used as "helper" lipid to enhance transfection efficiency in retina (Mashal et al., 2017). Polysorbates contain polyethylene glycol (PEG) chains that improve transfection efficiency of liposome formulations (Meyer et al., 1998). Therefore, polysorbates are classically incorporated into niosome for gene delivery applications as non-ionic surfactants.

4.2.Material and methods

4.2.1. Preparation of niosomes and nioplexes

The reverse phase emulsification evaporation technique was used for elaboration of niosomes as previously described (Mashal et al., 2017). Briefly, the cationic lipid DOTMA (0.1% w/v, Avanti Polar Lipids Inc. Alabama, USA), non-ionic surfactant Polysorbate 60 (0.5% w/ v, Sigma Aldrich, Madrid, Spain) and helper lipid Lycopene (0.02% w/ v, Sigma Aldrich Madrid, Spain) were mixed at a molar ratio of 1/4/0.4 and dissolved in 1 ml of the organic solvent dichloromethane (Panreac, Barcelona, Spain). The chemical structure of such components can be observed on Fig. 1. Next, 5 ml miliQ water were added and the emulsion was sonicated for 30 s at 45 W (Branson Sonifier 250, Danbury, USA). After 2 h of magnetic evaporation, the organic phase was removed, leaving DP60L cationic niosomes suspended in the aqueous phase at a 1 mg/ml cationic lipid DOTMA concentration. Nioplexes were formed by mixing a stock solution of pCMS-EGFP plasmid (0.5 mg/ml) with niosome suspension. Under gentle pipetting, different cationic lipid/DNA (w/w) ratios were elaborated. The mixture was left for 30 min at room temperature.

4.2.2. Size and zeta potential measurement

The hydrodynamic diameter and zeta potential of both niosomes and nioplexes, were measured by Dynamic Light Scattering (DLS) and Laser Doppler Velocimetry (LDV) using Zetasizer Nano ZS (Malvern Instrument, UK). Particle size reported as

hydrodynamic diameter was obtained by Z-average. All measurements were carried out in triplicates. Only data that met the quality criteria were included in the study.

4.2.3. Cryo-TEM analysis

The morphology of formulations was revealed by Cryo-TEM analysis and samples were examined by a TEM, TECNAI G2 20 TWIN (FEI), operating at an accelerating voltage of 200 KeV in a bright-field and low-dose image mode (Ojeda et al., 2015). Digital images were acquired with digital camera.

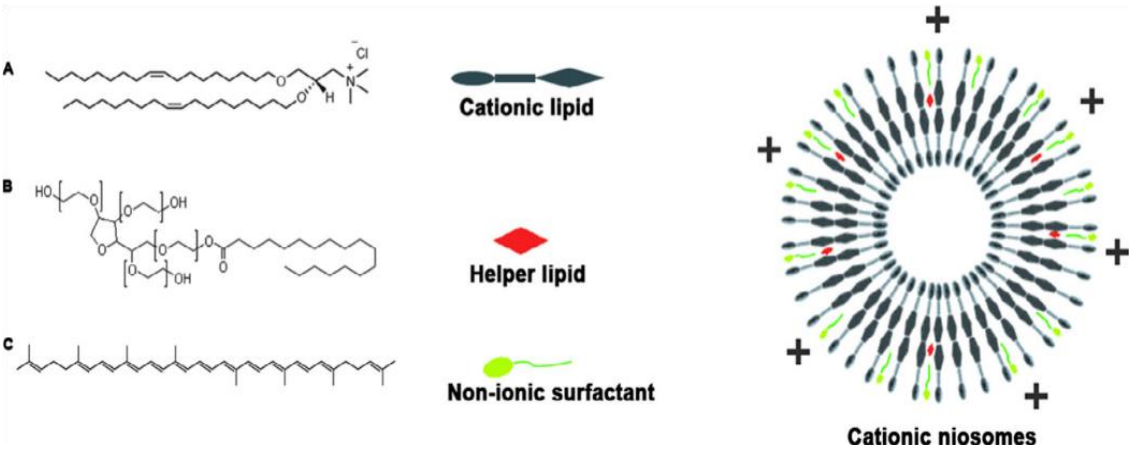

Fig. 1. Chemical composition of DP60L cationic niosomes. (A) Cationic lipid DOTMA-Cl, (B) Polysorbate 60 and (C) Lycopene.

4.2.4. Agarose gel electrophoresis studies

The ability of the niosomes to condense, release and protect plasmid DNA against enzymatic digestion was assayed by agarose gel electrophoresis. Nioplexes were analyzed at different cationic lipid/DNA (w/ w) ratios (200 ng of DNA/well). The agarose gel (0.8%, w/v) was immersed in a Tris-acetate-EDTA buffer and exposed for 30 min to 120 V. DNA bands were stained with GelRed® and observed with a ChemiDoc® MP Imaging System. SDS solution (3%) and DNase I enzyme (1 U DNase I/2.5 µg DNA) were added to the samples to evaluate the release and protection,

respectively. The integrity of DNA in each sample was compared to a control of untreated DNA.

4.2.5. NT2 cell culture and in vitro transfection

NT2 cells (ATCC®−CRL,1973) were cultivated in complete medium, Dulbecco's Modified Eagle's Medium (DMEM), enriched with 10% fetal bovine serum (FBS) and antibiotics (100 U/ml penicillin and 100 μg/ml streptomycin, Gibco®, Life Technologies S.A., Madrid, Spain). Before transfection, NT2 cells were seeded in 24-well plates at an initial density of 8×10^4 cells/well and allowed to grow to 70–80% confluence. Then, the medium was replaced with serum-free Opti-MEM (Gibco®, Life Technologies S.A., Madrid, Spain), and cells were exposed to nioplexes (1.25 μg of pCMS-EGFP/well). After 4 h of incubation, transfection medium was removed and refreshed with complete medium. Cells were allowed to grow for 24 h until being analyzed by flow cytometry (FACSCalibur, BD, San Jose, USA). Positive control (Lipofectamine® 2000, Gibco®, Life Technologies S.A., Madrid, Spain) was prepared following the manufacturer's protocol.

4.2.6. Cellular uptake and intracellular distribution studies

NT2 cells were cultured as previously mentioned. The regular growth media was removed and cells were exposed to nioplexes (prepared with FITC-labeled pCMS-EGFP plasmids, DareBio. Madrid, Spain). After 4 h of incubation, the transfection medium was removed and cells were washed with PBS, trypsinized and analyzed by FACSCalibur flow cytometer. 10.000 events were collected and analyzed for each sample. Each sample was analyzed in triplicate.

To determine the intracellular distribution of internalized nioplexes, cells were seeded on coverslips (24-well plates) and exposed to the nioplexes. The intracellular distribution of nioplexes was analyzed by confocal laser scanning microscopy (CLSM; Olympus Fluoview 500).

4.2.7. Endocytosis mechanism

The endocytosis mechanisms were analyzed by co-localization of nioplexes prepared with FITC-pCMS-EGFP plasmid with different fluorescence-labeled markers. To illustrate caveolae raft-mediated (CvME) or clathrin-mediated endocytosis (CME), AlexaFluor® 555Cholera Toxin (10 μg/ml) and AlexaFluor® 546-Transferrin (50 μg/ml, Thermo Fisher Scientific. Madrid, Spain), were used respectively. Additionally, 0.15 μM AlexaFluor® 594-labeled dextran (anionic, 10,000 MW), was added to stain macropinocytosis (MPC). LysoTracker® Red DND-99 (140 Nm, Thermo Fisher Scientific. Madrid, Spain) was used to determine co-localization with late endosomes. NT2 cells were seeded on coverslips and co-incubated with FITC-labeled nioplexes and one of the four markers for 4 h. Next, the medium was removed and cells were washed with PBS and fixed with a 2% paraformaldehyde (PFA) solution. Samples were mounted on DAPI Fluoromount-G and visualized by an Olympus Fluoview 500 confocal microscopy. Next, the Mander's co-localization coefficient (M), was calculated using the NIH Fiji© program. A minimum of three optical sections per sample were analyzed in three independent experiments (Zinchuk and Grossenbacher-Zinchuk 2011).

4.2.8. Inhibition of uptake by endocytosis inhibitors

In a 24-well plate, NT2 cells were incubated for 30 min with methylβ-cyclodextrin 3 mM, genistein 200 μM, wortmannin 50 nM and for 60 min with chlorpromazine hydrochloride 5 μg/ml (Thermo Fisher Scientific (Madrid, Spain) prior to addition of complexes. The FITC-labeled nioplexes were incubated with cells for 4 h at 37 °C. Then, the transfection medium was removed and cells were washed with PBS, detached from the wells and analyzed by flow cytometer.

4.2.9. pH-buffering capacity

The pH-buffering capacity of DP60L niosomes was evaluated by volumetric analysis. Briefly, aliquots of 100 μL of 0.1 M HCl were added to 10 ml of the niosome solution, and the resulting pH changes were monitored by a pH meter (RISON, GLP 21+, Barcelona, Spain).

4.2.10. Vulnerability assay of nioplexes in the late endosome

Anionic micelles of phosphatidyl serine (PS), considered as an analogue for endosome compartment, were prepared, as described previously (Agirre et al., 2015). PS micelles and nioplexes were incubated at a pCMS-EGFP/PS (w/w) ratio of 1/50 for 1 h. Then, the amount of the released DNA from each complex was determined by agarose gel electrophoresis.

4.2.11. Primary cortical neuron culture

Experimental procedures for in vitro isolation and culture of primary cortex cells were carried out according to the directive 2010/63/EU of the European Parliament and of the Council, and the RD 53/2013 Spanish regulation on the protection of animals use for scientific purposes. Additionally, all procedures were approved by the Miguel Hernandez University Committee for Animal use in Laboratory. Dissociated cultures from primary cortical neurons were obtained from E17-E18 rat embryos (Sprague Dawley) and preserved in HBSS (Gibco®, Life Technologies S.A., Madrid, Spain), during extraction. Then, trypsin was added to the medium and incubated at 37 °C for chemical dissociation. Subsequently, the tissue was dissociated in NB/FBS (Gibco®, Life Technologies S.A., Madrid, Spain), and cell density was determined using a hemocytometer. Cells were seeded on glass coverslips following the same transfection protocol previously described. Then, samples were fixed with PFA (4%), blocked for non-specific staining (10% normal bovine serum (Jackson, West Grove, PA, USA)) and then incubated overnight at 4 °C with rabbit anti-NeuN (Millipore, 1:300) antibody diluted in PBS containing TritonX100 (0.5%). Later, coverslips were washed in PBS and incubated for 1 h with Alexa Fluor 555conjugated donkey anti-rabbit IgG (1:100). Hoechst 33,342 was used to label the nuclei. Finally, coverslips were mounted for imaging and analyzed with a Leica TCS SPE fluorescence microscope.

4.2.12. In vivo studies in rat brains

Adult male Sprague–Dawley rats (6–7 weeks old,) were used as experimental animals. All experimental procedures were carried out in accordance with the Spanish

and European Union regulations for the use of animals in research and supervised by the Miguel Hernandez University Standing Committee for Animal Use in Laboratory. Pretreatment of rats and injection of nioplexes were performed as previously reported (Ojeda et al., 2016c).

4.2.13. Evaluation of EGFP expression in the rat brain

After 72 h of surgery, animals were sacrificed and intracardiac perfusion with PBS followed by PFA (4%) was performed for an initial fixation. Then, rat brains were preserved in PFA (4%) and cryoprotected in sucrose solution (30%) with PBS before slicing. A cryostat (HM 550; Microm International GmbH, Walldorf, Germany) was used to obtain slices of 20 μm from coronal frozen sections adjacent to the injection area. Once the slices were mounted for immunohistochemistry analysis, sections were processed as previously reported (Ojeda et al., 2016c).

4.2.14. Statistical analysis

Statistical differences at significance levels of ≥95% were calculated by ANOVA and Student's t test. In all cases, P values < 0.05 were regarded as significant. Normal distribution of samples was assessed by the Kolmogorov- Smirnov test and the homogeneity of the variance by the Levene test.

4.3.Results

4.3.1. Physicochemical characterization of formulations

Fig. 2 summarizes physicochemical characterization of both niosomes and nioplexes at different cationic lipid/DNA mass ratios (w/w) in terms of particle size, polydispersity index (PDI), zeta potential (ZP), morphology and capacity to condense, release and protect DNA against enzymatic digestion. The size of niosomes was in the nanoscale range, measuring about 100 nm; ZP value was in the positive territory, around +34 mV; and PDI was relatively high, 0.44. All these parameters were affected when DNA was incorporated into the surface of niosomes to obtain corresponding nioplexes at different cationic lipid/DNA (w/w) ratios. Size of nioplexes decreased from 154 nm at 6/1 (w/w)

ratio to 94 nm at 18/1 ratio. Regarding ZP of nioplexes, all readings were in the positive region, but inferior than that observed in the niosomes.

A

	Size (nm)	PDI	Zeta potential (mV)
Niosomes	101.6 ± 2.5	0.44	33.8 ± 1.1
Nioplexes			
6/1	154.3 ± 1.3	0.40	12.0 ± 0.8
10/1	107.8 ± 0.7	0.29	22.7 ± 1.6
14/1	118.7 ± 2.6	0.35	22.9 ± 2.3
18/1	94.03 ± 1.2	0.31	27.1 ± 3.1

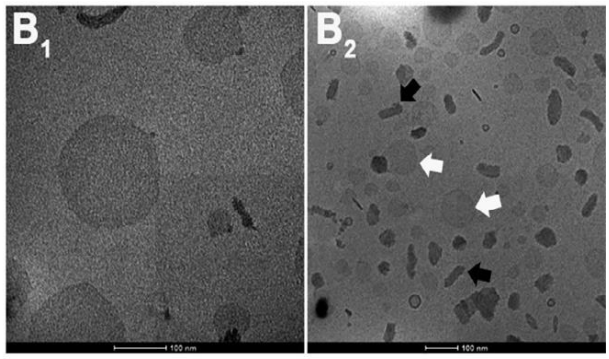

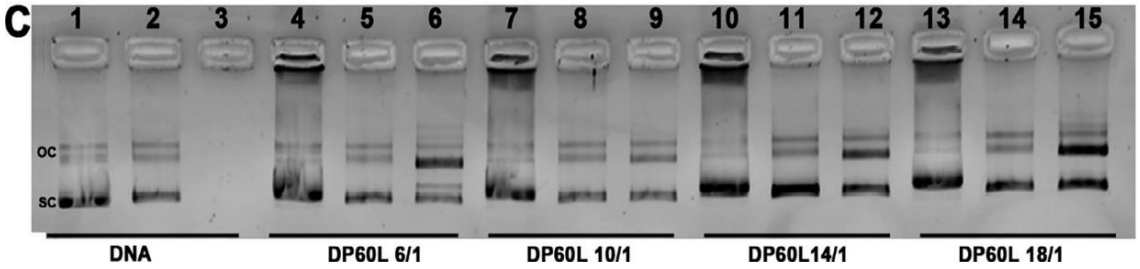

Fig. 2. Physicochemical characterization of DP60L niosomes and nioplexes. A) particle size (nm); polydispersity index (PDI); and Zeta potential (mV). Data represent mean ± SD (n = 3). CryoTEM micrographs of DP60L niosomes (B_1) and nioplexes at 14/1 cationic lipid/DNA mass ratio (w/w) (B_2). Scale bars 100 nm. C) DNA binding, SDS-induced release and protection at different cationic lipid/DNA mass ratios (w/w) of DP60L nioplexes. Lanes 1–3 correspond to uncomplexed DNA; lanes 4–6, cationic lipid/DNA mass ratio 6/1; lanes 7–9, cationic lipid/DNA mass ratio 10/1; lanes 10–12, cationic lipid/DNA mass ratio 14/1; lanes 13–15, cationic lipid/ DNA mass ratio 18/1. Lanes 2, 5, 8, 11 and 14 depict nioplexes treated with SDS, while lanes 3, 6, 9, 12 and 15 demonstrate DNase I + SDS-treated nioplexes. OC: open circular form, SC: supercoiled form.

Moreover, the positive charge gradually increased with the increase in the cationic lipid/DNA (w/w) ratio, from 12 mV at 6/1 ratio to 27.1 mV at 18/1 ratio, a value very similar to that found in the niosome formulation. Regarding PDI, the lowest value was observed at 10/1 cationic lipid/DNA (w/w) ratio, 0.29. When assessed by Cryo-TEM, niosomes adopted a discrete spherical morphology (Fig. 2-B_1), whereas the morphology of DP60L nioplexes at 14/1(w/w) ratio, showed heterogeneous construction, with various shapes, mostly elongated (Fig. 2-B_2, black arrows). In the same field, many uncomplexed niosomes appeared as electron lucent spheres with variable size (Fig. 2-B_2, white arrows).Agarose gel electrophoresis assays revealed a partial binding of DNA

to niosomes (lanes 4, 7, 10 and 13) which corresponded to 6/1, 10/1, 14/ 1 and 18/1 cationic lipid/DNA (w/w) ratios, respectively. Upon the addition of the tensioactive agent, SDS, the condensed DNA was completely released from all nioplexes, since no bands were observed on wells 5, 8, 11 and 14 (6/1, 10/1, 14/1 and 18/1 ratios, respectively). SC (supercoiled bands) bands on lanes 6, 9, 12 and 15 showed that released plasmid DNA was protected from enzymatic digestion at 6/1, 10/1, 14/1 and 18/1 cationic lipid/DNA(w/w), respectively.

4.3.2. Transfection efficiency and cell viability studies in NT2 cells.

Quantitative expression of EGFP and viability in NT2 cells were determined 24 h post-transfection by flow cytometer (Fig. 3). As the cationic lipid/DNA mass ratios increased, the percentages of transfected cells (bars) gradually increased from 2% at 6/1 mass ratio to a peak of 17% at 14/1 mass ratio (45% of transfection normalized to Lipofectamine® 2000). Then, the number of transfected cells gradually decreased at higher mass ratios, 18/1. NT2 cells were not transfected when free "uncomplexed" DNA was used. Regarding cell viability, it decreased gradually from 98% at 6/1 mass ratio to a minimum of 88% at 18/1 mass ratio. In any case, cell viability at all cationic lipid/DNA mass ratios was higher than viability of Lipofectamine® 2000 (83%).

4.3.3. Cellular uptake and intracellular distribution studies

The percentage of FITC-positive NT2 cells was quantified in Fig. 4. DP60L nioplexes at 14/1 cationic lipid /DNA (w/w) mass was about 60%, while the uptake of the positive control Lipofectamine® 2000 was around 85%. Control cells and naked DNA did not induce any notable uptake (Fig. 4-A, and B). In Fig. 4-C, it can be observed that FITC-labeled DP60L nioplexes were distributed within the cytoplasm, close to the nucleus of most cells in the field (white arrows).

4.3.4. Internalization studies

Internalization studies of FITC-labelled DP60L/DNA nioplexes (green) at 14/1 cationic lipid/DNA mass ratio (w/w) are represented in Fig. 5.

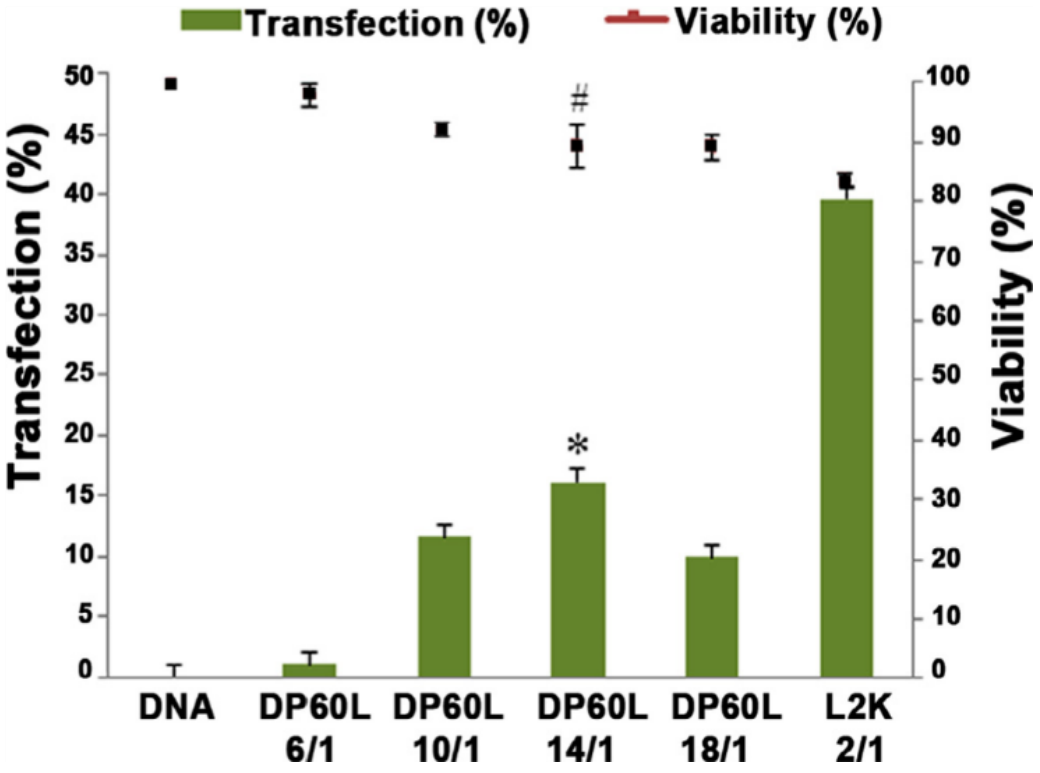

Fig. 3. In vitro transfection studies. Flow cytometry analysis of transfection efficiency and cell viability in NT2 cells at 24 h. Percentage of EGFP-positive cells (bars) and percentage of viable cells (line) at different cationic lipid/DNA mass ratios (w/w). Values represent mean ± SD. (n = 3). (L2K = Lipofectamine®™2000) ($^{*}P < 0.05$ vs. L2K transfection). ($^{\#}P < 0.05$ vs. L2K viability).

After 4 h of nioplexes incubation with corresponding specific markers (red) of CvME (AlexaFluor 555-Cholera Toxin, Fig. 5-A_1), CME (AlexaFluor 546-Transferrin, Fig. 5-A_2), MPC (AlexaFluor 594-Dextran, Fig. 5-A_3), and late endosome/lysosome (LysoTracker Red DND-99, Fig. 5-A_4), Mandeŕs M_1 colocalization coefficients were 0.86, 0.72, 0,69 and 0.60, respectively. As seen in Fig. 5-B, the inhibition of either CvME (by genistein) or CME (by chlorpromazine hydrochloride) uptake pathway had notable effects on cellular uptake of nioplexes, since cellular uptake decreased to around 45 and 30%, respectively. A similar value to that obtained when both previously

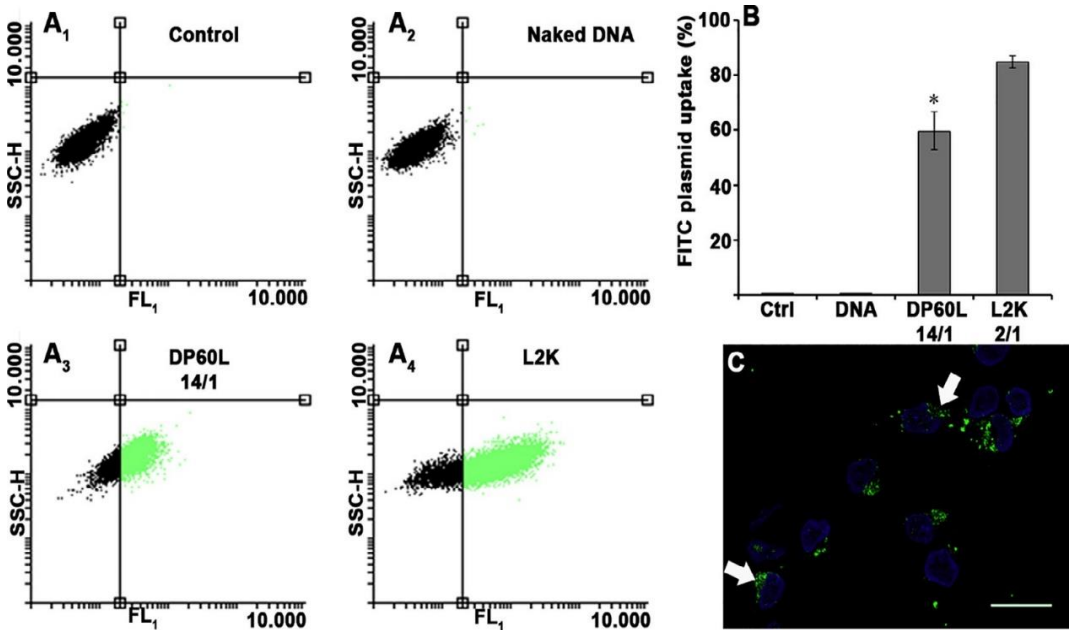

Fig. 4. Cellular uptake studies in NT2 cells 4 h post incubation. (A) Flow cytometry dot-plots (SSC-H and FL_1) of control cells without treatment (A_1), naked DNA (A_2), DP60L nioplexes at 14/1 (w/w) ratio (A_3), and lipofectamine 2000® (L2K) at 2/1(w/w) ratio (A_4). (B) Flow cytometry measurement of NT2 cells treated with FITC-labeled formulations. Error bars represent SD (n = 3). $^{*}p < 0.05$. (C) Fluorescence microscopy images of NT2 cells after 4 h of incubation with FITC-labeled DP60L nioplexes at 14/1 (w/w) ratio. Cells were stained with DAPI-fluoromount G (blue). White arrows indicate nanoparticles around the nucleus. (Scale bar =25 μm). (For interpretation of the references to colour in this figure legend, the reader is referred to the web version of this article.)

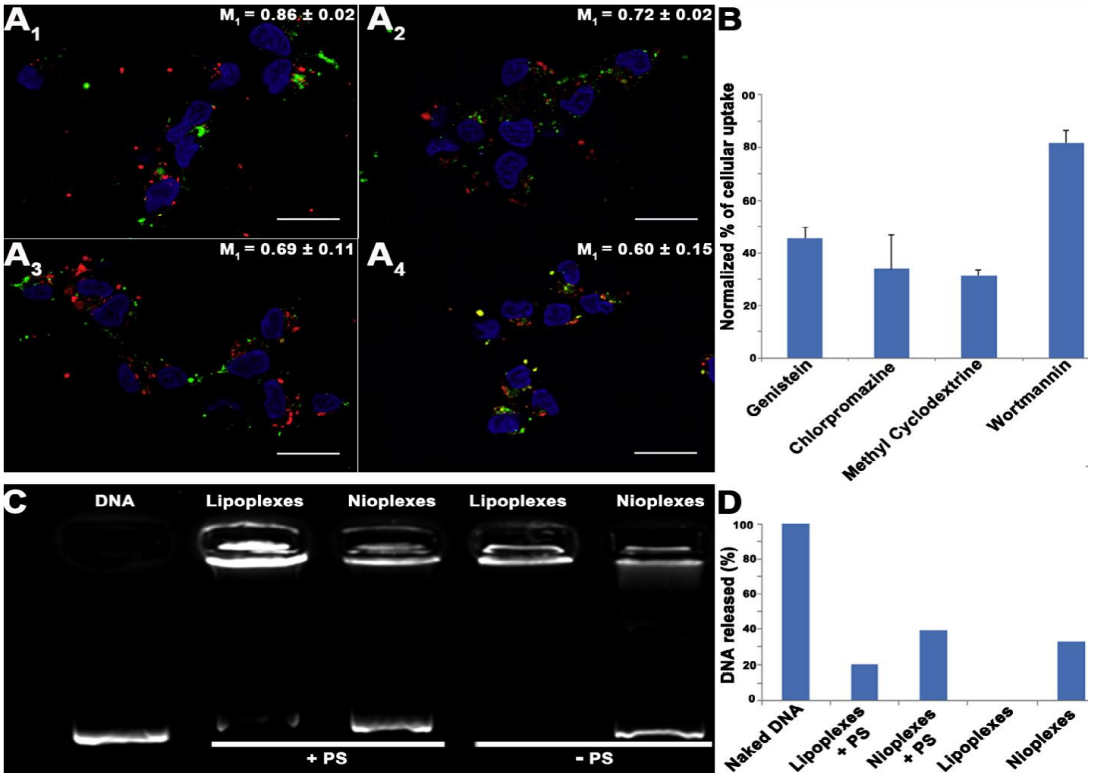

Fig. 5. Internalization studies. (A) Confocal microscopy images showing intracellular distribution in NT2 cells of nioplexes at 14/1 ratio labelled with FITC-pCMS EGFP (green) plasmid and AlexaFluor 555-Cholera Toxin (A1), AlexaFluor 546-Transferrin (A2), AlexaFluor 594-Dextran (A3), and LysoTracker Red DND-99 markers (A4), all in red. (M1 = Mandeŕs overlap coefficient). Scale bars =25 μm. (B) Effect of endocytic inhibitors on the cellular uptake of FITC-labeled nioplexes. Data were normalized to uptake without inhibitor. (C) Agarose gel electrophoresis DNA released profiles of lipoplexes and nioplexes incubated with or without PS. (D) Quantification of released DNA in agarose gel electrophoresis.

mentioned endocytosis mechanisms were simultaneously inhibited by prior treatment with methyl cyclodextrin (28%). However, MPC inhibition by wortmannin, as an inhibitor of MPC, had less effect on cellular uptake reduction, since uptake values where higher, around 80%. The capacity of DNA compacted with both DP60L niosomes and lipofectamine® 2000 to escape from the late endosome, simulated by PS micelles (167 nm, and −65 mV), was analyzed by agarose gel electrophoresis assay (Fig. 5-C). As noticed in Fig. 5-D, in the presence of PS micelles, the amount of DNA released from lipoplexes was around 20%, while in the case of nioplexes, approximately, double amount of DNA, 40%, was released. Without the previous incubation with the anionic PS micelles, the released DNA was almost 0% in the case

of lipoplexes, and about 30% with DP60L nioplexes. Additionally, the pH titration curve (Supplementary data, Fig. 1) provided evidence of the buffering capacity of DP60L formulation, since pH value, slightly decreased from 4.1 to 1.7, after the addition of 1.400 µL of HCl 0.1 M.

4.1.1. Primary cortical neuron and in vivo gene expression studies

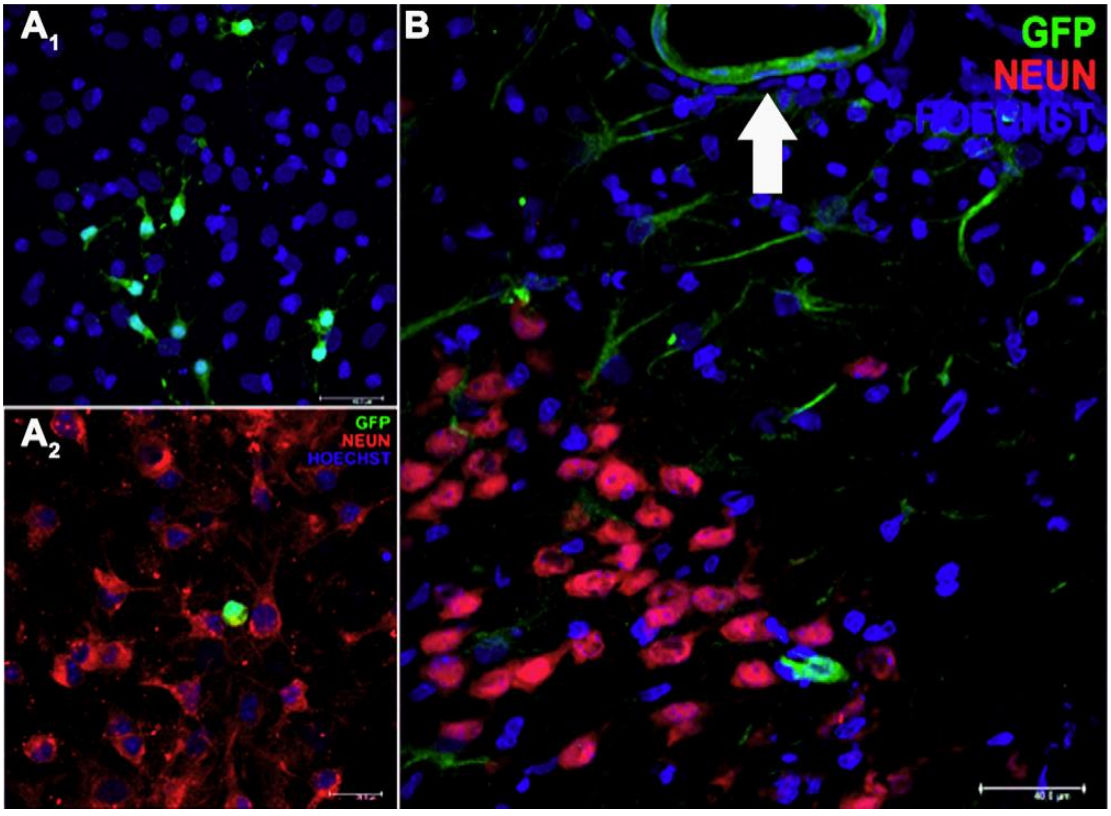

Fig. 6. Primary cortical culture and in vivo gene expression of EGFP carried by DP60 nioplexes at 14/1 mass ratio (w/w). A_1 and A_2, transfection of primary neuronal cell cultures 24 h post transfection. NeuN-positive neurons (red) and nuclei counterstained with Hoechst 33342 (blue) (Scale bars =20 and 40 µm, respectively). B, in vivo gene expression of pCMS-EGFP 72 h after intracortical administration of nioplexes. Nuclei are shown in blue (Hoechst), neurons in red ($NeuN^+$), and EGFP expression (GFP^+) in green. White arrow points a blood vessel. Scale bar 40 µm. (For interpretation of the references to colour in this figure legend, the reader is referred to the web version of this article.)

EGFP-expressing neural cell morphology were discerned on primary cortical cultures transfected with DP60L nioplexes at 14/1 mass ratio (w/w) in Fig. 6-A1. However, none of them were NeuN+ (Fig. 6-A2). 72 h after mice intracranial injection of nioplexes, immunochemistry of the cryopreserved sections showed NeuN− (non-neuronal) cells with glial morphology, expressing EGFP throughout dendritic processes. Interestingly, cells in the wall of some vessels were EGFP+ as well.

4.4.Discussion

Gene therapy directed to the CNS represents a great challenge to bring normal gene copies and correct mutant gene deficiencies in many neurodegenerative diseases (Maguire et al., 2014). However, in order to apply this promising technology into the regular clinic practice, safe and efficient gene carrier systems are needed. Compared with viral vector, non-viral vectors have several important advantages. For instance, they are easier and cheaper to produce, and there is no preexisting immunity to these vectors. Additionally, they are not derived from pathogens, and consequently show less safety concerns. However, their transfection efficiency is lower than their virus-based counterparts. Therefore, research on this topic merits special attention.

Based on the flattering properties showed recently by niosomes to transfect retinal cells after both intravitreal and subretinal administration (Mashal et al., 2017; Puras et al., 2014; Ochoa et al., 2014), we elaborated cationic niosomes based on DOTMA, polysorbate 60 and lycopene to deliver DNA into the brain cortex of rats after cerebral cortex administration. DOTMA is a highly water-soluble quaternary ammonium salt lipid that has been extensively used for gene delivery purposes, due to its ability to condense DNA (Zhang et al., 2012). Lycopene is a natural carotenoid that when used as “helper” lipid, enhances transfection efficiency in retinal cells (Mashal et al., 2017). Polysorbate 60 is the major component of the niosome formulation, and its poly(ethylene glycol) structure has been reported that increases in vivo transfection efficiency in CNS (Tang et al., 2003; Yao et al., 2012).

Prior to perform any biological study, we characterized in Fig. 2 our formulation in terms of size, superficial charge, morphology and capacity to condense, release and protect DNA against enzymatic digestion. Although there is no a general rule about the

optimal particle size of formulations for each gene delivery application, it is generally accepted that this parameter clearly influences the final performance, and that in case of niosomes, is affected by the cationic lipid/DNA mass ratio (Puras et al., 2015). Size of DP60L niosomes was around 100 nm. Interestingly, when DNA was incorporated to obtain nioplexes at 6/1 ratio, size increased up to 154 nm. However, at higher ratios, size decreased, probably due to the electrostatic interactions that condense DNA more efficiently, and therefore, decreased PDI values as well. Additionally, differences observed in PDI values could be due to different DNA topologies found in nioplexes (Cherng et al., 1999). Regarding ZP values, we found a positive correlation with the cationic lipid/DNA ratio, which suggests that cationic DOTMA binds and neutralize the negatively charged DNA (Paecharoenchai et al., 2012). Under TEM observation, niosomes appeared spherical, while nioplexes at 14/1 mass ratio showed heterogeneous shapes, but mostly elongated. Interestingly, at this ratio, spherical niosomes were also discerned (Fig. 2-B_2), which could accumulate on the surface of cell membranes and enhance DNA delivery (Smith et al., 1998; Song and Liu, 1998). To further analyze electrostatic interactions, we performed a gel retardation assay (Fig. 2-C), since an optimum balance is required for efficient gene delivery (Paecharoenchai et al., 2012). Despite the incomplete DNA condensation observed, which could be affect by different thermodynamic factors, kinetics mixing, or by the lycopene incorporation in to the niosome formulation or the high aqueous solubility of DOTMA (Mahato, 2005), all cationic lipid/DNA ratios analyzed, were able to protect plasmid DNA against enzymatic digestion.

Once physicochemical properties of nioplexes were analyzed, next, we performed in vitro studies to evaluate, initially, both transfection efficiency and viability in NT2 cells. These cells represent an interesting model to study the efficiency of gene delivery vectors into CNS due to their capacity to differentiate into bot neuronal and glial cells (Agirre et al., 2015). Unlike other teratocarcinoma cell lines, the NT2 cells depict an exclusive commitment to a neural lineage when exposed to retinoic acid (RA). Therefore, it has been considered as a promising human cell source in studies of cell in vivo therapeutic applications in many neurodegenerative diseases such as Parkinson disease (Cacciotti et al., 2017). Accordingly, we considered NT2 cells as an interesting

model to study the efficiency of gene delivery vectors into CNS. Additionally, these cells represent a promising platform in cell-based gene delivery as they could be genetically-modified and then transplanted (Tinsley and Eriksson, 2004).

Data obtained in Fig. 3 revealed that transfection efficiency increased in proportion to the cationic lipid/DNA mass ratio, reaching the peak at 14/1 ratio (17% of cells were transfected). Although the percentage of transfected cells were inferior to those obtained with commercially available lipifectamine®2000 (17% and 37%, respectively), viability values were higher (90% and 83%, respectively). The reported low cytotoxicity of nioplexes represents an appealing feature for potential further in vivo applications, since the in vivo use of lipifectamine®2000 is discouraged due to its cytotoxicity (Yang et al., 2014). To better understand the transfection process mediated by DP60L nioplexes in NT2 cells, we evaluated the cellular uptake and the intracellular trafficking of nioplexes, since those two factors clearly influence on the final performance of gene delivery carriers (Puras et al., 2015). Cellular uptake values were compared with lipifectamine®2000. As observed in Fig. 4, lipoplexes obtained with commercially available lipofectamine®2000, were more efficiently internalized than DP60L nioplexes (around 85% and 60%, respectively), which could explain the higher percentage of EGFP expression in NT2 cells transfected with lipofectamine®2000. Differences observed in cellular uptake between both formulations could be due to particular topologies of complexes or specific interactions of the complexes with cell membrane lipids (Cherng et al., 1999). In any case, percentage of transfected cells with DP60L nioplexes (17%, Fig. 3) were clearly inferior to the percentage of positive cells for FITC-labeled DP60L nioplexes (60%, Fig. 4-B), which suggest the influence of other biological events, such as intracellular trafficking or endosomal scape, in the final EGFP expression (Cardarelli et al., 2016). Therefore, we analyzed three of the most employed cellular internalization pathways such as clathrin-mediated endocytosis (CME), caveolae-mediated endocytosis (CvME) and macropinocytosis (MPC). Although there is not a clear consensus regarding the most efficient endocytosis pathway, the release of DNA into the cytoplasm, and therefore, the final performance, is clearly affected by the cellular uptake process (Nam et al., 2009). The results observed in Fig. 5 suggested that DP60L nioplexes were internalized, mainly, by CvME and CME, while MPC had

much less participation in the cellular uptake process. It is generally accepted that both CvME and CME are endocytosis routes that transfer genetic material to late endosomes/lysosomes, where the acidic environment degrades the DNA, making transfection process inefficient (Agirre et al., 2015). Therefore, the observation of nioplexes in the late endosome (Fig. 5-A_4) might explain the relatively low transfection efficiency values (17%) observed (Fig. 3), despite the fact that high number of NT2 cells (60%) captured the complexes (Fig. 4). Nonetheless, this hypothesis needs further verification since the endosomal escape capacity of nioplexes, if present, could evade degradation. Therefore, in next experiments, we evaluated the ability of nioplexes to escape from degradation in lysosomes. Several particle dependent endosomal escape mechanisms have been reported in the literature, being the proton-sponge mechanism one of the most widely described (Varkouhi et al., 2011).

Therefore, we analyzed the pH-buffering capacity of cationic DP60L niosomes. As observed (Supplementary data, Fig. 1), the incorporation of both cationic DOTMA and lycopene lipids into the niosome formulation, increased the pH-buffering capacity upon titration with 0.1 M HCl compared with niosomes elaborated only with polysorbate 60, which could suggest that those lipids could increase the proton sponge effect, and therefore, the endosomal scape capacity of DP60L niosomes. Another widely proposed endosomal scape mechanism consists on the destabilization of the endosomal membrane by electrostatic interactions between the cationic nanoparticles and the anionic lipids of the late endosome membrane, which could allow the DNA release to the cytoplasm (Varkouhi et al., 2011). To evaluate this endosomal scape mechanism, we added DP60L nioplexes to anionic micelles made with phosphatidyl serine (PS), that simulated the endosomal compartment, and the DNA release from PS micelles was evaluated in an agarose gel electrophoresis assay (Agirre et al., 2015). As observed in Fig. 5, about 40% of DNA was released form DP60L nioplexes, in the presence of PS, micelles. However, only 30% of DNA was released without previous incubation with the anionic PS micelles, which demonstrates the capacity of the DP60L nioplexes to release DNA once they contact the endosomal lipid bilayer membrane. In the case of lipoplexes based on lipofectamine®2000, all DNA was condensed with the formulation and up to 20% was released in the presence of PS micelles.

Next, and prior to perform in vivo studies, we evaluated transfection efficiency of DP60L nioplexes in primary cortical cultures of rat embryos, since primary cells normally express their tissue-specific receptors, and mimic in vivo conditions, where different kind of neurons and glial cells are mixed to set up neuronal-glial networks. In these conditions, we observed that, apparently, only glial cells, expressed EGFP (Fig. 6-A_1). This assumption was further confirmed by lack of $NeuN^+$-immunoreactivity in EGFP expressing cells (Fig. 6-A_2). Such preferential transfection of glial cells could be attributed to their higher mitotic and/or phagocytic activities (Schafer and Stevens, 2013).

Interestingly, in in vivo experiments performed by direct intracranial injection of nioplexes, again, NeuN negative cells (neuroglia and cells in blood vessel wall) were the only ones transfected by DP60L nioplexes (Fig. 6-B). These results reveal the incapacity of nioplexes to transfect neuron cells, probably due to the impaired uptake and/or intracellular trafficking (Bergen et al., 2008). Therefore, DP60L nioplexes could be of great interest to transfect glial cells in the CNS in glia-related neurological disorders. Glial cells constitute over 70% of the total cell population in the CNS, and they play a pivotal role for the normal development and function of nervous tissue (Alvarez et al., 2013; Fields and Stevens-Graham, 2002). Their perturbation is associated with several neurological disorders such as; stroke, multiple sclerosis, epilepsy, Alzheimer's and Parkinson's diseases (Barres, 2008; Milligan and Watkins, 2009). Therefore, the preferential transfection of glial cells could be of great importance in future applications in glia-related neurological disorders. Additionally, cells in the wall of some blood vessels were also transfected with DP60L nioplexes (Fig. 6-B, white arrow). Transfection at this level could be of great relevance in cerebrovascular diseases, such as; stroke, transient ischemic attacks, subarachnoid hemorrhage or vascular dementia, just to name a few.

4.5.Conclusion

In summary, we conclude that non-viral vector formulations based on niosome nanoparticles, where DOTMA is the cationic lipid, lycopene the "helper" lipid and polysorbate 60 the non-ionic surfactant, presents suitable physicochemical properties

for gene delivery applications in terms of size, superficial charge, polydispersity, or capacity to protect genetic material against enzymatic digestion. In addition, such formulation was able to transfect efficiently NT2 cultured cells, were both clathrin and caveolae-mediated endocytosis pathways predominated over macropinocytosis, exhibiting endosomal scape properties that could explain the high protein expression levels observed. Promising results obtained in both primary cortical cultures of rat embryos and in in vivo conditions after intracranial injection open the door for future application of such niosomes as efficient gene delivery tools for therapeutic treatment of some degenerative as well as malignant CNS disorders.

4.6.Acknowledgements

This project was supported by the Basque Country Government (GIC15/85), Spanish Grant MAT 2015 -69976-C3-1, SAF2013-42347-R, and by Research Chair “Bidons Egara”. The authors also wish to thank the intellectual and technical assistance from the ICTS “NANBIOSIS”, more specifically by the Drug Formulation Unit (U10) of the CIBER in Bioengineering, Biomaterials, and Nanomedicine (CIBER-BBN) at the University of Basque Country (UPV/EHU). Technical and human support provided by SGIker (UPV/EHU) is gratefully acknowledged

4.7. Supplementary data

Supplementary data to this article can be found online at https:// doi.org/10.1016/j.ijpharm.2018.09.038.

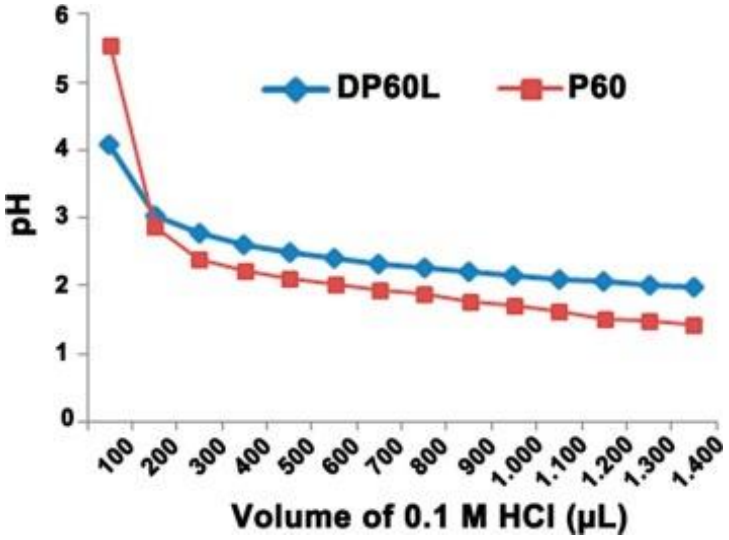

Supplementary figure 1. pH buffering capacity of assay of both DP60L and P60 niosomes.

4.8.References

Agirre, M., Ojeda, E., Zarate, J., Puras, G., Grijalvo, S., Eritja, R., Garcia del Cano, G., Barrondo, S., Gonzalez-Burguera, I., Lopez de Jesus, M., Salles, J., Pedraz, J.L., 2015. New insights into gene delivery to human neuronal precursor NT2 cells: a comparative study between lipoplexes, nioplexes, and polyplexes. Mol. Pharm. 12, 4056–4066. https://doi.org/10.1021/acs.molpharmaceut.5b00496.

Alvarez, J.I., Katayama, T., Prat, A., 2013. Glial influence on the blood brain barrier. Glia 61, 1939–1958. https://doi.org/10.1002/glia.22575.

Attia, N., Mashal, M., Grijalvo, S., Eritja, R., Zarate, J., Puras, G., Pedraz, J.L., 2017. Stem cell-based gene delivery mediated by cationic niosomes for bone regeneration. Nanomedicine S1549-9634(17)30200-9 [pii].

Barres, B.A., 2008. The mystery and magic of glia: a perspective on their roles in health and disease. Neuron 60, 430–440. https://doi.org/10.1016/j.neuron.2008.10.013.

Bergen, J.M., Park, I.K., Horner, P.J., Pun, S.H., 2008. Nonviral approaches for neuronal delivery of nucleic acids. Pharm. Res. 25, 983–998. https://doi.org/10.1007/s11095007-9439-5.

Cacciotti, I., Ceci, C., Bianco, A., Pistritto, G., 2017. Neuro-differentiated Ntera2 cancer stem cells encapsulated in alginate beads: first evidence of biological

functionality. Mater. Sci. Eng. C Mater. Biol. Appl. 81, 32–38 S0928-4931(17)30169-8 [pii].

Cardarelli, F., Digiacomo, L., Marchini, C., Amici, A., Salomone, F., Fiume, G., Rossetta, A., Gratton, E., Pozzi, D., Caracciolo, G., 2016. The intracellular trafficking mechanism of Lipofectamine-based transfection reagents and its implication for gene delivery. Sci. Rep. 6, 25879. https://doi.org/10.1038/srep25879.

Cherng, J.Y., Schuurmans-Nieuwenbroek, N.M., Jiskoot, W., Talsma, H., Zuidam, N.J., Hennink, W.E., Crommelin, D.J., 1999. Effect of DNA topology on the transfection efficiency of poly((2-dimethylamino)ethyl methacrylate)-plasmid complexes. J.Controlled Release 60, 343–353 S0168-3659(99)00089-9 [pii].

Fields, R.D., Stevens-Graham, B., 2002. New insights into neuron-glia communication. Science 298, 556–562. https://doi.org/10.1126/science.298.5593.556.

Huang, Y., Rao, Y., Chen, J., Yang, V.C., Liang, W., 2011. Polysorbate cationic synthetic vesicle for gene delivery. J. Biomed. Mater. Res. A 96, 513–519. https://doi.org/10. 1002/jbm.a.32999.

Krishnamoorthy, G., Selvakumar, K., Venkataraman, P., Elumalai, P., Arunakaran, J., 2013. Lycopene supplementation prevents reactive oxygen species mediated apoptosis in Sertoli cells of adult albino rats exposed to polychlorinated biphenyls. Interdiscip. Toxicol. 6, 83–92. https://doi.org/10.2478/intox-2013-0015.

Maguire, C.A., Ramirez, S.H., Merkel, S.F., Sena-Esteves, M., Breakefield, X.O., 2014. Gene therapy for the nervous system: challenges and new strategies. Neurotherapeutics 11, 817–839. https://doi.org/10.1007/s13311-014-0299-5.

Mahato, R.I., 2005. Water insoluble and soluble lipids for gene delivery. Adv. Drug Deliv.Rev. 57, 699–712 S0169-409X(05)00006-2 [pii].

Mansouri, S., Lavigne, P., Corsi, K., Benderdour, M., Beaumont, E., Fernandes, J.C., 2004. Chitosan-DNA nanoparticles as non-viral vectors in gene therapy: strategies to improve transfection efficacy. Eur. J. Pharm. Biopharm. 57, 1–8 S0939641103001553 [pii].

Mashal, M., Attia, N., Puras, G., Martinez-Navarrete, G., Fernandez, E., Pedraz, J.L., 2017. Retinal gene delivery enhancement by lycopene incorporation into cationic

niosomes based on DOTMA and polysorbate 60. J. Controlled Release 254, 55–64 S01683659(17)30491-1 [pii].

Meyer, O., Kirpotin, D., Hong, K., Sternberg, B., Park, J.W., Woodle, M.C., Papahadjopoulos, D., 1998. Cationic liposomes coated with polyethylene glycol as carriers for oligonucleotides. J. Biol. Chem. 273, 15621–15627.

Milligan, E.D., Watkins, L.R., 2009. Pathological and protective roles of glia in chronic pain. Nat. Rev. Neurosci. 10, 23–36. https://doi.org/10.1038/nrn2533.

Nagabhushan Kalburgi, S., Khan, N.N., Gray, S.J., 2013. Recent gene therapy advancements for neurological diseases. Discov. Med. 15, 111–119.

Nam, H.Y., Kwon, S.M., Chung, H., Lee, S.Y., Kwon, S.H., Jeon, H., Kim, Y., Park, J.H., Kim, J., Her, S., Oh, Y.K., Kwon, I.C., Kim, K., Jeong, S.Y., 2009. Cellular uptake mechanism and intracellular fate of hydrophobically modified glycol chitosan nanoparticles. J. Controlled Release 135, 259–267. https://doi.org/10.1016/j.jconrel. 2009.01.018.

Nobre, R.J., Almeida, L.P., 2011. Gene therapy for Parkinson's and Alzheimer's diseases: from the bench to clinical trials. Curr. Pharm. Des. 17, 3434–3445 BSP/CPD/E-Pub/ 000710 [pii].

Ochoa, G.P., Sesma, J.Z., Diez, M.A., Diaz-Tahoces, A., Aviles-Trigeros, M., Grijalvo, S.,Eritja, R., Fernandez, E., Pedraz, J.L., 2014. A novel formulation based on 2,3-di (tetradecyloxy)propan-1-amine cationic lipid combined with polysorbate 80 for efficient gene delivery to the retina. Pharm. Res. 31, 1665–1675. https://doi.org/10. 1007/s11095-013-1271-5.

Ojeda, E., Puras, G., Agirre, M., Zarate, J., Grijalvo, S., Pons, R., Eritja, R., Martinez Navarrete, G., Soto-Sanchez, C., Fernandez, E., Pedraz, J.L., 2015. Niosomes based on synthetic cationic lipids for gene delivery: the influence of polar head-groups on the transfection efficiency in HEK-293, ARPE-19 and MSC-D1 cells. Org. Biomol. Chem. 13, 1068–1081. https://doi.org/10.1039/c4ob02087a.

Ojeda, E., Puras, G., Agirre, M., Zarate, J., Grijalvo, S., Eritja, R., Martinez-Navarrete, G., Soto-Sanchez, C., Diaz-Tahoces, A., Aviles-Trigueros, M., Fernandez, E., Pedraz, J.L., 2016c. The influence of the polar head-group of synthetic cationic lipids on the

transfection efficiency mediated by niosomes in rat retina and brain. Biomaterials 77, 267–279. https://doi.org/10.1016/j.biomaterials.2015.11.017.

Ojeda, E., Agirre, M., Villate-Beitia, I., Mashal, M., Puras, G., Zarate, J., Pedraz, J.L., 2016a. Elaboration and physicochemical characterization of niosome-based nioplexes for gene delivery purposes. Methods Mol. Biol. 1445, 63–75. https://doi.org/10.1007/978-1-4939-3718-9_5.

Ojeda, E., Puras, G., Agirre, M., Zarate, J., Grijalvo, S., Eritja, R., DiGiacomo, L., Caracciolo, G., Pedraz, J.L., 2016b. The role of helper lipids in the intracellular disposition and transfection efficiency of niosome formulations for gene delivery to retinal pigment epithelial cells. Int. J. Pharm. 503, 115–126. https://doi.org/10.1016/j.ijpharm.2016.02.043.

Paecharoenchai, O., Niyomtham, N., Ngawhirunpat, T., Rojanarata, T., Yingyongnarongkul, B.E., Opanasopit, P., 2012. Cationic niosomes composed of spermine-based cationic lipids mediate high gene transfection efficiency. J. Drug Targeting 20, 783–792. https://doi.org/10.3109/1061186X.2012.716846.

Peluffo, H., Unzueta, U., Negro-Demontel, M.L., Xu, Z., Vaquez, E., Ferrer-Miralles, N., Villaverde, A., 2015. BBB-targeting, protein-based nanomedicines for drug and nucleic acid delivery to the CNS. Biotechnol. Adv. 33, 277–287. https://doi.org/10.1016/j.biotechadv.2015.02.004.

Pezzoli, D., Chiesa, R., De Nardo, L., Candiani, G., 2012. We still have a long way to go to effectively deliver genes!. J. Appl. Biomater. Funct. Mater. 10, 82–91. https://doi.org/10.5301/JABFM.2012.9707.

Puras, G., Mashal, M., Zarate, J., Agirre, M., Ojeda, E., Grijalvo, S., Eritja, R., Diaz Tahoces, A., Martinez Navarrete, G., Aviles-Trigueros, M., Fernandez, E., Pedraz, J.L., 2014. A novel cationic niosome formulation for gene delivery to the retina. J. Controlled Release 174, 27–36. https://doi.org/10.1016/j.jconrel.2013.11.004.

Puras, G., Martinez-Navarrete, G., Mashal, M., Zarate, J., Agirre, M., Ojeda, E., Grijalvo, S., Eritja, R., Diaz-Tahoces, A., Aviles-Trigueros, M., Fernandez, E., Pedraz, J.L., 2015. Protamine/DNA/Niosome ternary non-viral vectors for gene delivery to the retina: the role of protamine. Mol. Pharm. 12, 3658–3671. https://doi.org/10.1021/acs.molpharmaceut.5b00422.

Rajera, R., Nagpal, K., Singh, S.K., Mishra, D.N., 2011. Niosomes: a controlled and novel drug delivery system. Biol. Pharm. Bull. 34, 945–953 JST.JSTAGE/bpb/34.945 [pii].

Rezaee, M., Oskuee, R.K., Nassirli, H., Malaekeh-Nikouei, B., 2016. Progress in the development of lipopolyplexes as efficient non-viral gene delivery systems. J. Controlled Release 236, 1–14. https://doi.org/10.1016/j.jconrel.2016.06.023.

Schafer, D.P., Stevens, B., 2013. Phagocytic glial cells: sculpting synaptic circuits in the developing nervous system. Curr. Opin. Neurobiol. 23, 1034–1040. https://doi.org/10.1016/j.conb.2013.09.012.

Smith, J.G., Wedeking, T., Vernachio, J.H., Way, H., Niven, R.W., 1998. Characterization and in vivo testing of a heterogeneous cationic lipid-DNA formulation. Pharm. Res. 15, 1356–1363.

Song, Y.K., Liu, D., 1998. Free liposomes enhance the transfection activity of DNA/lipid complexes in vivo by intravenous administration. Biochim. Biophys. Acta 1372, 141–150 S0005-2736(98)00054-6 [pii].

Tang, M.X., Szoka, F.C., 1997. The influence of polymer structure on the interactions of cationic polymers with DNA and morphology of the resulting complexes. Gene Ther. 4, 823–832. https://doi.org/10.1038/sj.gt.3300454.

Tang, G.P., Zeng, J.M., Gao, S.J., Ma, Y.X., Shi, L., Li, Y., Too, H.P., Wang, S., 2003. Polyethylene glycol modified polyethylenimine for improved CNS gene transfer: effects of PEGylation extent. Biomaterials 24, 2351–2362 S0142961203000292 [pii].

Tinsley, R., Eriksson, P., 2004. Use of gene therapy in central nervous system repair. Acta Neurol. Scand. 109, 1–8 240 [pii].

Varkouhi, A.K., Scholte, M., Storm, G., Haisma, H.J., 2011. Endosomal escape pathways for delivery of biologicals. J. Controlled Release 151, 220–228. https://doi.org/10.1016/j.jconrel.2010.11.004.

Yang, Z., Jiang, Z., Cao, Z., Zhang, C., Gao, D., Luo, X., Zhang, X., Luo, H., Jiang, Q., Liu, J., 2014. Multifunctional non-viral gene vectors with enhanced stability, improved cellular and nuclear uptake capability, and increased transfection efficiency. Nanoscale 6, 10193–10206. https://doi.org/10.1039/c4nr02395a.

Yao, L., Yao, S., Daly, W., Hendry, W., Windebank, A., Pandit, A., 2012. Non-viral gene therapy for spinal cord regeneration. Drug Discov. Today 17, 998–1005. https://doi.org/10.1016/j.drudis.2012.05.009.

Yin, H., Kanasty, R.L., Eltoukhy, A.A., Vegas, A.J., Dorkin, J.R., Anderson, D.G., 2014. Non-viral vectors for gene-based therapy. Nat. Rev. Genet. 15, 541–555. https://doi. org/10.1038/nrg3763.

Zhang, X.X., McIntosh, T.J., Grinstaff, M.W., 2012. Functional lipids and lipoplexes for improved gene delivery. Biochimie 94, 42–58. https://doi.org/10.1016/j.biochi. 2011.05.005.

Zinchuk, V., Grossenbacher-Zinchuk, O., 2011. Quantitative colocalization analysis of confocal fluorescence microscopy images. Curr. Protoc. Cell. Biol. https://doi.org/10.1002/0471143030.cb0419s52.

Chapter 5

Gene delivery to the rat retina by non-viral vectors based on chloroquine-containing cationic niosomes

Gene delivery to the rat retina by non-viral vectors based on chloroquine-containing cationic niosomes

Mohamed Mashal[a,1], Noha Attia[a,b,c,1], Gema Martínez-Navarrete[d,e], Cristina Soto-Sánchez[d,e], Eduardo Fernández[d,e], Santiago Grijalvo[d,f], Ramón Eritja[d,f], Gustavo Puras[a,d,] , Jose Luis Pedraz[a,d,]

[a] NanoBioCel Group, Laboratory of Pharmaceutics, School of Pharmacy, University of the Basque Country (UPV/EHU), Paseo de la Universidad 7, 01006 Vitoria-Gasteiz, Spain
[b] Histology and Cell Biology Department, Faculty of Medicine, University of Alexandria, Alexandria, Egypt
[c] Department of Basic Sciences, The American University of Antigua-College of Medicine, Coolidge, Antigua and Barbuda
[d] Networking Research Centre of Bioengineering, Biomaterials and Nanomedicine (CIBER-BBN), Vitoria-Gasteiz, Spain
[e] Neuroprothesis and Neuroengineering Research Group, Miguel Hernández University, Elche, Spain
[f] Institute of Advanced Chemistry of Catalonia (IQAC-CSIC), Spain

Journal of Controlled Release 304 (2019) 181–190

ABSTRACT

The incorporation of chloroquine within nano formulations, rather than as a co-treatment of the cells, could open a new avenue for in vivo retinal gene delivery. In this manuscript, we evaluated the incorporation of chloroquine diphosphate into the cationic niosome formulation composed of poloxamer 188, polysorbate 80 non-ionic surfactants, and 2,3-di (tetradecyloxy) propan-1-amine (hydrochloride salt) cationic lipid, to transfect rat retina. Niosome formulations without and with chloroquine diphosphate (DPP80, and DPP80-CQ, respectively) were prepared by the reverse phase evaporation technique and characterized in terms of size, PDI, zeta potential, and morphology. After the incorporation of the pCMS-EGFP plasmid, the resultant nioplexes -at different cationic lipid/DNA mass ratios- were further evaluated to compact, liberate, and secure the DNA against enzymatic digestion. In vitro procedures were achieved in ARPE-19 cells to assess transfection efficacy and intracellular transportation. Both nioplexes formulations transfected efficiently ARPE-19 cells, although the cell viability was clearly better in the case of DPP80-CQ nioplexes. After subretinal and intravitreal injections, DPP80 nioplexes were not able to transfect the rat retina. However, chloroquine containing vector showed protein expression in many retinal cells, depending on the administration route. These data provide new insights for retinal gene delivery based on chloroquine-containing niosome non-viral vectors.

Keywords: Niosomes, Non-viral vector, Gene therapy, Retina, Chloroquine

5.1.Introduction

Retinal degeneration is a devastating ocular pathology caused by functional impairment of genes related mainly to the phototransduction process, the structure and metabolism of the retinal cells, and the maturation process of the mRNA needed to synthetize specific proteins. One of the most promising alternatives to treat retinal disorders like age-related macular degeneration [1], Leber congenital amaurosis (LCA) [2] retinitis pigmentosa [3] or choroideremia consists on the delivery of a normal copy of the mutated genes to the affected cells by means of gene therapy technology [4]. Since the success of first RPE65-gene-replacement trials for LCA type-2, further clinical trials of gene therapy have been conducted for other devastating retinal disorders [5]. In most of those clinical trials, viral-vectors have been used to deliver the genetic material. Among them, adeno-associated virus (AAV) stand out for their safety profile [6]. In fact, Luxturna, the first gene therapy-based medicine approved by the FDA in 2017 for the treatment of mutations in RPE65 gene linked to retinitis pigmentosa and Stargardt disease, is based on such AAV. However, the limited carrying capacity of genetic material, around 5 kb, hampers their ap-plication to deliver genes that over pass such size to the retina. For instance, ABCA4 and MYO7A genes, whose mutations can be related to Stargardt disease and Usher Syndrome Type 1B, respectively [7], have a size of around 7 kb. Therefore, the use of non-viral vectors represents an interesting alternative, since the size of DNA that can be inserted in some of these formulations is theoretically unlimited [8,9].

Despite their limited transfection efficiency and transient gene ex-pression, non-viral vectors have emerged as a promising alternative to deliver genetic material. Some of the main advantages of such gene delivery systems, in addition to their higher carrying capacity, include their low cost of production or their capacity to be easily modified in order to enhance their performance [10,11]. Hence, the research ac-tivity related to the design and characterization of novel non-viral vector formulations for gene delivery has considerably increased [12]. Cationic niosomes are self-assembled vesicular nanovehicles, similar to liposomes, with encouraging properties for gene delivery applications. To mention a few, the chemical structure of niosomes makes it possible to provide more stable and less cytotoxic formulations at a low cost [13]. The

amphiphilic nature of non-ionic surfactants enable niosomes to trap both hydrophobic and hydrophilic compounds [14].The cationic part here is the hydrochloride salt of the cationic lipid 2,3-di (tetra-decyloxy) propan-1-amine (D). Such cationic lipid contains the four pivotal components that manage the gene transfection process: a polar head, a backbone, a linker, and two non-polar tails [15].

One of the key limiting steps in the transfection process is the endosomal escape. Chloroquine is a known endosomal disrupting molecule and lysosomotropic agent that can cross the blood retinal barrier. Although chloroquine has been used in vitro as a pre-treatment of cultured cells to facilitate gene delivery [16], this study will be the first -to the best of our knowledge- to apply a chloroquine-containing nio-some formulation in gene delivery setting. The incorporation of one or more of the materials at the molecular level, within the nano-formulation, can dramatically affect the transfection process under in vitro and in vivo conditions [12]. Thereafter, scientists may face a great challenge in the near future to test a library of different materials that can be incorporated within the gene delivery vehicles.

Based on the aforementioned (D) cationic lipid, two niosome vehicles were formulated for retinal gene delivery with two non-ionic surfactants [polysorbate 80 (P80) and poloxamer 188 (P)], in the absence/presence of chloroquine (CQ), referred as DPP80 and DPP80-CQ, respectively (Fig. 1). The two vehicles were prepared by the emulsification/solvent evaporation system and characterized in terms of particle size, polydispersity index (PDI) and zeta potential. Then, the reporter pCMS-EGFP plasmid was added at different weight ratios of cationic lipid to obtain nioplexes. Such DPP80/DPP80-CQ nioplexes were further characterized by size, PDI, charge, morphology, and the capability to compact, liberate and protect the DNA from digestive enzymes. In vitro comparative studies of both vehicles in ARPE-19 cells were achieved respecting their cellular uptake, transfection efficiency, viability and internalization mechanism. Finally, the two formulations were administered to rat eyes via intravitreal and subretinal injections, as a probe of concept, to estimate transfection efficiency by confocal microscopy.

5.2.Materials and methods

5.2.1. Production of cationic niosomes

The synthesis of the hydrochloride salt form of the cationic lipid 2,3-di (tetradecyloxy) propan-1-amine (D) was performed as described in the literature, with slight modifications of the laboratory protocol [17]. Niosomes were composed by modified reverse-phase evaporation approach [18]. Concisely, 5 mg (0.1% w/v) of the lipid was dispersed in 1 ml of dichloromethane (organic phase). Subsequently, 5 ml milliQ water containing 12.5 mg (0.25% w/v) poloxamer 188 (P) (Sigma-Aldrich, Madrid, Spain), 12.5 mg (0.25% w/v) polysorbate 80 (P80) (Sigma-Aldrich, Madrid, Spain) and 2.5 mg (0.05% w/v) chloroquine diphosphate (CQ) (Sigma-Aldrich, Madrid, Spain) were added to the organic phase.

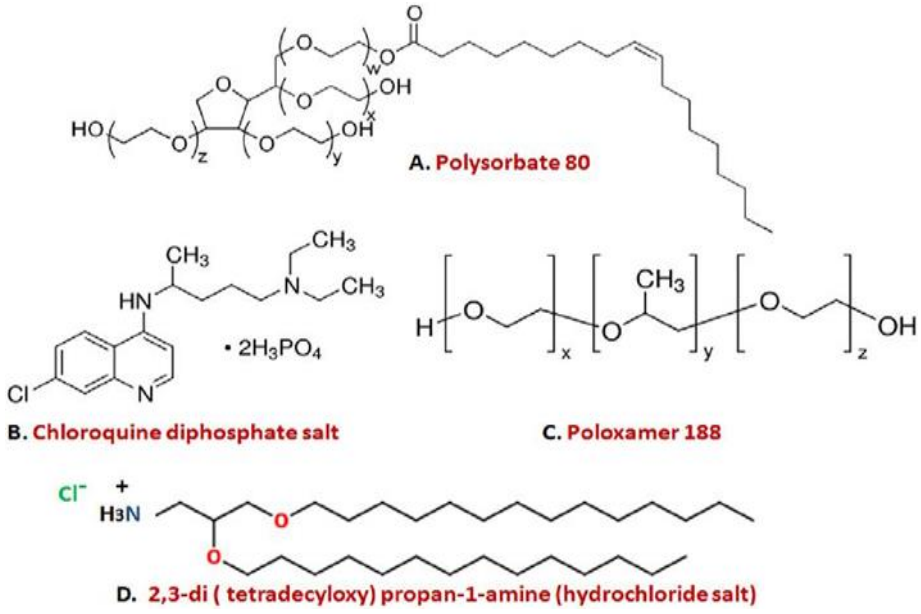

Fig. 1. Chemical structure of the components of DPP80 and DPP80-CQ niosomes. (A) Polysorbate80, (B) Chloroquine diphosphate salt, (C) Poloxamer188 and (D) cationic lipid (DTPA-Cl).

The emulsions were obtained by sonication of the mixture for 50 s at 45 W (Branson Sonifier 250®, Danbury, USA). Di-chloromethane was eliminated from emulsions by dissipation under magnetic stirring for 2 h, rendering the cationic niosomes in the aqueous medium. The molar ratios of both DPP80 and DPP80-CQ formulations were, 1.9/0.3/1.9 and 1.9/0.3/1.9/1, respectively.

5.2.2. Plasmid propagation and elaboration of nioplexes

The protocols for propagation, purification, and quantification of pCMS-EGFP plasmid (5541 bp, Plasmid Factory, Bielefeld, Germany), have been described previously [12]. The nioplexes (niosome/DNA complexes) of both DPP80 and DPP80-CQ were formed by mixing an adequate volume of pCMS-EGFP plasmid stock solution (0.5 mg/ml) with various amounts of the niosome suspension (1 mg cationic lipid/ ml) to get different cationic lipid/DNA mass ratios (w/w). To enhance the electrostatic interaction, the nioplexes mixture was allowed to settle for 30 min at room temperature.

5.2.3. Characterization of niosomes/nioplexes

Dynamic light scattering (DLS) technique was used to estimate both particle size and polydispersity index (PDI) measurements (Malvern Zetasizer Nano ZS, UK). Particle size, was determined by cumulative analysis of the recorded hydrodynamic diameter. Laser Doppler Velocimetry (LDV) was used to assess zeta potential (ZP). Samples were dispersed in a 0.1 mM NaCl solution. Triple measurements were carried out for all samples. The morphology of both niosomes and nioplexes was estimated by transmission electron microscopy (TEM). Shortly, onto glow-discharged carbon coated grids, 5 μl sample was allowed to adhere on the surface for 60 s. Samples were examined under TEM, Tecnai G2 20 Twin (FEI, Eindhoven, The Netherlands). In a bright-field image mode, the operation was done with an accelerating voltage of 200 keV. Digital images were captured by an Olympus SIS Morada di-gital camera. Niosomes' ability to compact, liberate and safeguard DNA from enzymatic digestion was assessed by agarose gel electrophoresis studies. Nioplexes samples (200 mg of plasmid DNA/20 μl) were com-pared to naked (uncomplexed) DNA. The agarose gel (0.8% w/v) was immersed in a Tris–acetate–EDTA buffer, and the DNA samples were run on the gel for 30 min at 120 V. Next, agarose gel was stained with GelGreen®. A digital ChemiDoc™ MP Imaging System (Bio-Rad, Madrid, Spain) was used for band observation. 20 μl of a 2% SDS solution (Sigma-Aldrich, Madrid, Spain) was added to the samples to estimate the liberation of DNA from both DPP80 and DPP80-CQ vehicles at different cationic lipid/DN mass ratios. In addition, DNase I (Sigma-Aldrich, Madrid, Spain) was added at a concentration of 1 unit of DNase I/2.5 μg DNA to

evaluate the protective ability of both vehicles against enzymatic digestion. Then, the samples were incubated at 37 ºC for 30 min and a 2% SDS solution was added to evaluate if released the DNA from the vehicles wad protected from the enzymatic digestion.

5.2.4. In vitro transfection experiments

ARPE-19 cells, purchased from the American Type Culture Collection (ATCC, CRL 2302®), were seeded in 24-well plates at a density of 8×10^4 cells/well, with 500 µl of complete medium, formed of D-MEM/F-12 containing 10% fetal bovine serum (Gibco®, California, USA). Then, at a confluence level of 70–80%, the media was removed, and cells were exposed to nioplexes at different cationic lipid/DNA mass ratios (w/w) (1.25 µg DNA/well) dispersed in serum free Opti-MEM® solution (Gibco®, California, USA) at 37 ºC for 4 h. Subsequently, transfection medium was removed, and cells were thoroughly washed 3 times with PBS. Then, cells were cultured in 1 ml of complete medium and allowed to grow for further 72 h until fluorescence microscopy imaging (Nikon TSM) and flow cytometry analysis (FACSCalibur™, BD Biosciences, USA) were done. FL_1 (530/30) was used to detect EGFP-expressing transfected cells, and FL_3 (670) was used to detect Propidium Iodide-stained dead/dying cells. Untransfected cells were used as negative control for all experiments, while cells transfected with Lipofectamine™ 2000 (Invitrogen, California, USA), according to manufacturer's protocol, were considered as positive controls. 10.000-gated events were acquired and analyzed using Flowing Software 2.5.1. Data represent the mean (± SD) of three independent experiments, each of them performed in triplicate.

5.2.5. Cellular uptake and endocytosis mechanism studies

FITC-labeled (pCMS-EGFP) plasmid (DareBio, Madrid, Spain) was used instead of pCMS-EGFP plasmid to estimate the cellular uptake of the vehicles. The same protocol described in the previous 5.2.4 section, was used to incubate and maintain ARPE-19 cells, and to evaluate cellular uptake. After removal of the transfection medium and multiple washes of the plates with PBS, the cells were assayed

by FACSCalibur flow cytometer. The negative control cells were transfected with naked DNA, and the percentage of FITC-positive cells represented the cellular uptake values. Each specimen was assayed in triplicate. Different up-take inhibitors were used to estimate the endocytosis mechanism of vehicles. Genistein, chlorpromazine hydrochloride, methyl-β-cyclo-dextrin and wortmannin were used as inhibitors for caveolae-mediated endocytosis (CvME), clathrin-mediated endocytosis (CME), both (CvME and CME) and macropinocytosis (MPC), respectively. Nioplexes at 10/1 cationic lipid/DNA mass ratio were complexed with pCMS-EGFP plasmid, and followed the same protocol described in the previous 5.2.4 section to transfect ARPE-19 cells. Prior to the addition of nioplexes, cells were incubated with either 200 μM genistein for 30 min, or with 5 mM methyl-β-cyclodextrin, 50 nM wortmannin, or with 5 μg/ml chlorpromazine hydrochloride for 60 min. Cells were incubated with serum-free Opti-MEM® solution for 4 h at 37 °C. Subsequently, cells were carefully washed with PBS after removal of the transfection medium. Then, complete medium was added, and cells were incubated to grow for a further 72 h until flow cytometer analysis was done to determine the transfection efficiency. Each specimen was analyzed in triplicate.

5.2.6. Buffering capacity of niosomes

The buffering capacity of both DPP80 and DPP80-CQ niosomes was assayed by volumetric analysis. Briefly, 10 ml formulation samples were titrated with aliquots of 100 μl 0.1 M HCl solution, and the changes in pH value were monitored by a pH meter (CRISON, GLP 21, Barcelona, Spain).

5.2.7. In vivo studies

Intravitreal (4 μl containing 100 ng of pDNA) and subretinal injection (1 μl containing 25 ng of pDNA) of both DPP80 and DPP80-CQ nioplexes suspension were performed into four adult female Sprague–Dawley rats (6–7 weeks old, 200–300 g weight) per formulation. Experiments were done according to the Spanish and European Union regulations for the use of animals in research and the Association for Research in Vision and Ophthalmology (ARVO) statement, as de-scribed in the

literature [12]. To deliver nioplexes to the subretinal space, a bent 33-gauge needle was introduced through a sclerotomy (1–2 mm) posterior to ora serrata and in a tangential direction toward the posterior retinal pole along the subretinal space. Successful administration was confirmed by the appearance of a partial retinal detachment by direct ophthalmoscopy of the eye fundus through the operating microscope (Zeiss OPMI® pico; Carl Zeiss Meditec GmbH, Jena, Germany). The untreated right eyes were injected only with the vehicles and served as negative controls.

Rats were sacrificed and perfused with 4% paraformaldehyde (PFA) after 72 h and eyes were removed, opened at the cornea and immersed in PFA. For whole mounts, retina was dissected from the eyecup and flattened onto Superfrost glass slides (Superfrost Plus, Fisher Scientific). For cryosections, the eyes were cryoprotected in sucrose and embedded in Tissue-Tek® OCT (optimum cutting temperature). The eyes were cryosectioned at 16 μm and transferred directly onto microscope slides (Superfrost, Fisher Scientific).

For immunohistochemistry, whole mounts or retinal sections were washed and blocked with 10% bovine serum albumin and 0,05% triton in PBS for 1 h (cryosections) or 2 h (whole mounts). Both sections and whole mounts were incubated overnight at 4 °C with primary antibodies: rabbit anti-NeuN (Merck Millipore, MA, USA), rabbit anti-recoverin (Merck Millipore, MA, USA), rabbit anti-Protein kinase C (PKC, Santa Cruz Biotechnology) and rabbit anti-GFAP (Santa Cruz Biotechnology). Samples were rinsed and incubated with Alexa Fluor 555 donkey anti rabbit (Thermofisher Scientific) and counterstained with Hoechst 33342 (Thermofisher Scientific). Finally, whole mounts and sections were mounted with antifade mounting meédium and evaluated with a Leica TCS SPE spectral confocal microscope (Leica Microsystems GmbH, Wetzlar, Germany).

5.2.8. Statistical analysis

INSTAT program (GraphPad Software, San Diego, CA, USA) was used to perform the statistical analysis. Differences between groups at significance levels of

95% were calculated by the ANOVA and the Student's t-test. In all cases, P values < .05 were regarded as significant. Normal distribution of samples was assessed by the Kolmogorov-Smirnov test and the homogeneity of the variance by the Levene test. Numerical data were presented as mean ± SD.

Table 1
Physical features of both DPP80 and DPP80-CQ niosomes in terms of size (nm), Polydispersity index (PDI), and zeta potential (mV). The values exemplify the mean ± SD (n = 3).

	Size (nm)	Zeta potential (mV)	PDI
DPP80	90.41 ± 0.65	44.3 ± 1.48	0.42 ± 0.01
DPP80-CQ	118.18 ± 1.46	28.9 ± 7.73	0.13 ± 0.02

5.3.Results

5.3.1. Characterization of niosomes/nioplexes

Both niosome vehicles were prepared by mixing [polysorbate 80 (P80) and poloxamer 188 (P)] non-ionic surfactants and cationic lipid (D). In the absence/presence of chloroquine (CQ), niosomes were referred as DPP80, or as DPP80-CQ, respectively (Fig. 1). Both niosomes were prepared by the emulsification/solvent evaporation method and were characterized in terms of particle size, zeta potential (ZP) and polydispersity index (PDI) as shown in Table 1. The incorporation of chloroquine into the DPP80 niosome formulation increased the size of those niosomes from 90 to118 nm. Moreover, upon chloroquine addition, the ZP values decreased remarkably to 29 mV in DDP80-CQ niosomes compared to 44 mV in DPP80 niosomes. Interestingly, the addition of chloroquine also decreased the PDI value from 0.42 in DPP80 formulation to 0.13 in DPP80-CQ formulation.

Fig. 2 illustrates the physicochemical characterization of DPP80 and DPP80-CQ nioplexes. In Section 2-A, the size and ZP values of both nioplexes at different ratios

(from 4/1 to 12/1) can be observed. The size of DPP80 nioplexes (light bar) generally decreased, with fluctuations, between 170 nm at 4/1cationic lipid/DNA mass ratio to 106 nm at 12/1 mass ratio. With respect to the size of DPP80-CQ nioplexes (dark bars), it depicted an evident decreasing pattern (from 300 nm at 4/1 to 140 nm at 12/1 cationic lipid/DNA mass ratios). Basically, the addition of chloroquine to the formulation increased the sizes at all cationic lipid/DNA mass ratios, in comparison to DPP80 nioplexes. Regarding the ZP, at all cationic lipid/DNA mass ratios, readings of DPP80 nioplexes (light lines) exceeded their DPP80-CQ counterparts (dark lines).

Concerning the PDI values (Supplementary data, Table. 1), except for the 4/1 cationic lipid/DNA mass ratio, the PDI values of DPP80 nioplexes surpassed those of DPP80-CQ. As depicted in Fig. 2-B_1, the morphology of DPP80 nioplexes by TEM, revealed distinct imperfectly spherical structure, while DPP80-CQ nioplexes morphology showed aggregated lamellar morphology (Fig. 2-B_2). Fig. 2-C represents the agarose gel electrophoresis assays of both DPP80 (C_1) and DPP80-CQ (C_2) nioplexes prepared at different cationic lipid/DNA mass ratios (4/1, 6/1, 8/1 and 10/1). At all cationic lipid/DNA ratios, both niosomes were able to condense the DNA, since clear white bands were recognized in wells 4, 7, 10, and 13. However, in the case of DPP80-CQ (C_2) dim supercoiled (SC) bands were noticed on 7, 10, and 13 wells. Upon SDS addition, the DNA was successfully released from both formulations at all cationic lipid/DNA ratios evaluated, since clear SC bands were observed on lanes 5, 8, 11, and 14. Furthermore, the DNA bound to the surface of both niosome structures was shielded from enzymatic digestion, as clear SC bands were observed on lanes 6, 9, 12, and 15. No SC bands were detected on lane 3, which proves that the plasmid DNA can be fully digested by the DNase I enzyme.

5.3.2. In vitro transfection and viability studies in ARPE-19 cells

Fig. 3-A depicts the transfection efficiency and cell viability of cationic niosome/DNA nioplexes in ARPE-19 cells. Cationic lipid/DNA mass ratios (w/w) higher than 4/1 showed about 20–30% of cells transfected by both DPP80 and DPP80-CQ nioplexes. However, the values of ARPE-19 cells transfected by DPP80 nioplexes at 6/1, 8/1 and 12/1 cationic lipid/DNA mass ratios (light bars) were significantly higher that values obtained at those same rations when ARPE-19 were transfected with DPP80-CQ (dark bars) formulation. In any case, transfection values for both formulations were significantly lower ($p < .05$) than those values gained with Lipofectamine™2000 (36.6%). Meantime, naked DNA plasmid did not show any transfection (data not shown).

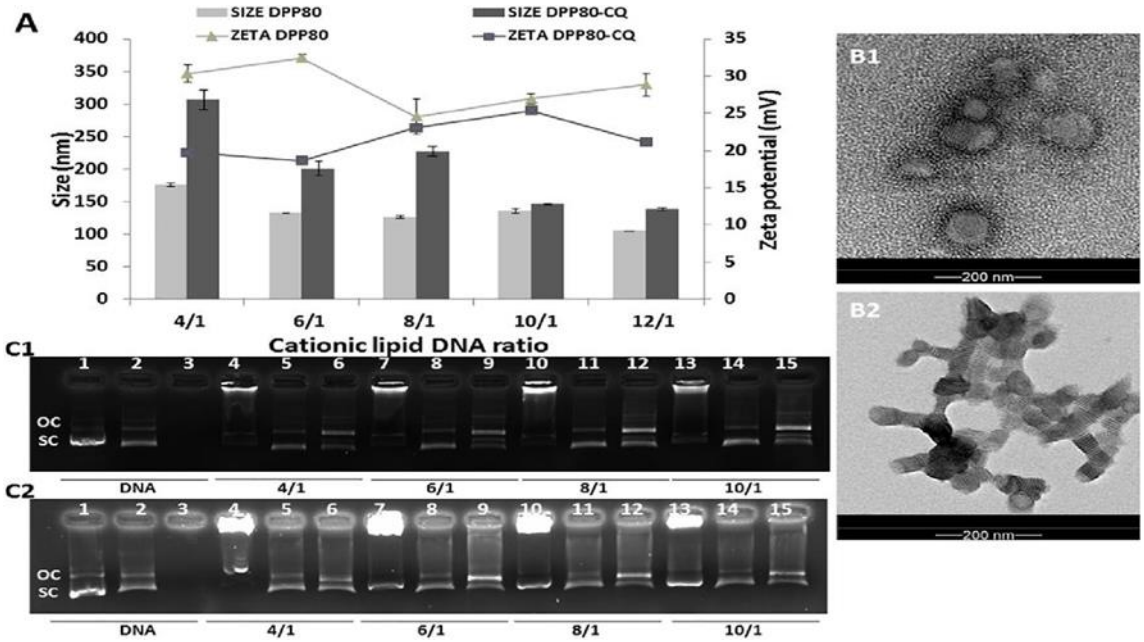

Fig. 2. Physicochemical features of nioplexes. (A) The impact of cationic lipid/DNA mass ratio (w/w) on the size (bars) and zeta potential (lines). The data represent the mean ± SD (n = 3). TEM images of DPP80 (B_1) and DPP80-CQ complexes (B_2) at 8/1 and 10/1cationic lipid/DNA mass ratio (w/w) respectively. Scale bar = 200 nm. (C) condensation, release by SDS and DNase I protection of DNA at various cationic lipid/DNA mass ratios (w/w) of nioplexes based on DPP80 (C_1) and DPP80-CQ (C_2) vehicles depicted by agarose gel electrophoresis. Lanes 1–3 represent uncondensed DNA; lanes 4–6, cationic lipid/DNA mass ratio 4/1; lanes 7–9, cationic lipid/DNA mass ratio 6/1; lanes 10–12, cationic lipid/DNA mass ratio 8/1; lanes 13–15, cationic lipid/DNA mass ratio 10/1. Complexes were processed with SDS (lanes 2, 5, 8, 11 and 14) and DNase I + SDS (lanes 3, 6, 9, 12 and 15). OC: open circular structures, SC: supercoiled structures.

Regarding cell viability, all cationic lipid/DNA mass ratios (w/w) studied above 6/1, had obviously revealed higher percentages of viability with DPP80-CQ nioplexes compared to their DPP80 counter-parts. The viability value of cells transfected with DPP80-CQ at 10/1 cationic lipid /DNA mass ratio (90%) was similar to the viability value obtained with Lipofectamine™ 2000 commercial reagent (89.5%). The micrographs observed in Fig. 3-B_1 for DPP80, and in Fig. 3-B_2 for DPP80-CQ nioplexes, confirmed the previously mentioned difference in the viability of transfected ARPE- 19 cells with both nioplexes at 8/1 and 10/1 cationic lipid/DNA mass ratios respectively.

5.3.3. Cellular uptake studies

Fig. 4-A illustrates the cellular uptake study of both DPP80 and DPP80-CQ nioplexes with FITC-labeled pDNA in ARPE-19 cells carried out by flow cytometry. Nioplexes at the cationic lipid/DNA mass ratio of the highest transfection efficiency, 8/1 and 10/1 for DPP80 and DPP80-CQ respectively, were used to evaluate the uptake percentage after 4 h of incubation. The uptake values of DPP80 and DPP80-CQ were 73.60% and 74%, respectively.

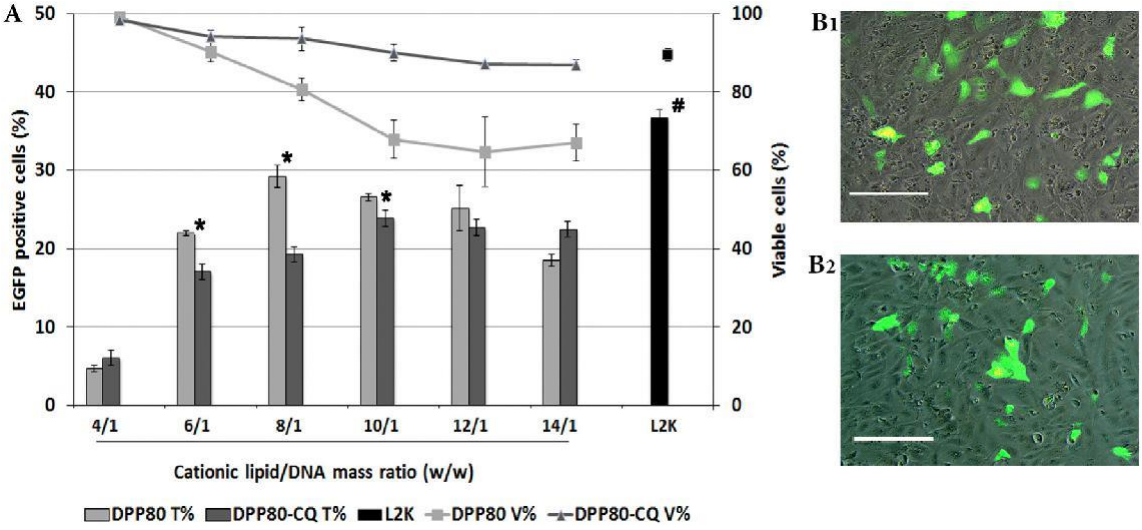

Fig. 3. In vitro transfection and viability performance of both DPP80 and DPP80-CQ nioplexes in ARPE-19 cells. (A) The percentage of EGFP-positive cells (bars) and the percentage of viable cells (lines) at various cationic lipid/DNA mass ratios (w/w) evaluated by flow cytometry at 72 h. Data are expressed in terms of mean ± SD, n = 3. L2K = Lipofectamine™2000. *P < .05 compared to DPP80, $^{\#}$P < .05 compared to nioplexes. (B_1 and B_2) fluorescence and phase-contrast overlay micrographs of ARPE-19 cells after 72 h transfection at 8/1 and 10/1 cationic lipid/DNA mass ratios (w/w) for DPP80 and DPP80-CQ, respectively. Scale bar = 100 μm.

5.3.4. The impacts of endocytosis inhibitors on cellular transfection

Fig. 4-B shows cellular transfection of pCMS-EGFP plasmid, medi-ated by DPP80 (light bars) and DPP80-CQ (dark bars) nioplexes, in ARPE-19 cells with different endocytosis inhibitors. The transfection results were calculated as percentages from the absolute transfection values obtained by DPP80 and DPP80-CQ nioplexes at 8/1 and 10/1 cationic lipid/DNA mass ratios, respectively, in the absence of en-docytosis inhibitors. Transfection efficiency of both nioplexes was slightly affected by the caveolae inhibitor, genistein (transfection values were about 93% for both DPP80 and DPP80-CQ), without statistically significant difference between both nioplexes ($p > 0.05$).

Additionally, selective inhibition of CME (by chlorpromazine hydro-chloride) had a more pronounced effect on DPP80 nioplexes than on DPP80-CQ ($p < 0.05$) (the normalized values of transfection were 67% and 89%, respectively). Nevertheless, transfection efficiency was more affected by methyl-β-cyclodextrin (inhibitor of both CME and CvME) (transfection values decreased to be 11% and 23% for DPP80 and DPP80-CQ nioplexes without inhibition, respectively). Interestingly, wortmannin, an inhibitor of MPC, had statistically reduced the normalized transfection efficiency of DPP80-CQ nioplexes (to be 57%) when compared to DPP80 counterparts (75%).

5.3.5. Buffering capacity of niosomes

Fig. 4-C shows the buffering capacity of both DPP80 and DPP80-CQ niosomes. After addition of successive volumes (100 μl) of a 0.1 M HCl aqueous solution to a fixed volume of niosomes (10.000 μl), the pH titration curve revealed that DPP80-CQ had a considerably higher buffering capacity than DPP80, whereas the initial pH values of both formulations were around 4.

5.3.6. In vivo study

5.3.6.1. Histological assessment after subretinal injections

At 10/1 cationic lipid /DNA mass ratio, DPP80-CQ nioplexes were administered subretinally. After 72 h, EGFP expression in rat retinae was analyzed by CLSM (Fig. 5). In retinal cross sections, EGFP protein expression was recognized in GCL (Fig. 5-A, and B, white arrows). Interestingly, EGFP expression was also observed in some photoreceptor cells (Fig. 5-A, and C, yellow arrows). Such EGFP expression colocalized with some recoverin positive photoreceptors (Fig. 5-B, yellow arrows). Transfection of DPP80-CQ nioplexes on photoreceptors after subretinal administration was also observed on Supplementary Fig. 3 (pink arrows). Additionally, blue arrows observed in Fig. 5-D suggest that some damaged and displaced RPE cells were transfected close to the injection site. It is worth mentioning that no co-localization was observed in the bipolar cells stained with PKC. No fluorescence was detected in the retinae injected with the vehicle (Supplementary Fig. 4-C).

5.3.6.2. Histological assessment after intravitreal injections

Fig. 6 revealed some EGFP expression in whole mount sections of the retina in both GCL (Fig. 6-A, white arrows) and INL (Fig. 6-B, yellow arrows), close to the injection site.

According to the morphology and the retinal layer examined, such fluorescence could correspond to ganglion and amacrine transfected cells. In any case, endothelial cells migrating to the injection site or glial cells could also have been transfected. Transfection in the GCL was also observed in retinal cross-sections (Fig. 6-D, white arrows) and, interestingly, in the OPL (Fig. 6-C, blue arrows).

After both intravitreal and subretinal injections, we did not observe GFP expression in regions distal from the injection sites (Fig. 4-A, B, Supplementary data).

5.4.Discussion

In this research work, we offer a novel approach to design, char-acterize and evaluate chemical vectors for retinal gene delivery. More precisely, we evaluated the role of chloroquine incorporation into niosomes composed of cationic lipid and a mixture of non-ionic surfactants.

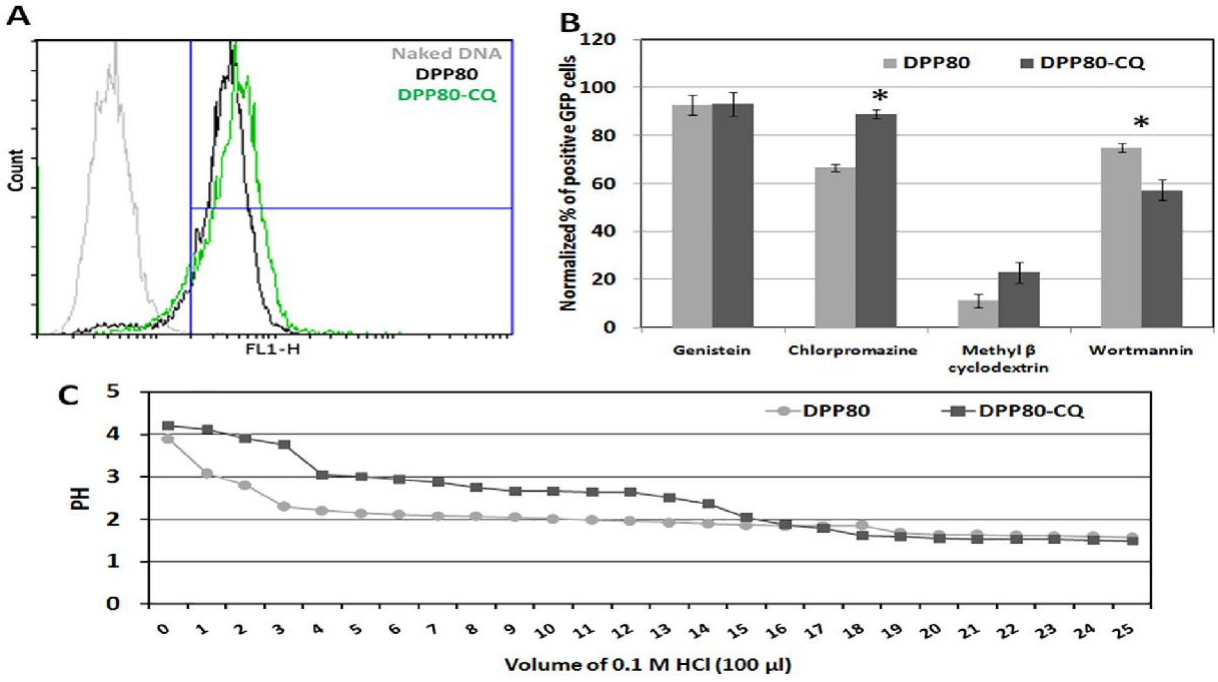

Fig. 4. Cellular uptake and internalization studies of both DPP80 and DPP80-CQ nioplexes at 8/1 and 10/1 cationic lipid/DNA mass ratio. (A) Flow cytometry histograms representing the FITC-labeled plasmid uptake in ARPE-19 cells after 4 h of incubation. (B) Endocytic inhibitors effect on the transfection performance of DPP80 and DPP80-CQ nioplexes. The values were normalized to the transfection without inhibitor. *P < .05 (C) pH buffering capacity analysis of DPP80 and DPP80-CQ niosomes.

Chloroquine, by itself, can enhance transfection efficiency whenever included to the cell culture medium or incorporated into cationic-peptide-DNA complexes [19] in a dose-dependent matter. However, the pre-treatment with chloroquine, has shown high toxicity levels that limit further clinical applications [20]. To avoid such noxious effect, in the current study, chloroquine was incorporated within the niosome formulation. Such inclusion of chloroquine into a niosome formulation, rather than as a co-/pre-treatment of cells, would be a more logical approach for in vivo settings. The amphiphilic nature of both non-ionic surfactants used (P80 and P) can deliver both hydrophilic and lipophilic molecules. Interestingly, propylene oxide chains of the P can interact with lipid membranes and induce their structural re-arrangement for better stability and translocation of the gene carriers [21]. In addition, the incorporation of P

to polycation-DNA complexes enhanced the expression level of the delivered genes in both in vitro and in vivo conditions at doses below the known toxicity levels [22]. P80 has been reported to act as a co-emulsifier along with P, in drug and gene delivery endeavors [23]. Moreover, the encouraging properties of P80 create a steric barrier that evades the aggregation of nano-vesicles, enhances the cell tolerance [11], and improves transfection efficiency due to the presence of polyethylene glycol (PEG) chains in its structure [24]. However, the ability P to form network structures might be more suitable than P80, if used with water-soluble cationic lipids, to enhance their flexibility and durability [25]. In such case, a mixture of two specific types of non-tensioactive molecules could provide a synergistic enhancement of nano-vesicle stabilization [26].

Regarding the cationic lipid, the high solubility of the D-Cl salt enhances biodistribution of lipid/plasmid complexes, and therefore, transfection efficiency [27]. However, in a previous study, we observed that the solubility of cationic lipid can dramatically shift the transfection results according to the type of the cells and the way of formulation. In that study, the DTPA cationic lipid (non-salt form) succeeded to transfect retinal cells in vitro conditions [11], while in such mentioned study, the salt form failed to transfect retinal cells in vivo. Interestingly, the same formulation with the same salt form of cationic lipid (DPP80) succeeded to transfect cerebral cortical cells in vivo [28]. Strikingly, both salt/non-salt forms of the cationic lipid were able to transfect ARPE-19 cells in vitro conditions. In any case, the non-salt form was superior in terms of transfection and cell viability. This contradiction emphasizes the lack of correlation between the in vivo and in vitro transfection conditions and the importance of the formulation at physical level.

To emphasize the impact of chloroquine, DPP80 and DPP80-CQ niosomes were elaborated and compared. The characterization data of both niosomes were analyzed (Table 1). The incorporation of chloroquine slightly increased the size of niosomes by about 28 nm, and reduced both PDI (about 69% decrease) and ZP (about 34% decrease). Drug/gene delivery vehicles are generally favored by small poly-dispersity values [29]. The positive ZP values (> +25 mV) detected for both niosomes would reflect a

potentially long-lasting stability. Once the niosomes were characterized in terms of size, PDI, and zeta potential, nioplexes were elaborated with the pCMS-EGFP plasmid at various cationic lipid/DNA mass ratios by adding the reporter plasmid to the niosomes and not the opposite to ensure proper condensation process [30].

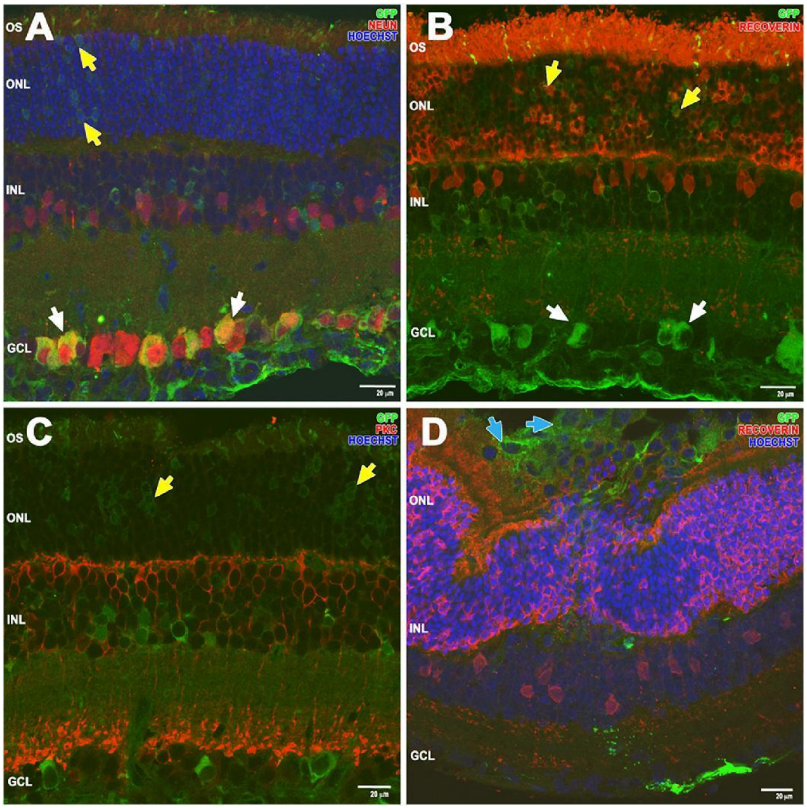

Fig. 5. Retinal cross sections micrographs obtained by confocal microscopy 3 days post subretinal injection of DPP80-CQ nioplexes (A–D). EGFP protein was observed mainly in GCL (white arrows), photoreceptors (yellow arrows) and RPE cells (blue arrows). Retinal sections were stained with antibodies against NeuN(A), recoverin (B, D) and protein kinase C (C). The cell nuclei were counterstained with Hoechst 33342. GCL, ganglion cell layer; INL, inner nuclear layer; ONL, outer nuclear layer; OS, photoreceptor outer segment Scale bars: 20 μm. (For interpretation of the references to colour in this figure legend, the reader is referred to the web version of this article.)

The ZP of DPP80 nioplexes was clearly lower when compared to the same niosomes without chloroquine (Fig. 2-A). On the other hand, ZP of chloroquine-containing nioplexes (DPP80-CQ) oscillated within a narrower range (19–25 mV) in comparison to DPP80-CQ niosomes (29 mV). Generally, the compaction of DNA is improved when 90% of the charge is compensated in an aqueous solution [31]. Strikingly, at 8/1 and 10/1 mass ratios for DPP80 and DPP80-CQ, respectively, ZP values fluctuated within a narrow range (23–27 mV) which represents a small reduction

in ZP for DPP80-CQ compared to ZP of niosomes (29 mV). This suggests a spontaneous electrostatic inter-action of pDNA with DPP80-CQ niosomes at 10/1 mass ratio which could be explained by a direct interaction of chloroquine with pDNA. Regarding PDI values of nioplexes, an obvious effect of chloroquine addition at all ratios studied above 4/1 was observed, as PDI values decreased in comparison to DPP80 formulation (Supplementary Table 1). The electron micrographs illustrated a discrete, almost spherical morphology and absence of aggregates in DPP80 complexes (Fig. 2-B_1). By contrast, DPP80-CQ nioplexes appeared as clusters of multilamellar planar structures that form string-like colloidal aggregates (Fig. 2-B_2). The lamellar spacing was around 5.5–6 nm, suggesting that the pDNA strands were complexed with the cationic lipid bilayers [15]. Similarly, many mixtures of neutral lipids (as DOPC and DOPE), along with cationic lipids (as DOTAP), extensively used for gene delivery purposes, are known to form lamellar complexes with DNA [32].

The agarose gel retardation assay showed that both niosomes, at all studied cationic lipid/DNA ratios, were able to condense, release and protect the DNA from enzymatic digestion (Fig. 2-C). Of note, the relatively lower DNA condensation, observed by the chloroquine-containing formulation (Fig. 2-C_2), did not hamper the release or the protection of the condensed DNA, which is of utmost importance during the transfection process. Any change in condensation efficiency might affect the pattern and topology of spatial DNA configuration. Even more, the state of DNA condensation can be affected by both the type and the content of the surfactant or other additives as chloroquine. Therefore, the fine-tuning of such molecules could be of importance to unveil the mechanism of condensation of different types of DNA molecules within different nano-vesicles. Even at high concentrations of chloroquine, 100 μg/ml, ARPE-19 cells appeared healthy with good viability, despite the appearance of many vacuoles in the cytoplasm (Supplementary Fig. 1). The transfection efficiency in vitro, ARPE-19 cells, fluctuated within a small range in both vectors at all mass ratios studied (Fig. 3). However, the cell viability was in favor of DPP80-CQ (Fig. 3-A). Noteworthy, chloroquine inhibits lysosomal enzymes by increasing the pH of the lysosomes and disturbing their fusion with autophagosomes, thus inhibits autophagy [33]. Moreover,

chloroquine and its autophagy inhibiting derivative, hydroxychloroquine, are both FDA-approved agents [34]. According to the cell type or the state of stress, autophagy might protect or promote cell death in the eye [35].

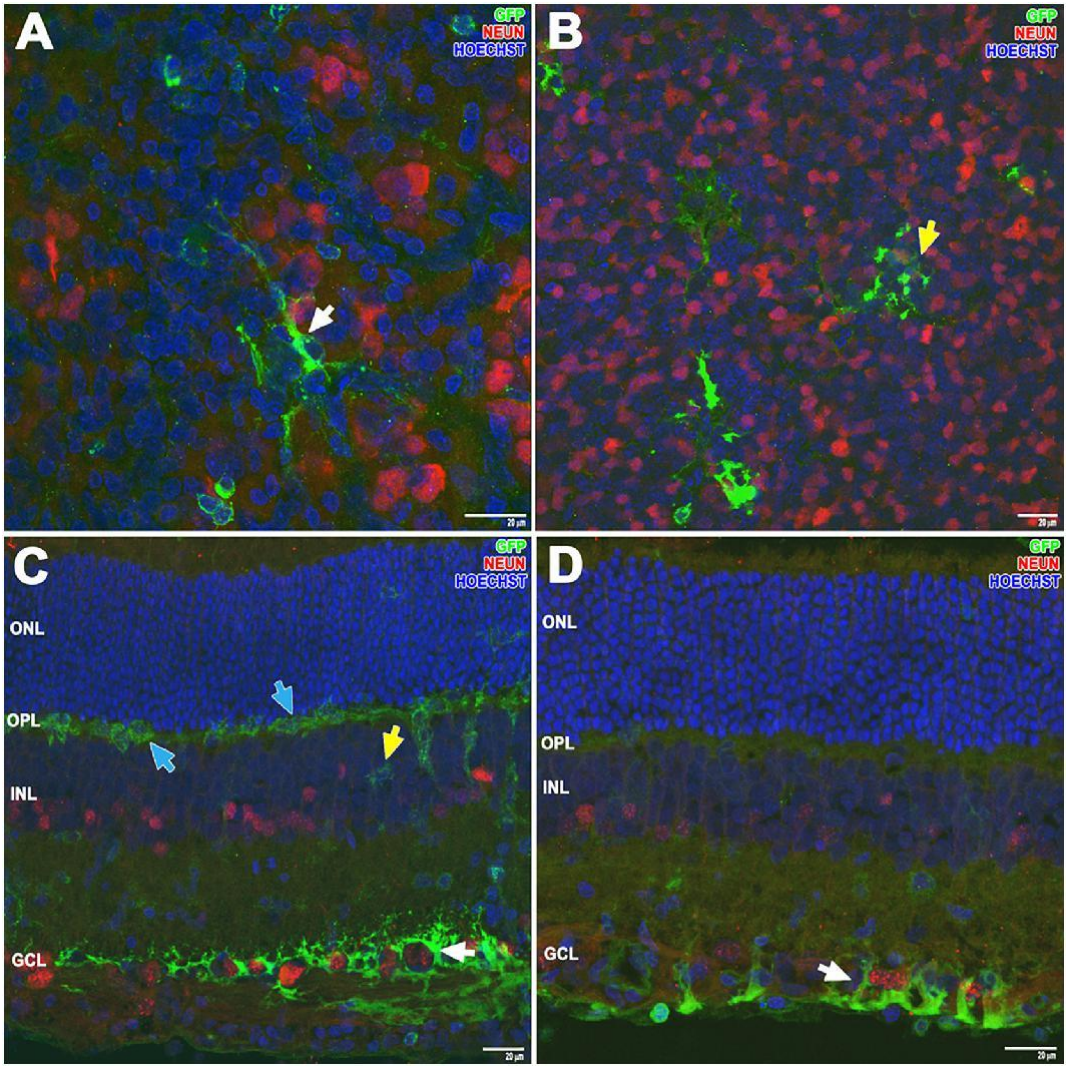

Fig. 6. Confocal fluorescence micrographs of whole mount (A, B) and cross-sections (C, D) of the retina 3 days after intravitreal administration of DPP80-CQ nioplexes. EGFP expression can be observed in both GCL (A, C and D, white arrows) and INL (B and C, yellow arrows). Interestingly, some protein expression was also observed in OPL (C, blue arrows). Whole mount and retinal sections were stained with NeuN (A-D). The cell nuclei were counterstained with Hoechst 33342 (blue). GCL, Ganglion cell layer; INL, inner nuclear layer; ONL, outer nuclear layer; OPL, outer plexiform layer. Scale bars: 20 μm. (For interpretation of the references to colour in this figure legend, the reader is referred to the web version of this article.)

This mutable nature of autophagy might be the reason for the increased cell viability observed with DDP80-CQ formulation in comparison with its chloroquine-free

counterpart, DPP80. Generally, cell viability and metabolism of ARPE-19 cells are relatively unaffected by the concentrations of chloroquine between 10 and 30 μg/ml, though affected in a dosage-dependent fashion afterward [36]. To analyze whether the enhanced cell internalization of nioplexes was among the effects that chloroquine could have on niosome formulations, we determined the percentage of ARPE-19 cell uptake of both DPP80 and DPP80-CQ formulations at the mass ratios of best transfection efficiency, 8/1 for DPP80 and 10/1 for DPP80-CQ (Fig. 4).

Interestingly, flow cytometry studies showed that chloroquine incorporation had an insignificant effect on the percentage of cellular uptake when compared to the DPP80 formulation (Fig. 4-A). Such observation is most probably due to the indifferent surface charge of both nioplexes at the aforementioned mass ratios (22.5 ± 7.3 and 25.3 ± 2.5 for DPP80 and DPP80-CQ, respectively, $P > .05$). The similar uptake percentages in such ratios could justify the unaltered transfection results depicted pre-viously (Fig. 3-A). The transfection efficiency can be markedly affected by the mechanism of endocytosis. Consequently, we studied three of the most active cellular internalization pathways: clathrin-mediated endocytosis (CME), caveolae-mediated endocytosis (CvME) and macro-pinocytosis (MPC). The results observed in Fig. 4-B suggested that DPP80-CQ nioplexes were internalized mainly by MPC, while CvME and CME had less participation in the cellular uptake process. Due to its ability to internalize larger structures, macropinocytosis pathway has been proposed to mediate the internalization of non-viral gene delivery vehicles [37]. Moreover, MPC is considered as the major pathway responsible for DNA transfection in certain cell types [38]. In contrary, DPP80 nioplexes were internalized mainly by CME and, to a lesser extent, by MPC, while CvME had a much less participation in the cellular uptake process. However, the minor fluctuation in transfection efficiency between the two nioplexes could be due to limited variations between the two main different mechanisms of internalization (CME for DPP80 and MPC for DPP80-CQ). The delivery of genetic material by CvME and CME passes through late endosomes/lysosomes, which in-creases the hazards of DNA degradation and lowers the transfection efficiency [39]. So, an expected trivial effect of CvME and especially CME pathways could explain the high percentages of EGFP expression in ARPE cells by both nioplexes (Fig. 3), compared to lipofectamine® 2000

(approximately, 80% and 75% of lipofectamine®2000 for DPP80 and DPP80-CQ, respectively).

Afterwards, we analyzed the pH-buffering capacity of both niosomes (Fig. 4-C). The incorporation of chloroquine into the niosome formulation increased the pH-buffering capacity upon titration with 0.1 M HCl, compared to the niosomes elaborated without chloroquine (at pH values > 2). Though, there was no change in the buffering capacity when the pH was < 2 for both niosomes. Chloroquine might induce endosomal and lysosomal escape via the proton sponge effect [40]. This result could suggest that chloroquine-containing formulation could increase the proton sponge effect, and therefore, the endosomal escape capacity of DPP80-CQ niosomes. However, as the predominant mechanism of internalization for DPP80-CQ was neither CvME nor CME, the impact of the proton sponge effect of chloroquine on the transfection efficiency was insignificant.

Based on the previously mentioned physicochemical and in vitro biological results, we were enthusiastic to perform a preliminary in vivo study to evaluate the transfection efficiency of our formulations, DPP80-CQ in particular, in rat retinae after both subretinal (Fig. 5), and intravitreal injections (Fig. 6). Subretinal injection is a well-known clinical route to deliver genetic/drug material to the back of the eye. In addition, it enables direct contact of the injected nucleic acids with the outer retinal layers, photoreceptors and RPE cells. Noteworthy, clinical trials to treat many inherited retinal diseases such as LCA type 2 used the subretinal injection route [41]. However, it is less desirable than the intravitreal route due to the possible complications; such as retinal detachment or the localized side effects around the site of injection. Generally, IV injection is more widely applicable in the clinical practice due to its ability to deliver genetic material to a larger retinal surface, in addition to less surgical trauma compared to the SR route [42].

Surprisingly, DPP80 did not induce any transfection to retinal cells in vivo after both subretinal or intravitreal injections (Supplementary Fig. 2), whereas the

chloroquine-containing formulation, DPP80-CQ did (Figs. 5 and 6). The lack of correlation between in vitro and in vivo transfection results has been widely reported as it is a context-dependent matter [12].

Based on previous physicochemical and in vitro biological results, we were enthusiastic to perform a preliminary in vivo study to evaluate the transfection efficiency of our formulations, DPP80-CQ in particular, in rat retinae after subretinal (Fig. 5) and intravitreal injections (Fig. 6). Subretinal injection is a well-known clinical viable route to deliver genetic material to the eye. It enables direct contact of the injected nucleic acids with the outer retinal layers, photoreceptors and RPE cells. Noteworthy, clinical trials to treat many inherited retinal diseases such as LCA type 2 use subretinal injection [41]. However, it is less desirable than the IV route due to the possible complications such as retinal detachment or the localized effect around the site of injection. Generally, intravitreal injection is more widely applicable in the clinical practice due to its ability to deliver genetic materials to a larger retinal surface and advantages of less surgical trauma compared to the SR route [42].

Subretinal administration allows direct contact of genetic material with RPE cells and outer layer of the retina. Although this route of administration is highly effective to locally transfect cells close to the site of the injection, the occasionally observed side effects, related to this invasive route, such as retinal detachment, hemorrhages or alterations in RPE cells can hamper its practice [43]. In any case, sub-retinal injections have been widely used on clinical trials to treat some devastating genetic disorders of the retina reporting excellent outcomes [44]. In addition, the recently FDA/EMA-approved Luxturna medicine
to deliver healthy copies of the RPE65 gene to the retina is administered by subretinal injection. In our in vivo experiments, after subretinal administration of nioplexes, we observed localized EGFP expression, mainly in some photoreceptor and RPE cells, close to the injection site. Transfection at this level can have clinical relevance because mutations of > 200 genes in RPE cells/photoreceptors are related to relevant ge-netic

disorders of the retina such as; Leber congenital amaurosis, retinitis pigmentosa, and Stargardt disease, to name just a few ones [45].

Compared to subretinal injection, intravitreal injection represents an interesting alternative to deliver genetic material to the back of the eye, and therefore to access retinal structure. It is a less invasive route, more easily to perform, and higher doses can be delivered [46]. Consequently, large retinal surfaces can be transfected by this route of administration [47]. When we administered 4 µl of DPP80-CQ nioplexes by intravitreal injection, the inner layers of the retina (GCL and INL) were mainly transfected as observed in Fig. 6. (white and yellow arrows, respectively). Transfection at this level can be of clinical relevance in treatment of devastating ocular pathologies that compromise the function of ganglion cells as glaucoma [48]. Interestingly, EGFP expression was also discerned in the OPL (Fig. 6-C, blue arrows) which suggests that nioplexes partially diffused, not only through the vitreous where they were administered, but also through the inner retinal layers until reach the OPL. Transfection of the outer layers of the retina by intravitreal administration of non-viral vectors represents a great challenge for the scientific community, since can avoid the subretinal injections and the corresponding side effects commonly associated to such injection.

Unfortunately, chloroquine, like other endolytic agents, has been found to be cytotoxic in several pre-clinical or clinical trials [49]. Chloroquine passes the blood-retinal barrier and is toxic to the retina. Nevertheless, such retinal toxicity is related to large doses and long-term use of chloroquine [50]. In this study, at 10/1 cationic lipid /DNA mass ratio, the final concentration of chloroquine was only 25 µg/ml which did not induce any significant cytotoxicity in accordance with Chen et al, [36]. The affinity of retinal cells to the modified salt form of the cationic lipid, in addition to the favorable properties of P and P80, along with the effect of chloroquine, raise the possibility to target different retinal cell layers safely and effectively after both subretinal and intravitreal administrations.

5.5.Conclusions

The addition of chloroquine to a niosome formulation retained its functionality in vitro, but most importantly, enhanced its transfection ability in vivo. This work highlights the use of chloroquine as a built-in component in the gene delivery vehicles to evade its toxicity and to provide new insights into the future of retinal gene therapy.

5.6.Acknowledgements and disclosures

This project was supported by the Basque Country Government (CGIC10/172), Spanish Ministry of Education (Grant CTQ2017-84415-R, MAT2015-69967-C3-1R), the Generalitat de Catalunya (2014/SGR/

and the Instituto de Salud Carlos III (CB06_01_0019, CB06_01_1028). The authors also wish to thank the intellectual and technical assistance from the ICTS "NANBIOSIS", more specifically by the Drug Formulation Unit (U10) of the CIBER in Bioengineering, Biomaterials, and Nanomedicine (CIBER-BBN) at the University of Basque Country (UPV/EHU). Technical and human support provided by SGIker (UPV/EHU) is acknowledged.

5.7. Supplementary data

Supplementary data to this article can be found online at https://
doi.org/10.1016/j.jconrel.2019.05.010.

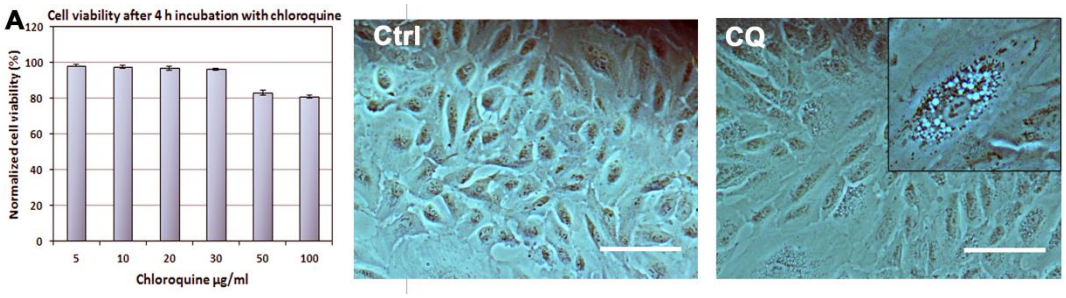

Supplementary fig.1. (A) ARPE-19 cell viability after 4h of incubation with different concentrations of chloroquine diphosphate. Phase contrast microscopy of ARPE-19 cells showing control cells (Ctrl) and cells with vacuolated cytoplasm (CQ) after their treatment with chloroquine diphosphate 100ug/ml.

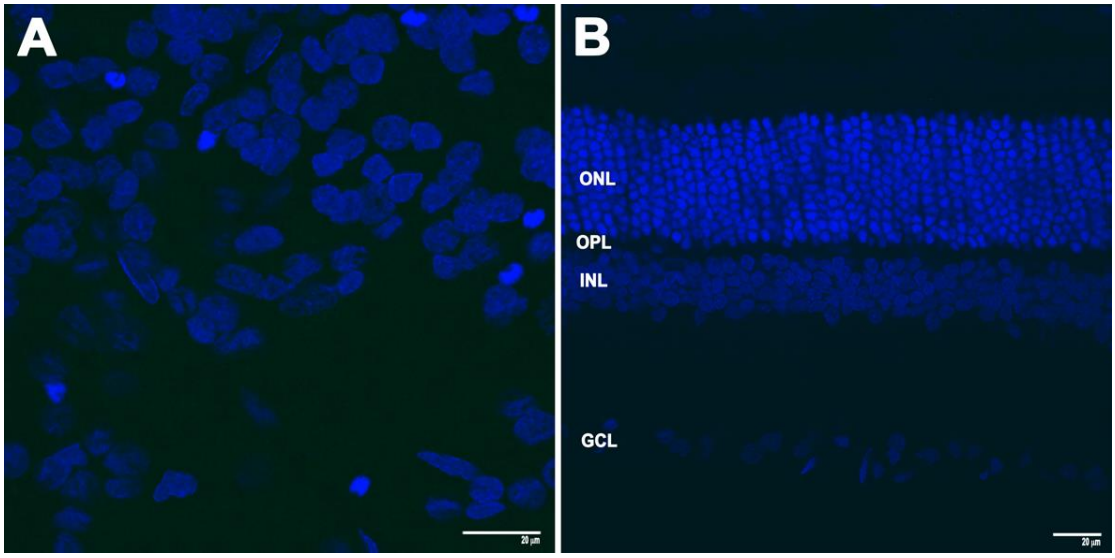

Supplementary fig. 2. Confocal fluorescence micrographs of (A) retinal whole mount after 3 days of intravitreal administration of **DPP80** nioplexes and of (B) retinal cross-sections after 3 days of subretinal administration of **DPP80** nioplexes. There is no GFP expression detected in different retinal layers. Scale bars: 20 µm.

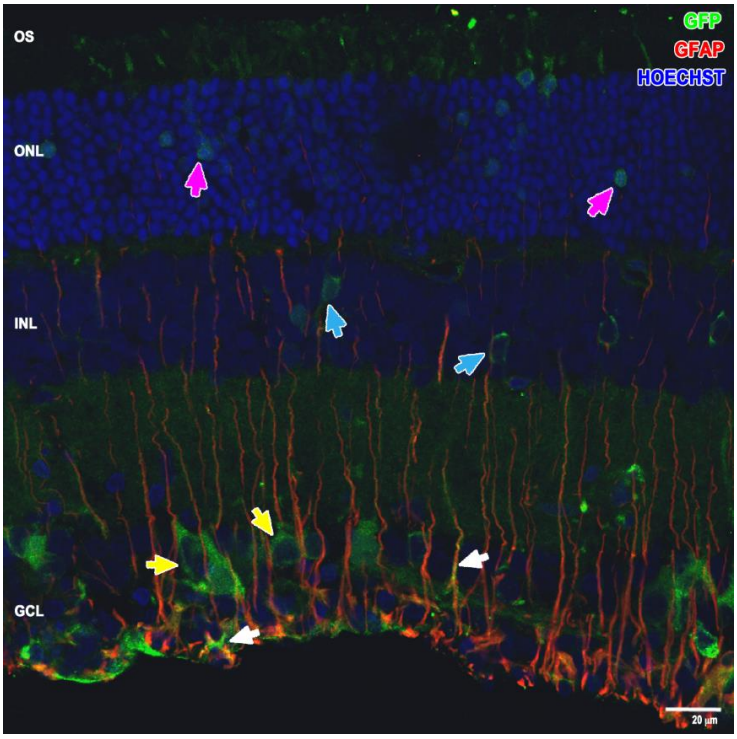

Supplementary Fig.3. EGFP expression after subretinal injection of DPP80-CQ nioplexes in retinal cross-section obtained close to the site of injection. EGFP expression colocalizes with GFAP-positive Müller glial cells (white arrows). EGFP expression can also be observed in the ganglion cell layer (yellow arrows), in the INL (blue arrows) and in the photoreceptors of the ONL (pink arrows). The cell nuclei were counterstained with Hoechst 33342 (blue). GCL, ganglion cell layer; INL, inner nuclear layer; ONL, outer nuclear layer; OS, photoreceptor outer segment. Scale bar: 20 µm.

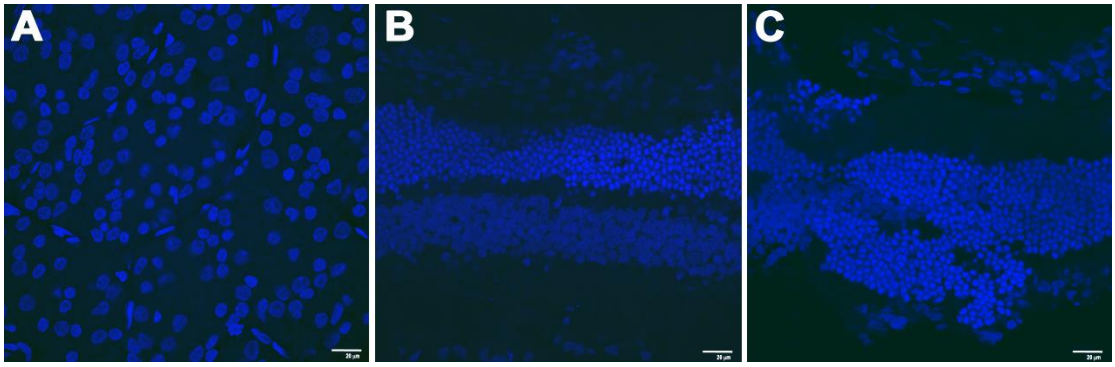

Supplementary Fig.4. Whole mount (A), and retinal cross-sections (B) after both intravitreal and subretinal injection of DPP80-CQ nioplexes. No EGFP fluorescence was observed neither in ganglion cell layer of whole mount (A) nor in retinal cross-sections (B) obtained approximately 300-400 µm away from the injection site after both injections. (C) Retinal cross-section at the site of subretinal injection of the vehicle alone in a control retina. No EGFP expression was observed. The cell nuclei were counterstained with Hoechst 33342 (blue). Scale bars: 20 µm.

Supplementary table 1. Polydispersity index values of both nioplexes (**DPP80** and **DDP80-CQ**). Data represent mean ± standard deviation, n=3.

N/P ratios	4/1	6/1	8/1	10/1	12/1
DPP80	0.211±0.017	0.260±0.014	0.217±0.003	0.288±0.032	0.202±0.005
DPP80-CQ	0.239±0.039	0.139±0.007	0.208±0.055	0.190±0.012	0.182±0.014

5.8.References

1 I.J. Constable, et al., Gene therapy for age-related macular degeneration, Asia Pacific J. Ophthalmol. 5 (4) (2016) 300–303.

2 A.M. Maguire, et al., Age-dependent effects of RPE65 gene therapy for Leber's congenital amaurosis: a phase 1 dose-escalation trial, Lancet 374 (9701) (2009) 1597–1605.

3 W.A. Beltran, et al., Gene therapy rescues photoreceptor blindness in dogs and paves the way for treating human X-linked retinitis pigmentosa, Proc. Natl. Acad. Sci. 109 (6) (2012) 2132–2137.

4 K. Balaggan, R. Ali, Ocular gene delivery using lentiviral vectors, Gene Ther. 19 (2) (2012) 145.

5 A.M. Maguire, et al., Safety and efficacy of gene transfer for Leber's congenital amaurosis, N. Engl. J. Med. 358 (21) (2008) 2240–2248.

6 M.F. Naso, et al., Adeno-Associated Virus (AAV) as a Vector for Gene Therapy, 31(4) (2017), pp. 317–334.

7 D.J. Jiang, C.L. Xu, S.H.J.G. Tsang, Revolution in Gene Medicine Therapy and Genome Surgery, 9(12) (2018), p. 575.

8 M. Agirre, et al., Delivery of an Adenovirus Vector Plasmid by Ultrapure Oligochitosan Based Polyplexes, 479(2) (2015), pp. 312–319.

9 M. Mashal, et al., Non-viral Vectors Based on Cationic Niosomes as Efficient Gene Delivery Vehicles to Central Nervous System Cells into the Brain, 552(1–2) (2018), pp. 48–55.

10 R. Zulliger, et al., Optimizing Non-viral Gene Therapy Vectors for Delivery to Photoreceptors and Retinal Pigment Epithelial Cells, in Retinal Degenerative Diseases, Springer, 2018, pp. 109–115.

11 G. Puras, et al., A novel cationic niosome formulation for gene delivery to the retina, J. Control. Release 174 (2014) 27–36.

12 M. Mashal, et al., Retinal gene delivery enhancement by lycopene incorporation into cationic niosomes based on DOTMA and polysorbate 60, J. Control. Release 254 (2017) 55–64.

13 S. Grijalvo, et al., Cationic Niosomes as Non-Viral Vehicles for Nucleic Acids: Challenges and Opportunities in Gene Delivery, 11(2) (2019), p. 50.

14 G.P. Kumar, P. Rajeshwarrao, Nonionic surfactant vesicular systems for effective drug delivery—an overview, Acta Pharm. Sin. B 1 (4) (2011) 208–219.

15 N. Attia, et al., Stem cell-based gene delivery mediated by cationic niosomes for bone regeneration, Nanomedicine 14 (2) (2018) 521–531.

16 P. Erbacher, et al., Putative role of chloroquine in gene transfer into a human hepatoma cell line by DNA/lactosylated polylysine complexes, Exp. Cell Res. 225 (1) (1996) 186–194.

17 G. Kokotos, R. Verger, A. Chiou, Synthesis of 2-oxo amide triacylglycerol analogues and study of their inhibition effect on pancreatic and gastric lipases, Chem. Eur. J. 6 (22) (2000) 4211–4217.

18 E. Ojeda, et al., Elaboration and Physicochemical Characterization of Niosome-Based Nioplexes for Gene Delivery Purposes, in Non-Viral Gene Delivery Vectors, Springer, 2016, pp. 63–75.

19 S. Yang, et al., Cellular uptake of self-assembled cationic peptide–DNA complexes: multifunctional role of the enhancer chloroquine, J. Control. Release 135 (2) (2009) 159–165.

20 X. Zhang, et al., The in vivo use of chloroquine to promote non-viral gene delivery to the liver via the portal vein and bile duct, J. Gene Med. 5 (3) (2003) 209–218.

21 M. Morille, et al., Progress in developing cationic vectors for non-viral systemic gene therapy against cancer, Biomaterials 29 (24–25) (2008) 3477–3496.

22 S. Sriadibhatla, et al., Transcriptional activation of gene expression by pluronic block copolymers in stably and transiently transfected cells, Mol. Ther. 13 (4) (2006) 804–813.

23 A.V. Kabanov, E.V. Batrakova, V.Y. Alakhov, Pluronic® block copolymers as novel polymer therapeutics for drug and gene delivery, J. Control. Release 82 (2–3) (2002) 189–212.

24 H. Lee, J.H. Jeong, T.G. Park, PEG grafted polylysine with fusogenic peptide for gene delivery: high transfection efficiency with low cytotoxicity, J. Control. Release 79 (1–3) (2002) 283–291.

[13] C. Freitas, R.H. Müller, Effect of light and temperature on zeta potential and physical stability in solid lipid nanoparticle (SLN™) dispersions, Int. J. Pharm. 168 (2) (1998) 221–229.

[14] McGregor, W.C., J. Stubstad, and C.P. Chang, Pharmaceutical compositions of bactericidal/permeability increasing protein (BPI). 2000, Google Patents.

[15] R.I. Mahato, Water insoluble and soluble lipids for gene delivery, Adv. Drug Deliv. Rev. 57 (5) (2005) 699–712.

[16] N. Attia, et al., Gene Transfer to Rat Cerebral Cortex Mediated by Polysorbate 80 and Poloxamer 188 Nonionic Surfactant Vesicles, (2018).

[17] N. Nafee, et al., Chitosan-coated PLGA nanoparticles for DNA/RNA delivery: effect of the formulation parameters on complexation and transfection of antisense oligonucleotides, Nanomedicine 3 (3) (2007) 173–183.

[18] L. Wasungu, D. Hoekstra, Cationic lipids, lipoplexes and intracellular delivery of genes, J. Control. Release 116 (2) (2006) 255–264.

[19] F. Ke, et al., Characterizing DNA condensation and conformational changes in organic solvents, PLoS One 5 (10) (2010) e13308.

[20] J.O. Rädler, et al., Structure of DNA-cationic liposome complexes: DNA intercalation in multilamellar membranes in distinct interhelical packing regimes, Science 275 (5301) (1997) 810–814.

[21] P. Maycotte, et al., Chloroquine sensitizes breast cancer cells to chemotherapy in-dependent of autophagy, Autophagy 8 (2) (2012) 200–212.

[22] S. Zhou, et al., Autophagy in tumorigenesis and cancer therapy: Dr. Jekyll or Mr. Hyde? Cancer Lett. 323 (2) (2012) 115–127.

[23] S.-J. Sheu, et al., Differential autophagic effects of vital dyes in retinal pigment epithelial ARPE-19 and photoreceptor 661W cells, PLoS One 12 (3) (2017) e0174736.

[24] P.M. Chen, Z.J. Gombart, J.W. Chen, Chloroquine treatment of ARPE-19 cells leads to lysosome dilation and intracellular lipid accumulation: possible implications of lysosomal dysfunction in macular degeneration, Cell Biosci. 1 (1) (2011) 10.

[25] C.M. Wiethoff, C.R. Middaugh, Barriers to nonviral gene delivery, J. Pharm. Sci. 92 (2) (2003) 203–217.

[26] X.-X. Zhang, P.G. Allen, M. Grinstaff, Macropinocytosis is the major pathway responsible for DNA transfection in CHO cells by a charge-reversal amphiphile, Mol. Pharm. 8 (3) (2011) 758–766.

[27] S. Xiang, et al., Uptake mechanisms of non-viral gene delivery, J. Control. Release 158 (3) (2012) 371–378.

[28] L.D. Cervia, et al., Distinct effects of endosomal escape and inhibition of endosomal trafficking on gene delivery via electrotransfection, PLoS One 12 (2) (2017) e0171699.

[29] J. Bennett, et al., AAV2 gene therapy readministration in three adults with con-genital blindness, Sci. Transl. Med. 4 (120) (2012) (p. 120ra15-120ra15).

[30] H. Koo, et al., The movement of self-assembled amphiphilic polymeric nano-particles in the vitreous and retina after intravitreal injection, Biomaterials 33 (12) (2012) 3485–3493.

[31] C. Bloquel, et al., Non-viral Ocular Gene Therapy: Potential Ocular Therapeutic Avenues, 58(11) (2006), pp. 1224–1242.

[32] Y. Peng, L. Tang, Y. Zhou, Subretinal Injection: A Review on the Novel Route of Therapeutic Delivery for Vitreoretinal Diseases, Ophthalmic Res. 58 (2017) 217–226.

[33] M. Hims, S. Daiger, C. Inglehearn, Retinitis pigmentosa: genes, proteins and prospects, Genetics in Ophthalmology, Karger Publishers, 2003, pp. 109–125.

[34] A. del Pozo-Rodríguez, et al., Applications of Lipid Nanoparticles in Gene Therapy, 109 (2016), pp. 184–193.

[35] P. Dureau, et al., Quantitative Analysis of Subretinal Injections in the Rat, 238(7) (2000), pp. 608–614.

[36] A. Bosco, et al., Complement C3-Targeted Gene Therapy Restricts Onset and Progression of Neurodegeneration in Chronic Mouse Glaucoma, 26(10) (2018), pp. 2379–2396.

[37] P. Lönn, et al., Enhancing endosomal escape for intracellular delivery of macro-molecular biologic therapeutics, Sci. Rep. 6 (2016) 32301.

[38] N. Kasturi, Long-term continuation of chloroquine-induced retinal toxicity in rheumatoid arthritis despite drug cessation, Rheumatology 55 (4) (2015) 766–768.

Chapter 6

General discussion

Presently, cationic niosomes, as non-viral gene delivery carrier, have become an important tool to deliver both genetic macromolecules and drug molecules. Development of efficient non-viral gene delivery systems could reduce the time and save expenses for coming new market therapies. In addition, they would be significantly safer than their viral counterparts. Development of safe and efficient non-viral vectors to deliver DNA into the CNS represents a huge challenge to face many neurological disorders. Despite its peripheral location, the retina or neural layer of the eye, is actually a part of the central nervous system.

In the current study, we have designed, prepared and characterized niosome formulations based on different cationic lipids and various helper molecules. *In vitro* studies were conducted to evaluate transfection efficiency, viability and internalization mechanism in ARPE-19 and NT2 cells. Subsequently, their *in vivo* application was evaluated in both retina and brain.

6.1 Lycopene enhances the efficacy of cationic niosomes based on DOTMA and polysorbate 60 for retinal gene delivery purposes

Due to its appealing chemical structure, the commercially available cationic lipid DOTMA has been used widely for gene delivery applications (1).

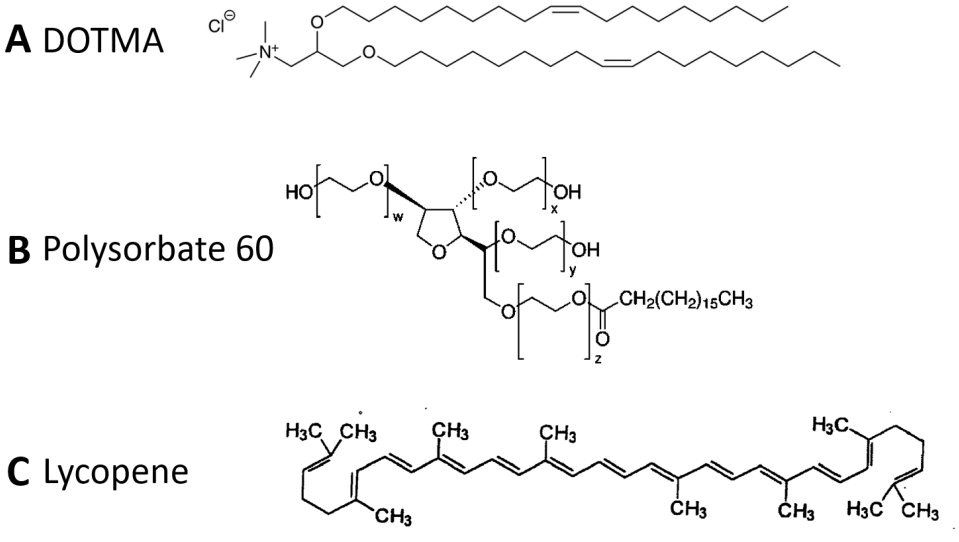

Fig. 1. Chemical structures of the cationic lipid, N-[1-(2,3-dioleoyloxy)propyl]-N,N,N-trimethylammonium chloride (DOTMA) (A), Polysorbate 60 (B), and Lycopene (C).

As shown in Fig. 1-A, its structure is composed of a polar head-group, two non-polar hydrophobic chains, a linker and a back-bone, which classically are known as the four domains that rule gene transfection process (2).

We combined DOTMA with the non-ionic surfactant polysorbate 60, in a niosome formulation at a molar ratio of 1:4 respectively, in order to enhance cell tolerance (3) and provide a steric barrier to avoid aggregation (4). It has been reported on the literature that the presence of PEG chains in the chemical structure of polysorbates (Fig. 1-B) provides physicochemical stability to lipid formulations (5), conserves effectiveness over time and boosts transfection efficiency (6).

Table 1

Physical characterization of DP60 and DP60L niosomes regarding particle size (nm); Polydispersity index (PDI), and Zeta potential (mV). Data represent mean ± SD (n = 3).

Particle	Size (nm)	PDI	Zeta potential (mV)
DP60 niosome	66.49 ± 1.17	0.46±0.02	45.30±1.57
DP60L niosome	101.60 ± 2.48	0.44±0.02	33.80±1.13

Compared with polysorbate 80, another polysorbate that has been widely used in the elaboration of niosome formulations for gene delivery applications, [15–17,31] polysorbate 60 could offer some important advances.

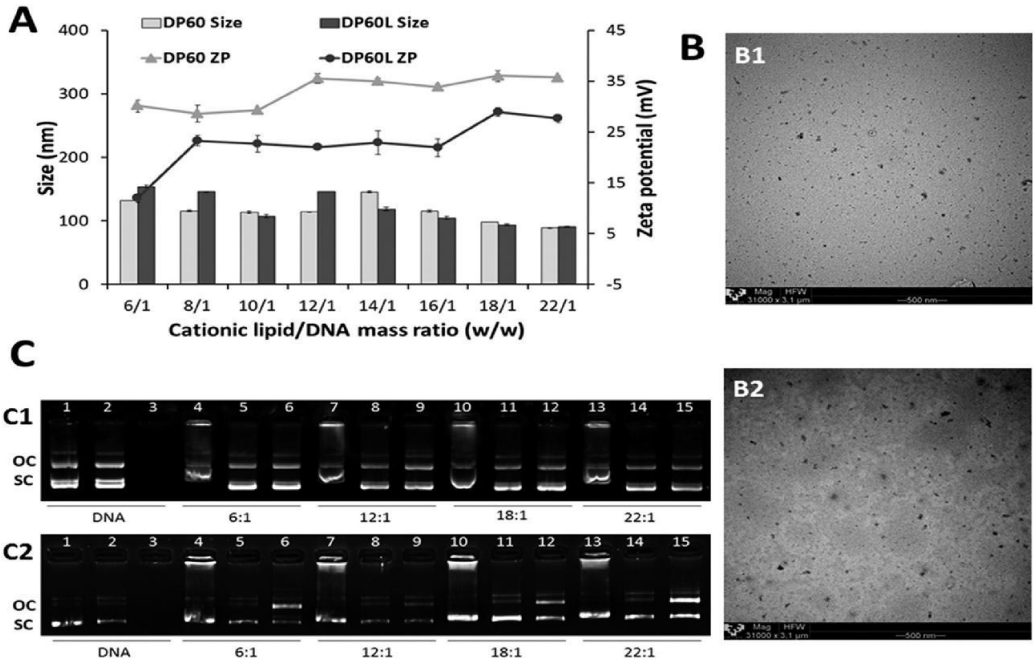

Fig. 2. Physicochemical characterization of nioplexes. A) Effect of cationic lipid/DNA mass ratio (w/w) on both particle size (bars) and zeta potential (lines). Each data point represents the mean ± SD (n = 3). TEM of DP60 (B1) and DP60L nioplexes (B2) at ratio of 18/1 cationic lipid/DNA mass ratio (w/w). Scale bar = 500 nm. Binding, SDS-induced release and protection of DNA at different cationic lipid/DNA mass ratios (w/w) of nioplexes based on both DP60 (C1) and DP60L (C2) visualized by agarose electrophoresis. Lanes 1–3 correspond to uncomplexed DNA; lanes 4–6, cationic lipid/DNA mass ratio 6/1; lanes 7–9, cationic lipid/DNA mass ratio 12/1; lanes 10–12, cationic lipid/DNA mass ratio 18/1; lanes 13–15, cationic lipid/DNA mass ratio 22/1. Nioplexes were treated with SDS (lanes 2, 5, 8, 11 and 14) and DNase I + SDS (lanes 3, 6, 9, 12 and 15). OC: open circular form, SC: supercoiled form.

For instance, the lack of double bonds in the hydrocarbon chains (Fig. 1-B) could provide low permeability of the vesicles, and therefore better stability of niosome membranes (5). Additionally, compared with other hydrophilic surfactants such as polysorbates 80, 40 or 20, the low hydrophilic-lipophilic balance (HLB) value of polysorbate 60 (14.9) could help to solubilize lycopene more efficiently (7). The addition of the natural and non-polar lipid lycopene (Fig. 1-C) into niosome bilaminar membrane could increase its fluidity, disturb membrane packing, and consequently vesicle susceptibility to environmental stresses (8).

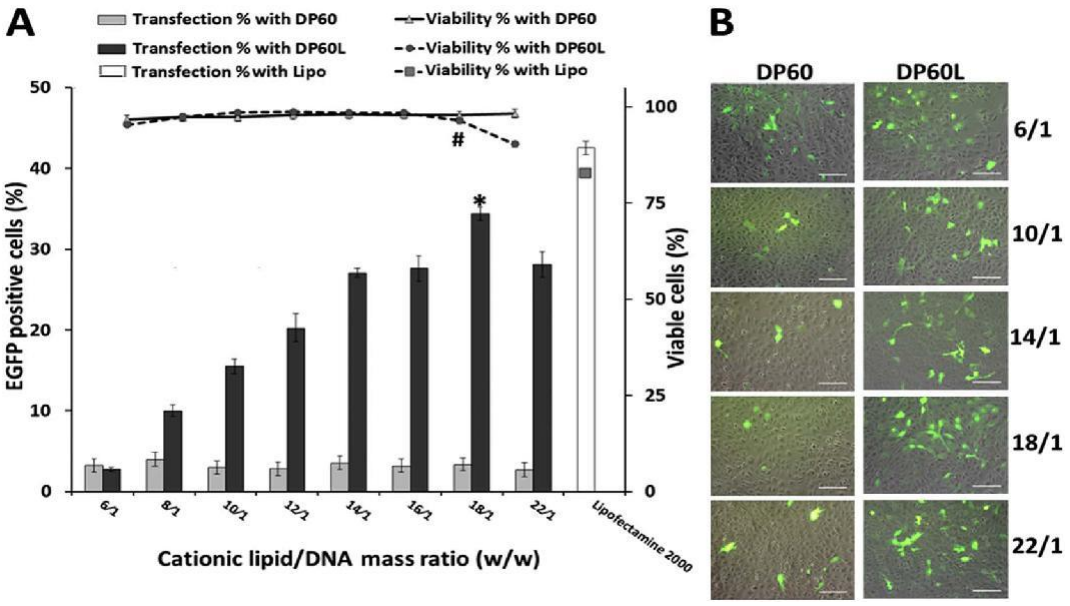

Fig. 3. In vitro transfection efficiency and cell viability in ARPE-19 cells at 72 h post-transfection. (A) Flow cytometry-based evaluation of the percentage of EGFP-positive cells (bars) and percentage of viable cells (lines) at different cationic lipid/DNA mass ratios (w/w). Values represent mean ± SD (n = 3). (*P < 0.05 vs. Lipofectamine™2000 transfection). ($^{\#}$P < 0.05 vs. Lipofectamine™2000 viability). (B) Overlay of fluorescence and phase-contrast micrographs of ARPE-19 cells 72 h post-transfection at different cationic lipid/DNA mass ratios (w/w). Scale bar = 100 μm.

Once elaborated by the reverse phase elaboration method, both DP60 and DP60L niosomes showed appropriate size (in the nanometric scale) and PDI values (below 0.5) for gene delivery purposes (Table 1). High positive ZP values (> +25 mV) ensure long-lasting stability (9), extempore electrostatic reciprocal action with DNA, along with binding of the nioplexes to the negatively charged units of the cell membrane previous to cellular uptake (2).

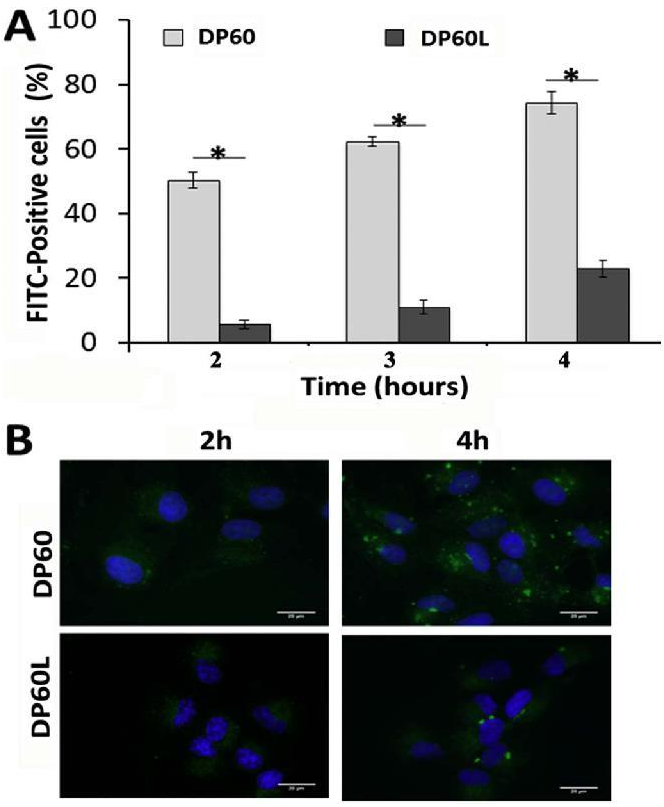

Fig. 4. Uptake of FITC-labeled nioplexes in ARPE-19 cells. Both DP60 and DP60L at a mass ratio of 18/1 (w/w). (A) Percentage of FITC-positive cells. Data represent mean ± SD (n = 3). *p < 0.05. (B) Fluorescence micrographs of ARPE-19 cells at 2 h and 4 h of incubation with FITC-labeled DP60 and DP60L nioplexes (green). Nuclei stained with Dapi (blue). Original magnification 63×. Scale bar = 20 μm. (For inter-pretation of the references to color in this figure legend, the reader is referred to the web version of this article.)

To elaborate nioplexes, we added pCMS-EGFP reporter plasmid to both niosome formulations at different cationic lipid/DNA mass ratios, since otherwise, the complex assembly process could be slowed down (10). The slight changes discerned in the size of nioplexes (100–150 nm, Fig. 2-A), at the mass ratios studied, might be due to the delicate balance of different events involved in the multistep self-assembled complex formation, such as: electrostatic interaction, further membrane merging, lipid mixing and aggregate growth (10). Regarding the ZP values, the gradual increase of superficial charge along with cationic lipid/DNA ratios (w/w) suggests the capacity of cationic

niosomes to bind to and neutralize the negatively charged phosphate groups of DNA (11). Lycopene addition reduced ZP value of DP60L nioplexes, compared to DP60, at all ratios studied. This fact could be explained by the perturbation of the lipid membrane bilayer, which could dissipate the electrical potential (Fig. 2-A) (12).

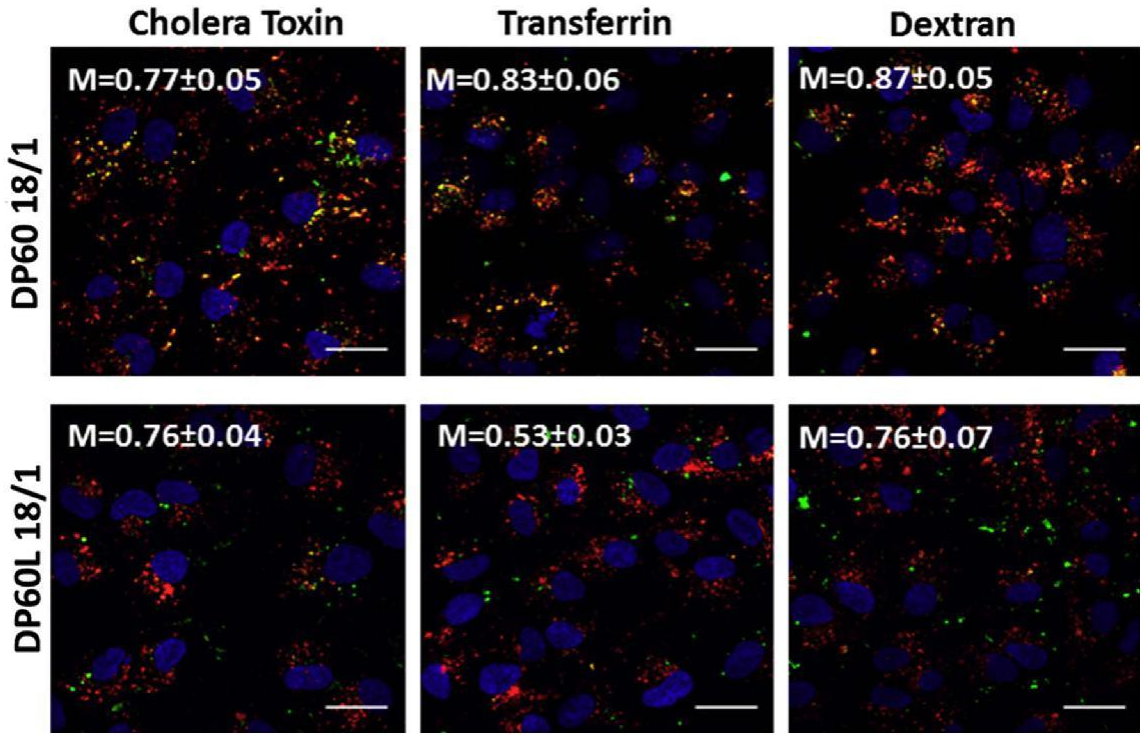

Fig. 5. Three-channel overlay RGB images of ARPE-19 cells showing nioplexes with FITC-labeled pCMS-EGFP (green) and one of the endocytosis markers in red (AlexaFluor® 555-Cholera Toxin, AlexaFluor® 546-Transferrin or AlexaFluor® 594-dextran). Presence of yellow/orange color represents the overlay of an endocytic marker and nioplexes. (M = Mander's overlap coefficient). Original magnification 63×, Scale bar = 25 μm. (For interpretation of the references to color in this figure legend, the reader is referred to the web version of this article.)

In any case, both formulations could function as gene delivery carriers, since complexes with positive charge could interact electrostatically with the anionic cell coat, inducing early steps of the endocytosis process (13). The high positive ZP value of both DP60 and DP60L nioplexes, especially at 18/1 mass ratio (42 and 27 mV,

respectively), could ensure the discrete morphology and absence of aggregates observed by TEM micrographs (Fig. 2-B) (14). Among other factors that can command transfection success, the van der Waals interactions between phosphate groups of the DNA (negatively charged) and amine groups of the cationic niosomes (positively charged) deserve special attention (11, 15, 16). We observed by agarose gel electrophoresis assay that at all cationic lipid/DNA ratios tested, both niosomes were capable to condense, release and protect the DNA from enzymatic digestion (Fig. 2-C1and C2).

Once we evaluated that our nano-formulations were biotechnologically fitting for gene delivery purposes, we proceeded to evaluate their biological performance in ARPE-19 cells.

ARPE-19 cell line has a normal karyotype and has functional and structural properties similar to retinal pigment epithelia (RPE) in vivo, expresses RPE-specific markers, hence it is considered a suitable transfection model to investigate our vectors' effectiveness and safety before its application in vivo (17). It has been reported that the non-ionic nature of surfactants makes niosomes well tolerated by cells (18). Our results in Fig. 3 show higher cell viability values in cells transfected with both nioplexes when compared with cells transfected with Lipofectamine™ 2000. Additionally, we observed under the fluorescence microscope that cells transfected with both nioplexes maintained their normal morphology, even at high cationic lipid/DNA ratios (Fig. 3-B). Although the percentage of transfected cells with DP60L niosomes at 18/1 mass ratio was significantly lower than that obtained with commercially available Lipofectamine™ 2000, our niosomes formulation was better tolerated by ARPE-19 cells. Therefore, it could be an interesting alternative to Lipofectamine™ 2000, since some authors have reported damage on the retina associated to the in vivo administration of Lipofectamine™ 2000 in the eye (19). Regarding the transfection efficiency, the lipid composition is considered a primary limiting factor that affects to this process (1). We clearly observed in Fig. 3 the impact that lycopene had on transfection efficiency in ARPE-19 cells, since values were clearly higher when lycopene was present in the niosome formulation.

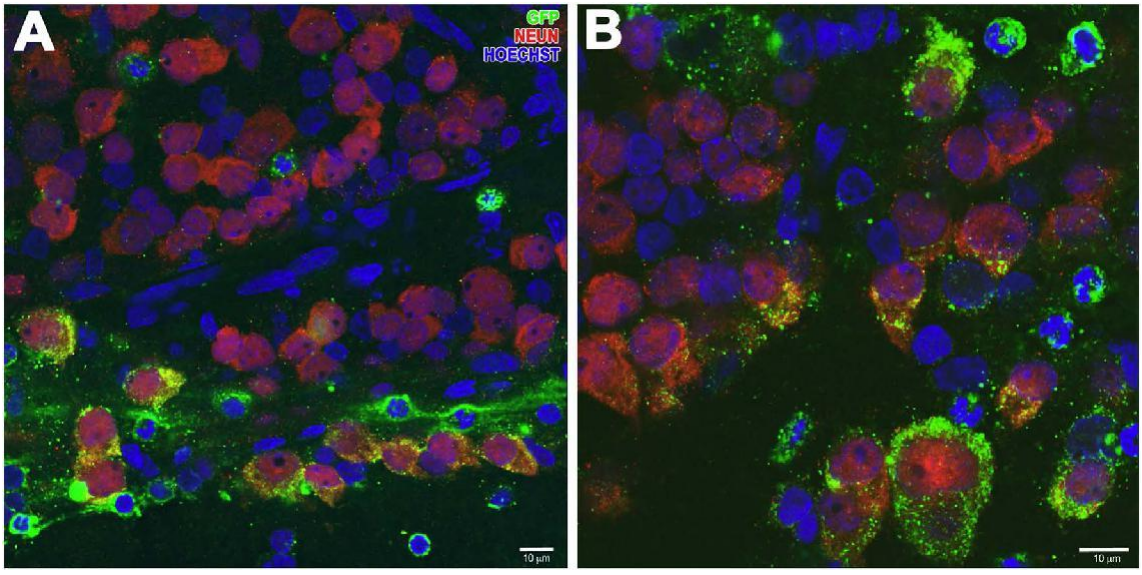

Fig. 6. Immunohistochemical study of EGFP expression in retinal whole-mount preparations 3 days after intravitreal administration of DP60L nioplexes. Partial colocalization of EGFP (green color) with NeuN-positive ganglion cells (red) was observed in the ganglion cell layer (GCL) (red). EGFP expression was observed as well in some cells with typical microglial morphology in GCL (NeuN-negative cells). Nuclei were stained with Hoechst 33342 (blue). Scale bars: 10 µm. (For interpretation of the references to color in this figure legend, the reader is referred to the web version of this article.)

Still, the definite mechanism of lycopene action has not yet been fully expounded, some authors suggest existence of a lycopene receptor and/or transporter in the nuclear membrane of cells (20). Additionally, other study has documented the capacity of lycopene to modulate transcription (21). Such effect could be either by direct interactions with transcription factors such as nuclear factor-kappa, or by indirect modifications of transcriptional activity.

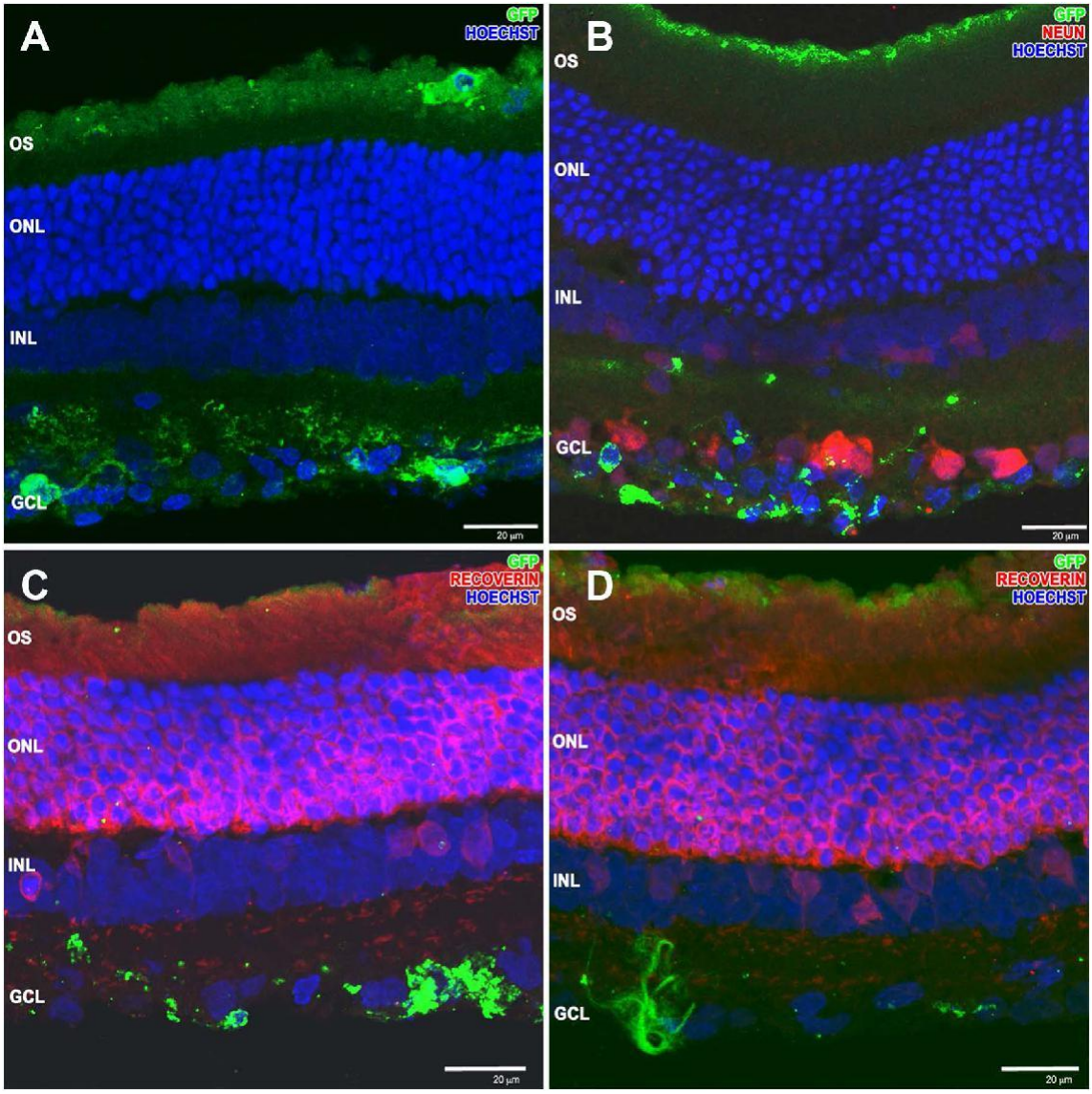

Fig. 7. Confocal fluorescence micrographs of retinal cross-sections after 3 days of intravitreal (A,B) and subretinal (C,D) administration of DP60L nioplexes. After intravitreal injections, EGFP fluorescence was observed in glial cells in the GCL, and in the outer segments of the photoreceptors. Localization of EGFP after subretinal injections was detected as well in OS of photoreceptors (stained with recoverin, in red) and some microglial cells. Cell nuclei were counterstained with Hoechst 33342 (blue). Scale bars: 20 µm. (For interpretation of the references to color in this figure legend, the reader is referred to the web version of this article.)

In any case, advanced research is still needed to determine the exact mechanism [44]. The ascending transfection percentages obtained by DP60L at high mass ratios might be attributed, partially, to the triggering effect of free niosomes absorbed on to the cell membrane. At higher cationic lipid/DNA mass ratios, there is a large excess of cationic lipid to DNA, therefore a population of free niosomes is expected (22). This free cationic lipid could prolong cellular retention or decreases degradation rate of DNA (1). Nonetheless, additional experiments are needed to elucidate the detailed mechanisms involved.

To determine whether enhanced internalization was among the effects that lycopene incorporation could have in niosome formulations, we studied the percentage of cellular uptake of both DP60 and DP60L formulations at the mass ratio of best transfection efficiency (18/1) in ARPE-19 cells at different times (Fig. 4). Surprisingly, flow cytometry studies showed that lycopene addition clearly reduced the percentage of cellular uptake at all times studies when compared to DP60 formulation (Fig. 4-A). Such reduction in the cellular uptake could probably be due to the lower zeta potential of DP60L formulation compared with DP60 (Fig. 2-A).

Additionally, CLSM studied (Fig. 4-B), excluded mere electrostatic adherence of cationic nioplexes to the negatively charged surface of ARPE-19 cell, since a clear intracellular distribution of both nioplexes was observed in the case of both formulations. In any case, the cytoplasmatic distribution of both nioplexes showed a different behavior. Whereas DP60L nioplexes maintained a homogeneous distribution in the cytoplasm over the time, DP60 nioplexes showed some aggregates at 4 h. The differences observed in the cytoplasmatic distribution of both formulations could suggest different internalization pathways. Therefore, and motivated by the differences observed between both formulation in terms of transfection efficiency and cellular uptake, we next studied the cellular trafficking of both nioplexes at the mass ratio of best transfection efficiency (18/1). Three of the pathways most employed in the uptake processes were assayed; clathrin-mediated endocytosis (CME), caveola-mediated endocytosis (CvME) and macropinocytosis (Fig. 5) (23). The performance of non-viral

vectors is known to be clearly affected by their distinct cellular internalization pathway, taking into account the variable effectiveness of every pathway in the release of DNA into the cytoplasm, which is one of the critical steps in the eventual transgene expression (10). Although there is not a clear consensus in the scientific community, it is widely accepted that the endolysosomal fate is the hallmark feature of CME (14, 24). In the other hand, CvME and macropinocytosis are widely related to non-acidic and non-digestive routes of cellular uptake (25, 26). Therefore, our results observed in Fig. 5 suggest that internalization of DP60L via these last pathways could be advantageous over CME internalization, in terms of both DNA delivery and integrity, since it could avoid lysosomal degradation (23).

Once the intracellular trafficking of both DP60 and DP60L nioplexes was studied, next, we performed a provisional in vivo study to estimate the transfection efficiency of DP60L vectors in rat retina after both intravitreal (IV) and subretinal (SR) administrations. These routes are considered the most clinically viable options to convey genetic material to the back of the eye in an effective way. IV injection has been extensively studied thanks mainly to its relative easiness and to the capacity to deliver high doses of genetic material to retinal cells. Additionally, it is less invasive and traumatic than the counterpart SR administration (27). Typically, after IV injection, the delivered genes are expressed, mainly, in the ganglion cell layer (GCL) of the retina (28). Among many applications, transfection at this level could be of clinical importance for the treatment of glaucoma, a devastating eye disease that is considered the first cause of blindness worldwide (29). However, our in vivo data showed not only a good and uniformly distributed EGFP expression at this level (Fig. 6 and Fig. 7-A, B), but also we observed EGFP expression in some of the outer segments (OS) of photoreceptors (Fig. 7-A, B), which suggests a partial diffusion of our DPL60 niosomes through the different layers of the retina. Diffusion of nioplexes could be probably explained by the PEG chains of the polysorbate 60 non-ionic tensioactive which could prevent aggregations with fibrillar structures in the retina. In any case, for further clinical applications, where the volume of the human vitreous is significantly bigger than the volume of the rat vitreous, we should also consider the possible electrostatic

interactions between the positively charged niosome based complexes and the negatively charged components of the vitreous such as hyaluronans, proteoglycans, hyalocytes or proteins. These interactions could affect to the final performance of the formulation. To avoid this scenario, positively charged complexes could be coated with negatively charged compounds such us hyaluronic acid, which has been recently reported that can enhance retinal gene delivery after intravitreal injection (30).

Transfection at the outer layers of the retina is highly desirable from a therapeutic point of view, since to date, mutations in over 200 genes expressed in photoreceptors and RPE cells have been associated with many inherited retinal disorder, that until know, do not have curative treatment, such as Retinitis Pigmentosa, Stargardt Disease, Age-related Macular Degeneration, or Leber's Congenital Amaurosis,(28) to name just a few. Although being able to deliver the EGFP gene to the same layers as IV administration (Fig. 7-C,D), SR injection bears the risk of retinal detachment [49]. Therefore, our preliminary in vivo study offers reasonable hope to target the outer retina by the much safer IV instead of SR administration route, which relevant clinical implications.

6.2 Cationic niosome vehicle based on lycopene helper lipid and DOTMA as efficient gene delivery vehicles to central nervous system cells into the brain

The flattering properties of the-lycopene containing-niosomes in retinal cells encouraged the team to use the same particles to transfect NT2 cells, primary cortical culture as well as brain cortex of rats, to investigate the safety and effectiveness of lycopene containing-niosome as non-viral vectors to deliver DNA into the CNS to face many neurological disorders.

Gene therapy aimed to the CNS represents an extreme challenge to bring normal gene copies and correct mutant gene deficiencies in many neurodegenerative diseases (31). However, in order to apply this promising technology into the regular clinic practice, safe and efficient gene carrier systems are needed. Compared with viral vector, non-

viral vectors have several important advantages. For instance, they are easier and cheaper to produce, and there is no preexisting immunity to these vectors. Additionally, they are not derived from pathogens, and consequently show less safety concerns. However, their transfection efficiency is lower than their virus-based counterparts. Therefore, research on this topic merits special attention.

Based on the flattering properties showed recently by niosomes to transfect retinal cells after both intravitreal and subretinal administration (11, 32, 33), we elaborated cationic niosomes based on DOTMA, polysorbate 60 and lycopene to deliver DNA into the brain cortex of rats after cerebral cortex administration. DOTMA is a highly water-soluble quaternary ammonium salt lipid that has been strongly used for gene delivery goals, due to its ability to condense DNA (34). Lycopene is a natural carotenoid that when used as "helper" lipid, enhances transfection efficiency in retinal cells (32). Polysorbate 60 is the major component of the niosome formulation, and its poly (ethylene glycol) structure has been reported that increases in vivo transfection efficiency in CNS (35).

Prior to perform any biological study, we characterized in Fig. 8 our formulation in the matter of size, superficial charge, morphology and capacity to compact, liberate and secure DNA against enzymatic digestion. Although there is no a general rule about the optimal particle size of formulations for each gene delivery application, it is generally accepted that this parameter clearly influences the final performance, and that in case of niosomes, is affected by the cationic lipid/DNA mass ratio (28). Size of DP60L niosomes was around 100 nm. Interestingly, when DNA was incorporated to obtain nioplexes at 6/1 ratio, size increased up to 154 nm. However, at higher ratios, size decreased, probably due to the electrostatic interactions that condense DNA more efficiently, and therefore, decreased PDI values as well.

A

	Size (nm)	PDI	Zeta potential (mV)
Niosomes	101.6 ± 2.5	0.44	33.8 ± 1.1
Nioplexes			
6/1	154.3 ± 1.3	0.40	12.0 ± 0.8
10/1	107.8 ± 0.7	0.29	22.7 ± 1.6
14/1	118.7 ± 2.6	0.35	22.9 ± 2.3
18/1	94.03 ± 1.2	0.31	27.1 ± 3.1

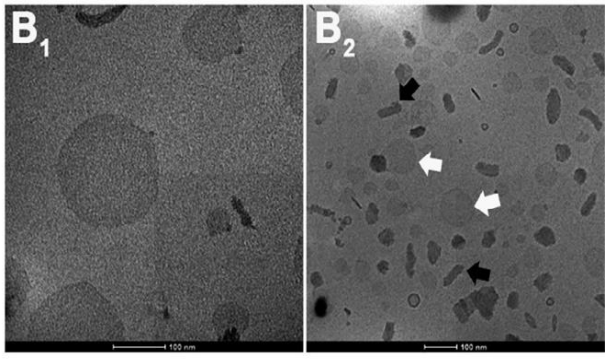

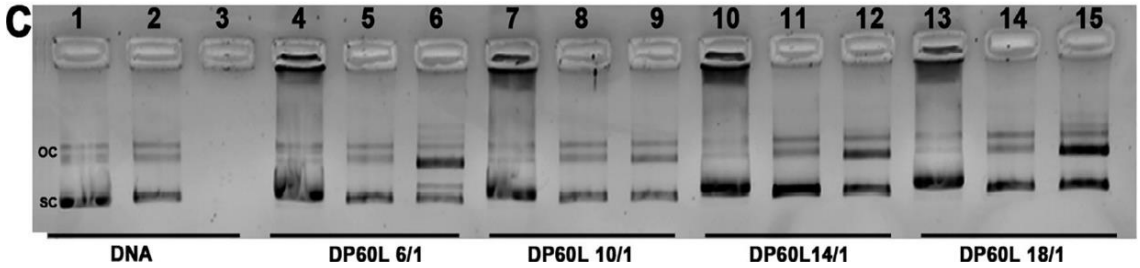

Fig. 8. Physicochemical characterization of DP60L niosomes and nioplexes. A) particle size (nm); polydispersity index (PDI); and Zeta potential (mV). Data represent mean ± SD (n = 3). CryoTEM micrographs of DP60L niosomes (B_1) and nioplexes at 14/1 cationic lipid/DNA mass ratio (w/w) (B_2). Scale bars 100 nm. C) DNA binding, SDS-induced release and protection at different cationic lipid/DNA mass ratios (w/w) of DP60L nioplexes. Lanes 1–3 correspond to uncomplexed DNA; lanes 4–6, cationic lipid/DNA mass ratio 6/1; lanes 7–9, cationic lipid/DNA mass ratio 10/1; lanes 10–12, cationic lipid/DNA mass ratio 14/1; lanes 13–15, cationic lipid/ DNA mass ratio 18/1. Lanes 2, 5, 8, 11 and 14 depict nioplexes treated with SDS, while lanes 3, 6, 9, 12 and 15 demonstrate DNase I + SDS-treated nioplexes. OC: open circular form, SC: supercoiled form.

Additionally, differences recognized in PDI values perhaps thanks to different DNA topologies found in nioplexes (36). Regarding ZP values, we found a positive correlation with the cationic lipid/DNA ratio, which suggests that cationic DOTMA binds and neutralize the negatively charged DNA (37). Under TEM observation, niosomes appeared spherical, while nioplexes at 14/1 mass ratio showed heterogeneous shapes, but mostly elongated. Interestingly, at this ratio, spherical niosomes were also discerned (Fig. 8-B_2), which could accumulate on the surface of cell membranes and enhance DNA delivery(38). To further analyze electrostatic interactions, we performed a gel retardation assay (Fig. 8-C), since an optimum balance is required for efficient gene delivery (37). Despite the incomplete DNA condensation observed, which could be affect by different thermodynamic factors, kinetics mixing, or by the lycopene

incorporation in to the niosome formulation or the high aqueous solubility of DOTMA (39), all cationic lipid/DNA ratios analyzed, were able to keep safe plasmid DNA against enzymatic digestion.

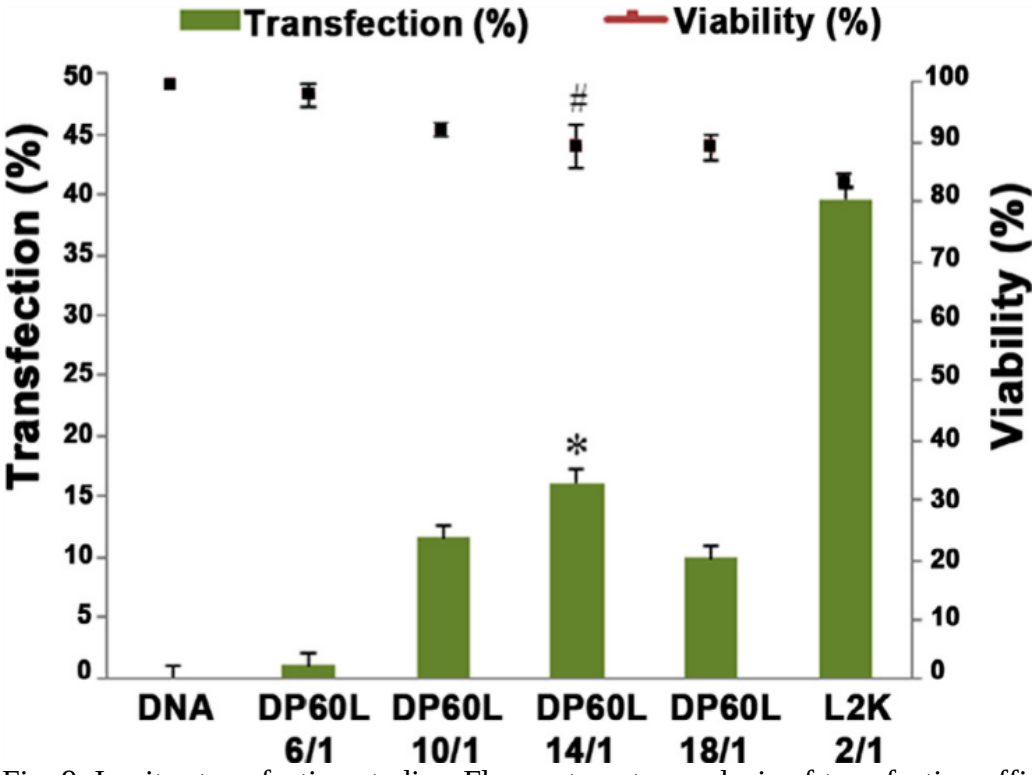

Fig. 9. In vitro transfection studies. Flow cytometry analysis of transfection efficiency and cell viability in NT2 cells at 24 h. Percentage of EGFP-positive cells (bars) and percentage of viable cells (line) at different cationic lipid/DNA mass ratios (w/w). Values represent mean ± SD. (n = 3). (L2K = Lipofectamine®2000) ($^{*}P < 0.05$ vs. L2K transfection). ($^{\#}P < 0.05$ vs. L2K viability).

Once physicochemical properties of nioplexes were analyzed, next, we performed in vitro studies to evaluate, initially, both transfection efficiency and viability in NT2 cells. These cells represent an interesting model to study the efficiency of gene delivery vectors into CNS due to their capacity to differentiate into bot neuronal and glial cells (40). Unlike other teratocarcinoma cell lines, the NT2 cells depict special obligation to a neural lineage upon exposure to retinoic acid (RA). Therefore, it has been considered as a promising human cell source in studies of cell in vivo therapeutic applications in many neurodegenerative disorder like Parkinson disease(41). Accordingly, we considered NT2 cells as an interesting model to study the efficiency of gene delivery

vectors into CNS. Additionally, these cells represent a promising platform in cell-based gene delivery as they could be genetically-modified and then transplanted(42).

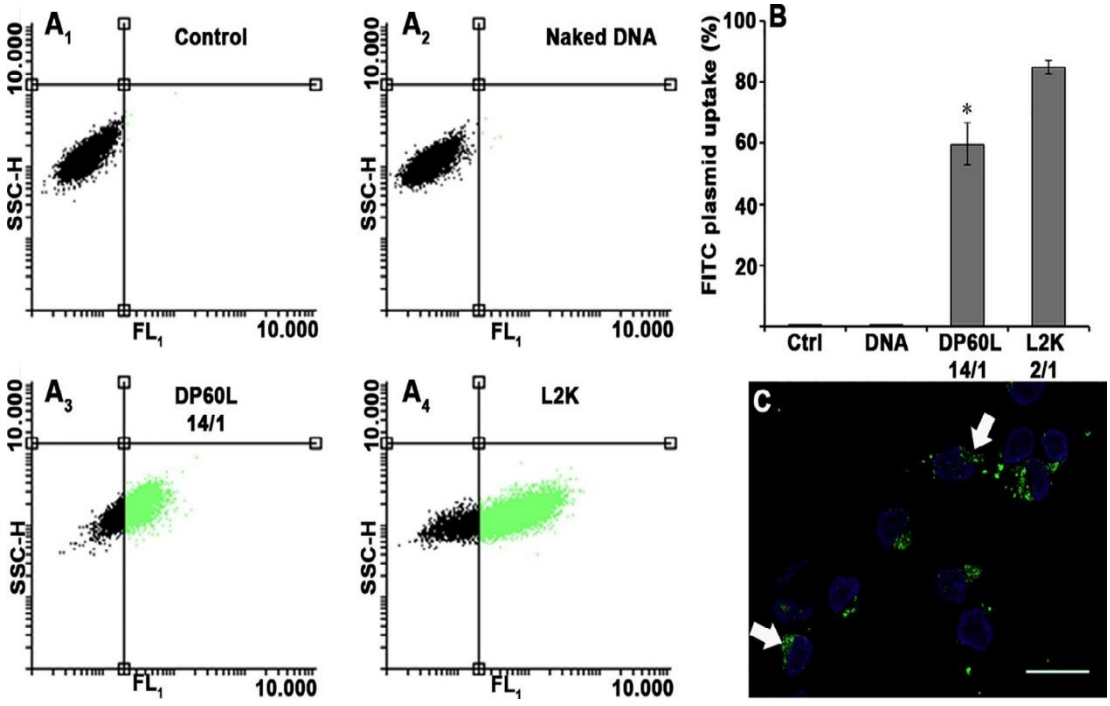

Fig. 10. Cellular uptake studies in NT2 cells 4 h post incubation. (A) Flow cytometry dot-plots (SSC-H and FL_1) of control cells without treatment (A_1), naked DNA (A_2), DP60L nioplexes at 14/1 (w/w) ratio (A_3), and lipofectamine 2000® (L2K) at 2/1(w/w) ratio (A_4). (B) Flow cytometry measurement of NT2 cells treated with FITC-labeled formulations. Error bars represent SD (n = 3). $^{*}p < 0.05$. (C) Fluorescence microscopy images of NT2 cells after 4 h of incubation with FITC-labeled DP60L nioplexes at 14/1 (w/w) ratio. Cells were stained with DAPI-fluoromount G (blue). White arrows indicate nanoparticles around the nucleus. (Scale bar =25 μm). (For interpretation of the references to colour in this figure legend, the reader is referred to the web version of this article.)

Data obtained in Fig. 9 revealed that transfection efficiency increased in proportion to the cationic lipid/DNA mass ratio, touching the peak at 14/1 ratio (17% of cells were transfected). Although the percentage of transfected cells were inferior to those obtained with commercially available lipifectamine®2000 (17% and 37%, respectively), viability values were higher (90% and 83%, respectively). The reported low cytotoxicity of nioplexes represents an appealing feature for potential further in vivo applications, since the in vivo use of lipifectamine®2000 is discouraged due to its cytotoxicity (43). To better understand the transfection process mediated by DP60L nioplexes in NT2 cells,

we estimated the cellular uptake and the intracellular trafficking of nioplexes, since those two factors clearly influence on the final performance of gene delivery carriers (28). Cellular uptake values were compared with lipifectamine®2000.

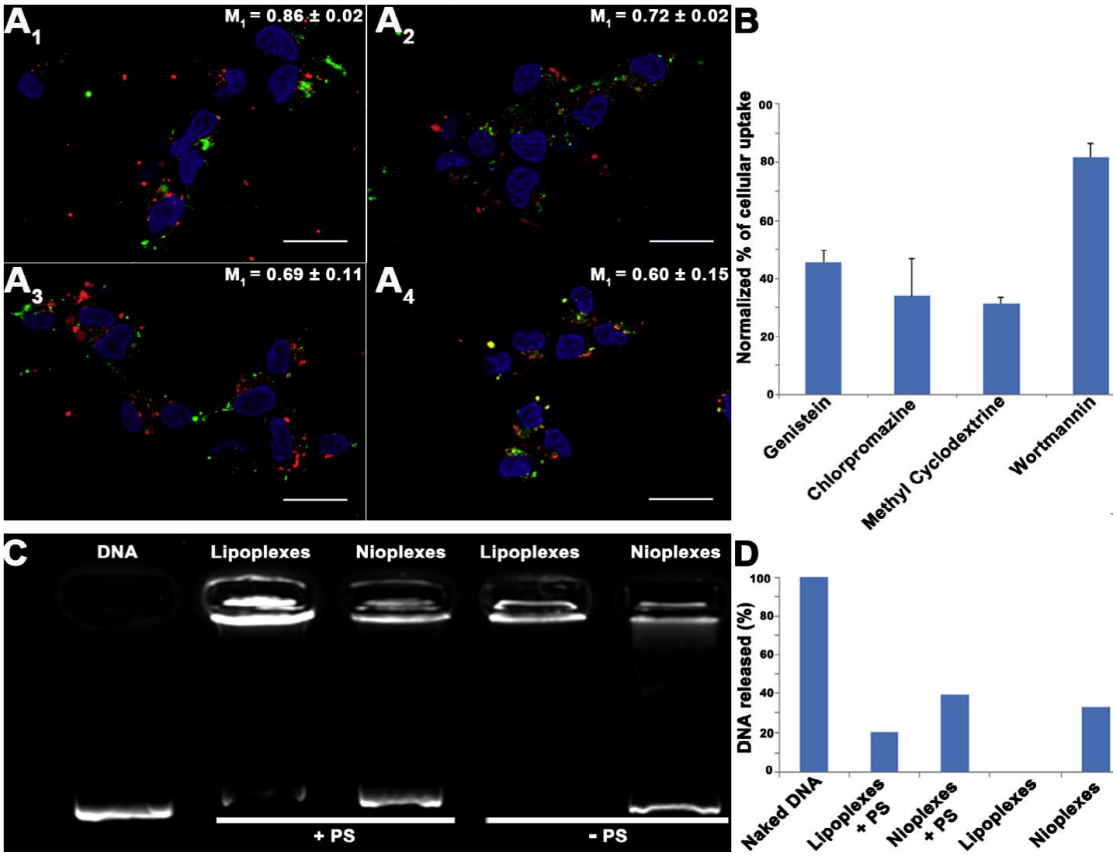

Fig. 11. Internalization studies. (A) Confocal microscopy images showing intracellular distribution in NT2 cells of nioplexes at 14/1 ratio labelled with FITC-pCMS EGFP (green) plasmid and AlexaFluor 555-Cholera Toxin (A1), AlexaFluor 546-Transferrin (A2), AlexaFluor 594-Dextran (A3), and LysoTracker Red DND-99 markers (A4), all in red. (M1 = Mandeŕs overlap coefficient). Scale bars =25 µm. (B) Effect of endocytic inhibitors on the cellular uptake of FITC-labeled nioplexes. Data were normalized to uptake without inhibitor. (C) Agarose gel electrophoresis DNA released profiles of lipoplexes and nioplexes incubated with or without PS. (D) Quantification of released DNA in agarose gel electrophoresis.

As observed in Fig. 10, lipoplexes obtained with commercially available lipofectamine®2000, were more efficiently internalized than DP60L nioplexes (around 85% and 60%, respectively), which could interpret the higher percentage of EGFP expression in NT2 cells transfected with lipofectamine®2000. Differences observed in cellular uptake between both formulations could be due to particular topologies of

complexes or specific interactions of the complexes with cell membrane lipids (36). In any case, percentage of transfected cells with DP60L nioplexes (17%, Fig. 9) were clearly inferior to the percentage of positive cells for FITC-labeled DP60L nioplexes (60%, Fig. 10-B), which suggest the influence of other biological events, such as intracellular trafficking or endosomal scape, in the final EGFP expression (44). Therefore, we analyzed three of the most employed cellular internalization pathways such as clathrin-mediated endocytosis (CME), caveolae-mediated endocytosis (CvME) and macropinocytosis (MPC). Although there is no general agreement in relation to the most efficient endocytosis pathway, the release of DNA into the cytoplasm, and therefore, the final performance, is clearly affected by the cellular uptake process (45).

The results observed in Fig. 11 suggested that DP60L nioplexes were internalized, mainly, by CvME and CME, while MPC had much less participation in the cellular uptake process. It is generally accepted that both CvME and CME are endocytosis routes that transfer genetic material to late endosomes/lysosomes, where the acidic environment degrades the DNA, making transfection process inefficient (40). Therefore, the observation of nioplexes in the late endosome (Fig. 11-A_4) might explain the relatively low transfection efficiency values (17%) observed (Fig. 9), despite the fact that high number of NT2 cells (60%) captured the complexes (Fig. 10). Nonetheless, this hypothesis needs further verification since the endosomal escape capacity of nioplexes, if present, could evade degradation. Therefore, in next experiments, we evaluated the ability of nioplexes to escape from degradation in lysosomes. Several particle dependent endosomal escape mechanisms have been reported in the literature, being the proton-sponge mechanism one of the most widely described (46). Therefore, we analyzed the pH-buffering capacity of cationic DP60L niosomes. As observed (Supplementary data, Fig. 1), the incorporation of both cationic DOTMA and lycopene lipids into the niosome formulation, increased the pH-buffering capacity upon titration with 0.1 M HCl compared with niosomes elaborated only with polysorbate 60, which could suggest that those lipids could increase the proton sponge effect, and therefore, the endosomal scape capacity of DP60L niosomes. Another widely proposed endosomal scape mechanism consists on the destabilization of the endosomal membrane by electrostatic interactions between the cationic nanoparticles

and the anionic lipids of the late endosome membrane, which could allow the DNA release to the cytoplasm (Varkouhi et al., 2011).

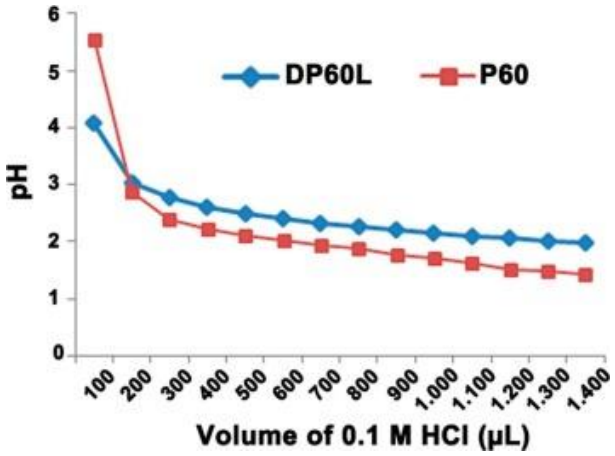

Supplementary figure 1

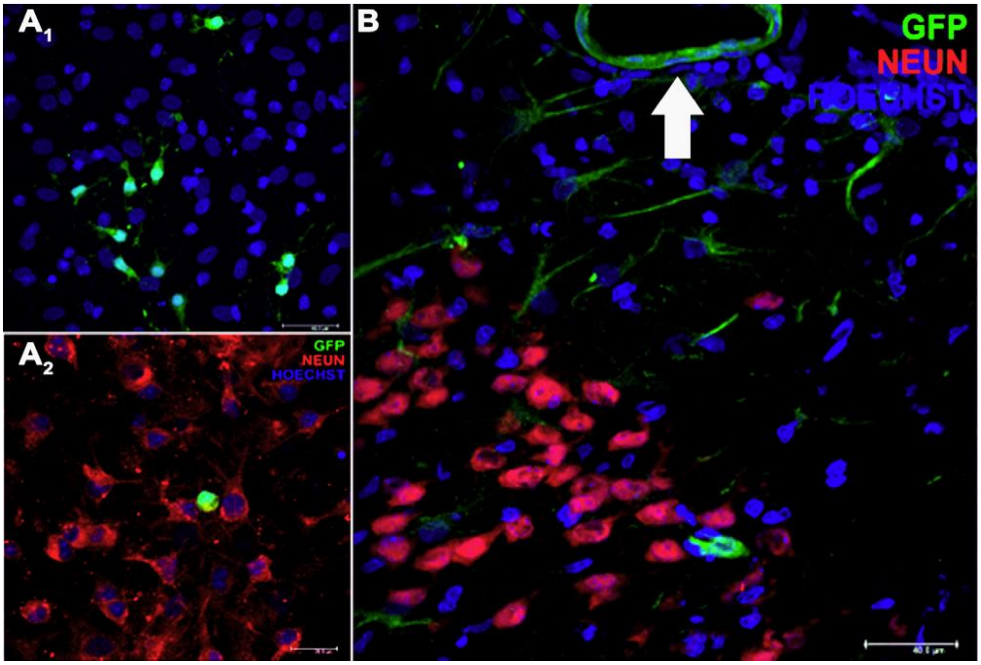

Fig. 12. Primary cortical culture and in vivo gene expression of EGFP carried by DP60 nioplexes at 14/1 mass ratio (w/w). A_1 and A_2, transfection of primary neuronal cell cultures 24 h post transfection. NeuN-positive neurons (red) and nuclei counterstained with Hoechst 33342 (blue) (Scale bars =20 and 40 µm, respectively). B, in vivo gene expression of pCMS-EGFP 72 h after intracortical administration of nioplexes. Nuclei are shown in blue (Hoechst), neurons in red ($NeuN^+$), and EGFP expression (GFP^+) in green. White arrow points a blood vessel. Scale bar 40 µm. (For interpretation of the

references to colour in this figure legend, the reader is referred to the web version of this article.)

To evaluate this endosomal scape mechanism, we added DP60L nioplexes to anionic micelles made with phosphatidyl serine (PS), that simulated the endosomal compartment, and the DNA release from PS micelles was evaluated in an agarose gel electrophoresis assay (40). As observed in Fig. 11, about 40% of DNA was released form DP60L nioplexes, in the presence of PS, micelles. However, only 30% of DNA was released without previous incubation with the anionic PS micelles, which demonstrates the capacity of the DP60L nioplexes to release DNA once they contact the endosomal lipid bilayer membrane. In the case of lipoplexes based on lipofectamine®2000, all DNA was condensed with the formulation and up to 20% was released in the presence of PS micelles. Next, and prior to perform in vivo studies, we evaluated transfection efficiency of DP60L nioplexes in primary cortical cultures of rat embryos, since primary cells normally express their tissue-specific receptors, and mimic in vivo conditions, where different kind of neurons and glial cells are mixed to set up neuronal-glial networks. In these conditions, we observed that, apparently, only glial cells, expressed EGFP (Fig. 12-A_1). This assumption was further confirmed by lack of $NeuN^+$-immunoreactivity in EGFP expressing cells (Fig. 12-A_2). Such preferential transfection of glial cells could be attributed to their higher mitotic and/or phagocytic activities (47). Interestingly, in in vivo experiments performed by direct intracranial injection of nioplexes, again, NeuN negative cells (neuroglia and cells in blood vessel wall) were the only ones transfected by DP60L nioplexes (Fig. 12-B). These results reveal the incapacity of nioplexes to transfect neuron cells, probably due to the impaired uptake and/or intracellular trafficking (48). Therefore, DP60L nioplexes could be of great interest to transfect glial cells in the CNS in glia-related neurological disorders. Glial cells constitute over 70% of the total cell population in the CNS, and they play a pivotal role for the normal development and function of nervous tissue (49, 50). Their perturbation is associated with several neurological disorders such as; stroke, multiple sclerosis, epilepsy, Alzheimer's and Parkinson's diseases (51, 52). Therefore, the preferential transfection of glial cells could be of great importance in future applications in glia-related neurological disorders. Additionally, cells in the wall of some blood

vessels were also transfected with DP60L nioplexes (Fig. 12-B, white arrow). Transfection at this level could be of great relevance in cerebrovascular diseases, such as; stroke, transient ischemic attacks, subarachnoid hemorrhage or vascular dementia, just to name a few.

6.3 Chloroquine-containing cationic niosomes as non-viral vectors for gene delivery to the rat retina

To emphasize the role and importance of helper molecule to turn on transfection efficiency, we designed a novel chemical vehicle for retinal gene delivery. More clearly, we probed the role of chloroquine embodiment into niosomes composed of cationic lipid and a blend of non-ionic surfactants. Interestingly, chloroquine, on its own, may improve efficiency of transfection whenever combined to the cell culture medium or included into cationic-peptide-DNA complexes (53) in a dose-dependent matter. Nonetheless, the pre-treatment with chloroquine, has shown high toxicity levels that limit further clinical applications(54). To escape such destructive effect, in the present work, chloroquine was embodied within the niosome preparation. Such insertion of chloroquine into a niosome formulation, rather than as a co-/pre-treatment of cells, would be a more rational approach for in vivo environment.

Table 2

Physical features of both DPP80 and DPP80-CQ niosomes in terms of size (nm), Polydispersity index (PDI), and zeta potential (mV). The values exemplify the mean ± SD (n = 3).

	Size (nm)	Zeta potential (mV)	PDI
DPP80	90.41 ± 0.65	44.3 ± 1.48	0.42 ± 0.01
DPP80-CQ	118.18 ± 1.46	28.9 ± 7.73	0.13 ± 0.02

Both non-ionic surfactants used (P80 and P) have amphiphilic nature and can deliver both water and lipid soluble molecules. Moreover, propylene oxide chains of the P can induce structural re-arrangement of lipid membrane for better stability and translocation of the gene carriers (55). Interestingly, the inclusion of P to polycation-DNA complexes augmented the expression level of the delivered genes in both in vitro and in vivo circumstances at doses below the known toxicity levels (56). P80 was reported to act as a co-emulsifier together with P, in drug and gene delivery efforts (57).

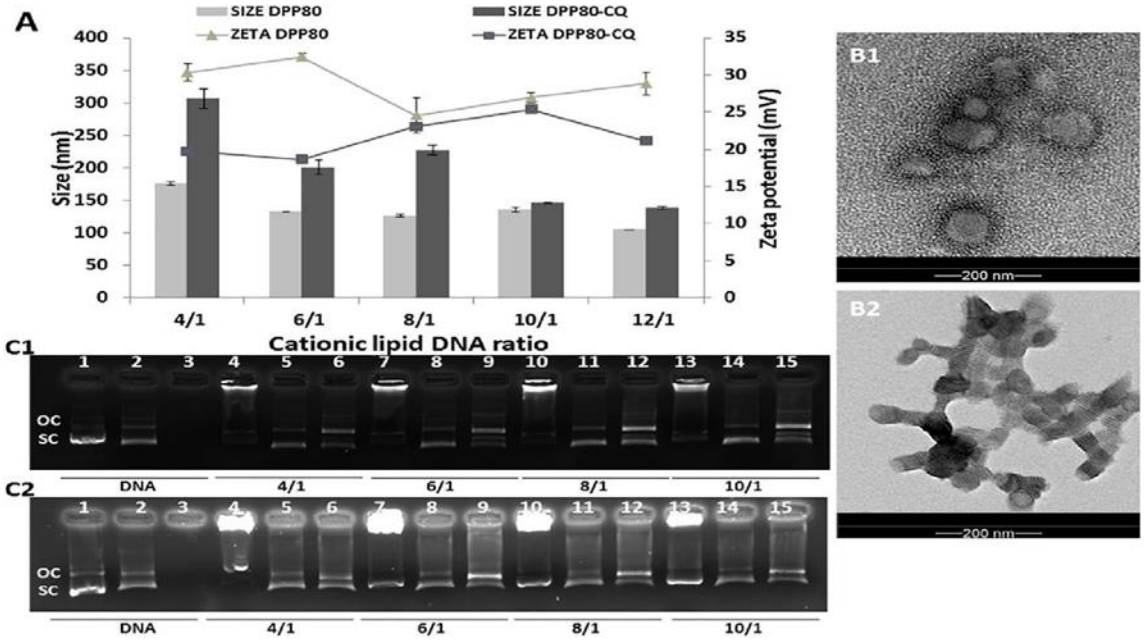

Fig. 13. Physicochemical features of nioplexes. (A) The impact of cationic lipid/DNA mass ratio (w/w) on the size (bars) and zeta potential (lines). The data represent the mean ± SD (n = 3). TEM images of DPP80 (B_1) and DPP80-CQ complexes (B_2) at 8/1 and 10/1cationic lipid/DNA mass ratio (w/w) respectively. Scale bar = 200 nm. (C) condensation, release by SDS and DNase I protection of DNA at various cationic lipid/DNA mass ratios (w/w) of nioplexes based on DPP80 (C_1) and DPP80-CQ (C_2) vehicles depicted by agarose gel electrophoresis. Lanes 1–3 represent uncondensed DNA; lanes 4–6, cationic lipid/DNA mass ratio 4/1; lanes 7–9, cationic lipid/DNA mass ratio 6/1; lanes 10–12, cationic lipid/DNA mass ratio 8/1; lanes 13–15, cationic lipid/DNA mass ratio 10/1. Complexes were processed with SDS (lanes 2, 5, 8, 11 and 14) and DNase I + SDS (lanes 3, 6, 9, 12 and 15). OC: open circular structures, SC: supercoiled structures.

In addition, the encouraging properties of P80 build a steric barrier that avert the aggregation of nano-vesicles, enhances the cell tolerance (11), and enhances the

performance of transfection by the inclusion of polyethylene glycol (PEG) chains in its structure (58). However, if used with water soluble cationic lipid, P's ability to shape network structures may be more suitable than P80 to increase their flexibility and durability (59). In these cases, a mixture of two different types of non-tensioactive molecules could provide a synergistic improvement of nano-vesicle stabilisation (60).

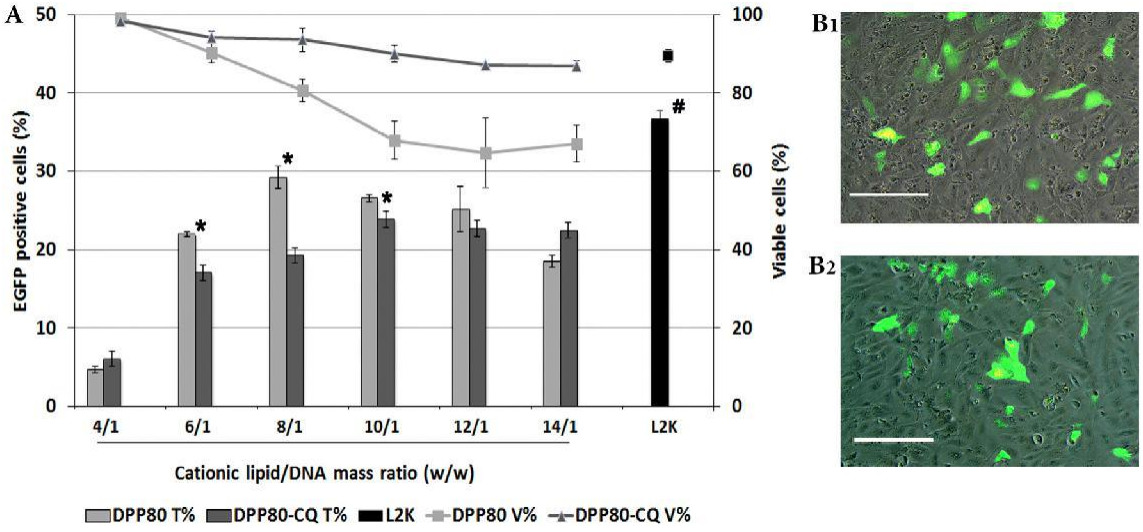

Fig. 14. In vitro transfection and viability performance of both DPP80 and DPP80-CQ nioplexes in ARPE-19 cells. (A) The percentage of EGFP-positive cells (bars) and the percentage of viable cells (lines) at various cationic lipid/DNA mass ratios (w/w) evaluated by flow cytometry at 72 h. Data are expressed in terms of mean ± SD, n = 3. L2K = Lipofectamine™2000. *P < .05 compared to DPP80, #P < .05 compared to nioplexes. (B_1 and B_2) fluorescence and phase-contrast overlay micrographs of ARPE-19 cells after 72 h transfection at 8/1 and 10/1 cationic lipid/DNA mass ratios (w/w) for DPP80 and DPP80-CQ, respectively. Scale bar = 100 μm.

With respect to cationic lipid, the high solubility of the D-Cl salt increases biodistribution of lipid/plasmid complexes, and hence, the efficiency of transfection (39). However, we observed in a previous study that the solubility of cationic lipid can drastically change the result of transfection according to the nature of the cells and the formulation process. In this analysis, the DTPA cationic lipid (non-salt form) was able to transfect retinal cells in vitro conditions (11), while the salt form did not transfect retinal cells in vivo. Interestingly, the same formulation with the same cationic lipid salt type (DPP80) has succeeded in transfecting *in vivo* cerebral cortical cells (61).

Strikingly, both formulations of the cationic lipid (salt/non-salt) were able to transfect ARPE-19 cells in vitro conditions. The non-salt type was, in any case superior in terms of transfection and cell viability.

This inconsistency emphasizes the lack of correlation between the conditions for *in vivo* and *in vitro* transfection, as well as, the importance of the formulation at physical level.

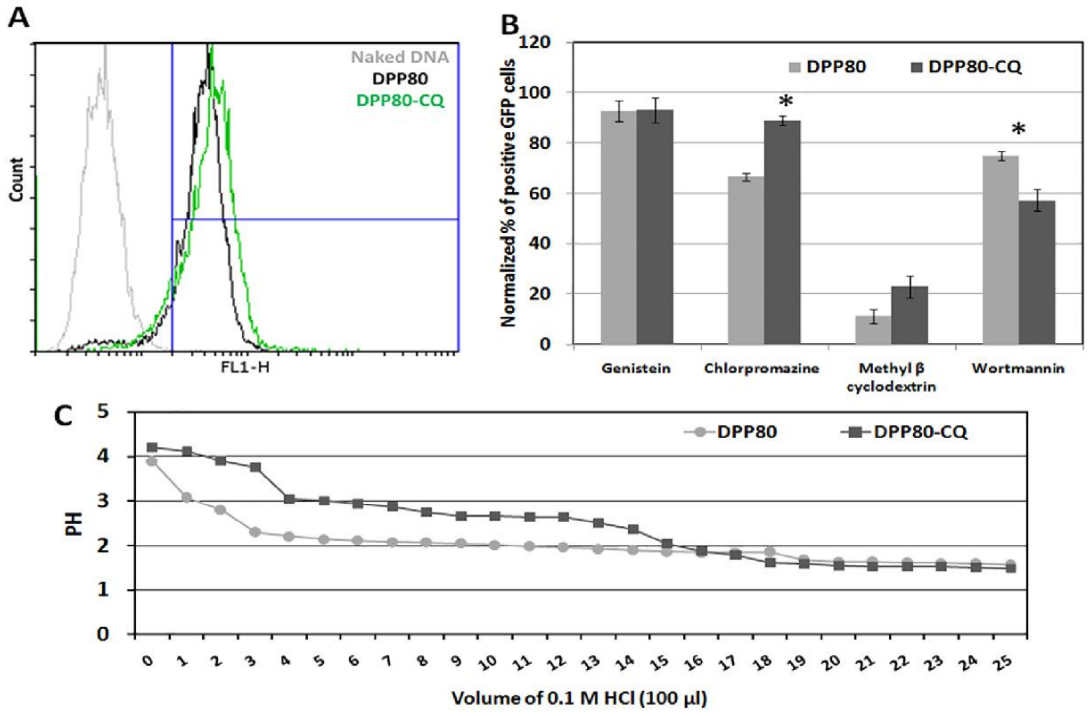

Fig. 15. Cellular uptake and internalization studies of both DPP80 and DPP80-CQ nioplexes at 8/1 and 10/1 cationic lipid/DNA mass ratio. (A) Flow cytometry histograms representing the FITC-labeled plasmid uptake in ARPE-19 cells after 4 h of incubation. (B) Endocytic inhibitors effect on the transfection performance of DPP80 and DPP80-CQ nioplexes. The values were normalized to the transfection without inhibitor. *P < .05 (C) pH buffering capacity analysis of DPP80 and DPP80-CQ niosomes.

Stressing the effect of chloroquine, DPP80 and DPP80-CQ niosomes were formulated and compared. Both niosomes characterization data was analyzed (Table 2). The addition of chloroquine slightly increased the size of niosomes by about 28 nm, and reduced both PDI (about 69% decrease) and ZP (about 34% decrease). Small poly-dispersity values are generally preferred when designing Drug/gene delivery vehicles

(62). The positive ZP values (> +25 mV) detected for both niosomes would reflect a potentially long-lasting stability.

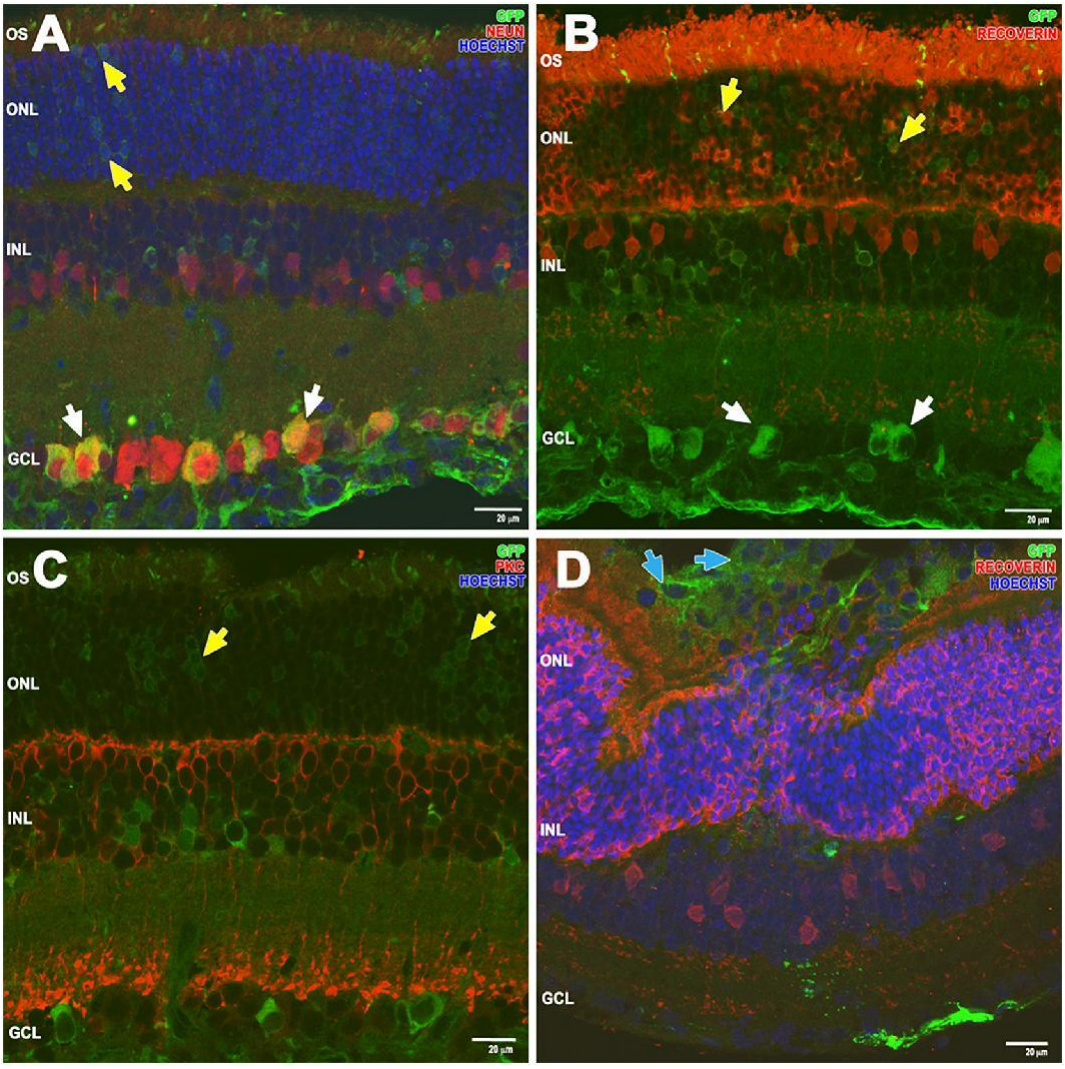

Fig. 16. Retinal cross sections micrographs obtained by confocal microscopy 3 days post subretinal injection of DPP80-CQ nioplexes (A–D). EGFP protein was observed mainly in GCL (white arrows), photoreceptors (yellow arrows) and RPE cells (blue arrows). Retinal sections were stained with antibodies against NeuN(A), recoverin (B, D) and protein kinase C (C). The cell nuclei were counterstained with Hoechst 33342. GCL, ganglion cell layer; INL, inner nuclear layer; ONL, outer nuclear layer; OS, photoreceptor outer segment Scale bars: 20 μm. (For interpretation of the references to colour in this figure legend, the reader is referred to the web version of this article.)

Once the niosomes were characterized in terms of size, PDI, and zeta potential, nioplexes were formed with the pCMS-EGFP plasmid at diverse cationic lipid/DNA mass ratios by adding the reporter plasmid to the niosomes and not the other way round to ensure proper condensation process (10). The ZP of DPP80 nioplexes was clearly lower as compared to the same chloroquine-free niosomes (13-A). In comparison to DPP80-CQ niosomes (29 mV), ZP of chloroquine-containing nioplexes (DPP80-CQ) oscillated within a narrower range (19–25 mV).

Generally, DNA compaction Typically improved by compensating 90% of the charge in an aqueous solution [31]. Strikingly, ZP values fluctuated within a narrow range (23–27 mV) at 8/1 and 10/1 mass ratios for DPP80 and DPP80-CQ, respectively, which reflects a slight reduction in ZP for DPP80-CQ relative niosomes' ZP (29 mV). This indicates a spontaneous electrostatic interaction of pDNA with DPP80-CQ niosomes at a mass ratio of 10/1 which could be explained by a direct chloroquine interaction with pDNA. With regard to nioplexes' PDI value, an obvious effect of chloroquine addition was observed at all ratios studied above 4/1, as PDI values decreased compared with DPP80 formulation (Supplementary Table 1).

Supplementary table 1. Polydispersity index values of both nioplexes (**DPP80** and **DDP80-CQ**). Data represent mean ± standard deviation, n=3.

N/P ratios	4/1	6/1	8/1	10/1	12/1
DPP80	0.211±0.017	0.260±0.014	0.217±0.003	0.288±0.032	0.202±0.005
DPP80-CQ	0.239±0.039	0.139±0.007	0.208±0.055	0.190±0.012	0.182±0.014

The electron micrographs demonstrated a distinct, almost spherical morphology in DPP80 complexes and lack of aggregates (Fig. 13-B_1). DPP80-CQ nioplexes, by contrast, appeared as clusters of multilamellar planar structures forming string-like colloidal aggregates (Fig. 13-B_2). The lamellar spacing was about 5.5–6 nm, indicating that the pDNA strands with the cationic lipid bilayers were complexed (63). Similarly,

several neutral lipids mixtures (such as DOPC and DOPE) along with cationic lipids (such as DOTAP), commonly used for gene delivery, are known to form lamellar complexes with DNA (64).

The agarose gel retardation assay showed that both niosomes, were able to condense, release and protect the DNA from enzymatic digestion at all cationic lipid/DNA ratios tested (Fig.13-C). Of note, the relatively lower DNA condensation, observed by the chloroquine-containing formulation (Fig. 13-C_2), did not hamper the release or the protection of the condensed DNA, which is of paramount importance in transfection performance. Any condensation efficiency shift might affect the pattern and topology of configuring spatial DNA. Even more, both the type and the amount of the surfactant or other additives as chloroquine may influence the state of DNA condensation. Therefore, the fine-tuning of such molecules may be critical in revealing the condensation mechanism of different types of DNA molecules by different nano-vesicles. Notwithstanding the presence of several vacuoles in the cytoplasm, ARPE-19 cells appeared healthy with good viability Even at high concentrations of chloroquine, 100 μg/ml (Supplementary Fig. 2).

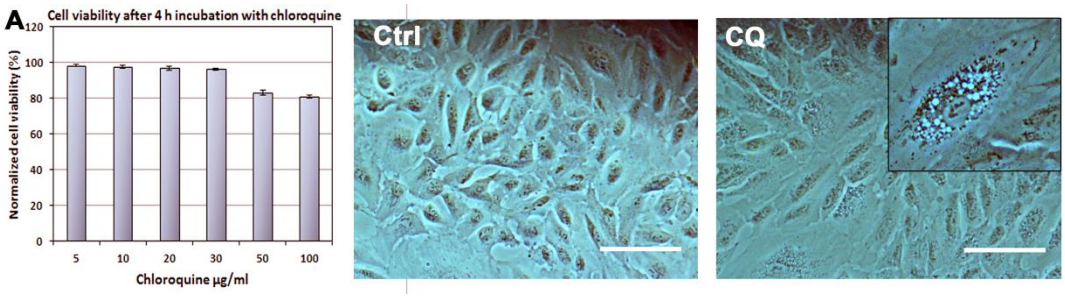

Supplementary fig.2. (A) ARPE-19 cell viability after 4h of incubation with different concentrations of chloroquine diphosphate. Phase contrast microscopy of ARPE-19 cells showing control cells (Ctrl) and cells with vacuolated cytoplasm (CQ) after their treatment with chloroquine diphosphate 100ug/ml.

In vitro, ARPE-19 cells, the transfection output fluctuated in both vectors within a small range at all mass ratios tested (Fig. 14). The cell viability was however in favor of DPP80-CQ (Fig. 14-A). Noteworthy, chloroquine increased the pH of the lysosomes by inhibiting lysosomal enzymes and disturbed their fusion with autophagosomes, thus

inhibits autophagy (65). In addition, chloroquine and its autophagy inhibiting derivative, hydroxychloroquine, are both FDA-approved agents (66). Autophagy may protect or encourage cell death in the eye depending on type of cell or the stress state (67). This mutable aspect of autophagy may be the explanation for DDP80-CQ's increased cell viability compared to its chloroquine-free counterpart, DPP80. Commonly, cell viability and metabolism of ARPE-19 cells are relatively uninfluenced by chloroquine concentrations between 10 and 30 μg/ml, but subsequently affected in a dosage-dependent manner (68). In order to examine whether the enhanced cell internalization of nioplexes was one of the effects that chloroquine could have on niosome formulations, we estimated the percentage of ARPE-19 cell uptake of both DPP80 and DPP80-CQ formulations at the best transfection efficiency mass ratios, 8/1 for DPP80 and 10/1 for DPP80-CQ (Fig. 15).

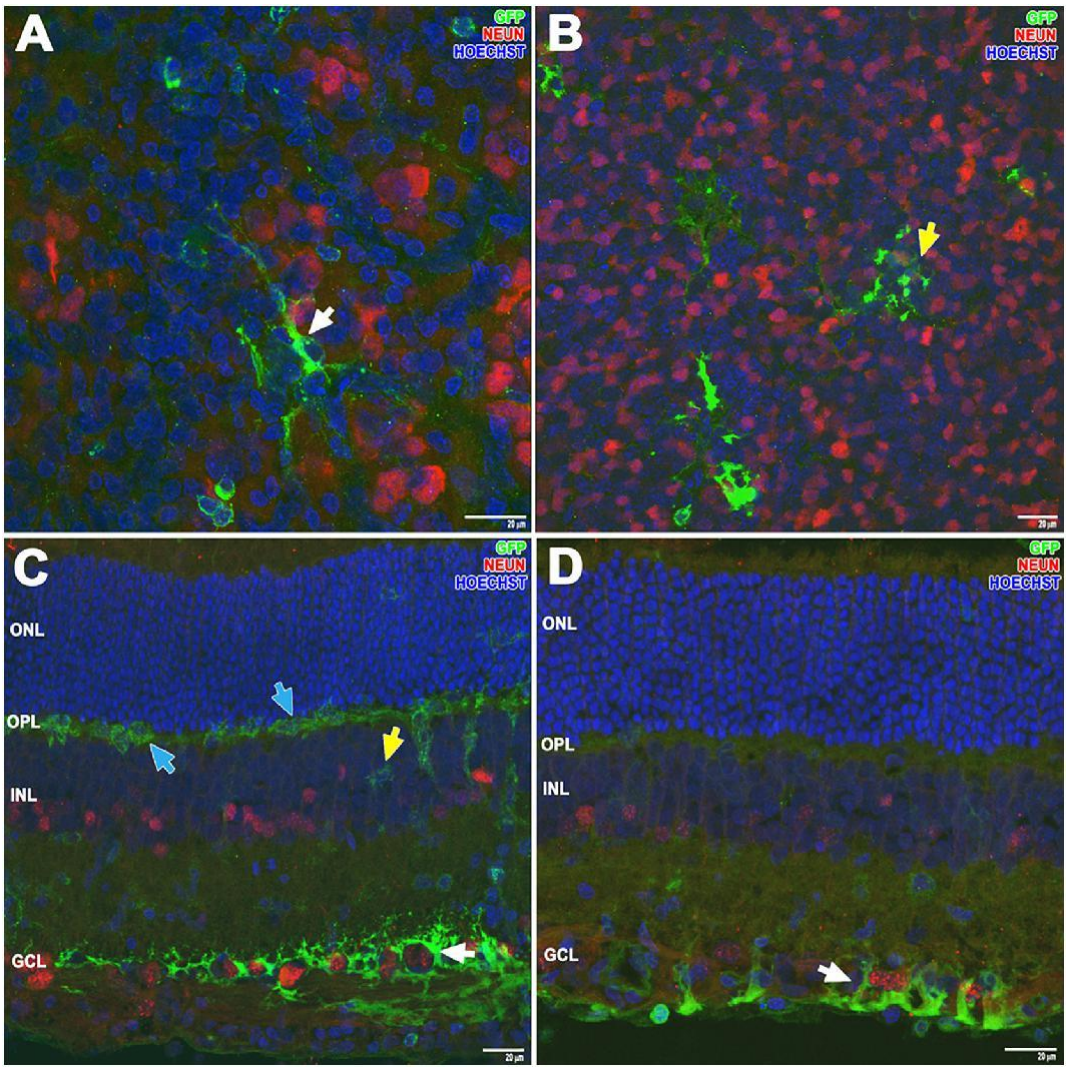

Fig. 17. Confocal fluorescence micrographs of whole mount (A, B) and cross-sections (C, D) of the retina 3 days after intravitreal administration of DPP80-CQ nioplexes. EGFP expression can be observed in both GCL (A, C and D, white arrows) and INL (B and C, yellow arrows). Interestingly, some protein expression was also observed in OPL (C, blue arrows). Whole mount and retinal sections were stained with NeuN (A-D). The cell nuclei were counterstained with Hoechst 33342 (blue). GCL, Ganglion cell layer; INL, inner nuclear layer; ONL, outer nuclear layer; OPL, outer plexiform layer. Scale bars: 20 μm. (For interpretation of the references to colour in this figure legend, the reader is referred to the web version of this article.)

Interestingly, flow cytometry studies showed that the addition of chloroquine had negligible effect on the percentage of cellular uptake relative to the DPP80 formulation (15-A). These findings are most likely due to the indifferent surface charge the two nioplexes at the above-mentioned mass ratios (22.5 ± 7.3 and 25.3 ± 2.5 for DPP80 and DPP80-CQ, respectively, $P > .05$). The similar percentages of uptake in such ratios may justify the previously seen unchanged transfection findings (Fig. 14-A). The transfection efficiency may be significantly impacted by the endocytosis mechanism. Three of the most active cellular internalization pathways were thus studied: clathrin-mediated endocytosis (CME), caveolae-mediated endocytosis (CvME) and macro-pinocytosis (MPC). Observed findings in Fig. 15-B indicated that DPP80-CQ nioplexes were internalized mainly by MPC, while CvME and CME had less involvement in the process of cellular uptake. Macropinocytosis pathway has been suggested to mediate the internalization of non-viral gene delivery vehicles because of its capacity to internalize larger structures (69). Moreover, in certain cell types MPC is known as the main pathway responsible for DNA transfection (70). In comparison, DPP80 nioplexes were internalized primarily by CME and, to a lesser extent, by MPC, while CvME had a much less involvement in the process of cellular uptake. Nonetheless, the slight fluctuation in transfection efficiency between the two nioplexes might be due to small differences between the two key different internalization mechanisms (CME for DPP80 and MPC for DPP80-CQ). The late endosomes/lysosomes proceed through The delivery of genetic material by CvME and CME, which raises the hazards of DNA degradation and decreases the transfection efficiency (23). Thus, an expected trivial effect of CvME and especially CME pathways might explain the high percentages of EGFP expression by both nioplexes in ARPE cells (Fig. 14), compared to lipofectamine® 2000 (approximately, 80% and 75% of lipofectamine®2000 for DPP80 and DPP80-CQ, respectively).

Afterwards, the pH-buffering potential of both niosomes was analyzed (Fig. 15-C). The introduction of chloroquine into the formulation of the niosome increased the pH-buffering potential with 0.1 M HCl after titration relative to the niosomes generated without chloroquine (at pH values > 2). However, the buffering capacity didn't change when the

pH for both niosomes was < 2. Chloroquine might induce endosomal and lysosomal escape via the proton sponge effect (71). This result may indicate that formulation containing chloroquine could increase the effect of proton sponge, and thus, the endosomal escape potential of DPP80-CQ niosomes. However, since the predominant internalization mechanism for DPP80-CQ was neither CvME nor CME, the impact of chloroquine's proton sponge effect on the transfection efficiency was negligible.

Based on the aforementioned physicochemical and in vitro biological findings, we were enthusiastic to perform a preliminary in vivo test to estimate the transfection efficiency of our formulations, DPP80-CQ in particular, in rat retinae after both subretinal (Fig. 16), and intravitreal injections (Fig. 17). Subretinal injection is a popular clinical route to transport genetic/drug content to the back of the eye. Furthermore, it allows direct contact of the injected nucleic acids with the outer retinal layers, photoreceptors and RPE cells. Noteworthy, clinical trials used the subretinal injection route to treat many inherited retinal disorders such as type 2 LCA (72). However, due to the possible risks, it is less suitable than the intravitreal route; such as retinal detachment or the localized side effects around the injection site. In general, IV injection is more widely applicable in the clinical practice because of its ability to deliver genetic material to a wider retinal surface, as well as less surgical damage compared to the SR route (73).

Surprisingly, after both subretinal or intravitreal injections, DPP80 did not cause any transfection of retinal cells in vivo after (Supplementary Fig. 3), while the chloroquine-containing formulation, DPP80-CQ did (Figs. 16 and 17). The lack of connection between the effects in vitro and in vivo transfection results was widely reported since it is a context dependent matter (32).

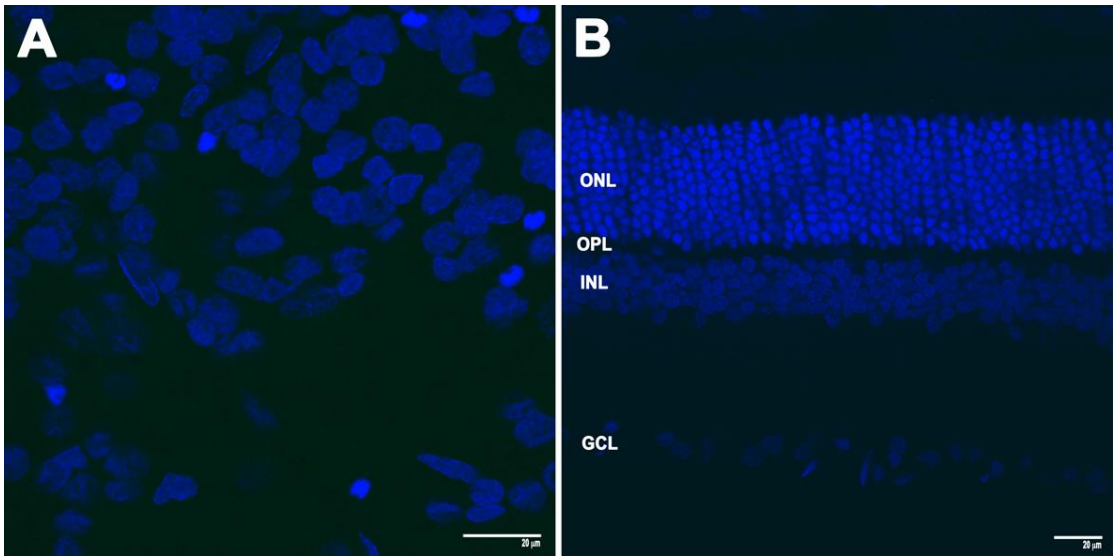

Supplementary fig. 3. Confocal fluorescence micrographs of (A) retinal whole mount after 3 days of intravitreal administration of **DPP80** nioplexes and of (B) retinal cross-sections after 3 days of subretinal administration of **DPP80** nioplexes. There is no GFP expression detected in different retinal layers. Scale bars: 20 μm.

Based on previous physicochemical and in vitro biological findings, we were enthusiastic to perform a preliminary in vivo analysis to assess the transfection efficiency of our formulations, notably DPP80-CQ, in rat retinae after subretinal (Fig. 16) and intravitreal injections (Fig. 17). Subretinal injection is a well proven, effective therapeutic route for delivering genetic material to the eye. This allows direct communication of the nucleic acids injected with the outer retinal layers, photoreceptors and RPE cells. Noteworthy, clinical studies use subretinal injection to treat many inherited retinal disorder such as type 2 LCA (72). However, due to the possible complications such as retinal detachment or the localized impact around the injection site, it is less preferable than the IV route. Generally speaking, intravitreal injection is more common in the clinical practice because its ability to deliver genetic materials to a larger retinal surface and advantages of less surgical damage relative to the SR route (73).

Subretinal administration enables direct contact with RPE cells and outer layer of the retina by genetic material. Though this route of administration is highly effective in transfecting cells locally close to the site of the injection, occasionally found side effects,

related to this invasive route, such as retinal detachment, hemorrhages or alterations in RPE cells can impede its operation (74). Nevertheless, sub-retinal injections were commonly used on clinical trials to treat some devastating retinal genetic disorders that show excellent outcomes (75). In addition, the Luxturna medicine recently approved by FDA/EMA for delivering safe copies of the RPE65 gene to the retina is administered by subretinal injection. In our in vivo experiments, we observed localized EGFP expression after subretinal administration of nioplexes, primarily in some photoreceptor and RPE cells, near to the injection site. Transfection at this level can be clinically relevant because mutations of > 200 genes in RPE cells/photoreceptors are liked to specific genetic disorders of the retina such as; Leber congenital amaurosis, retinitis pigmentosa, and Stargardt disease, to name just a few ones (76).

Similar to subretinal injection, intravitreal injection is an interesting alternative for delivering genetic material to the back of the eye, and thus for access retinal structure. It is a less invasive route, easier to execute, and it can deliver higher doses (77). Consequently, this route of administration can transfect large retinal surfaces (78). When 4 μl of DPP80-CQ nioplexes were administered by intravitreal injection, the inner layers of the retina (GCL and INL) were transfected primarily as seen in Fig. 17. (white and yellow arrows, respectively). Transfection at this level can be clinically relevant in treatment of devastating ocular pathologies that jeopardize the function of ganglion cells as glaucoma (79). Interestingly, expression of EGFP has also been discerned in the OPL (Fig. 17-C, blue arrows) which indicates that nioplexes are partially diffused, not only through the vitreous where they were administered, but also through the inner retinal layers before reach the OPL. Transfection of the outer layers of the retina by intravitreal administration of non-viral vectors represents a major challenge for the scientific community, as can avoid the subretinal injections and the resulting side effects commonly associated with such injection.

Unfortunately, in several pre-clinical or clinical trials, chloroquine was found to be cytotoxic as were other endolytic agents, (80). Chloroquine is toxic to the eye and passes the blood-retinal barrier. This retinal toxicity, however is associated with large doses and

long-term chloroquine use (81). In this analysis, the final concentration of chloroquine was only 25 μg/ml at 10/1 cationic lipid /DNA mass ratio, which according to Chen et al, did not cause any major cytotoxicity (68). In addition to the favorable properties of P and P80, along with the effect of chloroquine, the sensitivity of retinal cells to the modified salt form of the cationic lipid, raises the possibility to safely and effectively targeting different retinal cell after both subretinal and intravitreal administrations.

6.4. References

1. Song YK, Liu D. Free liposomes enhance the transfection activity of DNA/lipid complexes in vivo by intravenous administration. Biochimica et Biophysica Acta (BBA)-Biomembranes. 1998;1372(1):141-50.
2. Balazs DA, Godbey W. Liposomes for use in gene delivery. Journal of drug delivery. 2011;2011.
3. del Pozo-Rodríguez A, Delgado D, Solinís M, Gascón A, Pedraz J. Solid lipid nanoparticles: formulation factors affecting cell transfection capacity. International journal of pharmaceutics. 2007;339(1-2):261-8.
4. Liu F, Yang J, Huang L, Liu D. Effect of non-ionic surfactants on the formation of DNA/emulsion complexes and emulsion-mediated gene transfer. Pharmaceutical research. 1996;13(11):1642-6.
5. Abdelbary G, El-gendy N. Niosome-encapsulated gentamicin for ophthalmic controlled delivery. Aaps Pharmscitech. 2008;9(3):740-7.
6. Meyer O, Kirpotin D, Hong K, Sternberg B, Park JW, Woodle MC, et al. Cationic liposomes coated with polyethylene glycol as carriers for oligonucleotides. Journal of Biological Chemistry. 1998;273(25):15621-7.
7. Rhein LD, Schlossman M, O'Lenick A, Somasundaran P. Surfactants in personal care products and decorative cosmetics: crc press; 2006.
8. Xia S, Tan C, Zhang Y, Abbas S, Feng B, Zhang X, et al. Modulating effect of lipid bilayer–carotenoid interactions on the property of liposome encapsulation. Colloids and Surfaces B: Biointerfaces. 2015;128:172-80.
9. Szunerits S, Boukherroub R. Introduction to plasmonics: advances and applications: Jenny Stanford Publishing; 2015.
10. Wasungu L, Hoekstra D. Cationic lipids, lipoplexes and intracellular delivery of genes. Journal of Controlled Release. 2006;116(2):255-64.
11. Puras G, Mashal M, Zárate J, Agirre M, Ojeda E, Grijalvo S, et al. A novel cationic niosome formulation for gene delivery to the retina. Journal of Controlled Release. 2014;174:27-36.
12. Sung WS, Lee I-S, Lee DG. Damage to the cytoplasmic membrane and cell death caused by lycopene in Candida albicans. Journal of microbiology and biotechnology. 2007;17(11):1797-804.
13. Sakurai F, Inoue R, Nishino Y, Okuda A, Matsumoto O, Taga T, et al. Effect of DNA/liposome mixing ratio on the physicochemical characteristics, cellular uptake and intracellular trafficking of plasmid DNA/cationic liposome complexes and subsequent gene expression. Journal of controlled release. 2000;66(2-3):255-69.
14. Bareford LM, Swaan PW. Endocytic mechanisms for targeted drug delivery. Advanced drug delivery reviews. 2007;59(8):748-58.
15. Ojeda E, Puras G, Agirre M, Zarate J, Grijalvo S, Eritja R, et al. The role of helper lipids in the intracellular disposition and transfection efficiency of niosome formulations for gene

delivery to retinal pigment epithelial cells. International journal of pharmaceutics. 2016;503(1-2):115-26.
16. Ojeda E, Puras G, Agirre M, Zárate J, Grijalvo S, Pons R, et al. Niosomes based on synthetic cationic lipids for gene delivery: the influence of polar head-groups on the transfection efficiency in HEK-293, ARPE-19 and MSC-D1 cells. Organic & biomolecular chemistry. 2015;13(4):1068-81.
17. Kuznetsova AV, Kurinov AM, Aleksandrova MA. Cell models to study regulation of cell transformation in pathologies of retinal pigment epithelium. Journal of ophthalmology. 2014;2014.
18. Aramaki K, Yamada J, Tsukijima Y, Maehara T, Aburano D, Sakanishi Y, et al. Formation of bilayer membrane and niosomes by double-tailed polyglyceryl-type nonionic surfactant. Langmuir. 2015;31(39):10664-71.
19. Kachi S, Oshima Y, Esumi N, Kachi M, Rogers B, Zack DJ, et al. Nonviral ocular gene transfer. Gene therapy. 2005;12(10):843.
20. Liu A, Pajkovic N, Pang Y, Zhu D, Calamini B, Mesecar AL, et al. Absorption and subcellular localization of lycopene in human prostate cancer cells. Molecular cancer therapeutics. 2006;5(11):2879-85.
21. Palozza P, Simone RE, Catalano A, Mele MC. Tomato lycopene and lung cancer prevention: from experimental to human studies. Cancers. 2011;3(2):2333-57.
22. Sharoni Y, Danilenko M, Dubi N, Ben-Dor A, Levy J. Carotenoids and transcription. Archives of Biochemistry and Biophysics. 2004;430(1):89-96.
23. Xiang S, Tong H, Shi Q, Fernandes JC, Jin T, Dai K, et al. Uptake mechanisms of non-viral gene delivery. Journal of controlled release. 2012;158(3):371-8.
24. El-Sayed A, Harashima H. Endocytosis of gene delivery vectors: from clathrin-dependent to lipid raft-mediated endocytosis. Molecular Therapy. 2013;21(6):1118-30.
25. Ferrari A, Pellegrini V, Arcangeli C, Fittipaldi A, Giacca M, Beltram F. Caveolae-mediated internalization of extracellular HIV-1 tat fusion proteins visualized in real time. Molecular therapy. 2003;8(2):284-94.
26. Xiang S, Zhang X. Cellular uptake mechanism of non-viral gene delivery and means for improving transfection efficiency. Gene Therapy-Tools and Potential Applications: IntechOpen; 2013.
27. Berns KI. The parvoviruses: Springer Science & Business Media; 2013.
28. Puras G, Martínez-Navarrete G, Mashal M, Zarate J, Agirre M, Ojeda E, et al. Protamine/DNA/niosome ternary nonviral vectors for gene delivery to the retina: the role of protamine. Molecular pharmaceutics. 2015;12(10):3658-71.
29. Almasieh M, Wilson AM, Morquette B, Vargas JLC, Di Polo A. The molecular basis of retinal ganglion cell death in glaucoma. Progress in retinal and eye research. 2012;31(2):152-81.
30. Martens TF, Remaut K, Deschout H, Engbersen JF, Hennink WE, Van Steenbergen MJ, et al. Coating nanocarriers with hyaluronic acid facilitates intravitreal drug delivery for retinal gene therapy. Journal of controlled release. 2015;202:83-92.
31. Maguire CA, Ramirez SH, Merkel SF, Sena-Esteves M, Breakefield XO. Gene therapy for the nervous system: challenges and new strategies. Neurotherapeutics. 2014;11(4):817-39.
32. Mashal M, Attia N, Puras G, Martínez-Navarrete G, Fernández E, Pedraz JL. Retinal gene delivery enhancement by lycopene incorporation into cationic niosomes based on DOTMA and polysorbate 60. Journal of Controlled Release. 2017;254:55-64.
33. Ochoa GP, Sesma JZ, Díez MA, Díaz-Tahoces A, Avilés-Trigeros M, Grijalvo S, et al. A novel formulation based on 2, 3-di (tetradecyloxy) propan-1-amine cationic lipid combined with polysorbate 80 for efficient gene delivery to the retina. Pharmaceutical research. 2014;31(7):1665-75.
34. Zhang X-X, McIntosh TJ, Grinstaff MW. Functional lipids and lipoplexes for improved gene delivery. Biochimie. 2012;94(1):42-58.

35. Tang G, Zeng J, Gao S, Ma Y, Shi L, Li Y, et al. Polyethylene glycol modified polyethylenimine for improved CNS gene transfer: effects of PEGylation extent. Biomaterials. 2003;24(13):2351-62.
36. Cherng J-Y, Schuurmans-Nieuwenbroek N, Jiskoot W, Talsma H, Zuidam N, Hennink W, et al. Effect of DNA topology on the transfection efficiency of poly ((2-dimethylamino) ethyl methacrylate)–plasmid complexes. Journal of controlled release. 1999;60(2-3):343-53.
37. Paecharoenchai O, Niyomtham N, Ngawhirunpat T, Rojanarata T, Yingyongnarongkul B-e, Opanasopit P. Cationic niosomes composed of spermine-based cationic lipids mediate high gene transfection efficiency. Journal of drug targeting. 2012;20(9):783-92.
38. Smith JG, Wedeking T, Vernachio JH, Way H, Niven RW. Characterization and in vivo testing of a heterogeneous cationic lipid-DNA formulation. Pharmaceutical research. 1998;15(9):1356-63.
39. Mahato RI. Water insoluble and soluble lipids for gene delivery. Advanced drug delivery reviews. 2005;57(5):699-712.
40. Agirre M, Ojeda E, Zarate J, Puras G, Grijalvo S, Eritja R, et al. New insights into gene delivery to human neuronal precursor NT2 cells: a comparative study between lipoplexes, nioplexes, and polyplexes. Molecular pharmaceutics. 2015;12(11):4056-66.
41. Cacciotti I, Ceci C, Bianco A, Pistritto G. Neuro-differentiated Ntera2 cancer stem cells encapsulated in alginate beads: First evidence of biological functionality. Materials Science and Engineering: C. 2017;81:32-8.
42. Tinsley R, Eriksson P. Use of gene therapy in central nervous system repair. Acta neurologica scandinavica. 2004;109(1):1-8.
43. Yang Z, Jiang Z, Cao Z, Zhang C, Gao D, Luo X, et al. Multifunctional non-viral gene vectors with enhanced stability, improved cellular and nuclear uptake capability, and increased transfection efficiency. Nanoscale. 2014;6(17):10193-206.
44. Cardarelli F, Digiacomo L, Marchini C, Amici A, Salomone F, Fiume G, et al. The intracellular trafficking mechanism of Lipofectamine-based transfection reagents and its implication for gene delivery. Scientific reports. 2016;6:25879.
45. Nam HY, Kwon SM, Chung H, Lee S-Y, Kwon S-H, Jeon H, et al. Cellular uptake mechanism and intracellular fate of hydrophobically modified glycol chitosan nanoparticles. Journal of Controlled Release. 2009;135(3):259-67.
46. Varkouhi AK, Scholte M, Storm G, Haisma HJ. Endosomal escape pathways for delivery of biologicals. Journal of Controlled Release. 2011;151(3):220-8.
47. Schafer DP, Stevens B. Phagocytic glial cells: sculpting synaptic circuits in the developing nervous system. Current opinion in neurobiology. 2013;23(6):1034-40.
48. Bergen JM, Park I-K, Horner PJ, Pun SH. Nonviral approaches for neuronal delivery of nucleic acids. Pharmaceutical research. 2008;25(5):983-98.
49. Alvarez JI, Katayama T, Prat A. Glial influence on the blood brain barrier. Glia. 2013;61(12):1939-58.
50. Fields RD, Stevens-Graham B. New insights into neuron-glia communication. Science. 2002;298(5593):556-62.
51. Barres BA. The mystery and magic of glia: a perspective on their roles in health and disease. Neuron. 2008;60(3):430-40.
52. Milligan ED, Watkins LR. Pathological and protective roles of glia in chronic pain. Nature reviews neuroscience. 2009;10(1):23.
53. Yang S, Coles DJ, Esposito A, Mitchell DJ, Toth I, Minchin RF. Cellular uptake of self-assembled cationic peptide–DNA complexes: multifunctional role of the enhancer chloroquine. Journal of Controlled Release. 2009;135(2):159-65.
54. Zhang X, Sawyer GJ, Dong X, Qiu Y, Collins L, Fabre JW. The in vivo use of chloroquine to promote non-viral gene delivery to the liver via the portal vein and bile duct. The Journal of

Gene Medicine: A cross-disciplinary journal for research on the science of gene transfer and its clinical applications. 2003;5(3):209-18.
55. Morille M, Passirani C, Vonarbourg A, Clavreul A, Benoit J-P. Progress in developing cationic vectors for non-viral systemic gene therapy against cancer. Biomaterials. 2008;29(24-25):3477-96.
56. Sriadibhatla S, Yang Z, Gebhart C, Alakhov VY, Kabanov A. Transcriptional activation of gene expression by pluronic block copolymers in stably and transiently transfected cells. Molecular Therapy. 2006;13(4):804-13.
57. Kabanov AV, Batrakova EV, Alakhov VY. Pluronic® block copolymers as novel polymer therapeutics for drug and gene delivery. Journal of controlled release. 2002;82(2-3):189-212.
58. Lee H, Jeong JH, Park TG. PEG grafted polylysine with fusogenic peptide for gene delivery: high transfection efficiency with low cytotoxicity. Journal of Controlled Release. 2002;79(1-3):283-91.
59. Freitas C, Müller RH. Effect of light and temperature on zeta potential and physical stability in solid lipid nanoparticle (SLN™) dispersions. International journal of pharmaceutics. 1998;168(2):221-9.
60. McGregor WC, Stubstad J, Chang CP. Pharmaceutical compositions of bactericidal/permeability increasing protein (BPI). Google Patents; 2000.
61. Attia N, Mashal M, Soto-Sánchez C, Martínez-Navarrete G, Fernández E, Grijalvo S, et al. Gene transfer to rat cerebral cortex mediated by polysorbate 80 and poloxamer 188 nonionic surfactant vesicles. Drug design, development and therapy. 2018;12:3937.
62. Nafee N, Taetz S, Schneider M, Schaefer UF, Lehr C-M. Chitosan-coated PLGA nanoparticles for DNA/RNA delivery: effect of the formulation parameters on complexation and transfection of antisense oligonucleotides. Nanomedicine: Nanotechnology, Biology and Medicine. 2007;3(3):173-83.
63. Attia N, Mashal M, Grijalvo S, Eritja R, Zárate J, Puras G, et al. Stem cell-based gene delivery mediated by cationic niosomes for bone regeneration. Nanomedicine: Nanotechnology, Biology and Medicine. 2018;14(2):521-31.
64. Rädler JO, Koltover I, Salditt T, Safinya CR. Structure of DNA-cationic liposome complexes: DNA intercalation in multilamellar membranes in distinct interhelical packing regimes. Science. 1997;275(5301):810-4.
65. Maycotte P, Aryal S, Cummings CT, Thorburn J, Morgan MJ, Thorburn A. Chloroquine sensitizes breast cancer cells to chemotherapy independent of autophagy. Autophagy. 2012;8(2):200-12.
66. Zhou S, Zhao L, Kuang M, Zhang B, Liang Z, Yi T, et al. Autophagy in tumorigenesis and cancer therapy: Dr. Jekyll or Mr. Hyde? Cancer letters. 2012;323(2):115-27.
67. Sheu S-J, Chen J-L, Bee Y-S, Chen Y-A, Lin S-H, Shu C-W. Differential autophagic effects of vital dyes in retinal pigment epithelial ARPE-19 and photoreceptor 661W cells. PloS one. 2017;12(3):e0174736.
68. Chen PM, Gombart ZJ, Chen JW. Chloroquine treatment of ARPE-19 cells leads to lysosome dilation and intracellular lipid accumulation: possible implications of lysosomal dysfunction in macular degeneration. Cell & bioscience. 2011;1(1):10.
69. Wiethoff CM, Middaugh CR. Barriers to nonviral gene delivery. Journal of pharmaceutical sciences. 2003;92(2):203-17.
70. Zhang X-X, Allen PG, Grinstaff M. Macropinocytosis is the major pathway responsible for DNA transfection in CHO cells by a charge-reversal amphiphile. Molecular pharmaceutics. 2011;8(3):758-66.
71. Cervia LD, Chang C-C, Wang L, Yuan F. Distinct effects of endosomal escape and inhibition of endosomal trafficking on gene delivery via electrotransfection. PloS one. 2017;12(2):e0171699.

72. Bennett J, Ashtari M, Wellman J, Marshall KA, Cyckowski LL, Chung DC, et al. AAV2 gene therapy readministration in three adults with congenital blindness. Science translational medicine. 2012;4(120):120ra15-ra15.
73. Koo H, Moon H, Han H, Na JH, Huh MS, Park JH, et al. The movement of self-assembled amphiphilic polymeric nanoparticles in the vitreous and retina after intravitreal injection. Biomaterials. 2012;33(12):3485-93.
74. Bloquel C, Bourges J, Touchard E, Berdugo M, BenEzra D, Behar-Cohen F. Non-viral ocular gene therapy: potential ocular therapeutic avenues. Advanced drug delivery reviews. 2006;58(11):1224-42.
75. Peng Y, Tang L, Zhou Y. Subretinal injection: a review on the novel route of therapeutic delivery for vitreoretinal diseases. Ophthalmic research. 2017;58(4):217-26.
76. Hims M, Daiger S, Inglehearn C. Retinitis pigmentosa: genes, proteins and prospects. Genetics in Ophthalmology. 37: Karger Publishers; 2003. p. 109-25.
77. del Pozo-Rodríguez A, Solinís MÁ, Rodríguez-Gascón A. Applications of lipid nanoparticles in gene therapy. European Journal of Pharmaceutics and Biopharmaceutics. 2016;109:184-93.
78. Dureau P, Legat L, Neuner-Jehle M, Bonnel S, Pecqueur S, Abitbol M, et al. Quantitative analysis of subretinal injections in the rat. Graefe's archive for clinical and experimental ophthalmology. 2000;238(7):608-14.
79. Bosco A, Anderson SR, Breen KT, Romero CO, Steele MR, Chiodo VA, et al. Complement C3-targeted gene therapy restricts onset and progression of neurodegeneration in chronic mouse glaucoma. Molecular Therapy. 2018;26(10):2379-96.
80. Lönn P, Kacsinta AD, Cui X-S, Hamil AS, Kaulich M, Gogoi K, et al. Enhancing endosomal escape for intracellular delivery of macromolecular biologic therapeutics. Scientific reports. 2016;6:32301.
81. Kasturi N. Long-term continuation of chloroquine-induced retinal toxicity in rheumatoid arthritis despite drug cessation. Rheumatology. 2015;55(4):766-8.

Chapter 7
Conclusions

According with the results obtained in the previously described experiments, the main conclusions of this work include:

1. The elaboration and characterization of a novel non-viral formulation based on DOTMA cationic lipid and polysorbate 60 non-ionic surfactant. Interestingly, the incorporation of natural lipid- lycopene- to the formulation clearly increased transfection efficiency in ARPE-19 cells, without affecting cell viability, probably due to the particular endocytosis pathway, where CvME and macro-pinocytosis pathways could avoid DNA degradation in the lysosome. In vivo administrations to the rat retina showed that DP60L niosomes were able to transfect the outer segments of the retina, which offer reason-able hope for the treatment of many inherited retinal diseases by a safe non-viral formulation after IV administration.

2. Non-viral vector formulations based on niosome nanoparticles, where DOTMA is the cationic lipid, lycopene the "helper" lipid and polysorbate 60 the non-ionic surfactant, presents suitable physicochemical properties for gene delivery applications in terms of size, superficial charge, polydispersity, or capacity to protect genetic material against enzymatic digestion. In addition, such formulation was able to transfect efficiently NT2 cultured cells, were both clathrin and caveolae-mediated endocytosis pathways predominated over macropinocytosis, exhibiting endosomal scape properties that could explain the high protein expression levels observed. Promising results obtained in both primary cortical cultures of rat embryos and in in vivo conditions after intracranial injection open the door for future application of such niosomes as efficient gene delivery tools for therapeutic treatment of some degenerative as well as malignant CNS disorders.

3. The addition of chloroquine to a niosome formulation retained its functionality in vitro, but most importantly, enhanced its transfection ability in vivo. This work highlights the use of chloroquine as a built-in component in the gene delivery vehicles to evade its toxicity and to provide new insights into the future of retinal gene therapy.